A Thesis Submitted for the Degree of PhD at the University of Warwick

Permanent WRAP URL:

http://wrap.warwick.ac.uk/1326139

Copyright and reuse:

This thesis is made available online and is protected by original copyright.

Please scroll down to view the document itself.

Please refer to the repository record for this item for information to help you to cite it.

Our policy information is available from the repository home page.

For more information, please contact the WRAP Team at: wrap@warwick.ac.uk

warwick.ac.uk/lib-publications

Investigating the selectivity of sequence-controlled antimicrobial polymers synthesised by RAFT polymerisation

Agnès Mari Kuroki

A thesis submitted in partial fulfilment of the requirements for the degree of

Doctor of Philosophy in Chemistry

Department of Chemistry

University of Warwick

May 2019

Table of Contents

List of Figures

List of Tables

List of Schemes

Abbreviations

ACN	Acetonitrile
A-D30	poly(NIPAM$_{70}$-b-AEAM$_{30}$)
A-D50	poly(NIPAM$_{50}$-b-AEAM$_{50}$)
A-D70	poly(NIPAM$_{30}$-b-AEAM$_{70}$)
AEAM	Amino-ethylacrylamide
A-M30	poly(NIPAM$_{18}$-b-AEAM$_{10}$-b-NIPAM$_{18}$-b-AEAM$_{10}$-b-NIPAM$_{18}$-b-AEAM$_{10}$-b-NIPAM$_{18}$)
A-M50	poly(NIPAM$_{10}$-b-AEAM$_{10}$-b-NIPAM$_{10}$-b-AEAM$_{10}$-b-NIPAM$_{10}$-b-AEAM$_{10}$-b-NIPAM$_{10}$-b-AEAM$_{10}$-b-NIPAM$_{10}$-b-AEAM$_{10}$)
A-M70	poly(AEAM$_{18}$-b-NIPAM$_{10}$-b-AEAM$_{18}$-b-NIPAM$_{10}$-b-AEAM$_{18}$-b-NIPAM$_{10}$-b-AEAM$_{18}$)
AMP	Antimicrobial peptide
A-S30	poly(NIPAM$_{70}$-s-AEAM$_{30}$)
A-S50	poly(NIPAM$_{50}$-s-AEAM$_{50}$)
A-S70	poly(NIPAM$_{30}$-s-AEAM$_{70}$)
A-T30	poly(NIPAM$_{35}$-b-AEAM$_{15}$-b-NIPAM$_{35}$-b-AEAM$_{15}$)
ATRP	Atom transfer radical polymerisation
BMA	Butyl methacrylate
BOC	$tert$-butoxycarbonyl
BocAEAM	N-t-butoxycarbonyl-N'-acryloyl-1,2-diaminoethane
c_H	Lowest concentration at which aggregation of RBCs is observed
CL	Cardiolipin sodium salt from bovine heart
CMC	Critical micelle concentration
Con A	Concanavalin A
CPP	Cell penetrating peptide

CTA	Chain Transfer Agent
C_{tr}	Chain transfer coefficient
$Đ$	Molar mass distribution (M_w/M_n)
DCM	Dichloromethane
diBocGEAM	1,3-Di-Boc-guanidinoethyl acrylamide
DLS	Dynamic Light Scattering
DMAEMA	2-(Dimethyl)aminoethylmethacrylate
DMEM	Dulbecco's Modified Eagle's Medium
DMF	*N,N*-Dimethyl formamide
DMSO	Dimethyl sulfoxide
DMSO-d_6	Deuterated DMSO
DP	Degree of polymerisation
E. coli	*Escherichia coli*
EDC	1-Ethyl-3-(3-dimethylaminopropyl)carbodiimide
EtOAc	Ethyl acetate
FA	Facially amphiphilic
G-D30	poly(NIPAM$_{70}$-*b*-GEAM$_{30}$)
GEAM	Guanidino-ethylacrylamide
GPC	Gel permeation chromatography
G-S30	poly(NIPAM$_{70}$-*s*-GEAM$_{30}$)
G-T30	poly(NIPAM$_{35}$-*b*-GEAM$_{15}$-*b*-NIPAM$_{35}$-*b*-GEAM$_{15}$)
HC$_{10}$	Lowest concentration at which 10 % of haemolysis is observed
HPLC	High performance liquid chromatography
IC$_{50}$	Inhibitory concentration of 50 % of cells
LAM	Less-activated monomer
LCST	Lower critical solution temperature
LRP	Living radical polymerisation

MAM	More-activated monomer
MHB	Müller-Hinton Broth
MIC	Minimum inhibitory concentration
MOPS	3-(N-morpholino)propanesulfonic acid
MRSA	Methicillin-resistant *S. aureus*
MS	Mass spectroscopy
MSSA	Methicillin-sensitive *S. aureus*
NaCl	Sodium chloride
NaOH	Sodium hydroxide
NEt$_3$	Triethylamine
NHS	N-hydroxysuccinimide
NIPAM	N-isopropylacrylamide
NMP	Nitroxide mediated polymerisation
NMR	Nuclear Magnetic Resonance
P. aeruginosa	*Pseudomonas aeruginosa*
PABTC	(propanoic acid)yl butyl trithiocarbonate
PBS	Phosphate Buffered Saline
PE	1,2 dioleoyl-*sn*-glycero-3-phosphoethanolamine
PEG	Poly(ethylene glycol)
PG	1,2 dioleoyl-*sn*-glycero-3-phospho-*rac*(1-glycerol) sodium salt
PMS	N-methyl dibenzopyrazine methyl sulphate
RAFT	Reversible Addition-Fragmentation chain Transfer
RBC	Red blood cell
RDRP	Reversible-deactivation radical polymerisation
ROMP	Ring-opening metathesis polymerisation
RPMI	Roswell Park Memorial Institute medium
S. aureus	*Staphylococcus aureus*

S. epidermidis	*Staphylococcus epidermidis*
SMAMP	Synthetic mimic of antimicrobial peptides
SEC	Size exclusion chromatography
TFA	Trifluoroacetic acid
THF	Tetrahydrofuran
TI	Therapeutic index
VA-044	2,2'-azobis[2-(2-imidazolin-2-yl)propane]dihydrochloride
XTT	2,3-Bis-(2-Methoxy-4-Nitro-5-Sulfophenyl)-2H-Tetrazolium-5-Carboxanilide

Acknowledgements

As I have been spoiled with support over the course of my PhD I am afraid this section will be lengthy but since this section is the most read part of any thesis I would rather use it wisely to thank all the people who have contributed to the thesis.

I would like to start by thanking my supervisor Prof Seb Perrier. Starting during my Master's degree, you provided me with guidance, helped me with finding my industrial placement but also PhD funding. I am also grateful for the funding provided by the Commonwealth Scientific and Industrial Research Organisation (CSIRO) for the PhD scholarship scheme. I have been lucky enough to have Dr. Katherine Locock as a co-supervisor for my PhD. Your enthusiasm and advice have been extremely helpful and you made my stint at CSIRO very enjoyable! I would also like to thank Dr. Elizabeth Williams, Dr. Parveen Sangwan, Dr. Yue Qu, Ivan Martinez and Dr. Christian Hornung with whom I had the chance to collaborate with during my stay and who were so welcoming.

During my Master's degree placements Dr. Andrew Slark and Dr. Paul Wilson provided me with precious advice which helped me in the decision of starting a PhD, which I am very grateful for.

I would like to thank Dr. Matthias Hartlieb: from advice on how to make tables look less terrible (thanks IMGUR) to experimental tips, your help has been essential during my PhD. I would also like to thank Dr. Guillaume Gody and Dr. Carlos Sanchez for teaching me RAFT and bio stuff, respectively.

As my PhD dangerously but inescapably progressed towards biological applications, I had the opportunity to collaborate with a few people who made the ride up to Gibbet Hill less arduous. I would like to thank John Moat and Prof. Chris Dowson for their help as well as Assoc. Prof. Meera Unnikrishnan, for collaborating with me and hosting me in her lab. Special thanks to Dr. Arnaud Kengmo Tchoupa for being an amazing teacher (I've never seen anyone mouth-pipette as fast as you do), and of course Ji Song for making the Perrier group's life easier in SLS and teaching me how not to contaminate mammalian cells! I would also like to thank Dr. Sandra Bédarida and Séverine Rangama for being a constant source of fun.

I should thank the t=0 Warwick Perrier group with Drs. Tammie Barlow, Junliang Zhang, Alex Cook, Majda Akrach, Johannes Brendel and Ming Koh for all the hiking and socialising. I would also like to thank Drs. Sophie Larnaudie and Ximo Sanchis-Martinez for taking the time to read and correct my thesis, as well as Dr. Alex Simula, seeing you work in the lab was quite inspiring (except when you played Kendrick!)

Declaration

Experimental work contained in this thesis is original research carried out by the author, in the Department of Chemistry at the University of Warwick, and at the Commonwealth Scientific and Industrial Research Organisation in Melbourne between October 2015 and March 2019. No material contained here has been submitted for any other degree, or at any other institution.

Results from other others are references throughout the text in the usual manner.

The work presented was carried out by the author with the following exceptions:

Chapter 2: The bacterial resistance assay was performed by John Moat and the XTT assays by Carlos Sanchez-Cano (University of Warwick, School of Life Sciences).

Chapter 3: The XTT assay with HaCaT cells by Raoul Peltier (University of Warwick, School of Life Sciences).

Date: _____   _____

                                                                  Agnès Kuroki

Chapter 1   Introduction

Bacterial resistance has become a pressing clinical issue for which the World Health Organisation has raised awareness due to the low levels of infection control reached recently.[1-2] This global issue has been considered as a failure in antibiotic drug discovery and new types of antibiotics have recently been investigated to tackle it.

For this reason, new types of antibiotics have recently been investigated. Among these, antimicrobial peptides (AMPs) have attracted an increased interest and a few of them are currently undergoing clinical trials.[3] AMPs are peptides comprised of 10-50 amino-acids with cationic and hydrophobic residues, present in the innate immune system of multicellular organisms, hence the terminology host-defence peptides.[4-5] The majority of these peptides, adopt an amphipathic helical conformation with the cationic functionalities on one side of the coil and the hydrophobic ones on the other.[6] AMPs have demonstrated a broad-range antimicrobial activity, which is associated to their mechanism of action based on bacterial membrane disruption. Indeed, the positively charged residues of AMPs have been shown to interact with the negatively charged phospholipids of bacterial membranes (Scheme 1.1).[7] Following the binding of AMPs to bacterial membranes, the hydrophobic residues of AMPs insert into the membrane, inducing the formation of pores. Once the integrity of the bacterial membrane is compromised, there is leakage of the intracellular material, which leads to bacterial cell death.[8] Remarkably, as AMPs seem to target bacterial membrane instead of a specific ligand, they do not seem to evoke bacterial resistance against these peptides.[9-10] Indeed, only minor structural changes are required for bacteria to exhibit a reduced susceptibility towards conventional antibiotics, whereas more significant changes in the structure of the bacterial membrane would be necessary to prevent the antimicrobial action of AMPs.[11-12] This membrane interaction based on electrostatic interactions allows AMPs to be selective towards bacteria over mammalian cells to a certain extent.[13]
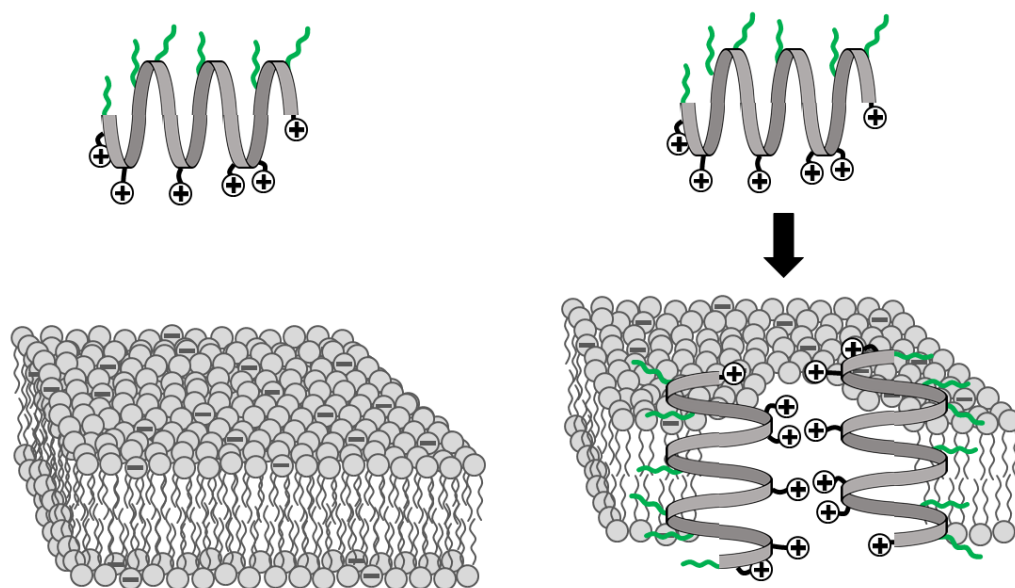
Scheme 1.1 - Schematic representation of the mode of action of AMPs

Despite the aforementioned advantages, AMPs can present a high toxicity profile towards mammalian cells, in particular with red blood cells.[14-15] Furthermore, peptides are not typically ideal drug candidates as they are costly to produce on large scale and show limited pharmacokinetic stability.[16] To overcome these challenges, synthetic mimics of AMPs (SMAMPs) which possess similar physico-chemical properties to naturally occurring AMPs and therefore mimic their mode of action, have been extensively investigated.

1.1   Key parameters influencing the selectivity of SMAMPs

The discovery that the helical chirality of AMPs did not affect their antimicrobial activity,[17] led researchers to examine a wider range of synthetic strategies.[18-20] Perhaps the most promising of these are the AMP mimicking polymers since their compositions are readily tuneable and easily scalable.[21] Remarkably, Mowery *et al.* reported the antimicrobial activity of polymers with a flexible backbone using nylon copolymers, hence demonstrating that a specific or regular conformation was not required for SMAMPs to exhibit antimicrobial activity.[22]

Because most SMAMPs are designed with both cationic and hydrophobic functionalities, the balance between positive charge and hydrophobicity on the selectivity towards mammalian cells has been extensively studied. Since positive charge, which enables the polymers to preferentially interact with bacterial membranes over mammalian cells, often confers hydrophilic character to the material, some additional hydrophobic character is typically introduced to facilitate membrane disruption (Scheme 1.2).[23] Kuroda and co-workers synthesised a library of polymethacrylates bearing positive charge with side chains of increasing hydrophobicity.[24] Highly hydrophobic materials exhibited less selectivity with high haemolytic activity, whereas no antimicrobial activity was observed with the most cationic (and therefore hydrophilic) polymers. This balance was shown to be quite delicate, as an increase in the overall hydrophilicity of the polymer, from polymethacrylate to polymethacrylamide, reduced their potency towards bacteria but also their haemolytic activity.[25] Similar trends were observed with polynorbornenes, with hydrophobicity being necessary to disrupt bacterial membranes, but inducing haemolysis if in excess.[26-27]
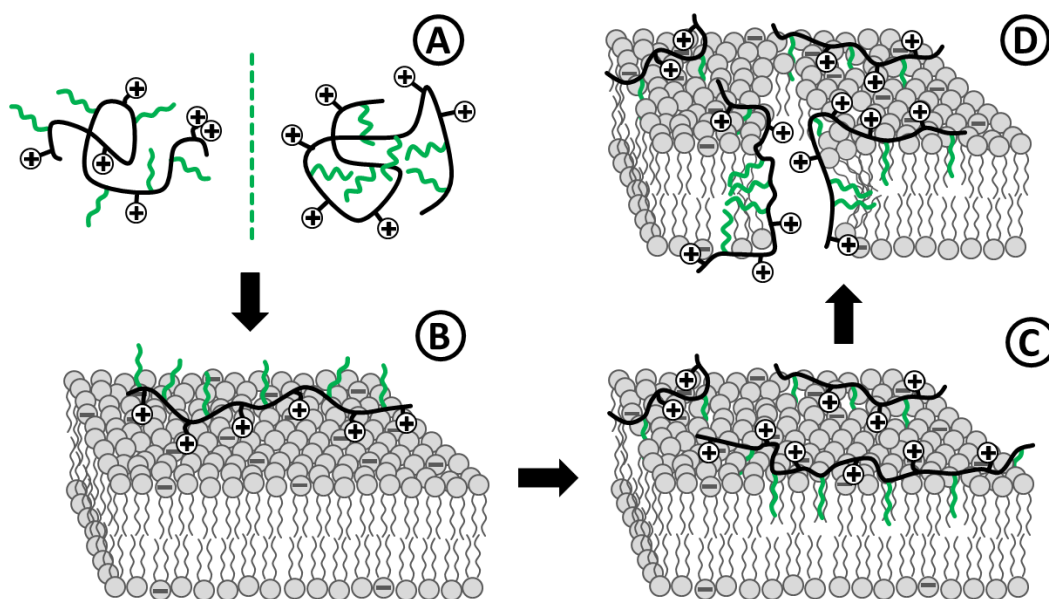
Scheme 1.2 - Schematic representation of the mode of action of AMP mimicking polymers. (A) Polymer in solution as either random coil (left) or partially segregated (and possibly aggregated, right). (B) Attachment to bacterial membrane by electrostatic interaction. (C) Insertion into the hydrophobic domain of the membrane. (D) Membrane disruption leading to cell death.

In addition, they observed that the molar mass of the polymers played a central role in optimising selectivity towards bacteria. Both the antimicrobial and the haemolytic activity

increased with the degree of polymerisation for polynorbornenes.[27] A similar trend was observed with oligomers bearing guanidine moieties, for which a minimum molar mass of 500 g.mol^{-1} was required to obtain an active compound.[28] However, above a molar mass of 50000 g.mol^{-1} there was also a loss of activity, which was attributed to the inability of the longest polymers to effectively cross the outer peptidoglycan layer.[26] Moreover, control over the molar mass distribution is crucial: Mowery and co-workers showed that for the same number average molar mass of 3000 g.mol^{-1}, a nylon-3 cationic SMAMP with a broader dispersity resulted in greater haemotoxicity than that of the polymer with a lower dispersity: the minimum haemolytic concentration varied from 12.5 to 800 μg.mL^{-1} for a *Đ* value of 1.15 and 1.06, respectively.[22] Indeed, it was found that the high molar mass chains within the population were responsible for an increase in toxicity towards red blood cells.

Various studies investigating the type of charge, counter-ion or the length of the spacer between the charged pendant moiety and the polymeric backbone have also been undertaken.[29-32] However, the results generally correlated to the variation in charge to hydrophobicity ratio, hence no ulterior structure-activity relationship could be elucidated.[29]
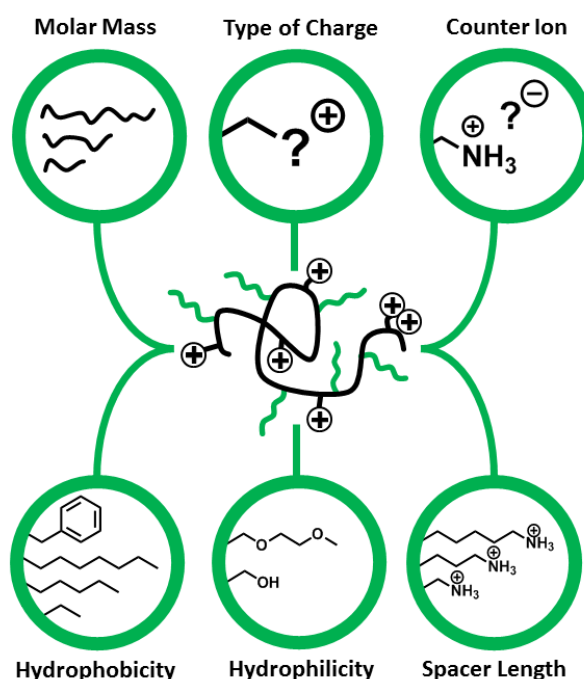
Scheme 1.3 - Parameters reported to influence the efficiency of polymeric AMP mimics.

1.2 Sequence Control in Polymeric AMP Mimics

As mentioned earlier, the *α*-helical secondary structure of AMPs is not necessary to exhibit antimicrobial activity. However, the physico-chemical properties of an AMP seem to have a direct impact on their interaction with bacterial membranes, and therefore on the antimicrobial activity. One approach to controlling the balance of positive charge to hydrophobicity, and hence antimicrobial activity, is to dictate the positioning of relative functionalities along a polymeric backbone. In this section, the influence of the distribution of functionalities and micellisation of SMAMPs on biological activity is reviewed.

1.2.1 Structural Control *via* Monomer Architecture

One typical and simple synthetic approach which allows for a degree of spatial control of functionalities in SMAMPs is the copolymerisation of hydrophobic and cationic monomers. In such cases the distance between functionalities is defined, on one level, by the nature of the polymer backbone, and secondly by the sequence of monomers. However, to investigate the impact of the relative distance between functionalities, other design strategies have also been developed.

In order to establish the influence of the spacing between the alkyl chain and the cationic centre, Sambhy *et al.* designed two types of random copolymers both containing pyridinium and methacrylate units.[33] For one series, methyl methacrylate was copolymerised with a pyridinium monomer quaternised by an alkyl chain substituent. The other copolymer series contained a pyridinium monomer quaternised by a methyl group and methacrylate monomers bearing pendant alkyl chains (Scheme 1.4A). The separation of the alkyl chain from the cationic centre slightly increased the antibacterial activity and significantly increased the haemolytic activity. Indeed, for similar composition and alkyl chain length, the disruption of cell membranes was promoted by the separation of the charge and the tail, in particular for mammalian cells. Therefore, the selectivity against bacteria was increased by situating the alkyl chain at the cationic centre. A possible explanation for this effect could be found in the mechanism of action of polymeric AMP mimics. When hydrophobicity is spatially separated from the charge it is more likely to insert into the hydrophobic domain of the cell membrane, rendering these polymers more membrane active. This research underlines the importance of the spatial control of hydrophobic and cationic units relative to each other.
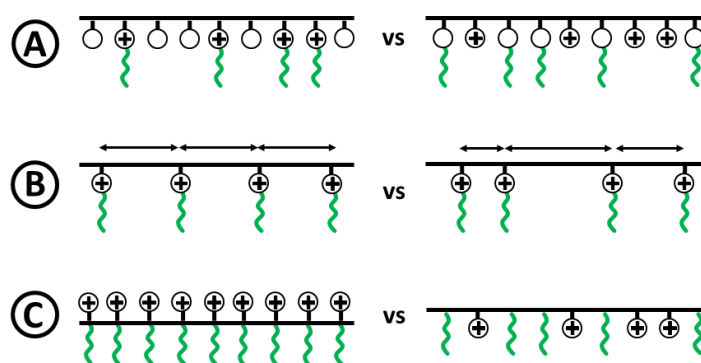
Scheme 1.4 - Different strategies to vary the biological activity of polymer by changes in sequence/monomer distribution. (A) Controlled distance of cationic charges. (B) Variations in proximity of cationic charge and hydrophobic units along the polymer chain. (C) Comparison of facial amphiphilic monomers with random copolymers.

Song and co-workers developed alternating copolymers obtained by alternated ring-opening metathesis polymerisation (AROMP) of cationic and hydrophobic monomers.[34] Random copolymer counterparts and homopolymers were synthesised for comparison of their antimicrobial activity. Regular spacing between functional groups was shown to improve the potency of alternating polymers, which exceeded the antimicrobial activity of the random copolymers with similar functionalities in which the distance between pendant groups is not strictly periodic (Scheme 1.4B). By comparing the potency of homopolymers and alternating polymers towards bacteria, the authors furthermore concluded that a distance of 8 - 10 Å between cationic units in an alternating copolymer backbone resulted in optimal membrane interaction. However, since the synthesised polymers possessed broad molar mass distributions (Đ up to 2.4 for alternating copolymers and 3.5 for homopolymers), it is difficult to clearly conclude on the structure-property relationship.

Further investigation of the distribution of functional groups along the polymer backbone was undertaken by Gabriel *et al.*[35] The study was directed towards the comparison of facially amphiphilic (FA) polynorbornenes synthesised *via* ring opening metathesis polymerisation (ROMP) of dual functional monomers with random amphiphilic copolymers derived from mono-functional monomers (Scheme 1.4C). The random amphiphilic polymers offered segregation of cationic primary amine moieties and hydrophobic alkyl chains *via* the polymer backbone, whereas FA polymers directed the separation of functionalities perpendicularly to the backbone. The FA polymers exhibited higher antimicrobial activity and lower toxicity against red blood cells than the segregated counterparts, thus a better selectivity. The FA structure might enhance membrane interactions, thus enhancing their disruption.[35] The rigidity of the polynorbornene backbone might emphasize the effect of the facial

amphiphilicity of the monomers. A more flexible backbone could allow the polymer chains to adapt their conformation more readily in presence of a membrane, thus rendering the initial distribution of the functionalities along the polymer backbone less important. Another observation was that the change in the ratio of cationic to hydrophobic segregated monomers did not influence the antimicrobial or the haemolytic activity. However, as the length of the alkyl pendant group had a direct impact on the selectivity, it seems that the local charge to hydrophobicity ratio is of greater importance than that of the overall polymer.

In order to mimic the facially amphiphilic structure of AMPs, Tew and co-workers designed oligomers using aromatic rings and other functionalities enabling hydrogen-bonding to rigidify the polymeric structure. They observed that by limiting rotational degrees of freedom around the backbone, the potency against bacteria was increased.[36-37] Further systems were explored using monomers bearing both a cationic and a hydrophobic pendant group,[27] or introducing modification in FA monomers affecting the structure of the backbone.[38] The design of monomers chosen to build the AMP mimics and any modification in the sequence of these monomers seemed to have an impact on the local amphiphilicity, therefore affecting the interaction of the resulting polymers with cell membranes. These FA systems, among other synthetic mimics of AMPs, have been discussed more extensively in a review by Lienkamp *et al.*[39]

1.2.2   Influence of Monomer Sequence

The self-assembly of AMPs has been demonstrated to play an important role in reducing the cytotoxicity and improving the stability of these peptides.[40,41] The self-assembly of antimicrobial polymers might also have an impact on their activity. Extensive work on the modelling of the interactions of antimicrobial polymers with bacterial membrane was carried out by Baul and co-workers (Scheme 1.5A).[42] Although specific conformations are not necessary, it was established that the interactions of polymers with bacterial membranes were enhanced by their ability to segregate cationic and hydrophobic groups. Additional simulations showed that the strength of the adsorption of antimicrobial polymers to bacterial membranes depended on the monomer sequence, correlating to their ability to phase segregate.[43] Amphiphilic block copolymers, in comparison to their random copolymer anologues, are more likely to undergo phase segregation in an aqueous environment and are therefore the subject of recent studies.

An early investigation performed by Sauvet and co-workers compared multiblock poly(siloxane)s bearing quarternised ammonium units with their statistical counterparts (Scheme 1.5B).[44] No influence of the polymer architecture on the antimicrobial activity was observed. However, the haemolytic activity of the macromolecules were not investigated, preventing a conclusion about their selectivity.
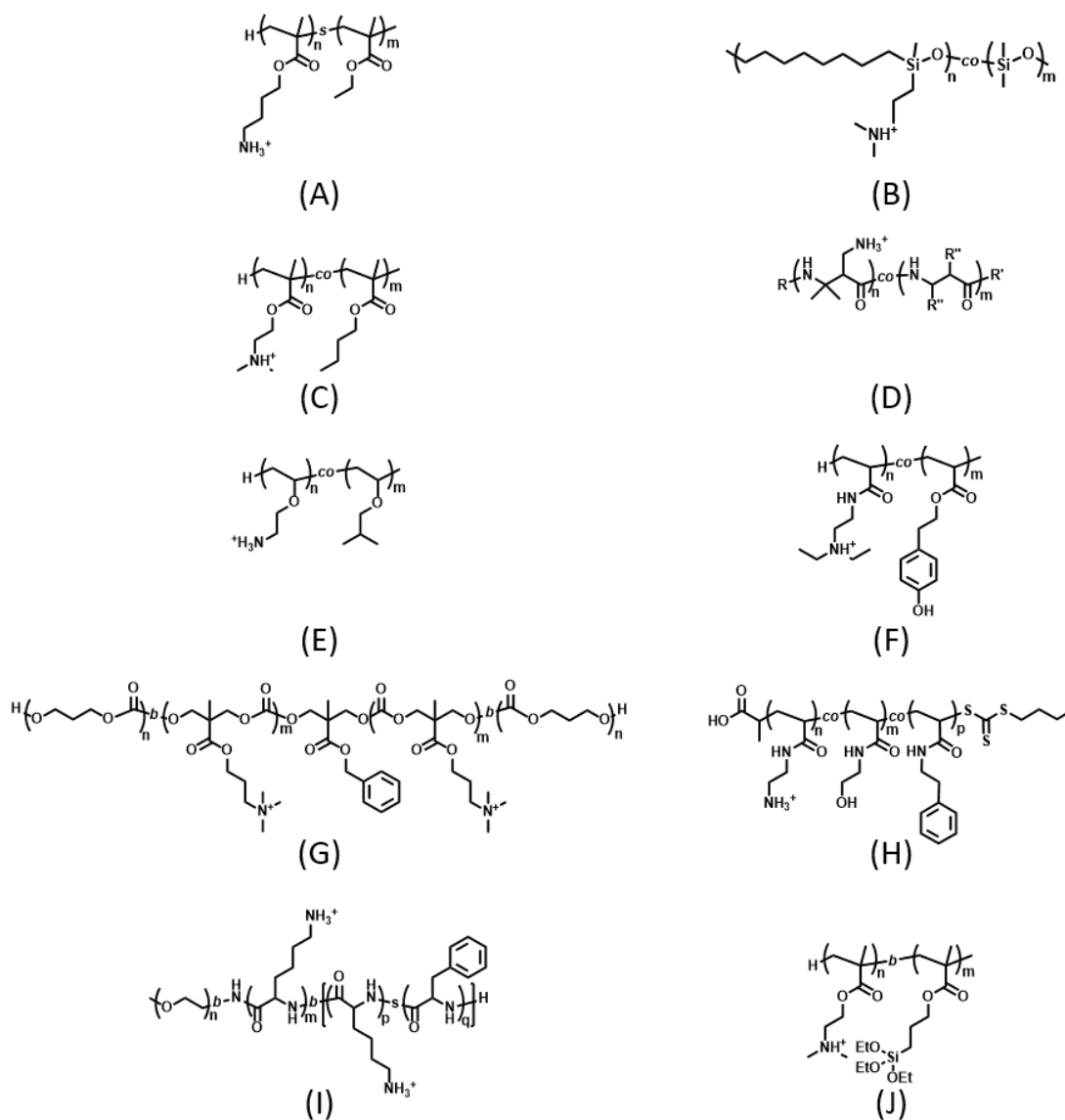
Scheme 1.5 – Structures of the statistical, gradient or block copolymers.

Similarly, Wang *et al.* explored the antimicrobial activity of diblock and random copolymers of 2-(dimethyl)aminoethylmethacrylate (DMAEMA) and butylmethacrylate (BMA) as shown in Scheme 1.5C.[45] Despite the level of activity against microorganisms not varying with the segmentation of the polymers, the haemolytic activity was substantially

decreased for diblock copolymers making them more selective against bacteria, in comparison to their random copolymer equivalents. A study of gradient and diblock nylon-3 copolymers synthesised from *β*-lactams bearing primary amine and hydrophobic pendant groups was performed by Liu and co-workers (Scheme 1.5D).[46] While haemolytic activity was diminished, the antimicrobial activity was also reported to be lower for the diblocks as compared to gradient copolymers. However, none of these works investigated the presence of self-assemblies in solution.

Oda *et al.* designed diblock and random copolymers of cationic and hydrophobic vinyl ethers using cationic polymerisation (Scheme 1.5E).[47] Although the antimicrobial activity was similar for both types of polymers, the study demonstrated that the block copolymers were far less haemolytic than their random copolymer equivalents. Interestingly, block copolymers displayed antimicrobial activity below their critical micelle concentration (CMC). However, they were considered to form unimolecular aggregates with a cationic shell at low concentration, which allowed a shielding of the hydrophobic domain from red blood cells, thus reducing the haemolytic activity. This is supported by molecular dynamic investigations on statistical copolymers performed by Taresco and co-workers (Scheme 1.5F).[48] A flower-like micelle model was used to fit the structure adopted by the random copolymers in solution indicating the formation of phase segregated systems even without a block or block-like architecture. A further difference with the block copolymers in the study by Oda *et al.* was the increased levels of haemagglutination (RBC aggregation) in comparison to the random copolymers. This could be a result of the phase separation of block copolymers leading to enhanced presentation of cationic charges compared to statistical copolymers. The increased interaction with anionic groups on RBC membranes would consequently result in cross-linking and aggregation.

A study by Nederberg and co-workers on triblock poly(carbonate)s synthesised by ring-opening polymerisation revealed similar observations concerning antimicrobial activity and haemolysis (Scheme 1.5G).[49] The polymers self-assembled in aqueous solution into flower-like micelles, which were able to efficiently disrupt bacterial membranes while maintaining low haemolysis levels. Indeed, in this case minimum inhibitory concentration (MIC) values were higher than the reported CMC of the polymers in buffer, hence the antimicrobial activity was attributed to the micellar structure. On the contrary, Judzewitsch and co-workers found that with a ternary copolymer system (hydrophobic, neutral hydrophilic and cationic monomers), segregating all three functionalities resulted in a lower antimicrobial activity compared to a statistical counterpart (Scheme 1.5H).[50] This reduction in activity was

attributed to the formation of stable micelles, preventing interactions of the hydrophobic moieties with bacterial membrane. However, when the hydrophobic and hydrophilic monomers were incorporated in the same block and the cationic functionalities segregated in a different block, the MIC towards both Gram-negative and Gram-positive bacteria was improved.[50]

Costanza *et al.* investigated block copolymers obtained by the coupling of polypeptides, containing phenyl alanine and lysine, with poly(ethylene glycol) (PEG) of varied lengths (Scheme 1.5I).[51] These block copolymers formed particles in aqueous solution, and it was found that a long PEG block (5000 g.mol^{-1}), shielded the biologically active block, which reduced the haemolytic activity, as well as the antimicrobial activity.

The influence of the shape of polymeric nano-objects on the inhibition of bacterial growth was investigated by Yao and co-workers through comparison of a diblock copolymer comprising a cationic polyDMAEMA block and a hydrophobic methacrylate-derived block bearing triethoxysilyl pendant groups which were synthesised *via* RAFT polymerisation (Scheme 1.5J).[52] Phase separated bulk materials were cross-linked and re-dispersed resulting in spherical, cylindrical and sheet-like assemblies. However, the antimicrobial activity was not affected by the morphology, indicating that increased contact area is not needed to improve antibacterial activity for these polymers. Furthermore, cross-linking of the polymers may have interfered with the effective insertion into the hydrophobic membrane domain. However, the impact of the shape on the toxicity against mammalian cells was not investigated.

In summary, although an alpha-helical shape, as found for AMPs, is not necessary for a successful antimicrobial polymer, the distribution of functionalities along the polymer chain certainly has an impact on their biological activity. However, while empirical evidence proves that distance between charges or the proximity of cationic domains to hydrophobic domains influence the membrane activity, no clear correlation for that effect has been established as yet. Nonetheless, in the case of polymers which possess a controlled segregation of functionalities *i.e.* block copolymers and facially amphiphilic polymers, the inluence is more definitive, and certainly micellisation seems to profoundly influence antimicrobial behavior. With the cationic corona shielding the hydrophobic domain, disruption of bacterial membranes seems less favoured within stable micelles.

The precise distribution of functionality, positive charge and hydrophobic moieties along the backbone has been demonstrated to have an impact on the selectivity of AMP

mimics. Although achieving such defined sequences in SMAMPs can be synthetically challenging, reversible-deactivation radical polymerisation (RDRP) techniques have made promising progress in the synthesis of sequence-controlled block copolymers with robust and easily scalable approaches.[53-55]

1.3   Design of well-defined multiblock copolymers using RAFT

Radical polymerisation is now widely exploited for the synthesise of precision polymers with the emergence of RDRP techniques which allows control over the molar mass, molar mass distribution and, crucially, confers "living" character to the polymer chains (i.e. the opportunity to reinitiate from the ω-chain end, yielding block copolymers).[56] Amongst those methods, nitroxide-mediated polymerisation (NMP),[57-59] atom transfer radical polymerisation (ATRP)[60-62] and reversible addition-fragmentation chain transfer (RAFT)[63-64] polymerisation have been the most extensively studied and utilised.[65] This part of the introduction will focus on the latter and its application in the synthesis of block copolymers.

1.3.1   Introduction to RAFT polymerisation

RAFT polymerisation is an extremely robust and versatile technique which is used to readily obtain polymers of defined molar mass with narrow molar mass distributions for a range of monomer families including (meth)acrylates, (meth)acrylamides, styrenics and vinyl ethers.[64, 66-67] RAFT is based on the degenerative transfer of the radical centre between polymers chains through addition to a chain transfer agent (CTA) (or RAFT agent), providing a reversible activation/deactivation mechanism which affords all polymeric chains an equal opportunity to grow using only a small fraction of radical species.[67] The mechanism of RAFT polymerisation is shown in Scheme 1.6.

Initiation

$$\text{Initiator} \xrightarrow{k_d} \text{I}^\bullet \xrightarrow[k_i]{M} \text{P}_1^\bullet \xrightarrow[k_p]{M} \xrightarrow[k_p]{M} \text{P}_n^\bullet$$

Pre-equilibrium

Re-initiation

$$\text{R}^\bullet \xrightarrow[k_{iR}]{M} \text{P}_1^\bullet \xrightarrow[k_p]{M} \xrightarrow[k_p]{M} \text{P}_m^\bullet$$

Main equilibrium

Termination

$$\text{P}_n^\bullet + \text{P}_m^\bullet \xrightarrow{k_{tc}} \text{P}_n\text{-P}_m$$

$$\text{P}_n^\bullet + \text{P}_m^\bullet \xrightarrow{k_{td}} \text{P}_n^= + \text{P}_m^H$$

Scheme 1.6 - The RAFT mechanism.

As in conventional radical polymerisation, radical species ($\text{I}^\bullet$) are generated and may undergo radical addition to monomer to form a polymeric radical species $\text{P}^\bullet_n$ (k_p). In the pre-equilibrium stage of the polymerisation, $\text{P}^\bullet_n$ will add (k_{add}) to the thiocarbonylthio of the CTA (1). The intermediate radical (2) can revert back to (1) and $\text{P}^\bullet_n$ ($-k_{add}$) or fragment (k_β) to yield a polymer chain with a thiocarbonylthio end-group (3), or macro-CTA, and a new CTA-derived radical $\text{R}^\bullet$. The latter can in turn undergo addition to monomer (k_{iR} then k_p) to form a polymeric radical $\text{P}^\bullet_m$, during the re-initiation step. The process then reaches the main equilibrium, ideally once all of the CTA (1) is consumed to give macro-CTA (3). At this stage, the radical is exchanged between two polymer chains, through the formation (k_{addP}) and fragmentation ($-k_{addP}$) of a radical intermediate (4). Since the process nonetheless involves the co-existence of radical species, bimolecular termination events will inevitably occur *via* either combination (k_{tc}) or disproportionation (k_{td}), yielding "dead chains". However, this mechanism of degenerative transfer offers all polymer chains the opportunity to propagate at a uniform rate with only a small fraction of the population existing as radical species, thereby limiting the extent of termination events. Thus, when the amount of CTA present is greater

than the amount of radical species produced by the initiator, the majority of the α-chain ends will be derived from the R group of the CTA, whilst ω-chain ends will possess the thiocarbonylthio group. Provided that the CTA is consumed rapidly and quantitatively, and exchange of radical species *via* the thiocarbonylthio moiety is efficient, the molar mass of the polymer chains is dictated by the ratio [M]/[CTA] and the population possesses a narrow molar mass distribution. The theoretical number-average molar mass ($M_{n,th}$) is calculated using Equation 1.1.

$$M_{n,th} = \frac{([M]_0 - [M]_t) \times M_M}{[CTA]_0 + 2f[I]_0(1 - e^{-k_d t})(1 - \frac{f_c}{2})} + M_{CTA}$$

Equation 1.1 - Calculation of $M_{n,th}$.

Where $[M]_0$, $[CTA]_0$, $[I]_0$ are the initial concentrations (in mol.L^{-1}) of the monomer, CTA and the initiator respectively; $[M]_t$ is the monomer concentration at time t; M_M and M_{CTA} are the molar masses (in g.mol^{-1}) of the monomer and the CTA, respectively; k_d is the decomposition rate constant (in s^{-1}) of the azo-initiator; and *t* represents the polymerisation time (in seconds). The factor "2" accounts for the fact that one molecule of azo-initiator yields two primary radicals with the efficiency *f* (assumed to be equal to 0.5 in this study). The term $1 - (f_c/2)$ represents the number of chains produced in a radical-radical termination event with f_c representing the coupling factor. An f_c value of 1 means that 100 % of bimolecular terminations occur *via* combination, whereas a value of 0 indicates that 100 % of bimolecular terminations occur *via* disproportionation. However, in an optimal experimental design, the fraction of dead chains should be negligible compared to CTA-derived chains, hence Equation 1 can be simplified to give Equation 1.2.

$$M_{n,th} \approx \frac{([M]_0 - [M]_t) \times M_M}{[CTA]_0} + M_{CTA}$$

Equation 1.2 - Approximation on the calculation of $M_{n,th}$.

During a RAFT polymerisation, control over molar mass distribution is dictated by the R and Z group of the CTA, which should be selected in accordance to monomer reactivity. Indeed, the type of R group affects the pre-equilibrium stage, during which a rapid and full consumption of the radical R˙ should occur, as mentioned previously. In order to achieve this, the fragmentation of the intermediate (2) towards R˙ (k_β), the radical derived from the R group

of the CTA, has to be more favourable than towards $P_n^{\bullet}$ ($k_{\text{-add}}$), followed by a rapid addition of $R^{\bullet}$ to monomer ($k_{iR} > k_p$).[67] The fragmentation of the intermediate (2) is determined by the partition coefficient Φ given by Equation 1.3:

$$\Phi = \frac{k_{\beta}}{k_{-add} + k_{\beta}}$$

Equation 1.3 - Determination of the partition coefficient Φ.

Polymers with narrow molar mass distributions can be obtained when $\Phi \geq 0.5$ ($k_{\beta} \geq k_{\text{-add}}$), corresponding to $R^{\bullet}$ being a better homolytic leaving group than $P_n^{\bullet}$. The fragmentation of the intermediate (2) will depend on the monomer being polymerised, since $k_{\text{-add}}$ decreases in the following order: methacrylates ≥ methacrylamides >> styrenics ≥ acrylates >> acrylamides > vinyl esters. The stability of $R^{\bullet}$ is related to polar and steric effects. Hence the R group should be designed according to the type of monomer being polymerised. A series of typical R-group structures given in order of their ability as a homolytic leaving group are shown in Scheme 1.7.[68] When the appropriate relative reactivity is chosen, the CTA is fully consumed at the start of the process, allowing for the main equilibrium to take place.
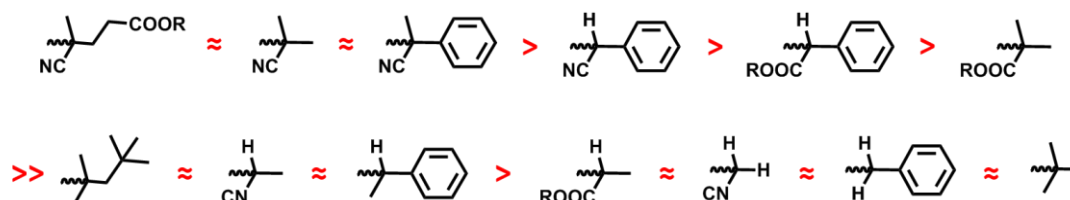
Scheme 1.7 – Structure of the R groups of RAFT agents. The leaving group ability (k_{β}) decreases from left to right.

During the main equilibrium, the exchange rate of the radical centre between the polymer chains should be greater than the propagation rate. This difference is ensured by a greater reactivity of the polymeric radical towards the thiocarbonylthio group compared to the monomer ($k_{addP} >> k_p$).[69] These kinetics considerations can be translated into the chain transfer coefficient (C_{tr}) which depends on the rate of chain transfer (k_{tr}) and propagation (k_p) as shown in Equations 1.4 and 1.5.

$$C_{tr} = \frac{k_{tr}}{k_p}$$

Equation 1.4 – Determination of the chain transfer constant C_{tr}.

$$k_{tr} = \Phi . k_{add}$$

Equation 1.5 – Determination of the rate of chain transfer k_{tr}.

In order to obtain polymers with low molar mass distribution ($Đ < 1.2$), CTAs with high C_{tr} (at least 10) are recommended.[70] The C_{tr} of a reaction depends on the monomer and the Z group of the CTA.[69] Indeed, there are two categories of vinyl monomers: the more-activated monomers (MAMs), such as (meth)acrylates, (meth)acrylamides and styrenic derivatives, which have a high reactivity to radicals, and the less-activated monomers (LAMs) such as vinyl esters and vinyl amides. The propagating radicals derived from LAMs are less stable than those produced from MAMs. By varying the Z group, the reactivity of the CTA and its derived radical intermediate (4) can be modified. Dithioesters and trithiocarbonates (Scheme 1.8A and B) were shown to be highly reactive, thus are suited for the polymerisation of MAMs. However, for the polymerisation of LAMs xanthates and dithiocarbamates are more appropriate (Scheme 1.8C and D) RAFT agents, as they have a lower reactivity towards radical addition. The variety in this R and Z group chemistry, which has been extensively reviewed, offer the ability to polymerise a wide range of different monomer types with control over molar mass and molar mass distribution.[64, 66, 68-69, 71-72]
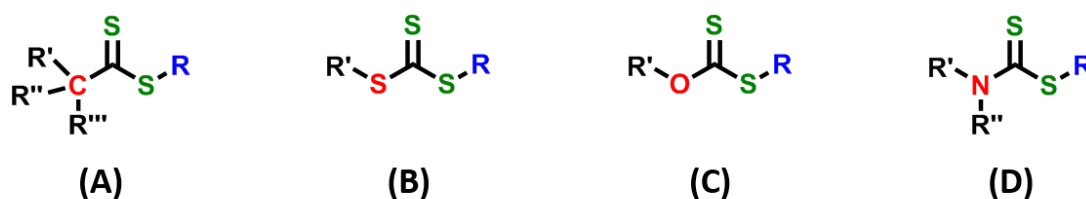
Scheme 1.8 – Categories of RAFT agents with different Z groups. Dithioester (A), trithiocarbonate (B), xanthate (C) and dithiocarbamate (D).

1.3.2   Synthesis of block copolymers *via* RAFT

The livingness of RAFT polymerisation permits the sequential addition of monomer to obtain highly defined structures called block copolymers comprised of blocks of different monomers.[73-74] The RAFT mechanism allows all polymer chains to grow using only a small fraction of active radical species, meaning a high proportion of the polymer chains are "living" i.e. possessing the thiocarbonylthio moiety, as expressed by Equation 1.6.[53]

$$L\ (\%) = \frac{[CTA]_0}{[CTA]_0 + 2f[I]_0(1 - e^{-k_d t})(\dfrac{1 - f_c}{2})}$$

Equation 1.6 - Theoretical determination of the relative amount of living polymer chains using an azo-initiator compound.

The fraction of living chains, L (%), can be calculated using Equation 1.3, where $[CTA]_0$ and $[I]_0$ are the initial concentrations of CTA and initiator, respectively, k_d and f describe the thermal decomposition of the initiator and 1-f_c/2 the termination mechanisms. Utilising a high ratio of $[CTA]/[I]_{consumed}$ results in a very high fraction of the "living" ω-chain ends, offering the possibility of efficient chain extension(s). In this regard, a low flux of radical species is beneficial. However, the rate of propagation (R_p) in RAFT polymerisation is proportional to the concentration of active radical species, which itself is related to the initial initiator concentration and the rate at which is decomposes, as for conventional radical polymerisation (Equation 1.7).[63]

$$R_p = k_p[M][P^\cdot] = k_p[M]\sqrt{\frac{f.k_d[I]_0 e^{-k_d t}}{k_t}}$$

Equation 1.7 - Theoretical determination of the rate of propagation for RAFT polymerisation.

Where [M] and [P·] are the concentrations of monomer and polymeric radical species, respectively; k_p and k_t are the rate of propagation and termination, respectively; f is the initiator efficiency and $[I]_0$ is the initiator concentration at time t. Therefore, monomer conversion is strongly correlated to the initiator concentration. In order to successfully conduct a RAFT

polymerisation to high monomer conversion, yielding polymers with a narrow molar mass distribution and also a high fraction of living chains, a fine optimisation of the [M]/[CTA]/[I] ratio has to be established.

When synthesising a block copolymer by RAFT, one of the key parameters to take into account is the choice of the Z group of the CTA, since its ability to stabilise the intermediate radical must be compatible with the radical derived from each monomer.[70] Additionally, the order of the chain extensions is governed by the reactivity of the monomers.[75] The first block acts as a macroCTA for the polymerisation of the second block, hence the reactivity of the propagating radical of the first block will affect the chain extension with the second monomer. Indeed, conditions which allow to proceed to the main equilibrium (i.e. R being an efficient homolytic leaving group and R˙ adding to monomer) must again be satisfied. The order of the synthesis of block copolymers require careful optimisation: the more activated monomers, which polymers are better homolytic leaving group, should be polymerised prior to the LAMs in order to ensure the successful chain extension of all the polymer chains.[64, 70]

The other aspect to take into consideration in the preparation of block copolymers using a degenerative transfer mechanism such as RAFT is that a continuous source of exogenous radicals are required.[70] The radicals generated from the decomposition of the initiator will react with the newly added monomer and propagate, yielding homopolymers of the second monomer. The proportion of this undesired homopolymer is related to the ratio of (macro)CTA to radicals introduced. Under conventional RAFT conditions, this ratio will be relatively low, and therefore the majority of polymer chains in the final population will be the desired AB block copolymer. However, when targeting further block extensions, the presence of undesired polymer chains (dead chains and initiator derived chains) is compounded and can become non-negligible, typically leading to a poorly defined population.

When targeting multiple block extensions via RAFT, to yield multiblock copolymers, conditions must be carefully considered in order to minimise the contribution of dead and initiator derived chains.[76] Traditionally, this entails using a relatively high ratio of CTA to initiator and stopping each polymerisation cycle at moderate monomer conversion (<70 %), thereby requiring timely and costly purification steps between each block extension.[77-78] However, in 2013 Gody and co-workers demonstrated how well-defined multiblock copolymers could be readily prepared via RAFT in a one-pot system through a rigorously considered approach.[53, 76, 79] By polymerising acrylamide monomers, which possess a high

$k_p/(k_t)^{1/2}$ compared to most other vinyl monomers, and working at high monomer concentrations, near-quantitative monomer conversion could be achieved for each polymerisation cycle with very low initiator concentrations. This system could be further optimised by using water as solvent, which further increases the k_p of acrylamides. Finally, it was shown how targeting a low degree of polymerisation for each RAFT polymerisation cycle and using rapidly decomposing azo-initiators permitted the one-pot synthesis of a well-defined multiblock copolymer with an unprecedented number of blocks (21) in a short time frame (2 h per block).[79] Well-defined polyacrylate and polymethacrylate multiblock copolymers have also since been successfully prepared by carefully optimising the conditions of the RAFT process.[80-82] With such time and resource-efficiency, complex multiblock copolymer architectures are becoming increasingly accessible and offer enormous potential for industrial applications.[83-84]

1.4   Conclusion and scope of the thesis

The activity and selectivity of antimicrobial polymers are governed by the interactions of the polymer chains with bacterial membranes. Recent studies investigated variations in polymer structure which dictate the relative distribution of cationic moieties and hydrophobic domains. In this context, the distribution of the functionalities along the polymer backbone seems to alter the interactions of the polymer chains with bacterial membrane. The multiblock approach provides access to an intermediate in terms of distribution of functional groups compared to other typical sequences (alternating, statistical, gradient, diblock). The activity of the defined copolymers could then be compared with that of the statistical monomer distributions, which would help in establishing an in-depth structure-activity relationship for these antimicrobial systems. Therefore, this study could be a starting point for the exploration of more efficient antimicrobial polymers. Additionally, as multiblock copolymers can easily be scaled up by using RAFT technology, and that their production cost is relatively low, they could be a potentially attractive alternative to current antibiotics.

The aim of this thesis is to study the structure-activity relationship of antimicrobial block copolymers obtained by RAFT. The first experimental chapter focuses on the synthesis of amphiphilic ammonium SMAMPs. The content of positive charge (0, 30, 50, 70 and 100 %), as well as the degree of segmentation (statistical, multiblock and diblock) were varied. This library will permit to determine the optimal charge content for these primary amine-functional SMAMPs, but also to investigate the effect of their sequence on the activity against a range of bacteria in addition to their compatibility towards mammalian cells.

Subsequently, guanidinium-rich polymers are synthesised in order to mimic AMPs containing arginine residues. For this system, a single chemical composition is targeted (30 % charge content), but the monomer distribution is varied in a similar fashion to the lysine mimics. A systematic comparison of guanidinium containing polymers with their ammonium counterparts is established to determine the ideal candidates to tackle MRSA (type of charge and polymer sequence).

In the final chapter, the interactions of guanidinium SMAMPs of different sequence with bacterial membrane is described. In order to explain the impact of monomer distribution on the antimicrobial activity, guanidinium homopolymers of comparable length to the cationic block of the block copolymers are investigated. Due to the similarities of the guanidinium-rich polymers with cell penetrating peptides (CPPs), their use as treatment against intracellular bacteria is explored.

1.5   References

1.   Antimicrobial resistance: Global report on surveillance; World Health Organization: 2014.

2.   Brown, E. D.; Wright, G. D., Antibacterial drug discovery in the resistance era. *Nature* **2016,** *529* (7586), 336-343.

3.   Sun, E.; Belanger, C. R.; Haney, E. F.; Hancock, R. E. W., 10 - Host defense (antimicrobial) peptides. In *Peptide Applications in Biomedicine, Biotechnology and Bioengineering*, Koutsopoulos, S., Ed. Woodhead Publishing: 2018; pp 253-285.

4.   Wang, G.; Wang, Z., APD: the Antimicrobial Peptide Database. *Nucleic Acids Research* **2004,** *32* (suppl_1), D590-D592.

5.   Tavares, L. S.; Silva, C. d. S. F. d.; Souza, V. C.; Silva, V. L. d.; Diniz, C. G.; Santos, M. D. O., Strategies and molecular tools to fight antimicrobial resistance: resistome, transcriptome and antimicrobial peptides. *Frontiers in Microbiology* **2013,** *4*.

6.   Tossi, A.; Sandri, L.; Giangaspero, A., Amphipathic, α-helical antimicrobial peptides. *Biopolymers* **2000,** *55* (1), 4-30.

7.   Zasloff, M., Antimicrobial peptides of multicellular organisms. *Nature* **2002,** *415* (6870), 389-395.

8.   Shai, Y., Mode of action of membrane active antimicrobial peptides. *Peptide Science* **2002,** *66* (4), 236-248.

9.   Seo, M.-D.; Won, H.-S.; Kim, J.-H.; Mishig-Ochir, T.; Lee, B.-J., Antimicrobial Peptides for Therapeutic Applications: A Review. *Molecules* **2012,** *17* (10), 12276.

10.   Phoenix, D. A.; Dennison, S. R.; Harris, F., Antimicrobial Peptides. Wiley: 2013; pp 1-37.

11.   Stapleton, P. D.; Taylor, P. W., Methicillin resistance in Staphylococcus aureus: mechanisms and modulation. *Science progress* **2002,** *85* (Pt 1), 57-72.

12.   Van Bambeke, F.; Mingeot-Leclercq, M.-P.; Struelens, M. J.; Tulkens, P. M., The bacterial envelope as a target for novel anti-MRSA antibiotics. *Trends in Pharmacological Sciences* **2008,** *29* (3), 124-134.

13.   Matsuzaki, K., Control of cell selectivity of antimicrobial peptides. *Biochimica et Biophysica Acta (BBA) - Biomembranes* **2009,** *1788* (8), 1687-1692.

14.   Izumiya, N., Kato, T., Aoyagi, H., Waki, M., Kondo, M., Synthetic Aspects of Biologically Active Cyclic Peptides-Gramicidin S and Tyrocidine. *Halsted Press* **1979**, 16-27.

15.   Ahmad, A.; Azmi, S.; Srivastava, R. M.; Srivastava, S.; Pandey, B. K.; Saxena, R.; Bajpai, V. K.; Ghosh, J. K., Design of Nontoxic Analogues of Cathelicidin-Derived Bovine Antimicrobial Peptide BMAP-27: The Role of Leucine as Well as Phenylalanine Zipper Sequences in Determining Its Toxicity. *Biochemistry* **2009,** *48* (46), 10905-10917.

16.   Craik, D. J.; Fairlie, D. P.; Liras, S.; Price, D., The Future of Peptide-based Drugs. *Chemical Biology and Drug Design* **2013,** *81* (1), 136-147.

17.   Papo, N.; Oren, Z.; Pag, U.; Sahl, H.-G.; Shai, Y., The Consequence of Sequence Alteration of an Amphipathic α-Helical Antimicrobial Peptide and Its Diastereomers. *The Journal of Biological Chemistry* **2002,** *277* (37), 33913-33921.

18.   Budhathoki-Uprety, J.; Peng, L.; Melander, C.; Novak, B. M., Synthesis of Guanidinium Functionalized Polycarbodiimides and Their Antibacterial Activities. *ACS Macro Letters* **2012,** *1* (3), 370-374.

19.   Rotem, S.; Mor, A., Antimicrobial peptide mimics for improved therapeutic properties. *Biochimica et Biophysica Acta (BBA) - Biomembranes* **2009,** *1788* (8), 1582-1592.

20.   Ganewatta, M. S.; Tang, C., Controlling macromolecular structures towards effective antimicrobial polymers. *Polymer* **2015,** *63*, A1-A29.

21.   Kenawy, E.-R.; Worley, S. D.; Broughton, R., The Chemistry and Applications of Antimicrobial Polymers: A State-of-the-Art Review. *Biomacromolecules* **2007,** *8* (5), 1359-1384.

22.   Mowery, B. P.; Lindner, A. H.; Weisblum, B.; Stahl, S. S.; Gellman, S. H., Structure−activity Relationships among Random Nylon-3 Copolymers That Mimic Antibacterial Host-Defense Peptides. *J. Am. Chem. Soc.* **2009,** *131* (28), 9735-9745.

23.   Timofeeva, L.; Kleshcheva, N., Antimicrobial polymers: mechanism of action, factors of activity, and applications. *Appl Microbiol Biotechnol* **2011,** *89* (3), 475-492.

24.   Kuroda, K.; Caputo, G. A.; DeGrado, W. F., The Role of Hydrophobicity in the Antimicrobial and Hemolytic Activities of Polymethacrylate Derivatives. *Chem. Eur. J.* **2009,** *15* (5), 1123-1133.

25.   Palermo, E. F.; Sovadinova, I.; Kuroda, K., Structural Determinants of Antimicrobial Activity and Biocompatibility in Membrane-Disrupting Methacrylamide Random Copolymers. *Biomacromolecules* **2009,** *10* (11), 3098-3107.

26.   Lienkamp, K.; Kumar, K.-N.; Som, A.; Nüsslein, K.; Tew, G. N., "Doubly Selective" Antimicrobial Polymers: How Do They Differentiate between Bacteria? *Chem. Eur. J.* **2009,** *15* (43), 11710-11714.

27.   Lienkamp, K.; Madkour, A. E.; Musante, A.; Nelson, C. F.; Nüsslein, K.; Tew, G. N., Antimicrobial Polymers Prepared by ROMP with Unprecedented Selectivity: A Molecular Construction Kit Approach. *J. Am. Chem. Soc.* **2008,** *130* (30), 9836-9843.

28.   Albert, M.; Feiertag, P.; Hayn, G.; Saf, R.; Hönig, H., Structure−Activity Relationships of OligoguanidinesInfluence of Counterion, Diamine, and Average Molecular Weight on Biocidal Activities. *Biomacromolecules* **2003,** *4* (6), 1811-1817.

29.   Palermo, E. F.; Vemparala, S.; Kuroda, K., Cationic Spacer Arm Design Strategy for Control of Antimicrobial Activity and Conformation of Amphiphilic Methacrylate Random Copolymers. *Biomacromolecules* **2012,** *13* (5), 1632-1641.

30.   Engler, A. C.; Tan, J. P. K.; Ong, Z. Y.; Coady, D. J.; Ng, V. W. L.; Yang, Y. Y.; Hedrick, J. L., Antimicrobial Polycarbonates: Investigating the Impact of Balancing Charge and Hydrophobicity Using a Same-Centered Polymer Approach. *Biomacromolecules* **2013,** *14* (12), 4331-4339.

31.   Punia, A.; He, E.; Lee, K.; Banerjee, P.; Yang, N.-L., Cationic amphiphilic non-hemolytic polyacrylates with superior antibacterial activity. *Chem. Commun.* **2014,** *50* (53), 7071-7074.

32.   Lienkamp, K.; Madkour, A. E.; Kumar, K.-N.; Nüsslein, K.; Tew, G. N., Antimicrobial Polymers Prepared by Ring-Opening Metathesis Polymerization: Manipulating Antimicrobial Properties by Organic Counterion and Charge Density Variation. *Chem. Eur. J.* **2009,** *15* (43), 11715-11722.

33.   Sambhy, V.; Peterson, B. R.; Sen, A., Antibacterial and Hemolytic Activities of Pyridinium Polymers as a Function of the Spatial Relationship between the Positive Charge and the Pendant Alkyl Tail. *Angew. Chem. Int. Ed.* **2008,** *47* (7), 1250-1254.

34.   Song, A.; Walker, S. G.; Parker, K. A.; Sampson, N. S., Antibacterial Studies of Cationic Polymers with Alternating, Random and Uniform Backbones. *ACS chemical biology* **2011,** *6* (6), 590-599.

35.   Gabriel, G. J.; Maegerlein, J. A.; Nelson, C. F.; Dabkowski, J. M.; Eren, T.; Nüsslein, K.; Tew, G. N., Comparison of Facially Amphiphilic versus Segregated Monomers in the Design of Antibacterial Copolymers. *Chem. Eur. J.* **2009,** *15* (2), 433-439.

36.   Tew, G. N.; Scott, R. W.; Klein, M. L.; DeGrado, W. F., De Novo Design of Antimicrobial Polymers, Foldamers, and Small Molecules: From Discovery to Practical Applications. *Accounts of Chemical Research* **2010,** *43* (1), 30-39.

37.   Liu, D.; Choi, S.; Chen, B.; Doerksen, R. J.; Clements, D. J.; Winkler, J. D.; Klein, M. L.; DeGrado, W. F., Nontoxic Membrane-Active Antimicrobial Arylamide Oligomers. *Angew. Chem. Int. Ed.* **2004,** *43* (9), 1158-1162.

38.   Ilker, M. F.; Nüsslein, K.; Tew, G. N.; Coughlin, E. B., Tuning the Hemolytic and Antibacterial Activities of Amphiphilic Polynorbornene Derivatives. *J. Am. Chem. Soc.* **2004,** *126* (48), 15870-15875.

39.   Lienkamp, K.; Madkour, A.; Tew, G., Polymer composites - polyolefin fractionation - polymeric peptidomimetics - collagens. Springer Berlin Heidelberg, 2013; Vol. 251, pp 141-172.

40.   Chen, L.; Liang, J. F., Peptide fibrils with altered stability, activity, and cell selectivity. *Biomacromolecules* **2013,** *14* (7), 2326-2331.

41.   Tian, X.; Sun, F.; Zhou, X.-R.; Luo, S.-Z.; Chen, L., Role of peptide self-assembly in antimicrobial peptides. *Journal of Peptide Science* **2015,** *21* (7), 530-539.

42.   Baul, U.; Kuroda, K.; Vemparala, S., Interaction of multiple biomimetic antimicrobial polymers with model bacterial membranes. *The Journal of Chemical Physics* **2014,** *141* (8), 084902.

43.   Mondal, J.; Zhu, X.; Cui, Q.; Yethiraj, A., Sequence-Dependent Interaction of β-Peptides with Membranes. *The Journal of Physical Chemistry B* **2010,** *114* (42), 13585-13592.

44.   Sauvet, G.; Fortuniak, W.; Kazmierski, K.; Chojnowski, J., Amphiphilic block and statistical siloxane copolymers with antimicrobial activity. *Journal of Polymer Science Part A: Polymer Chemistry* **2003,** *41* (19), 2939-2948.

45.   Wang, Y.; Xu, J.; Zhang, Y.; Yan, H.; Liu, K., Antimicrobial and Hemolytic Activities of Copolymers with Cationic and Hydrophobic Groups: A Comparison of Block and Random Copolymers. *Macromolecular Bioscience* **2011,** *11* (11), 1499-1504.

46.   Liu, R.; Chen, X.; Chakraborty, S.; Lemke, J. J.; Hayouka, Z.; Chow, C.; Welch, R. A.; Weisblum, B.; Masters, K. S.; Gellman, S. H., Tuning the Biological Activity Profile of Antibacterial Polymers via Subunit Substitution Pattern. *J. Am. Chem. Soc.* **2014,** *136* (11), 4410-4418.

47.   Oda, Y.; Kanaoka, S.; Sato, T.; Aoshima, S.; Kuroda, K., Block versus Random Amphiphilic Copolymers as Antibacterial Agents. *Biomacromolecules* **2011,** *12* (10), 3581-3591.

48.   Taresco, V.; Gontrani, L.; Crisante, F.; Francolini, I.; Martinelli, A.; D'Ilario, L.; Bordi, F.; Piozzi, A., Self-Assembly of Catecholic Moiety-Containing Cationic Random Acrylic Copolymers. *The Journal of Physical Chemistry B* **2015,** *119* (26), 8369-8379.

49.   Nederberg, F.; Zhang, Y.; Tan, J. P. K.; Xu, K.; Wang, H.; Yang, C.; Gao, S.; Guo, X. D.; Fukushima, K.; Li, L.; Hedrick, J. L.; Yang, Y.-Y., Biodegradable nanostructures with selective lysis of microbial membranes. *Nat Chem* **2011,** *3* (5), 409-414.

50.   Judzewitsch, P. R.; Nguyen, T.-K.; Shanmugam, S.; Wong, E. H. H.; Boyer, C., Towards Sequence-Controlled Antimicrobial Polymers: Effect of Polymer Block Order on Antimicrobial Activity. *Angew. Chem. Int. Ed.* **2018,** *57* (17), 4559-4564.

51.   Costanza, F.; Padhee, S.; Wu, H.; Wang, Y.; Revenis, J.; Cao, C.; Li, Q.; Cai, J., Investigation of antimicrobial PEG-poly(amino acid)s. *RSC Advances* **2014,** *4* (4), 2089-2095.

52.   Yao, D.; Guo, Y.; Chen, S.; Tang, J.; Chen, Y., Shaped core/shell polymer nanoobjects with high antibacterial activities via block copolymer microphase separation. *Polymer* **2013,** *54* (14), 3485-3491.

53.   Gody, G.; Maschmeyer, T.; Zetterlund, P. B.; Perrier, S., Exploitation of the Degenerative Transfer Mechanism in RAFT Polymerization for Synthesis of Polymer of High Livingness at Full Monomer Conversion. *Macromolecules* **2014,** *47* (2), 639-649.

54.   Zamfir, M.; Lutz, J.-F., Ultra-precise insertion of functional monomers in chain-growth polymerizations. *Nature Communications* **2012,** *3*, 1138.

55.   Moriceau, G.; Gody, G.; Hartlieb, M.; Winn, J.; Kim, H.; Mastrangelo, A.; Smith, T.; Perrier, S., Functional multisite copolymer by one-pot sequential RAFT copolymerization of styrene and maleic anhydride. *Polym. Chem.* **2017,** *8* (28), 4152-4161.

56.   Stenzel, M. H.; Barner-Kowollik, C., The living dead – common misconceptions about reversible deactivation radical polymerization. *Materials Horizons* **2016,** *3* (6), 471-477.

57.   Nicolas, J.; Guillaneuf, Y.; Lefay, C.; Bertin, D.; Gigmes, D.; Charleux, B., Nitroxide-mediated polymerization. *Progress in Polymer Science* **2013,** *38* (1), 63-235.

58.   Hawker, C. J.; Bosman, A. W.; Harth, E., New Polymer Synthesis by Nitroxide Mediated Living Radical Polymerizations. *Chemical Reviews* **2001,** *101* (12), 3661-3688.

59.   Moad, G.; Rizzardo, E., Alkoxyamine-Initiated Living Radical Polymerization: Factors Affecting Alkoxyamine Homolysis Rates. *Macromolecules* **1995,** *28* (26), 8722-8728.

60.   Matyjaszewski, K., Atom Transfer Radical Polymerization (ATRP): Current Status and Future Perspectives. *Macromolecules* **2012,** *45* (10), 4015-4039.

61.   Percec, V.; Guliashvili, T.; Ladislaw, J. S.; Wistrand, A.; Stjerndahl, A.; Sienkowska, M. J.; Monteiro, M. J.; Sahoo, S., Ultrafast Synthesis of Ultrahigh Molar Mass Polymers by Metal-Catalyzed Living Radical Polymerization of Acrylates, Methacrylates, and Vinyl Chloride Mediated by SET at 25 °C. *J. Am. Chem. Soc.* **2006,** *128* (43), 14156-14165.

62.   Ayres, N., Atom Transfer Radical Polymerization: A Robust and Versatile Route for Polymer Synthesis. *Polymer Reviews* **2011,** *51* (2), 138-162.

63.   Perrier, S., 50th Anniversary Perspective: RAFT Polymerization—A User Guide. *Macromolecules* **2017,** *50* (19), 7433-7447.

64.   Moad, G.; Rizzardo, E.; Thang, S. H., Living Radical Polymerization by the RAFT Process – A Third Update. *Australian Journal of Chemistry* **2012,** *65* (8), 985-1076.

65.   Shipp, D. A., Reversible-Deactivation Radical Polymerizations. *Polymer Reviews* **2011,** *51* (2), 99-103.

66.   Chiefari, J.; Chong, Y. K.; Ercole, F.; Krstina, J.; Jeffery, J.; Le, T. P. T.; Mayadunne, R. T. A.; Meijs, G. F.; Moad, C. L.; Moad, G.; Rizzardo, E.; Thang, S. H., Living Free-Radical Polymerization by Reversible Addition−Fragmentation Chain Transfer: The RAFT Process. *Macromolecules* **1998,** *31* (16), 5559-5562.

67.   Perrier, S.; Takolpuckdee, P., Macromolecular design via reversible addition–fragmentation chain transfer (RAFT)/xanthates (MADIX) polymerization. *Journal of Polymer Science Part A: Polymer Chemistry* **2005,** *43* (22), 5347-5393.

68.   Chong, Y. K.; Krstina, J.; Le, T. P. T.; Moad, G.; Postma, A.; Rizzardo, E.; Thang, S. H., Thiocarbonylthio Compounds [SC(Ph)S−R] in Free Radical Polymerization with Reversible Addition-Fragmentation Chain Transfer (RAFT Polymerization). Role of the Free-Radical Leaving Group (R). *Macromolecules* **2003,** *36* (7), 2256-2272.

69.   Chiefari, J.; Mayadunne, R. T. A.; Moad, C. L.; Moad, G.; Rizzardo, E.; Postma, A.; Thang, S. H., Thiocarbonylthio Compounds (SC(Z)S−R) in Free Radical Polymerization with Reversible Addition-Fragmentation Chain Transfer (RAFT Polymerization). Effect of the Activating Group Z. *Macromolecules* **2003,** *36* (7), 2273-2283.

70.   Keddie, D. J., A guide to the synthesis of block copolymers using reversible-addition fragmentation chain transfer (RAFT) polymerization. *Chemical Society Reviews* **2014,** *43* (2), 496-505.

71.   Barner, L.; Davis, T. P.; Stenzel, M. H.; Barner-Kowollik, C., Complex Macromolecular Architectures by Reversible Addition Fragmentation Chain Transfer Chemistry: Theory and Practice. *Macromolecular Rapid Communications* **2007,** *28* (5), 539-559.

72.   Moad, G.; Rizzardo, E.; Thang, S. H., Toward Living Radical Polymerization. *Accounts of Chemical Research* **2008,** *41* (9), 1133-1142.

73.   Chaduc, I.; Zhang, W.; Rieger, J.; Lansalot, M.; D'Agosto, F.; Charleux, B., Amphiphilic Block Copolymers from a Direct and One-pot RAFT Synthesis in Water. *Macromolecular Rapid Communications* **2011,** *32* (16), 1270-1276.

74.   Jennings, J.; Beija, M.; Richez, A. P.; Cooper, S. D.; Mignot, P. E.; Thurecht, K. J.; Jack, K. S.; Howdle, S. M., One-Pot Synthesis of Block Copolymers in Supercritical Carbon Dioxide: A Simple Versatile Route to Nanostructured Microparticles. *J. Am. Chem. Soc.* **2012,** *134* (10), 4772-4781.

75.   Chong, Y. K.; Le, T. P. T.; Moad, G.; Rizzardo, E.; Thang, S. H., A More Versatile Route to Block Copolymers and Other Polymers of Complex Architecture by Living Radical Polymerization: The RAFT Process. *Macromolecules* **1999,** *32* (6), 2071-2074.

76.   Gody, G.; Maschmeyer, T.; Zetterlund, P. B.; Perrier, S., Pushing the Limit of the RAFT Process: Multiblock Copolymers by One-Pot Rapid Multiple Chain Extensions at Full Monomer Conversion. *Macromolecules* **2014,** *47* (10), 3451-3460.

77.   Vandenbergh, J.; de Moraes Ogawa, T.; Junkers, T., Precision synthesis of acrylate multiblock copolymers from consecutive microreactor RAFT polymerizations. *Journal of Polymer Science Part A: Polymer Chemistry* **2013,** *51* (11), 2366-2374.

78.   Hadjiantoniou, N. A.; Krasia-Christoforou, T.; Loizou, E.; Porcar, L.; Patrickios, C. S., Alternating Amphiphilic Multiblock Copolymers: Controlled Synthesis via RAFT Polymerization and Aqueous Solution Characterization. *Macromolecules* **2010,** *43* (6), 2713-2720.

79.   Gody, G.; Maschmeyer, T.; Zetterlund, P. B.; Perrier, S., Rapid and quantitative one-pot synthesis of sequence-controlled polymers by radical polymerization. *Nat Commun* **2013,** *4*.

80.   Martin, L.; Gody, G.; Perrier, S., Preparation of complex multiblock copolymers via aqueous RAFT polymerization at room temperature. *Polym. Chem.* **2015,** *6* (27), 4875-4886.

81.   Engelis, N. G.; Anastasaki, A.; Nurumbetov, G.; Truong, N. P.; Nikolaou, V.; Shegiwal, A.; Whittaker, M. R.; Davis, T. P.; Haddleton, D. M., Sequence-controlled methacrylic multiblock copolymers via sulfur-free RAFT emulsion polymerization. *Nat Chem* **2017,** *9* (2), 171-178.

82.   Engelis, N. G.; Anastasaki, A.; Whitfield, R.; Jones, G. R.; Liarou, E.; Nikolaou, V.; Nurumbetov, G.; Haddleton, D. M., Sequence-Controlled Methacrylic Multiblock Copolymers: Expanding the Scope of Sulfur-Free RAFT. *Macromolecules* **2018,** *51* (2), 336-342.

83.   Becer, C. R.; Groth, A. M.; Hoogenboom, R.; Paulus, R. M.; Schubert, U. S., Protocol for Automated Kinetic Investigation/Optimization of the RAFT Polymerization of Various Monomers. *QSAR & Combinatorial Science* **2008,** *27* (8), 977-983.

84.   Hornung, C. H.; Nguyen, X.; Kyi, S.; Chiefari, J.; Saubern, S., Synthesis of RAFT Block Copolymers in a Multi-Stage Continuous Flow Process Inside a Tubular Reactor. *Australian Journal of Chemistry* **2013,** *66* (2), 192-198.

Chapter 2 Sequence control as a powerful tool for improving the selectivity of antimicrobial polymers
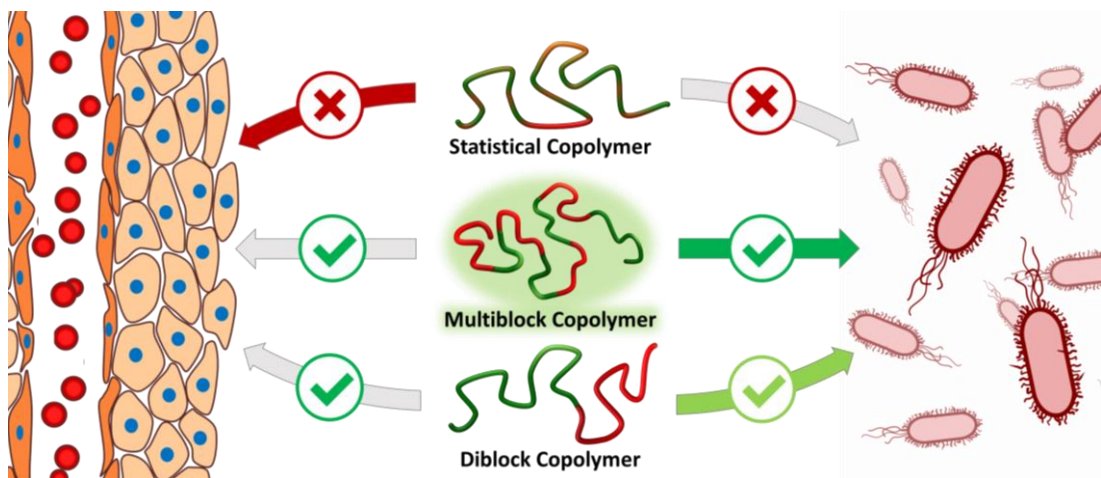
Abstract

In order to tackle the current development of bacterial resistance against conventional antibiotics, antimicrobial polymers represent a promising alternative since their mechanism of action relies on bacterial membrane disruption. This study investigates the effect of segregation of hydrophobic and cationic functionalities within antimicrobial polymers on their selectivity between bacteria and mammalian cells. Using RAFT polymerisation, statistical, highly segmented multiblock and diblock copolymers were synthesised in a controlled manner. Polymers were analysed by HPLC and the monomer sequence was found to have a significant influence on their overall hydrophobicity. In addition, the molar ratio of cationic co-monomer was varied to yield a small library of bioactive macromolecules. The antimicrobial properties of these compounds were probed against pathogenic bacteria (*Escherichia coli*, *Pseudomonas aeruginosa*, *Staphylococcus aureus* and *Staphylococcus epidermidis*) and their biocompatibility was assessed with haemolysis and erythrocyte aggregation assays, as well as mammalian cell viability assays. In all cases, the diblock and multiblock copolymers were found to outperform statistical copolymers, and for polymers with a low content of cationic co-monomer (30 %), the multiblock copolymer showed tremendously increased selectivity for *P. aeruginosa* and *S. epidermidis* compared to its statistical and diblock copolymer analogues. This work highlights the remarkable effect of monomer distribution on both the physical properties of the materials and their interaction with biological systems. Due to the selectivity of multiblock copolymers towards certain bacterial strains, the presented materials are a promising platform for the treatment of infections and a valuable tool to combat antimicrobial resistance.

2.1   Introduction

As an increasing number of studies emphasise the alarming situation concerning life-threatening infectious diseases caused by antibiotic resistant bacteria,[1-3] health organizations urge the discovery of novel antibiotics.[4-6] The development of antimicrobial resistance (AMR) is partly due to the narrow range of available antibiotics which have reached their limitations in infection treatment because of their high target specificity.[7] In such context, antimicrobial peptides (AMPs) have recently attracted interest as they were shown to target bacterial membranes instead of specific ligands.[8-9] These peptides have an amphipathic structure which can adopt a facially amphiphilic arrangement with hydrophobic groups on one side and cationic moieties on the other side of the molecule.[8] Although the precise mechanism of their toxicity towards bacterial is still under investigation, the cationic groups of the AMPs are thought to bind to the negatively charged phospholipids present on bacterial membranes *via* electrostatic interactions, upon which the hydrophobic functionalities induce membrane disruption, hence inducing cell death.[8] Due to the less anionic surface of mammalian cells, AMPs preferentially interact with bacterial membranes. Despite their selectivity, AMPs can be relatively toxic towards mammalian cells.[10-11] Furthermore, their isolation or production on a large scale is expensive and they showed limited pharmacokinetic stability.[12] In order to overcome these issues, a wide range of synthetic mimics have been developed in recent years from oligomers to polymers using different methodologies.[13] The key structural parameters which were found to affect the antimicrobial activity of polymers were the balance of cationic to hydrophobic moieties, the nature of the charge, as well as the molar mass of the polymer.[14-25] Current research focuses on reducing the toxicity of synthetic mimics of antimicrobial peptides (SMAMPs) against mammalian cells, and more interestingly towards red blood cells (RBCs), by investigating new structural parameters.[26-28]

The activity of some AMPs is highly dependent on their structural organisation, and mimicking their quaternary structure using polymers by self-assembly into nano-sized objects, is a substantial challenge which could potentially improve the performance of SMAMPs.[8, 29-30] As mentioned in the previous chapter, Yao *et al.* studied the influence of the morphology of cationic nano-objects on antimicrobial activity, using self-assembled diblock copolymer comprised of polyDMAEMA and a hydrophobic methacrylate-derived block bearing triethoxysilyl pendant groups.[28] Interestingly, spherical, cylindrical and sheet-like assemblies had similar potency towards bacteria after cross-linking. A different study using PEGylated cationic nanoparticles based on a diblock copolymer of PEG and a cationic polypeptide looked into the influence of the length of the PEG block. A clear reduction in both antimicrobial and

haemolytic activity of the nanoparticles was observed with a long PEG block (5000 g.mol^{-1}).[31-32] However, the effect of the morphology of cationic nanoparticles on the toxicity against mammalian cells was not addressed in those studies.

Intramolecular interactions of SMAMPs have been studied to a greater extent, since the helical structure of certain AMPs was thought to be responsible for their activity. However, it was demonstrated that this structural feature was not required for SMAMPs to exhibit antimicrobial activity. A flexible polymeric backbone was sufficient for the polymers to adopt a facially amphiphilic conformation which can induce bacterial membrane disruption, according to Mowery and co-workers.[21] The influence of polymer conformation on the potency of SMAMPs was highlighted with the study of single-chain nanoparticles (SCNPs). Nguyen *et al.* reported a high antimicrobial activity of SCNPs obtained from statistical copolymers of PEGacrylates with a primary amine functionalised acrylamide and an acrylate bearing a hydrophobic group (the hydrophobicity of the acrylate was screened to optimise the antimicrobial activity of the SCNPs).[33] Similarly, unimolecular aggregates with a cationic shell and a hydrophobic core obtained from the folding of a diblock copolymer were studied by Oda and co-workers.[34] The diblock copolymer exhibited reduced haemolytic activity compared to the statistical copolymer, which did not aggregate in solution, but increased haemagglutination. These results demonstrate the effect of the conformation of single polymeric chains on the interactions with bacterial and mammalian cells.

The effect of monomer sequence on the biological properties of SMAMPs was investigated using poly(DMAEMA-*co*-BMA) by comparing a diblock copolymer with its statistical counterpart.[35] The antimicrobial activity was similar for both structures, but the haemolytic activity was decreased for the diblock copolymer. Similar observations were reported using gradient and diblock cationic nylon-3 copolymers: haemolytic activity was decreased with the diblock copolymer whilst the antimicrobial properties were unchanged.[36] As the micellisation of these systems were not analysed, the difference in haemolytic activity could either be attributed to the formation of self-assemblies or to the segregation of the cationic and hydrophobic functionalities of SMAMPs. Monomer sequence not only affects the intermolecular interactions of SMAMPs *i.e.* self-assembly, but also their intramolecular interactions resulting in self-folding.[37-38] As previously discussed, inter- and intramolecular assemblies of cationic polymers seem to have an important effect on their antimicrobial activity and haemocompatibility, but beyond diblock and gradient copolymers, SMAMPs with controlled monomer sequences have yet to be investigated.

In this context, multiblock copolymers can provide an intermediate degree of functional segregation somewhere in between diblock and statistical copolymers.[39] Indeed, by varying the number of discreet functional blocks while (maintaining an overall composition), and thereby the length of cationic and hydrophobic domains within the polymer chain, a structure-activity relationship in terms of their antimicrobial activity/selectivity could potentially be established. The synthesis of well-defined multiblock copolymers has been reported *via* living radical polymerisation (LRP)[40-41] techniques, namely Cu(0)-mediated radical polymerisation[42-43] and reversible addition-fragmentation chain transfer (RAFT)[44-45] polymerisation. The latter was shown to be a versatile and robust technique, compatible with a wide range of monomers and solvent systems to obtain polymers with narrow molar mass distributions.[40-41] Furthermore, careful optimisation of the reaction conditions allows for the preparation of multiblock copolymers using a one-pot sequential polymerisation approach.[46] Although the process is indeed more complicated than that required to synthesise diblock or statistical copolymers, multiblock copolymers are still more suitable for scale-up than AMPs, as recently demonstrated *via* RAFT polymerisation in emulsion or in tubular reactors.[47-49]

This chapter describes the design and synthesis of poly(aminoethyl acrylamide)-*co*-poly(*N*-isopropylacrylamide) copolymers containing different molar ratios of primary amine functionality (30, 50 and 70 %) and monomer distributions (statistical, multiblock and diblock copolymers) *via* RAFT polymerisation. The influence of AEAM content and monomer sequence on the biological activity was assessed, through consideration of the different physico-chemical properties of the cationic polymers. The antimicrobial activity of the polymers against Gram-negative and Gram-positive bacterial strains were evaluated, followed by the study of their compatibility towards mammalian cells (erythrocytes, fibroblasts and colorectal epithelial cells). The selectivity of the ammonium SMAMPs could then be established, following which an ideal charge content and monomer distribution can be selected within the library with which to direct further studies.

2.2   Results and discussion

2.2.1   Design and synthesis of SMAMPs

In order to study the effect of monomer distribution on the biological properties of SMAMPs, a library of ammonium polymers were synthesised *via* RAFT polymerisation. Acrylamides were chosen as a monomer family for this study due to their high rate constant of propagation (k_p) and their limited susceptibility to degradation, allowing the synthesis of multiblock copolymers in a straightforward manner.[45, 50] The hydrophobic monomer which was selected for the synthesis of SMAMPs was *N*-isopropylacrylamide (NIPAM) as it bears the same pendant functionality as leucine. Furthermore, its hydrophobicity is relatively low compared to monomers which have been used in previous studies, and therefore should lead to polymers with a high biocompatibility and reduce the chances of inducing self-assembly in aqueous solution, hence the fundamental influence of monomer distribution may be assessed.[51-53] The cationic monomer chosen for the design of antimicrobial polymers was an acrylamide-based lysine mimic: amino-ethylacrylamide (AEAM). Although AEAM could be polymerised in a buffer to avoid aminolysis of the trithiocarbonate group of the CTA during the polymerisation process, the solution polymerisation of NIPAM in aqueous conditions would be challenging as it is a thermo-responsive monomer.[54-55] In order to conduct the polymerisation in an organic solvent, the Boc-protected equivalent of AEAM (Boc-AEAM) was polymerised, which also facilitated the characterisation of the polymers (Figures 2.14-2.17).

As mentioned previously, the balance between cationic and hydrophobic character is a key parameter for the optimisation of the properties of SMAMPs, a range of AEAM content was screened (0, 30, 50, 70 and 100 mol %). In order to study the influence of monomer sequence on antimicrobial activity and toxicity against mammalian cells, monomer distribution was varied from statistical, multiblock and diblock copolymers for the copolymers with 30, 50 and 70 % of AEAM (Scheme 2.1). The SMAMPs were labelled according to their type of charge (A for ammonium), degree of segregation (H, S, M and D for homopolymer, statistical, multiblock and diblock copolymers, respectively) and their content of cationic co-monomer in molar % (0, 30, 50, 70 and 100) with protected polymers labelled Boc.
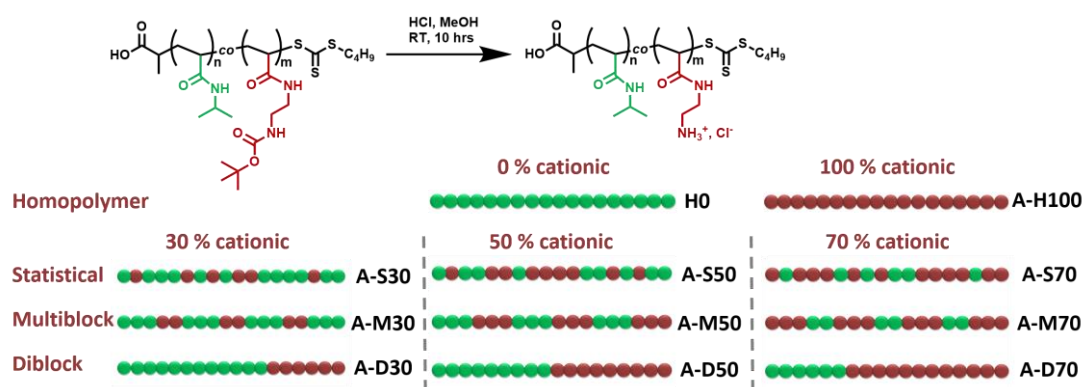
Scheme 2.1 - Schematic representation of structure, composition and monomer sequence of synthesised polymers.

As a loss in antimicrobial activity was shown with polymers of over 50000 g.mol⁻¹, the targeted molar mass of the SMAMPs had to be chosen carefully.[56] In this study, copolymers with a final molar mass of around 10000 g.mol⁻¹ was targeted, setting the degree of polymerisation (DP) to 100, as the maximum number of blocks increases with the length of the polymer chain. Since monomer to initiator ratio is related to conversion, and that CTA to initiator ratio affects livingness, it follows that higher livingness is obtained when a lower DP is targeted, meaning more chain extensions may be successfully performed. The shortest block length that was targeted was a DP of 10, since it has been shown that, for a polyNAM multiblock copolymer, a significant number of living chains would fail to contain the total number of blocks, by targeting DPs below 6, considering the molar mass distribution of well-defined polymers.[57] By taking this limitation into consideration, multiblock copolymers were designed with the highest number of blocks compatible for each composition. Therefore, seven blocks were targeted for polymers with 30 and 70 % BocAEAM content, (A-M30^Boc and A-M70^Boc, respectively) and ten blocks for A-M50^Boc which contained 50 % of BocAEAM, each in an alternating fashion (Table 2.1). From the design of these polymers, modifying the structure from statistical to multiblock and diblock copolymer should demonstrate the effect of the segregation of cationic and hydrophobic functionalities, whilst maintaining the overall polymer length and chemical composition.

Table 2.1 - Library of synthesised Boc-protected polymers.

BocAEAM content (%)	30	50	70
Statistical copolymers	NIPAM$_{70}$-s- BocAEAM$_{30}$	NIPAM$_{50}$-s- BocAEAM$_{50}$	NIPAM$_{30}$-s- BocAEAM$_{70}$
Diblock copolymers	NIPAM$_{70}$-b- BocAEAM$_{30}$	NIPAM$_{50}$-b- BocAEAM$_{50}$	NIPAM$_{30}$-b- BocAEAM$_{70}$
Multiblock copolymers	NIPAM$_{18}$-b- BocAEAM$_{10}$-b- NIPAM$_{18}$-b- BocAEAM$_{10}$-b- NIPAM$_{18}$-b- BocAEAM$_{10}$-b- NIPAM$_{18}$	NIPAM$_{10}$-b- BocAEAM$_{10}$-b- NIPAM$_{10}$-b-BocAEAM$_{10}$-b- NIPAM$_{10}$-b-BocAEAM$_{10}$-b- NIPAM$_{10}$-b- BocAEAM$_{10}$-b- NIPAM$_{10}$-b- BocAEAM$_{10}$	BocAEAM$_{18}$-b-NIPAM$_{10}$-b- BocAEAM$_{18}$-b-NIPAM$_{10}$-b- BocAEAM$_{18}$-b-NIPAM$_{10}$-b- BocAEAM$_{18}$

(Propanoic acid)yl butyl trithiocarbonate (PABTC) was chosen as the chain transfer agent (CTA) since it permits the control of the polymerisation of acrylamides and its alkyl chain is relatively short compared to the overall length of the polymer chain, hence allows to better study the influence of monomer sequence (Figures 2.18 and 2.19).[46] Additionally, a carboxylic acid end-group on SMAMPs has been shown previously to exhibit lower haemotoxicity.[58] The solvent system which was chosen for the polymerisations was a mixture of 1,4-dioxane and water (8/2). Dioxane solubilised the monomers as well as the polymers, while the presence of water permitted the use of VA-044, a water-soluble initiator with a high decomposition rate coefficient (k_d) and a 10 hour half-life of 44 °C (in water), and has been shown to increase the k_p of acrylamide monomers (Tables 2.8-2.12).[59] Optimisation of monomer and initiator concentrations enabled quantitative monomer conversion to be achieved after each block extension, confirmed by ^{1}H NMR spectroscopy (Figures 2.20-2.25), to obtain the desired (protected) statistical, multiblock and diblock copolymers in a one-pot sequential polymerisation process. SEC traces exhibited a clear shift to higher molar mass with each block extension, and molar mass distribution remained relatively narrow throughout (Đ ≤ 1.38) for all copolymers (Table 2.2, 2.13-2.16, Figures 2.1A, 2.26-2.28). However, populations at both low and high molar mass was observed on the SEC chromatograms of multiblock copolymers, particularly after the 4th chain extension (Figures 2.1A and 2.28). The tail at low molar mass indicate the presence of initiator derived chains, whereas the shoulder at high molar mass can be attributed to the accumulation of dead polymer chains (which have terminated by combination). These defects can be related to the decrease in the livingness of

the polymer chains after each chain extension, due to the addition of initiator. Furthermore, the discrepancy between the experimental molar mass values and the theoretical values can be attributed to differences in hydrodynamic volume between the polymers and the PMMA standards used to calibrate the SEC system.

A kinetic study of the statistical copolymer A-S30[Boc] was undertaken using ^{1}H NMR and high performance liquid chromatography (HPLC) to determine the rate of incorporation for each monomer in the polymer, as the vinyl peaks of NIPAM and BocAEAM overlap in ^{1}H NMR spectra. The ratio of the concentrations of unconsumed NIPAM to BocAEAM against the overall monomer conversion did not follow a pyramidal or inverse-pyramidal trend, hence the monomers should be evenly distributed in the statistical copolymers (Figure 2.29).

Table 2.2 - Characterisation data of Boc-protected polymers.

	Sample	BocAEAM content (%)	$M_{n,th}$ [a] (g mol^{-1})	$M_{n,SEC}$ [b] (g mol^{-1})	$Đ$ [b]
Homopolymer	H0	0	12000	14400	1.10
	A-H100[Boc]	100	21200	21000	1.11
Statistical	A-S30[Boc]	32	15400	17900	1.09
	A-S50[Boc]	50	17400	18800	1.09
	A-S70[Boc]	70	19600	21600	1.12
Multiblock	A-M30[Boc]	30	13800	15800	1.29
	A-M50[Boc]	50	16600	17100	1.38
	A-M70[Boc]	70	19400	17400	1.34
Diblock	A-D30[Boc]	30	15000	16200	1.10
	A-D50[Boc]	49	14900	17500	1.17
	A-D70[Boc]	71	18500	19000	1.20

[a] Theoretical molar mass of the protected polymers calculated from equation 2.5.

[b] Determined for the protected polymers by SEC/RI in DMF using PMMA as molecular weight standards.

The polymers were then quantitatively deprotected using hydrochloric acid, which was confirmed by the disappearance of the signal (1.3 ppm) associated with the Boc-protecting groups in ^{1}H NMR spectra as well as by the shift of the CH_2 (from 3.3 to 3.1 ppm) adjacent to the amine pendant groups (Figures 2.1B, 2.30 and 2.31).[60]
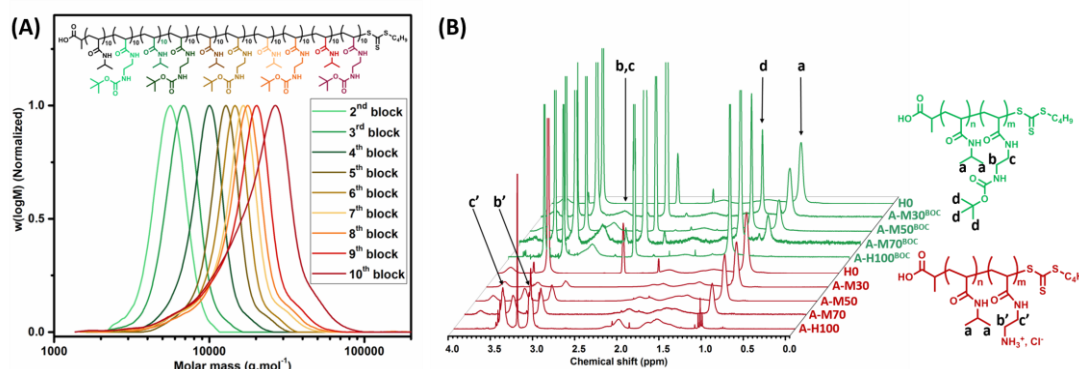
Figure 2.1 - DMF-SEC chromatograms for successive chain extensions of A-M50^{Boc} (A) and ^{1}H NMR spectra of SMAMPs on the example of homopolymers and multiblock copolymers before and after deprotection in DMSO-d_6 and D$_2$O, respectively (B).

2.2.2 Physico-chemical properties of SMAMPs

As electrostatic interactions play a major role in the binding of SMAMPs to bacterial membranes, the polymers should possess net positive charge in a physiological environment. The protonation of the primary amines was investigated using potentiometric titration. By comparing the behaviour of statistical, multiblock and diblock copolymers of similar AEAM content (A-S50, AM-50 and A-D50), the effect of segregation of functionalities on the pK_a of the primary amine pendant groups can be evaluated. The pK_a of the primary amines of the cationic homopolymer A-H100 (Figure 2.2) was of 8.1, which was significantly reduced compared to the pK_a of the amine from the lysine side chain at 8.9.[61] Indeed, the deprotonation of the primary amines of A-H100 is favoured by the suppression of electrostatic repulsion between amine functionalities in close proximity.[62] The three copolymers had similar pK_a values compared to A-H100: 7.9 for both A-S50 and A-M50, 7.8 for A-D50. As the majority of the primary amines are protonated at physiological pH, the library of ammonium copolymers would be positively charged during biological assays. However, the titration curves of A-D50 and A-M50 were steeper than that of A-S50 (Figure 2.2). Therefore, A-S50 would have a higher buffering capacity than its diblock and multiblock copolymer counterparts. Indeed, a study using poly(ethyleneimine)s suggested that once the pKa of the secondary amine was reached, the polymer chain would avoid having neighbouring positive

charges by protonating every second site, until the pH was decreased even further.[63] In the case of polyAEAM-*co*-NIPAM, the deprotonation of amine functionalities which are in close proximity to one another would be promoted by electrostatic repulsion. Therefore, it is postulated that deprotonation is favoured in the diblock and multiblock copolymers (A-M50 and A-D50), for which primary amines are comprised in segments, compared to the statistical copolymer, explaining the results obtained from potentiometric titration.
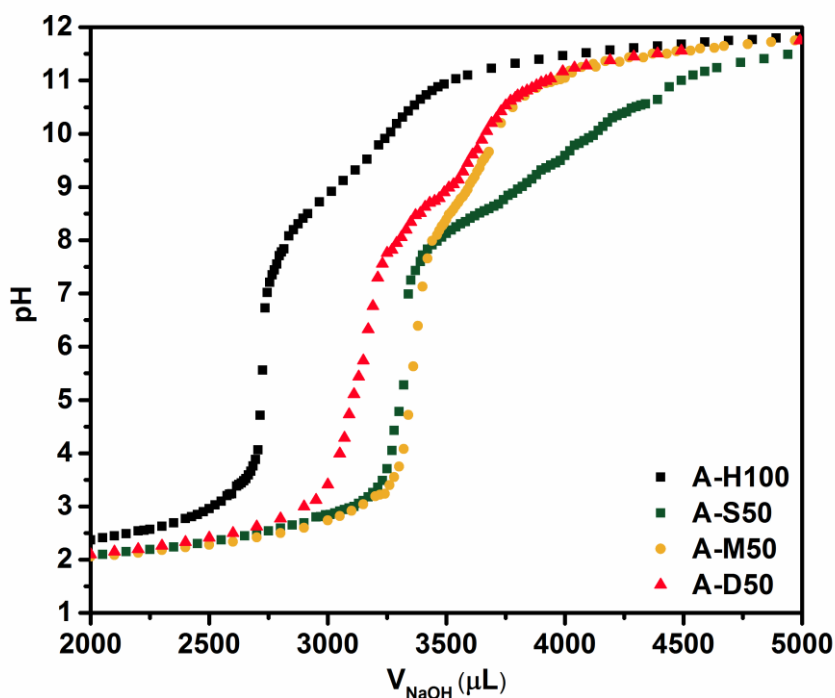
Figure 2.2 - Titration curves of acidified solutions of the cationic polymers A-H100, A-S50, A-D50 and A-M50 (concentration of around 0.5 mg.mL^{-1}) neutralised with sodium hydroxide (0.2 M).

While positively charged groups are necessary for the antimicrobial activity of SMAMPs, the balance between positive charge and hydrophobicity has a significant impact on their selectivity.[13-14] For this reason, the effect of monomer distribution on the overall hydrophobicity of SMAMPs was assessed using reverse-phase HPLC (RP-HPLC). Non water-soluble diblock and statistical copolymers have previously been studied by RP-HPLC, showing that for a similar chemical composition, the elution time varied between the two structures.[64] By monitoring the elution profiles of the ammonium polymer library the hydrophobicity of the polymers can be assessed, with longer elution time indicating a more hydrophobic polymer in a reverse-phase system (Figures 2.3 and 2.4).
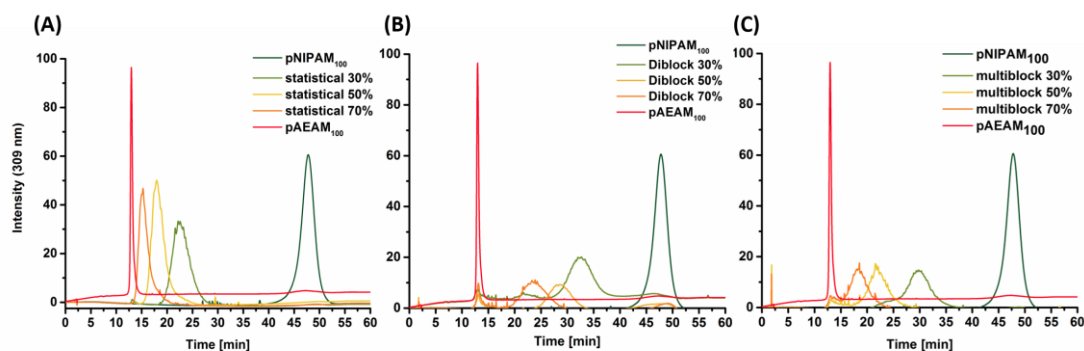
Figure 2.3 - Reverse-phase HPLC chromatograms of ammonium polymer library organised by monomer distribution: statistical (A), diblock (B) and multiblock (C) copolymers. The runs were performed with a gradient of 1 to 95 % ACN over 50 minutes at 37 °C.

For each copolymer architecture (statistical, multiblock or diblock), the elution time decreased with increasing AEAM content (Figure 2.3). This is to be expected since the hydrophilicity of the polymers would increase substantially when the molar content of AEAM is increased. Measurements were also conducted at 20 and 60 °C to assess if it would modify the elution profile of polyNIPAM, which is known to have a low LCST in water. No significant difference was observed in the elution profile of the homopolymer, which could be explained by the presence of ACN in the eluent mixture or to the concentration of the sample in the column (Figure 2.32).[65]
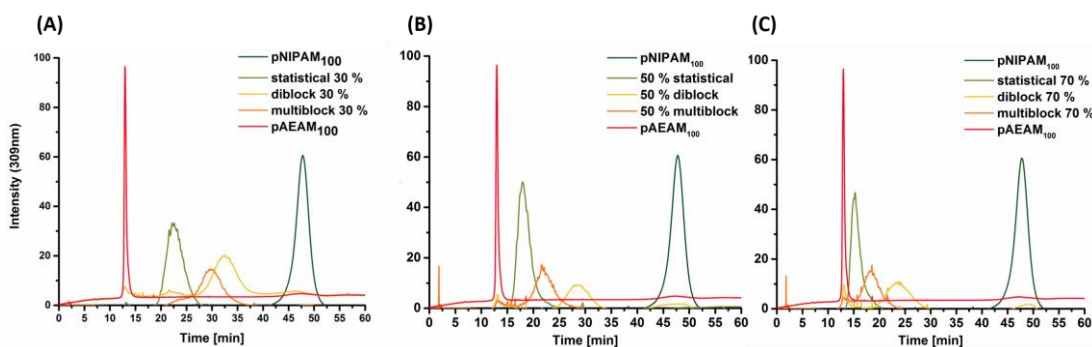
Figure 2.4 - Reverse-phase HPLC chromatograms of ammonium polymer library organised by molar content of AEAM: 30 % (A), 50 % (B) and 70 % (C) charge content. The runs were performed with a gradient of 1 to 95 % ACN over 50 minutes at 37 °C.

Additionally, for similar AEAM content, the elution profile varied with monomer distribution, indicating the diblock copolymers were the most hydrophobic, followed by multiblock copolymers and finally, the statistical counterparts (Figure 2.4). Interestingly, this

trend was observed for all three compositions (30, 50 and 70 % AEAM content). Since the multiblock copolymers represent an intermediate level of monomer distribution between diblock and statistical copolymers, it is unsurprising that their elution profiles lie between their counterparts: the more segregated the functionalities, the higher the overall hydrophobicity of the copolymer (Figure 2.5). This observation demonstrates that the hydrophobicity of the polymers do not only depend on their composition but also on the monomer sequence, which could have an impact on their biological properties.
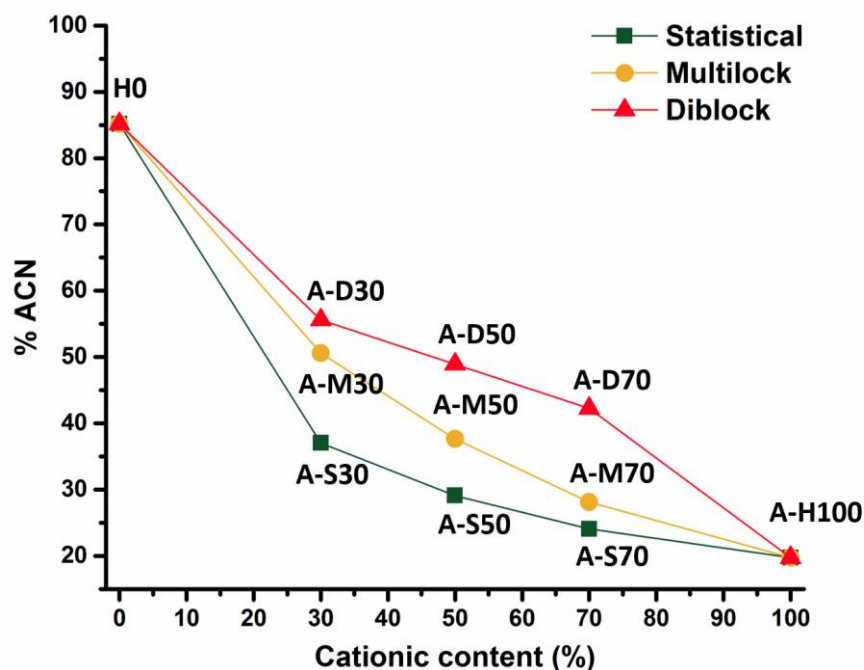
Figure 2.5 –Percentage of acetonitrile corresponding to the elution time of SMAMPs by RP-HPLC depending on the composition and the architecture (▲ Diblock copolymers, ● Multiblock copolymers, ■ Statistical copolymers).

As the amphiphilic properties of the polymers might induce self-assembly, dynamic light scattering (DLS) was used to investigate the behaviour of the polymers in phosphate buffer saline (PBS) at 37 °C (Figure 2.33, Table 2.17).[66] Population under 10 nm in size was observed by DLS for all the cationic copolymers at 1 mg.mL^{-1}, indicating single polymer chains, whereas aggregation was observed with the polyNIPAM homopolymer H0 (580 nm). Although the domains of statistical and multiblock copolymers might be too small to induce any self-assembly, the absence of micelles in solutions of diblock copolymers might be related to the concentration. This result further supports that the variation in hydrophobicity depending on monomer sequence is not associated with intermolecular interactions. Furthermore, any variation in biological activity with monomer distribution can be directly

linked to the segregation level of the hydrophobic and cationic functionalities, and not with the self-assemblies.

2.2.3   Dye leakage study

Before investigating the antimicrobial activity, the ability of ammonium SMAMPs to disrupt bacterial membranes was examined using a dye leakage assay. Liposomes comprised of 1,2 dioleoyl-*sn*-glycero-3-phosphoethanolamine/1,2 dioleoyl-*sn*-glycero-3-phospho-*rac*(1-glycerol) (4:1) (PE/PG) or cardiolipin, mimicking Gram-negative and Gram-positive bacteria, respectively, were loaded with calcein, a self-quenching fluorescent dye.[56] Upon dye leakage, the fluorescence level of the vesicle solution increases, indicating membrane disruption. All polymers, except for H0, induced an increase in fluorescence intensity against both Gram-positive (Figure 2.34) and Gram-negative (Figures 2.6 and 2.35) bacteria models. In most cases, the fluorescence intensity of the vesicle solution increased with increasing charge content of SMAMPs, which demonstrates the importance of their electrostatic interactions in membrane disruption. Statistical, multiblock and diblock copolymers exhibited similar dye leakage profiles (Figures 2.6, 2.34 and 2.35). Although this assay is not quantitative, as demonstrated by Tew *et al.*, it indicates that the SMAMPs are membrane active, a property which seems to be independent of the monomer distribution.[56]
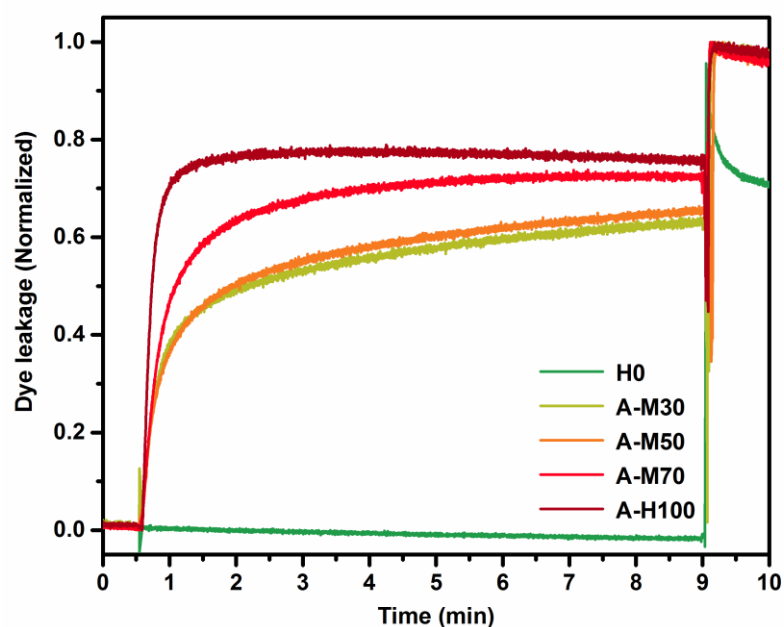
Figure 2.6 - Calcein leakage study on Gram-negative bacterial model (using liposomes comprised of a mixture of PE/PG (4:1)) with multiblock copolymers (A-M30, A-M50 and A-M70) and the homopolymers H0 and A-H100. Normalised fluorescence intensity at

λ_{em}=537 nm with λ_{ex}=492 nm. The sample was added at 30 s time point and vesicles were lysed by addition of Triton X at 9 min.

2.2.4   Antibacterial susceptibility assays

Growth inhibition was studied using two strains of Gram-negative bacteria: *Escherichia coli* (*E. coli*) and *Pseudomonas aeruginosa* (*P. aeruginosa*); and two Gram-positive strains: *Staphylococcus aureus* (*S. aureus*) and *Staphylococcus epidermidis* (*S. epidermidis*). The minimum inhibitory concentration (MIC) against each strain, the minimum concentration at which no bacterial growth was observed, was determined for each polymer as a measure of their antimicrobial activity (Table 2.3 and Figure 2.36). For statistical and diblock copolymers, the antimicrobial activity against all four strains increased with AEAM content as shown on Table 2.3, which is consistent with previous studies.[17] As demonstrated with the calcein leakage assay, an increased charge content promotes interaction of the polymers with bacterial membrane. However, for multiblock copolymers no clear trend with AEAM content could be established.

The influence of monomer distribution on antimicrobial activity was first assessed for the set of polymers with 30 % AEAM. A drastic reduction in MIC was observed moving from the statistical copolymer (A-S30), which was inactive towards most bacterial strains tested (MIC > 1024 μg.mL^{-1}, except against *S. epidermidis* with MIC=32 μg.mL^{-1}), to the multiblock and diblock copolymers (A-D30 and A-M30), which had MIC values as low as 4 μg.mL^{-1}. Activity against the Gram-negative *P. aeruginosa*, was particularly affected by monomer distribution, with MICs decreasing from over 1000 (A-S30) to 32 and 8 μg.mL^{-1} for A-D30 and A-M30, respectively (Table 2.3), which could be due to the difference in the composition of the bacterial cell envelope.[67] Indeed, Gram-negative bacteria possess an outer membrane (OM), which is a lipid bilayer comprised of an outer leaflet of lipopolysaccharides and an inner leaflet of phospholipids.[68] As lipopolysaccharides have long saturated acyl chains (leading to an increased membrane stiffness) combined with hydrophilic saccharides, they provide Gram-negative bacteria with an additional protective barrier, compared to Gram-positive bacteria. The multiblock copolymer was shown to have an intermediate hydrophobicity between that of its statistical and diblock copolymer counterparts, hence the difference in its antimicrobial activity seems more likely to be related to the presence of segments, rather than to the difference in hydrophobicity of the overall copolymer. Indeed, the cationic domains in the multiblock structure might lead to stronger interactions of SMAMPs

with the hydrophilic outer layer of the OM, compared its statistical copolymer counterpart, therefore enhancing OM permeabilisation.

Table 2.3 – Comparison of the antimicrobial activity of the ammonium SMAMPs. MIC values determined against Gram-negative bacteria *E.coli* and *P. aeruginosa* and Gram-positive bacteria *S. aureus* and *S. epidermidis*.

Sample	MIC[a] ($\mu g.mL^{-1}$)			
	E. coli	*P. aeruginosa*	*S. aureus*	*S. epidermidis*
H0	> 1024	> 1024	> 1024	> 1024
A-H100	4	4	4	32
A-S30	> 1024	> 1024	> 1024	32
A-S50	64	128	8	2
A-S70	64	64	4	2
A-M30	128	8	64	4
A-M50	1024	64	32	8
A-M70	1024	32	4	4
A-D30	512	32	128	32
A-D50	64	64	8	4
A-D70	32	32	8	4

[a] MIC is the minimum inhibitory concentration at which no visible bacteria growth can be observed.

2.2.5   Haemocompatibility of SMAMPs

Although the main requirement for SMAMPs is a high potency against bacteria, their toxicity towards mammalian cells has to be minimised in order to be considered as a viable alternative to antibiotics. Since blood is the principal vector distributing active compounds to cells, and that cationic compounds have been shown to exhibit a high toxicity towards red blood cells (RBCs), the haemocompatibility of the ammonium SMAMPs was investigated.[53] The first assay was directed towards the investigation of the lysis of the RBCs in the presence of the polymers, since they were shown to be membrane active in the calcein leakage studies. The haemolytic concentration HC_{10} (concentration to elicit 10 % haemolysis following 2 h incubation), was determined at concentrations between 2 and 1024 $\mu g.mL^{-1}$ in PBS.[69] Remarkably, only A-H100 lysed RBCs (Table 2.4, Figure 2.7), indicating that the presence of isopropyl groups of NIPAM is responsible for reducing the haemolytic activity of the rest of the polymer library.
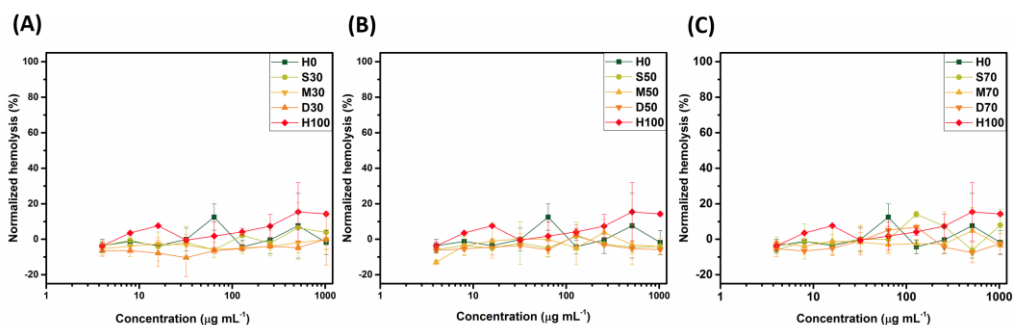
Figure 2.7 – Haemolytic activity of ammonium SMAMPs. Normalised haemolysis of human red blood cells following incubation at 37 °C for 2 hours in PBS with ammonium SMAMPs with 30 (A), 50 (B) and 70% (C) charge content.

To obtain a complete picture of the haemocompatibility of the polymers, haemagglutination, which is not necessarily related to haemolytic activity, was studied as well since positively charged polymers can interact with negatively charged sialic acid groups at the surface of RBCs, leading to intercellular binding.[19] The haemagglutination concentration c_H, which is the lowest concentration at which agglutination of RBCs is induced, was determined (Tables 2.4 and 2.5).[34] In line with the screening of cationic polymethacrylates of varying charge content by Locock and co-workers, A-H100 induced haemagglutination at low concentration (16 µg.mL^{-1}), whereas no aggregates were observed for H0, which further indicates the haemocompatibility of polyNIPAM.[19] Interestingly, the three diblock copolymers (A-D30, A-D50 and A-D70) and A-M30, had c_H values of over 1000 µg.mL^{-1}, whilst their statistical copolymer counterparts induced haemagglutination from 32 µg.mL^{-1}. Therefore, with similar AEAM content, the segregation of cationic and hydrophobic functionalities seems to affect the aggregation of RBCs. These observations could be explained by the cross-linking of RBCs being more efficient when the cationic moieties are distributed along the full length of the chain, as opposed to when charges are located on specific domains of the macromolecule. Although A-M30 has 3 cationic segments separated by polyNIPAM blocks, it did not induce any haemagglutination, whereas A-M50 and A-M70 did. This result could be explained by the fact that A-M30 is the only multiblock copolymer without cationic functionalities at the end of the polymer chain. Furthermore, the four cationic copolymers which did not induce any haemagglutination (A-D30, A-D50, A-D70 and A-M30), are also the most hydrophobic SMAMPs, according to HPLC data (Figure 2.5). Another hypothesis would be that the aggregation of RBCs could be prevented by maintaining a certain level of hydrophobicity. In any case, monomer distribution appears a key structural parameter affecting the haemocompatibility of SMAMPs.

Table 2.4 – SMAMP-induced erythrocytes aggregation. Observation of haemagglutination of human red blood cells following incubation with ammonium SMAMPs in PBS for 2 hours at 37 °C.

sample /concentration ($\mu g.mL^{-1}$)	1024	512	256	128	64	32	16	8	4	2
H0	-	-	-	-	-	-	-	-	-	-
A-H100	+++	+++	+++	+++	+++	++	+	-	-	-
A-S30	++	++	++	++	+	+	-	-	-	-
A-S50	+++	+++	+++	++	+	+	-	-	-	-
A-S70	+++	+++	+++	++	++	+	-	-	-	-
A-M30	-	-	-	-	-	-	-	-	-	-
A-M50	+++	+++	++	++	++	+	-	-	-	-
A-M70	+++	+++	+++	+++	++	+	-	-	-	-
A-D30	-	-	-	-	-	-	-	-	-	-
A-D50	-	-	-	-	-	-	-	-	-	-
A-D70	-	-	-	-	-	-	-	-	-	-

Haemagglutination strength: +++ strong; ++ moderate; + weak; - none.

Table 2.5. Comparison of the haemocompatibility of the ammonium SMAMPs. HC_{10}, c_H and haemocompatibility concentration across the SMAMPs of various composition and structure determined by haemolysis and haemagglutination assay.

Sample	HC_{10}[a] ($\mu g.mL^{-1}$)	c_H[b] ($\mu g.mL^{-1}$)	Haemocompatibility concentration[c] ($\mu g.mL^{-1}$)
H0	> 1024	> 1024	> 1024
A-H100	512	16	16
A-S30	> 1024	32	32
A-S50	> 1024	32	32
A-S70	> 1024	32	32
A-M30	> 1024	> 1024	> 1024
A-M50	> 1024	32	32
A-M70	> 1024	32	32
A-D30	> 1024	> 1024	> 1024
A-D50	> 1024	> 1024	> 1024
A-D70	> 1024	> 1024	> 1024

[a] HC_{10} is the minimum concentration at which at least 10 % of the maximum lysis was observed following 2 h incubation.

[b] c_H is the lowest concentration at which the polymers induce aggregation of RBCs.

[c] The haemocompatibility concentration was determined as the lowest value between HC_{10} and c_H. All polymers were non-haemolytic within the range of concentrations tested (except H100, for which HC10 was still higher than c_H), hence the haemocompatibility concentration was identical to c_H for all present SMAMPs.

In order to simultaneously compare the haemocompatibility and the antimicrobial activity for the library of SMAMPs, a selectivity value was determined for each bacterial strain using the ratio between the haemocompatibility concentration (which is the lowest value of HC_{10} and c_H, Table 2.5) and the MIC against the given strain (Table 2.3). This value is a powerful tool to measure the potential of SMAMPs, as only those with a pronounced activity against bacteria and no effect on RBCs, would exhibit high selectivity values.[20] As none of the SMAMPs were haemolytic, the haemocompatibility concentration was identical to the haemagglutination concentration, hence the latter was used to calculate the selectivity for bacteria over RBCs (Equation 2.1, Table 2.6).

$$Selectivity = \frac{c_H}{MIC}$$

Equation 2.1 – Equation for the selectivity against RBCs for a specific bacterial strain.

The highest selectivity values against all four bacterial strains over RBCs were obtained with the diblocks (A-D30, A-D50, A-D70) and A-M30. Additionally, monomer distribution was shown to affect the selectivity of the polymers: at 30 % AEAM content, A-M30 was found to be the most selective, followed by A-D30, then A-S30 (for example the values for *P. aeruginosa* were 0.03, 32 and 128, respectively).

Table 2.6 - Selectivity values for *E. coli*, *P. aeruginosa*, *S. aureus* and *S. epidermidis* over RBCs.

Sample	Selectivity[a]			
	E. coli	*P. aeruginosa*	*S. aureus*	*S. epidermidis*
H0	> 1	> 1	> 1	> 1
A-H100	4	4	4	0.5
A-S30	0.03	0.03	0.03	1
A-S50	0.5	0.25	4	16
A-S70	0.5	0.5	8	16
A-M30	> 8	> 128	> 16	> 256
A-M50	0.03	0.5	1	4
A-M70	0.03	1	8	8
A-D30	> 2	> 32	> 8	> 32
A-D50	> 16	> 16	> 128	> 256
A-D70	> 32	> 32	> 128	> 256

[a] Selectivity was determined using equation 2.1.

Additionally, the selectivity of the ammonium SMAMPs towards bacteria over RBCs was illustrated by comparing the MIC of a particular bacterial strain against the haemocompatibility concentration. Figure 2.8 depicts the selectivity of the SMAMPs by dividing them into categories with the most inactive and haemotoxic polymers in the bottom-right corner (highlighted in red; IV), most potent and haemocompatible species in the top-left corner (I), and two yellow intermediate zones in the top-right (II) and bottom-left (III) corner being the inactive but haemocompatible polymers and active but haemotoxic polymers, respectively. For statistical and diblock copolymers, increasing AEAM content improved the selectivity towards the four species of bacteria studied. The most selective polymers against all four strains over RBCs appear to be the diblock copolymers (A-D30, A-D50 and A-D70) and the multiblock copolymer A-M30, which is also highlighted with the selectivity values (Table 2.6). The most noteworthy variation in selectivity with monomer distribution was observed for SMAMPs with an AEAM content of 30 %: A-S30 was haemotoxic and non-

active towards bacteria except against *S. epidermidis* (red zone IV), whereas A-M30 and A-D30 were haemocompatible and highly active against all four strains (green zone I). This trend was also illustrated with the selectivity values. For SMAMPs with 50 and 70 % AEAM content, the diblock had a higher selectivity for bacteria over RBCs compared to its statistical and multiblock copolymer counterparts due to an increased haemocompatibility. Altering the monomer distribution of SMAMPs, whilst maintaining an overall chemical composition, can significantly influence the selectivity for bacteria over RBCs.
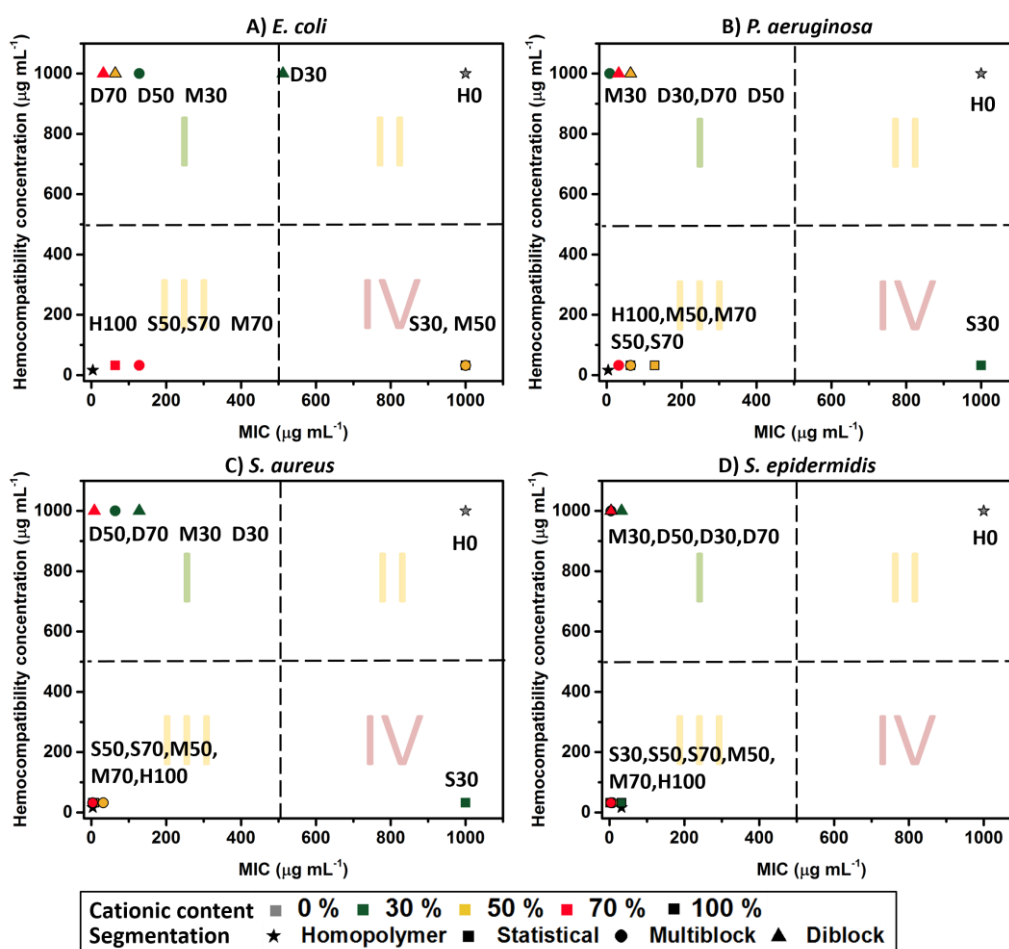
Figure 2.8 - Selectivity of the SMAMPs for Gram-negative and Gram-positive bacteria over RBCs. Haemocompatibility concentration against the MIC for *E. coli* (A), *P. aeruginosa* (B), *S. aureus* (C) and *S. epidermidis* (D) over RBCs.

2.2.6 Biocompatibility of SMAMPs

Potential applications for SMAMPs include their use as wound dressings or as oral antibiotics. As such, murine embryonic fibroblasts (NIH 3T3) and human colorectal epithelial cells (Caco-2) were pertinent *in vitro* models to determine the biocompatibility of the SMAMPs. NIH 3T3 are one of the most commonly used fibroblast cell lines, and is involved in the synthesis of extracellular matrix, hence playing a critical role in wound healing. Additionally, Caco-2 cells are well characterised colorectal cells that can be used as a model for intestinal absorption.[70]

To determine the toxicity of SMAMPs towards these mammalian cells, NIH 3T3 and Caco-2 cells were incubated with polymer concentrations ranging from 32 to 1024 μg.mL^{-1} for 3 days. As expected, H0 displayed no toxicity at any of the concentrations used, while A-H100 showed pronounced interference with cell viability (Figure 2.9) for both cell lines.
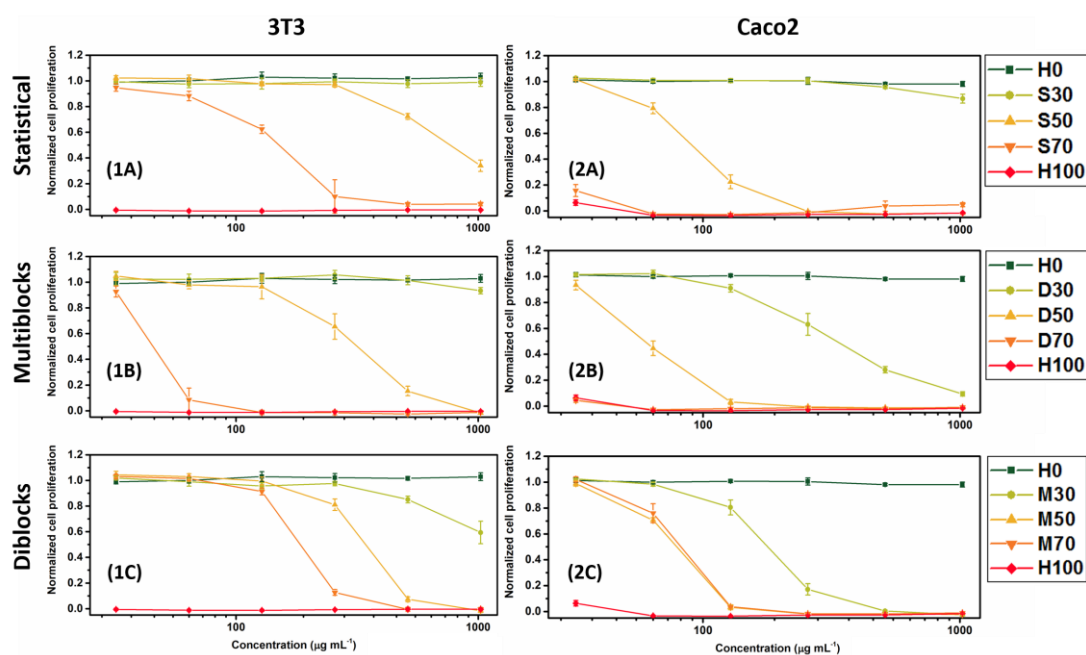
Figure 2.9 - Cytotoxicity of ammonium SMAMPs. Viability of 3T3 cells incubated for 72 hours in presence of statistical (1A), multiblock (1B) and diblock (1C) SMAMPs; and of Caco-2 cells incubated for 72 hours in presence of statistical (2A), multiblock (2B) and diblock (2C) copolymers, using XTT assay.

The inhibitory concentration (IC$_{50}$) values, which is the polymer concentration at which cell viability is inhibited by 50 %, were calculated for NIH 3T3 and Caco-2 using the toxicity curves from Figure 2.9 (Table 2.7, Figure 2.10). As expected, the toxicity towards

both cell lines increased with content of cationic functionalities, which is similar to the trend observed with haemotoxicity. These results could be attributed to an enhancement of the interactions of the polymers with the cell membrane when their charge content is increased. For both cell lines, the IC_{50} value was similar for the statistical, multiblock and diblock copolymers of 50 and 70 % AEAM content (Figure 2.10). Monomer distribution did not appear to significantly influence the toxicity of the SMAMPs towards fibroblasts and epithelial cells, except for the SMAMPs with 30 % AEAM content, as their IC_{50} towards Caco-2 cells decreased with segregation of functionalities from A-S30, to A-M30 and A-D30 (> 1024, 310 and 180 $\mu g.mL^{-1}$, respectively).
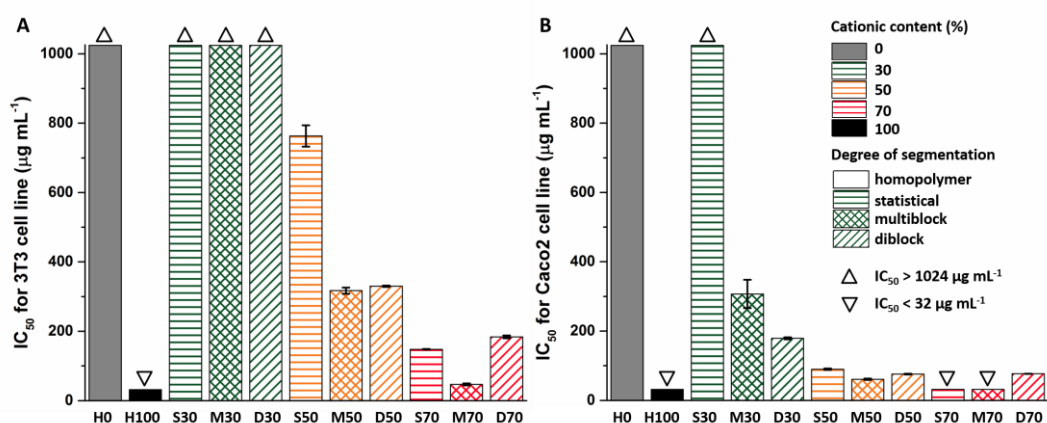
Figure 2.10 – Comparison of IC_{50} values for ammonium SMAMPs. IC_{50} of the SMAMPs for NIH 3T3 (A) and Caco-2 cells (B) after a 72-hour incubation at 37˚C in presence of the cationic polymers, using XTT assay.

Additionally, the SMAMPs were more toxic towards Caco-2 cells than NIH 3T3 cells, which might be due to increased uptake by colorectal cells.[71] These cytotoxicity results seem to indicate the potential application of the SMAMPs lies in the direction of skin wound treatment rather than oral use. Therefore, the following discussions relative to cytotoxicity will be based on the results obtained with NIH 3T3 cells. Similarly to the selectivity of bacteria over RBCs which was previously introduced, the therapeutic index (TI), which was obtained from the ratio of the IC_{50} for the mammalian cells to the MIC for each bacterial strain, indicated the relative toxicity of a SMAMP towards bacteria in comparison to mammalian cells (Equation 2.2, Table 2.7).[72]

$$TI = \frac{IC_{50}}{MIC}$$

Equation 2.2 – Equation for the therapeutic index (TI) with a cell line for a specific bacteria species.

Interestingly, the TI of A-M30 over 3T3 cells appeared to be the highest for the four bacterial strains studied: > 8, 128, 16 and 256 for *E.coli*, *P. aeruginosa*, *S. aureus* and *S. epidermidis*, respectively. Therefore, the ammonium multiblock copolymer with 30 % AEAM content appears to be a broad spectrum SMAMP which can target both Gram-negative and Gram positive bacteria whilst maintaining a low toxicity towards fibroblasts (and epithelial cells).

Table 2.7 - Cytotoxicity of SMAMPs. IC_{50} values of the SMAMPs against NIH 3T3 and Caco-2 cells obtained using XTT assays after incubation with the cationic polymers at 37 °C for 72 hours and TI of SMAMPs over 3T3 cells.

Sample name	IC_{50}[a] ($\mu g.mL^{-1}$)		Therapeutic Index (TI) [b]			
			3T3			
	3T3	Caco-2	*E. coli*	*P. aeruginosa*	*S. aureus*	*S. epidermidis*
H0	> 1024	> 1024	> 1	> 1	> 1	> 1
A-H100	< 32	< 32	< 8	< 8	< 8	< 1
A-S30	> 1024	> 1024	> 1	> 1	> 1	> 1
A-S50	760	90	12	6	95	381
A-S70	150	< 32	2	2	37	74
A-M30	> 1024	310	> 8	> 128	> 16	> 256
A-M50	320	60	0.3	5	10	40
A-M70	50	< 32	0.4	1.5	12	12
A-D30	> 1024	180	> 2	> 32	8	> 32
A-D50	330	80	5	5	41	83
A-D70	180	80	6	6	23	46

[a] IC_{50} was determined as the concentration at which 50 % inhibition occurred.

[b] Therapeutic index (TI) was calculated as the ratio the IC_{50} towards 3T3 against the MIC of the bacterial species.

In parallel to the selectivity graphs for RBCs, the IC_{50} was compared against the MIC for each bacterial strain to illustrate the TI over NIH 3T3 (Figure 2.11). A-M30 appeared as the ideal candidate against the four strains of bacteria studied. Indeed, at 30 % AEAM content, the segregation of AEAM and NIPAM functionalities allowed for the improvement of the selectivity: A-S30 was non-toxic towards 3T3 cells combined with a poor antimicrobial activity, whereas A-D30 and A-M30 exhibited a low mammalian cell toxicity and a high potency against Gram-negative and Gram-positive bacteria. Although A-D50 and A-D70 were

shown to be as selective as A-M30 over RBCs, their selectivity for bacteria over NIH 3T3 was much lower, as displayed in Figure 2.11.
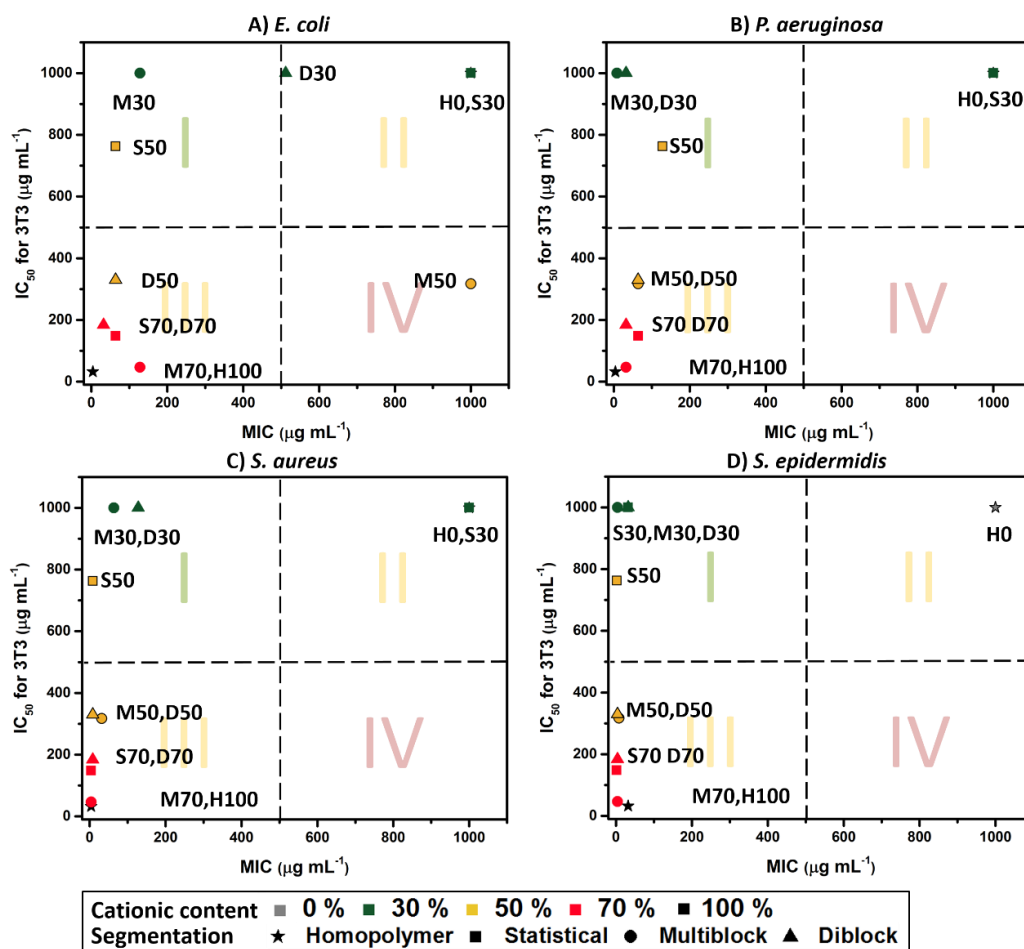
Figure 2.11 - Selectivity of SMAMPs for Gram-negative and Gram-positive bacteria over NIH 3T3 cells. IC_{50} of the SAMPs with NIH 3T3 cells against their MIC for *E. coli* (A), *P. aeruginosa* (B), *S. aureus* (C) and *S. epidermidis* (D).

The overall performance of SAMPs was analysed for each bacterial species by illustrating the TI for NIH 3T3 cells against the selectivity over RBCs (Figure 2.12 only displays the samples with a value of at least 1 for both parameters, whereas Figure 2.37 includes all data). The most promising polymers are located in the top-right green corner which represents the SMAMPs with selectivity and TI values of 10 and above. The most outstanding candidate from these graphs was A-M30, as it displayed the highest values regarding selectivity for both *P. aeruginosa* and *S. epidermidis* over 3T3 cells and RBCs.
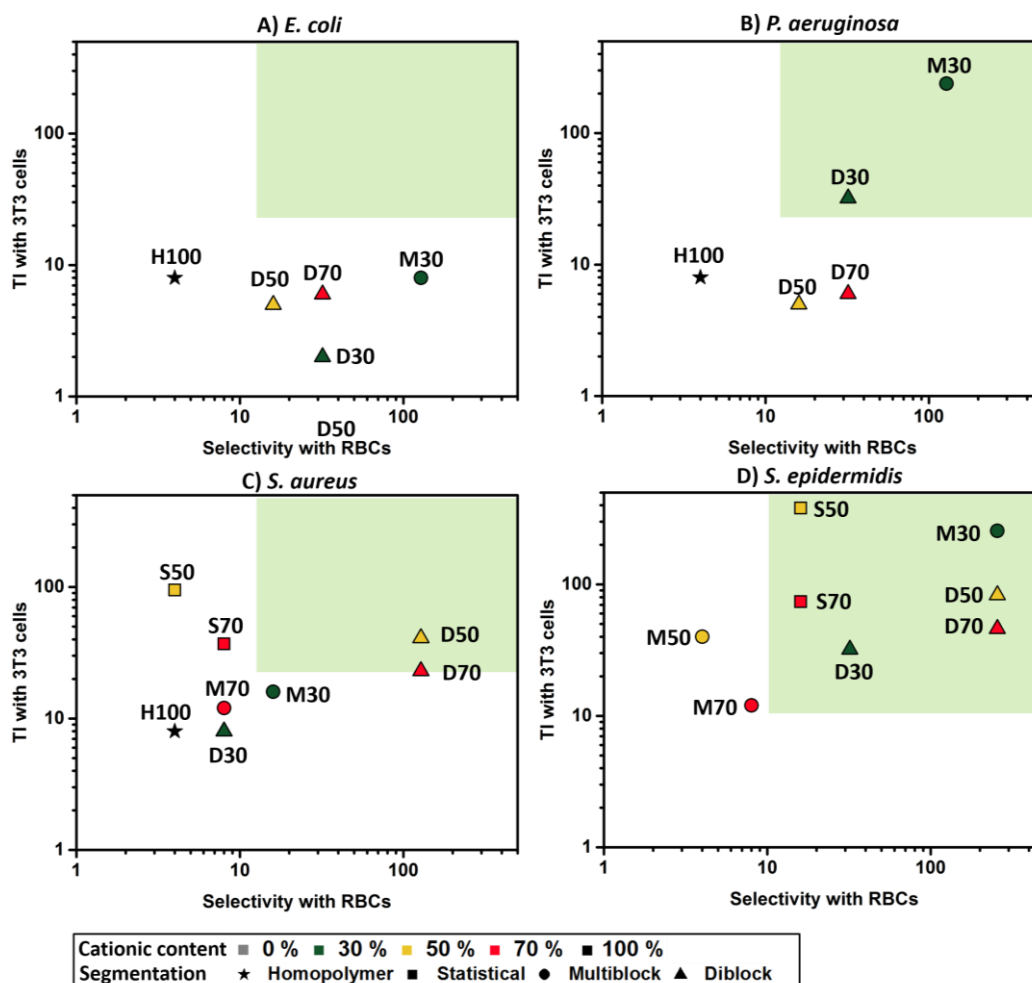
Figure 2.12 - Comparison of selectivity of SMAMPs for bacteria over RBCs and NIH 3T3 cells. TI of the SMAMPs over NIH 3T3 cells against their selectivity over RBCs for *E. coli* (A), *P. aeruginosa* (B), *S. aureus* (C) and *S. epidermidis* (D).

Despite similar chemical composition, A-M30 outperforms A-S30 and A-D30, which highlights the importance of charge segregation on the overall performance of the ammonium SMAMPs. The multiblock copolymer did not induce erythrocyte aggregation, unlike its statistical copolymer counterpart, and was less toxic towards mammalian cells as compared to its diblock copolymer analogue. Furthermore, A-M30 displayed a high membrane activity against a wide range of pathogenic bacteria. It should be emphasised that the present polymers show a pronounced activity against Gram-negative bacteria despite the additional protection from their outer membrane. Therefore, the multiblock copolymer with 30 % charge content appeared as a promising candidate for the treatment of bacterial infections. The compatibility of the ammonium SMAMPs with fibroblasts renders them interesting candidates as antimicrobial material in skin wound healing treatments.

2.2.7 Bacterial resistance

One of the main issues with currently used antibiotics is the ability of bacteria to develop resistance against them, rendering the antibiotics inactive following prolonged contact with the bacteria (at non-lethal doses).[1] However, as previously mentioned, bacteria do not seem to acquire resistance against SMAMPs as easily, since the polymers are designed to directly target bacterial membrane. In order to demonstrate the potential of the SMAMPs in this study for long-term treatment of bacterial infections, the evolution of the MIC value against a MRSA strain (USA 300) was studied for A-S30, A-M30 and A-D30 over the course of 4 weeks, with exposure at a sub-MIC (1/10) concentration. The antibacterial activity did not vary throughout the assay (Figure 2.13) and no resistant mutants could be detected in the final bacterial suspension. Therefore, the development of bacterial resistance against these polymers is not easily acquired, and this observation is valid across the different monomer distributions studied (statistical, multiblock and diblock copolymers). Indeed, a similar mechanism of antimicrobial action based on membrane disruption for the herein presented SMAMPs, as supported by the dye leakage assays, would explain the retention of antimicrobial activity.
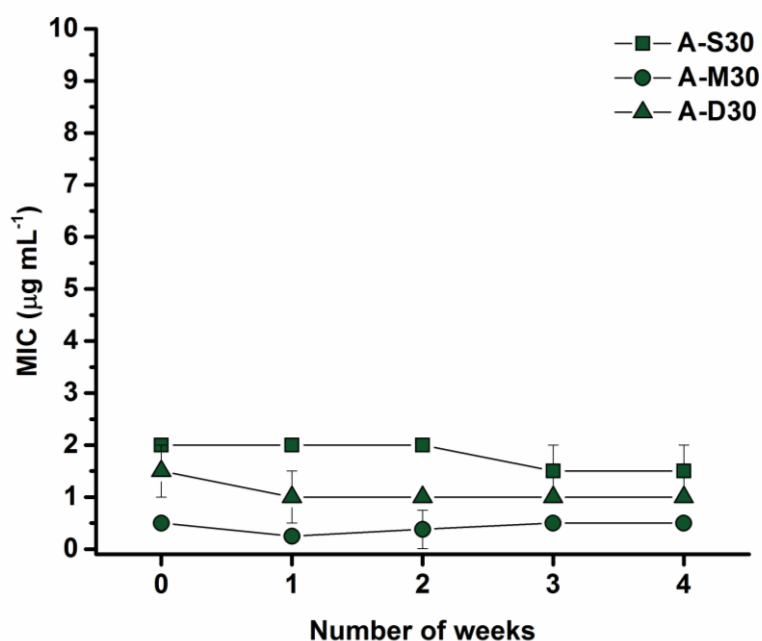
Figure 2.13 - Determination of bacterial resistance for copolymers with 30 % AEAM content. Evolution of the MIC value of A-S30, A-M30 and A-D30 against a MRSA strain USA300 over the course of 4 weeks, after incubating the bacteria in presence of sub-MIC concentrations of SMAMPs.

2.3   Conclusion

SMAMPs based on a cationic (AEAM) and a hydrophobic monomer (NIPAM) were synthesised with different AEAM content (30, 50 or 70 %) and various degrees of segregation, by exploiting RAFT polymerisation. NIPAM was a suitable choice of co-monomer since no haemolytic activity was observed for the copolymers, whilst the antimicrobial potency of the copolymers was maintained. From this study, monomer distribution appeared to have an impact on various levels. Firstly, the hydrophobicity of the polymers increased with increasing length and decreasing number of discreet segments, thus introducing an additional handle to tune hydrophobicity. Furthermore, at 30 % charge content, antimicrobial activity was shown to be affected by monomer distribution, particularly against Gram-negative bacteria. This improvement in activity could be the result of enhanced interactions of cationic moieties with the outer membrane of bacteria, when these functionalities are organised in domains. The antimicrobial activity of the ammonium copolymers was attributed to bacterial membrane disruption, following dye leakage assays.

After establishing the antimicrobial activity of the ammonium polymers, the selectivity with erythrocytes, epithelial cells and fibroblasts was examined. In all cases, diblock copolymers were found to outperform statistical copolymers, and at 30 % AEAM content, the multiblock copolymer exhibited much greater selectivity for *P. aeruginosa* and *S. epidermidis* compared to its statistical and diblock analogues. These results are independent to any self-assembling behaviour as, within the tested concentrations, the SMAMPs are likely to be in their unimolecular form. The one-pot multiblock copolymer synthesis approach utilised in this study has highlighted the influence of monomer distribution on the physical properties of the materials, which in turn influences their interaction with biological systems. By investigating a range of design parameters using SMAMPs in order to reduce toxicity towards mammalian cells and limit bacterial resistance, this study might aid in finding alternatives to standard antibiotics.

2.4   Experimental

2.4.1   Materials

Acetone (97 %), acryloyl chloride (97 %), 2-bromopropionic acid (≥99 %), butanethiol (99 %), carbon disulphide (≥99 %), chloroform (CHCl₃, 99 %), dichloromethane (DCM, 99 %), 1,4-dioxane (99 %), ethylacetate (EtOAc, 99 %), ethylenediamine (≥99 %), hydrochloric acid (HCl), sodium hydroxide (NaOH), triethylamine (NEt₃, ≥99 %) and trifluoroacetic acid (TFA, 99 %) were purchased from Sigma-Aldrich and used without further purification. Sodium chloride (NaCl, Fischer-Scientific, ≥99 %), Boc-anhydride (Fluka, 98 %) and 2,2'-azobis[2-(2-imidazolin-2-yl)propane]dihydrochloride (VA-044, Wako) were also used without further purification. Mili-Q water was directly used as a solvent for polymerisations. *N*-isopropylacrylamide (NIPAM, Sigma-Aldrich, 97 %) was recrystallised in *n*-hexane. Lipids 1,2 dioleoyl-*sn*-glycero-3-phosphotehanolamine (PE), 1,2 dioleoyl-*sn*-glycero-3-phospho-*rac*(1-glycerol) sodium salt (PG), Cardiolipin sodium salt from bovine heart (CL), Nutrient Agar, Dulbecco's Modified Eagle's Medium (DMEM), Müller-Hinton Broth (MHB), Roswell Park Memorial Institute medium (RPMI-1640) , 3-(*N*-morpholino)propanesulfonic acid (MOPS), Phosphate Buffered Saline (PBS) tablets, Concanavalin A (Con A) and Triton X were purchased from Sigma-Aldrich. Milli-Q filtered water was used to prepare solutions, according to their recommended concentration and the solutions were autoclaved prior to their usage in order to ensure sterility. The utilised bacteria strains were *P. aeruginosa* ATCC® 27853™, *E. coli* ATCC® 25922™, *S. epidermidis* ATCC® 35984™, *S. aureus* ATCC® 29213™ and *S. aureus* USA 300 (for the development resistance assay). Human red blood cells were obtained from the Australian Redcross.

2.4.2   Methods

2.4.2.1   Nuclear Magnetic Resonance (NMR) Spectroscopy

¹H NMR spectra were recorded on a Bruker Advance 300 spectrometer (300 MHz) at 27 °C in DMSO, CDCl₃ or D₂O. For ¹H NMR, the delay time (dl) was 2 s. Chemical shift values (δ) are reported in ppm. The residual proton signal of the solvent was used as internal standard.

2.4.2.2　Size exclusion chromatography (SEC)

Molar mass distributions were measured using an Agilent 390-LC MDS instrument equipped with differential refractive index (DRI), viscometry (VS), dual angle light scatter (LS) and dual wavelength UV detectors. The system was equipped with 2 x PLgel Mixed D columns (300 x 7.5 mm) and a PLgel 5 μm guard column. The eluent was DMF with 5 mmol NH_4BF_4 additive. Samples were run at 1 mL.min^{-1} at 50°C. Poly(methyl methacrylate) standards (Agilent EasyVials) were used for calibration between 955,000 - 550 gmol^{-1}. Analyte samples were filtered through a nylon membrane with 0.22 μm pore size before injection. Respectively, experimental molar mass ($M_{n,SEC}$) and dispersity ($Đ$) values of synthesized polymers were determined by conventional calibration using Agilent GPC/SEC software.

2.4.2.3　Mass spectroscopy (MS)

MS analysis was carried out with Agilent1100 HPLC coupled with Agilent 6130B single quadruple mass spectrometer equipped with electrospray ionisation source. Mobile phase was 80 % methanol with 20 % water at flow rate at 0.2 mL.min^{-1}. Mass spectrometer was operated in electrospray positive (or negative) ion mode with a scan range 50-500 m/z. Source conditions are: capillary at (-)4000V; nebuliser gas (N_2) at 15 psi; dry gas (N_2) at 7 L.min^{-1};Temperature at 300 °C. Calibration was done with ESI tuning mix from Agilent.

2.4.2.4　Fluorescence spectrometer

The fluorescent intensity was monitored using Agilent Technologies Cary Eclipse Fluorescence Spectrophotometer. The solutions of vesicles were introduced in a polystyrene cuvette for the measurements.

2.4.2.5　High performance liquid chromatography (HPLC)

HPLC was performed using an Agilent 1260 infinity series stack equipped with an Agilent 1260 binary pump and degasser. The flow rate was set to 1.0 mL.min^{-1} and samples were injected using Agilent 1260 autosampler with a 100 μL injection volume. The temperature of the column was set at 37 °C. The HPLC was fitted with a phenomenex Lunar C18 column (150 x 4.6 mm) with 5 micron packing (100Å). Detection was achieved using an Agilent 1260 variable wavelength detector. UV detection was monitored at λ = 309 nm. Methods were edited and run using Agilent OpenLAB online software and data was analysed using Agilent OpenLAB offline software. Mobile phase solvents used were HPLC grade (ACN was 'far UV') and consisted of mobile phase A: 100 % ACN, 0.04 % TFA; mobile phase B: 100 % water, 0.04 % TFA with a gradient of 1 to 95 % ACN over 50 minutes.

An elution ratio was calculated from Equation 2.3, relative to the difference in elution times of pAEAM$_{100}$ and pNIPAm$_{100}$.

$$Elution\ ratio\ =\ \frac{Elution\ time\ (sample)\ -\ Elution\ time\ (pAEAM_{100})}{Elution\ time\ (pNIPAM_{100})\ -\ Elution\ time\ (pAEAM_{100})}$$

Equation 2.3 - Determination of the elution ratio.

2.4.2.6 Dynamic Light Scattering (DLS) measurements

DLS measurements were taken using a Malvern instruments Zetasizer Nano at 37 °C with a 4 mW He-Ne 633 nm laser at a scattering angle of 173° (back scattering). For DLS aggregation studies, 1.024 mg of polymer sample was dissolved in 1 mL of PBS buffer at pH 7.4 and a total of 0.5 mL of the solution was introduced in a 1.5 mL polystyrene cuvette after filtering with a 0.2 μm filter.

2.4.2.7 Determination of pKa

20 mg (5 mg.mL^{-1}) of H100 and 1.17 g (0.05 M) of NaCl were dissolved in 40 mL of water. 100 μL of a 6M HCl solution was added to the polymer solution in order to make sure all the amine groups were protonated. The titration was performed manually at room temperature with a syringe pump to control the added volume and a pH meter (HI2211 Hanna Instruments) using a solution of 0.2 M of NaOH as the titrant. For each polymer, the range of pKa was determined using the maximum of the first derivative of the titration curve (Figure 2.2).

2.4.2.8 Dye leakage assays

Formation of vesicles. The synthesis of vesicles was performed according to a protocol detailed by Lienkamp *et al.*[56] 100 mL of a first buffer (buffer A) was prepared by dissolving 120 mg (1.00 mmol) of NaH$_2$PO$_4$ in 90 mL of H$_2$O. The pH was then adjusted to 7.0 with a 1 mol.L^{-1} solution of NaOH. The total volume of the solution was then taken to 100 mL. The calcein solution was obtained by dissolving 249 mg (0.400 mmol) of calcein dye in 8 mL of previously prepared buffer A. The pH of the solution was adjusted to 7.0 with a 1 mol.L^{-1} solution of NaOH in order to dissolve the calcein. The total volume was then taken up to 10 mL in order to yield a buffer of 40 mmol.L^{-1} of calcein.

A second buffer (buffer B) was prepared by dissolving 1.20 g (10.0 mmol) of NaH$_2$PO$_4$ and 5.26 g (90.0 mmol) of NaCl in 980 mL of H$_2$O. The pH was adjusted to 7.0 with a 1 mol.L^{-1} solution of NaOH. The volume of the solution was then taken up to 1000 mL.

For the PE/PG 4:1 vesicles, 6.0 mg (8 μmol) of PE and 1.6 mg (2 μmol) of PG in 0.8 mL of CHCl$_3$, for the CL vesicles, 6 mg (10 μmol) of CL was dissolved in 0.6 mL of CHCl$_3$ in a 25-mL round bottom flask, in order to obtain a solution of roughly 10 mg.mL^{-1}. A film was formed at the bottom of the flask by removing the solvent under reduced pressure, the flask kept as

vertical as possible. After the film was dried under vacuum, it was hydrated with 1 mL of buffer A and stirred for an hour with a magnetic stirring bar. After complete dissolution of the lipid, the solution underwent 5 freeze-thaw cycles. The solution was then filtered 15 times by extrusion, using an extruder from Avanti Polar Lipids (Mini-Extruder, Whatman) and 400 nm-membranes. 96-well plates were sourced from Thermo-Fischer. The free dye was filtered through a Sephadex G-50 column using buffer B. The vesicle fraction from the column was diluted for the dye-leakage experiments according to the initial fluorescence of the solution.

Fluorescence monitoring. Interactions of the polymers with model bacterial membranes composed of lipid bilayers were evaluated using liposomes consisting of a mixture of phosphatidylethanolamine (PE) and phosphatidylglycerol (PG) with a ratio of 4 to 1 to model Gram-negative bacteria and Cardiolipin (CL) for Gram-positive bacteria. The fluorescent dye calcein was encapsulated in a self-quenching concentration. When the membrane is compromised by the addition of a sample, the dye leakage would result in an increased fluorescence. To that end the fluorescence of the vesicle solution was monitored by recording the fluorescence intensity at a wavelength of 537 nm with the excitation wavelength set at 492 nm. The intensity of the vesicle solution was measured, then 20 μL of 1.4 mg mL^{-1} solution of polymer was added 30 seconds after the start of the run, followed by the addition of 20 μL of a 20 % solution of Triton X 9 minutes later. The intensities were normalised by setting the baseline at the intensity before polymer addition and the maximum at the intensity reached after addition of Triton X, corresponding to 100 % leakage.

2.4.2.9 Antibacterial susceptibility tests

Antibacterial susceptibility was studied using two strains of Gram-negative bacteria: *Escherichia coli* (*E. coli*) and *Pseudomonas aeruginosa* (*P. aeruginosa*); and two Gram-positive strains: *Staphylococcus aureus* (*S. aureus*) and *Staphylococcus epidermidis* (*S. epidermidis*). Minimum inhibitory concentrations (MICs) were determined according to the standard Clinical Laboratory Standards Institute (CLSI) broth microdilution method (M07-A9-2012). A single colony of bacteria was picked up from a fresh (24 hour) culture plate and inoculated in 5 mL of Mueller-Hinton (MH) broth, then incubated at 37 °C overnight. On the next day, the concentration of cells was assessed by measuring the optical density at 600 nm (OD$_{600}$). Culture suspension was then diluted to an OD$_{600}$ = 0.1 with RPMI with 0.165 mol L^{-1} of MOPS in order to reach a bacterial concentration of ~ 10^8 colony forming unit per mL (CFU mL^{-1}). The solution was diluted further by 100 fold to obtain a concentration of 10^6 CFU mL^{-1}. Polymers were dissolved in distilled water and 100 μL of each test polymer was added to micro-wells followed by the addition of the same volume of bacterial suspension (10^6 CFU mL^{-1}). The micro-wellplates were incubated at 37 °C for 24 hours, and growth was evaluated

by measuring the OD_{600} using a plate reader. Triplicates were performed for each concentration and readings were taken twice. The growth in the well was normalised using negative controls, wells without any bacteria introduced, and positive controls, wells only containing bacterial solution.

2.4.2.10 Haemolysis and haemagglutination assays

Human red blood cells (RBCs) were prepared by washing freshly collected human blood with PBS *via* centrifugation. Polymers were dissolved in PBS at desired concentration. The normalisation of results was achieved using positive controls (50 $\mu g.mL^{-1}$ Concanavalin A for haemagglutination and 2 % Triton X-100 in PBS for haemolysis) and negative control (PBS) which were included on each plate. A suspension of 3 % in volume of RBCs was added to each well and the contents were mixed before being incubated at 37°C for 2 hours. The 96-well plates were centrifuged at 600 x g for 10 minutes then 100 μL of the supernatant was transferred into a new plate. The absorbance at 540 nm was measured and normalised using the positive and negative control.

2.4.2.11 Cell Culture

Caco-2 human colorectal adenocarcinoma cells were grown in a 50:50 mixture of Ham's F12 and Dulbecco's Modified Eagle's Medium (DMEM) supplemented with 10 % of foetal calf serum, 1 % of 2 mM glutamine and 1 % penicillin/streptomycin. NIH/3T3 mouse embryonic fibroblasts were grown in DMEM medium supplemented with 10% of bovine calf serum, 1 % of 2 mM glutamine and 1 % penicillin/streptomycin. Both cell lines were grown as adherent monolayers at 37 °C in a 5% CO_2 humidified atmosphere and passaged at approximately 70-80% confluence.

2.4.2.12 *In vitro* growth inhibition assays

The anti-proliferative activity of the polymers was determined in CaCo-2 colorectal cancer cells and NIH/3T3 embryonic fibroblasts. 96-well plates were used to seed 5000 cells per well which were left to pre-incubate with drug-free medium at 37 °C for 24 hours before adding different concentrations of the compounds to be tested (1024 $\mu g\ mL^{-1}$ - 32 $\mu g\ mL^{-1}$). A drug exposure period of 72 hours was allowed. The XTT assay was used to determine cell viability. The IC_{50} values (concentrations which caused 50% of cell death), were determined as duplicates of triplicates in two independent sets of experiments and their standard deviations were calculated.

2.4.2.13 Resistance detection assay

The detection of the development of bacterial resistance was studied using the methodology described by Gullberg *et al.*[73] Overnight cultures of a methicillin-resistant strain of *S. aureus* (USA 300) in MH broth obtained from agar plates. Cells serially passaged by 400 fold into 1 mL batch cultures every 24 hours for 24 days, in MH broth containing 1/10 MIC value of the antimicrobial agent. After every 100 generations (4 days), an antibacterial susceptibility was performed as described above to observe any variation in the MIC values. To confirm the absence of any resistant mutants, a further detection method was used. 100 µL of the final bacterial suspension from the resistance generation assay was taken and serially diluted by 10 to 10^7. 100 µL from each dilution was added on an agar plate containing 1 x MIC of the test compound and using a sterile spreader, the solution was spread across the entire agar plate. After incubation at 37 °C for 24 hours, the agar plate with countable single colonies (if present) were used to perform an antibacterial susceptibility test on each colony separately to confirm any increase in resistance from prior MIC values. No resistant mutants were detected.

2.4.3   Synthesis

2.4.3.1   Synthesis of Boc-AEAM

Boc-AEAM was synthesised according to the literature.[60]

Synthesis of *N*-t-butoxycarbonyl-1,2-diaminoethane. A solution of ethylenediamine (4.41 g, 4.90 mL, 73.0 mmol) in 40 mL of DCM was added in a two-necked 100 mL flask fitted with a condenser, a pressure equalising dropping funnel and nitrogen inlet. After the solution was cooled with an ice-bath, a mixture of Boc-anhydride (3.98 g, 18.0 mmol) in DCM (20 mL) was added dropwise over 2 hours with stirring. The mixture was allowed to warm to RT and stirred overnight. The solvent was removed by rotary evaporation and a precipitate identified as *N,N'*-(bis-*t*-butoxycarbonyl)-1,2-diaminoethane was observed upon addition of water (50 mL). The filtrate was saturated with NaCl and extracted with EtOAc (3 x 60 mL). The combined organic phases were concentrated under vacuum to obtain a pale oil. Residual NaCl was removed by dissolving the oil in $CHCl_3$ and filtering. The solvent was removed under reduced pressure to give a colourless oil identified as *N-t*-butoxycarbonyl-1,2-diaminoethane (1.51 g, 9.00 mmol, 50 %). ^1H NMR ($CDCl_3$): δ = 4.93 (bs, 1H, amide

proton), 3.16 (m, 2H, CH$_2$), 2.78 (m, 2H, CH$_2$), 1.44 (s, 9H, CH$_3$), 1.20 (m, 2H, NH$_2$) as shown on Figure 2.13

Synthesis of *N*-t-butoxycarbonyl-*N'*-acryloyl-1,2-diaminoethane. Acryloyl chloride (0.67 g, 0.60 mL, 7.4 mmol) was dissolved in CHCl$_3$ (30 mL). The solution was cooled in an ice bath and a solution of NEt$_3$ (0.63 g, 0.90 mL, 6.2 mmol) and *N*-*t*-butoxycarbonyl-1,2-diaminoethane (1.0 g, 6.2 mmol) in CHCl$_3$ (15 mL) was added dropwise over an hour and a half. After addition, the reaction mixture was allowed to warm to RT and stirred for an hour before the solvent was removed under reduced pressure. The residue was washed with water (20 mL) and extracted with CHCl$_3$ (3 x 20 mL). The collected organic fractions were combined and the solvent was removed under vacuum to obtain *N*-*t*-butoxycarbonyl-*N'*-acryloyl-1,2-diaminoethane as a white powder. The product was recrystallised in Et$_2$O to yield white crystals (1.0 g, 4.9 mmol, 80 %); mp=110 °C. ^{1}H NMR (300 MHz, 298 K, CDCl$_3$, δ): 7.0 (bs, 1H, amide proton), 6.31-6.25 (dd, *J*=15 Hz, *J*=1 Hz, 1H, vinyl proton), 6.14-6.05 (dd, *J*=15 Hz, *J*=9 Hz, 1H, vinyl proton), 5.67-5.63 (dd, *J*=12 Hz, *J*=1 Hz, 1H, vinyl proton), 5.39 (bs, 1H, amide proton), 3.45 (m, 2H, CH$_2$), 3.32 (m, 2H, CH$_2$), 1.37 (s, 9H, CH$_3$) as shown on Figure 2.15. ^{13}C NMR (300 MHz, 298 K, CDCl$_3$, δ): 166.73 (CH$_2$=CH−(***C***=O)−NH−), 157.38 (=N−(***C***=O)−O−), 131.46 (CH$_2$=***C***−(C=O)−), 126.67 (***C***H$_2$=C−), 79.91 (−O−***C***((CH$_3$)$_3$), 40.98 (−NH−***C***H$_2$−CH$_2$−NH−), 40.45 (−NH−CH$_2$−***C***H$_2$−NH−), 28.63 (−O−C((***C***H$_3$)$_3$) as shown on Figure 2.16. MS: [M+Na$^+$] 237.3 (calculated) 237.2 (found), [2M+Na$^+$] 451.5 (calculated), 451.4 (found). The IR spectrum of BocAEAM can be found on Figure 2.17.

2.4.3.2 Synthesis of (propanoic acid)yl butyl trithiocarbonate (PABTC)

The RAFT agent was synthesised according to the literature.[74]

A 50% w/w aqueous sodium hydroxide solution (4.40 g, 2.20 g NaOH, 55.0 mmol) was added to a stirred mixture of butanethiol (5.00 g, 5.90 mL, 55.0 mmol) and water (8.5 mL). Acetone (2.8 mL) was then added, and the resulting clear solution was stirred for 30 min at room temperature. Carbon disulfide (4.75 g, 1.13 eq., 62.4 mmol) was added and the resulting orange solution was stirred for 30 min, then cooled to < 10°C. 2-Bromopropionic acid (8.69 g, 1.03 eq., 56.8 mmol) was slowly added under temperature supervision, followed by the slow addition of a 50% w/w aqueous NaOH solution (4.50 g, 2.25 g NaOH, 57.0 mmol). When the exotherm stopped, water (8 mL) was added and the reaction was left to stir at RT for 20 hours. A further aliquot of water (15 mL) was added to the reaction mixture, which was subsequently cooled to below 10 °C. A 10 M solution of HCl was slowly added, keeping the temperature below 10 °C and stopping when pH reached 3. The orange solid separated, crystallised and was recovered by filtration under reduced pressure. The solid was then

recrystallised in *n*-hexane to yield yellow crystals (7.20 g, 30.3 mmol, 55 %); mp=58 °C. ^{1}H-NMR (CDCl$_3$, 300 MHz, δ): 4.88 (q, 1H, J = 9 Hz, C**H**(CH$_3$)), 3.39 (t, 2H, J = 9 Hz, S-C**H$_2$**-CH$_2$-CH$_2$-CH$_3$), 1.70 (m, 2H, S-CH$_2$-C**H$_2$**-CH$_2$-CH$_3$), 1.64 (d, 3H, J = 9 Hz, CH(C**H$_3$**)), 1.44 (m, 2H, S-CH$_2$-CH$_2$-C**H$_2$**-CH$_3$), 0.94 (t, 3H, J = 9 Hz, CH$_2$-C**H$_3$**) as shown on Figure 2.18. ^{13}C NMR (300 MHz, 298 K, CDCl$_3$, δ): 222.1 (S$_2$**C**=S), 177.4 (**C**OOH), 47.8 (**C**H(CH$_3$)), 37.4 (S-**C**H$_2$-CH$_2$-CH$_2$-CH$_3$), 30.2 (S-CH$_2$-**C**H$_2$-CH$_2$-CH$_3$), 22.3 (S-CH$_2$-CH$_2$-**C**H$_2$-CH$_3$), 16.9 (CH(**C**H$_3$)), 13.9 (S-CH$_2$-CH$_2$-CH$_2$-**C**H$_3$) as shown on Figure 2.19.

2.4.3.3 Typical synthesis of homopolymers and statistical copolymers

For the synthesis of A-S30^{Boc}, BocAEAM (257 mg, 1.20 mmol), NIPAM (317 mg, 2.80 mmol), PABTC (9.54 mg, 0.0400 mmol) were dissolved in 980 µL of 1,4-dioxane and 180 µL of water. 86 µL of a 15 mg.mL^{-1} stock solution of VA-044 in H$_2$O was added to the mixture which was introduced in a test tube equipped with a mechanical stirrer and a rubber septum. The solution was then degassed with nitrogen for *ca.* 15 min and the polymerisation was then performed in a thermostated oil bath set at 46 °C. After 6 hours, the test tube was withdrawn from the oil bath. The quantity of reagents needed for the homopolymers and the statistical copolymers can be found in Table 2.8.

2.4.3.4 Multiblock copolymer synthesis by iterative RAFT polymerisation
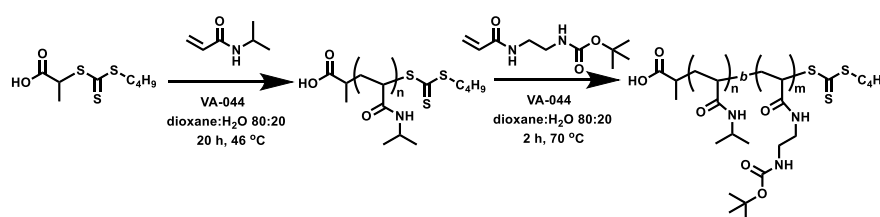
Typical synthesis of the initial block. For the synthesis of the first block of A-D30^{Boc}, NIPAM (339 mg, 3 mmol) and PABTC (10.216 mg, 0.04 mmol) were dissolved in 800 µL of 1,4-dioxane and 100 µL of water. 97 µL of a 10 mg.mL^{-1} stock solution of VA-044 in H$_2$O was added to the mixture which was introduced in a test tube equipped with a mechanical stirrer and a rubber septum. The solution was deoxygenated by bubbling nitrogen through it for 20 min and the polymerisation was then performed in a thermostated oil bath set at 46 °C. After 6 hours, the test tube was withdrawn from the oil bath and a sample was taken for ^{1}H NMR and SEC analysis.

Typical synthesis of subsequent blocks. The test tube with the reaction mixture was opened and BocAEAM (275 mg, 1.3 mmol) was added with 125 µL of 1,4-dioxane and 40 µL of a 15 mg.mL^{-1} stock solution of VA-044 in H$_2$O. After the vial was re-sealed with a septum, the solution was degassed for *ca.* 20 min, then placed in an oil bath set at 70 °C for the polymerisation to occur. The tube was withdrawn from the oil bath after 2 hours and a sample was taken for ^{1}H NMR and SEC analysis. The quantity of reagents added for each block extension for all diblock and mutliblock copolymers can be found in Tables 2.9-2.12.

Determination of monomer conversions. Monomer conversions (*p*) were calculated from ^{1}H NMR data using Equation 2.4.

$$p = 1 - (\int I_{5.4-6.4\text{ppm}} / \int I_a / DP_{\text{targeted}})$$

Equation 2.4 - Calculation of monomer conversion p

Where $\int I_{5.4-6.4\text{ppm}}$ is the integral of the three vinyl protons of the monomer, $\int I_a$ is the integral of the three methyl protons belonging to the terminal methyl of the Z group of the CTA and DP_{targeted} is the average degree of polymerisation targeted.

Calculation of $M_{n,th}$. The theoretical number-average molecular weight ($M_{n,th}$) is calculated using Equation 2.5.

$$M_{n,th} = \frac{[M]_0 p M_M}{[CTA]_0 + 2f[I]_0(1 - e^{-k_d t})(1 - \frac{f_c}{2})} + M_{CTA}$$

Equation 2.5 - Calculation of $M_{n,th}$.

Where $[M]_0$, $[CTA]_0$, $[I]_0$ are the initial concentrations (in mol.L^{-1}) of the monomer, CTA and the initiator respectively; *p* is the monomer conversion as determined by equation 2.4; M_M and M_{CTA} are the molar masses (in g.mol^{-1}) of the monomer and the CTA, respectively; k_d is the decomposition rate constant (in s^{-1}) of the azo-initiator; and *t* represents the polymerisation time (in seconds). The factor "2" accounts for the fact that one molecule of initiator yields two primary radicals with the efficiency *f* (assumed to be equal to 0.5 in this study). The decomposition rate constant for VA-044 at the temperature *T* ($k_{d,VA\text{-}044(T)}$) was determined from the values obtained from Wako ($k_{d,VA\text{-}044(44 °C)}$ = 1.92 10^{-4} s^{-1} and E_a = 108000 J.mol^{-1}) using the Arrhenius equation ($k_{d,VA\text{-}044(70 °C)}$ = 4.30 10^{-4} s^{-1}). The term $1 - (f_c /2)$ represents the number of chains produced in a radical-radical termination event with f_c representing the coupling factor. An f_c value of 1 means that 100 % of bimolecular terminations occur by combination, whereas a value of 0 indicates that 100 % of bimolecular

terminations result in disproportionation. In this study, 100 % terminations by disproportionation are assumed ($f_c = 0$).

Determination of livingness (*L*). The fraction of living chains can be calculated using Equation 2.6, the parameters being $[CTA]_0$ and $[I]_0$ initial CTA and initiator concentration, whereas k_d, f and 1-$f_c/2$ are related to the thermal decomposition of the initiator.

$$L\ (\%) = \frac{[CTA]_0}{[CTA]_0 + 2f[I]_0(1 - e^{-k_dt})(\frac{1 - f_c}{2})}$$

Equation 2.6 - Theoretical determination of the relative amount of living polymer chains using an azo-initiator compound.

2.4.3.5 Deprotection of the polymers

The polymers were dissolved at a concentration of 5 mg.mL^{-1} in a mixture of methanol and 1M aqueous solution of HCl (3:1) and stirred for 2 hours at 40°C. They were then dialysed against water and freeze-dried.

2.5   Supporting Figures
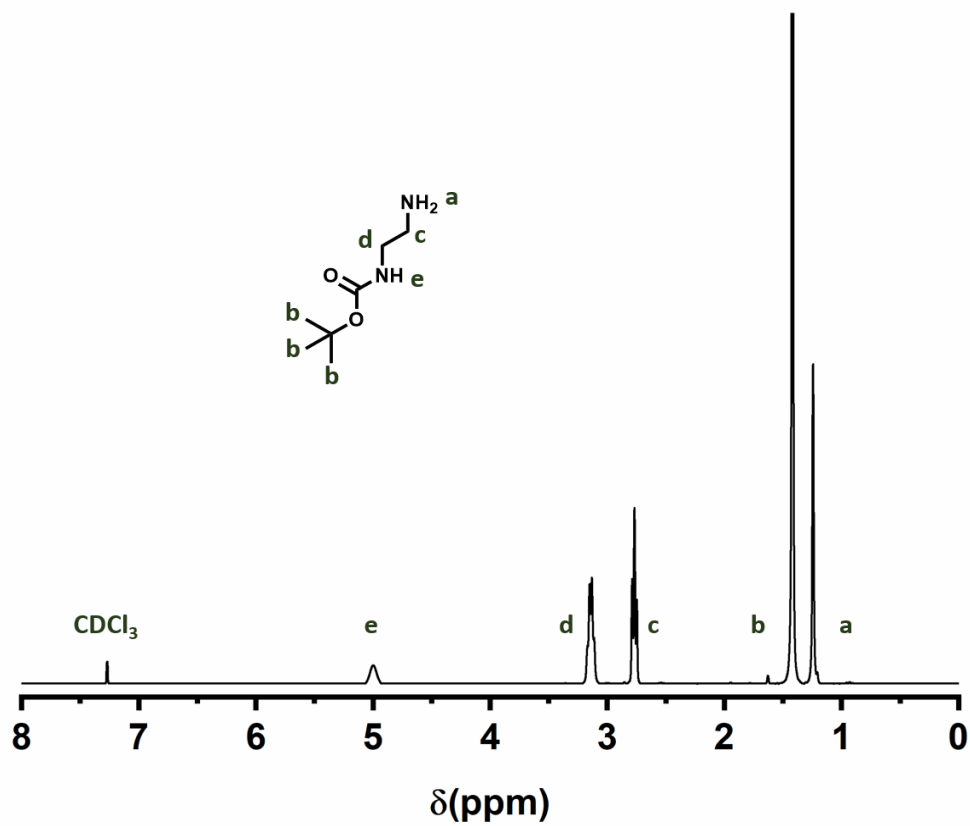
Figure 2.14 - ^{1}H NMR spectrum of the intermediate product *N*-t-butoxycarbonyl-1,2-diaminoethane in CDCl₃.
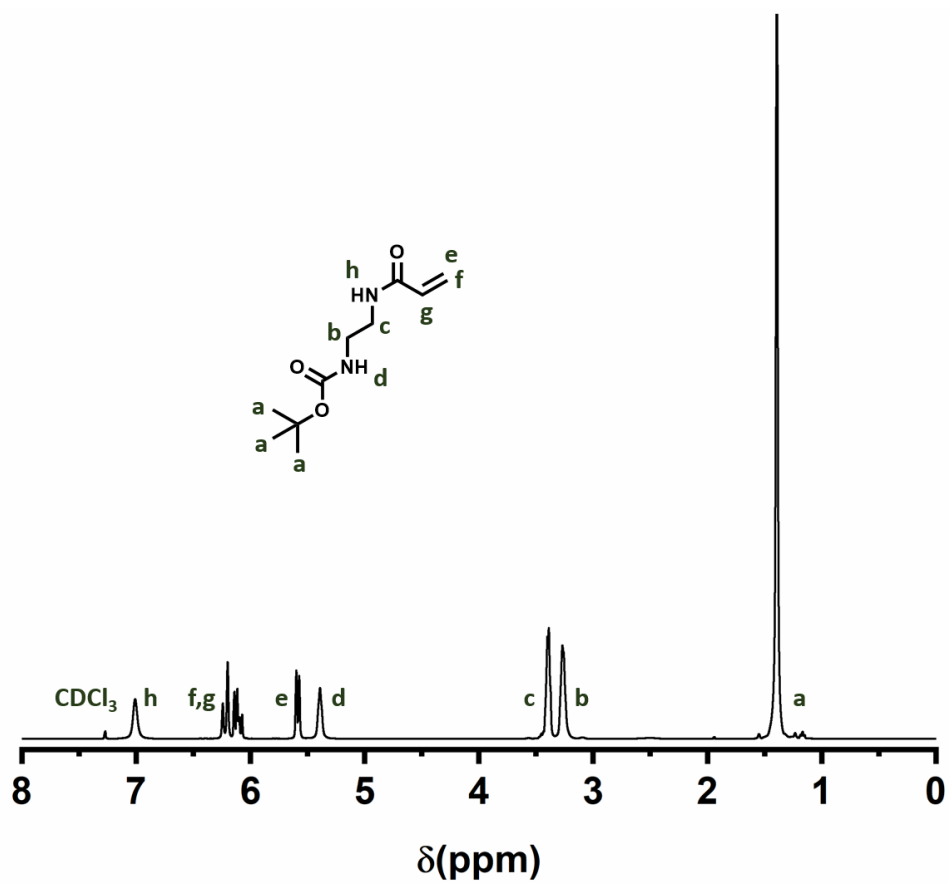
Figure 2.15 - ¹H NMR spectrum of Boc-AEAM in CDCl₃.
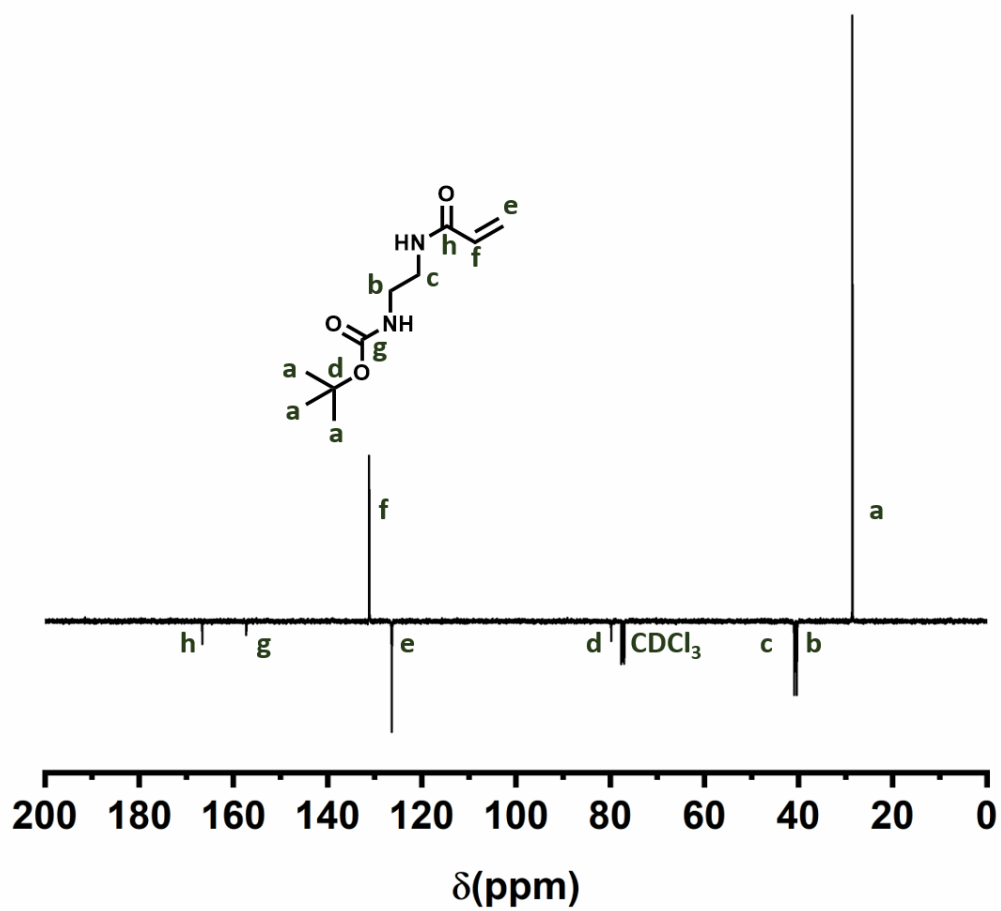
Figure 2.16 - ¹³C NMR spectrum of BocAEAM in CDCl₃.
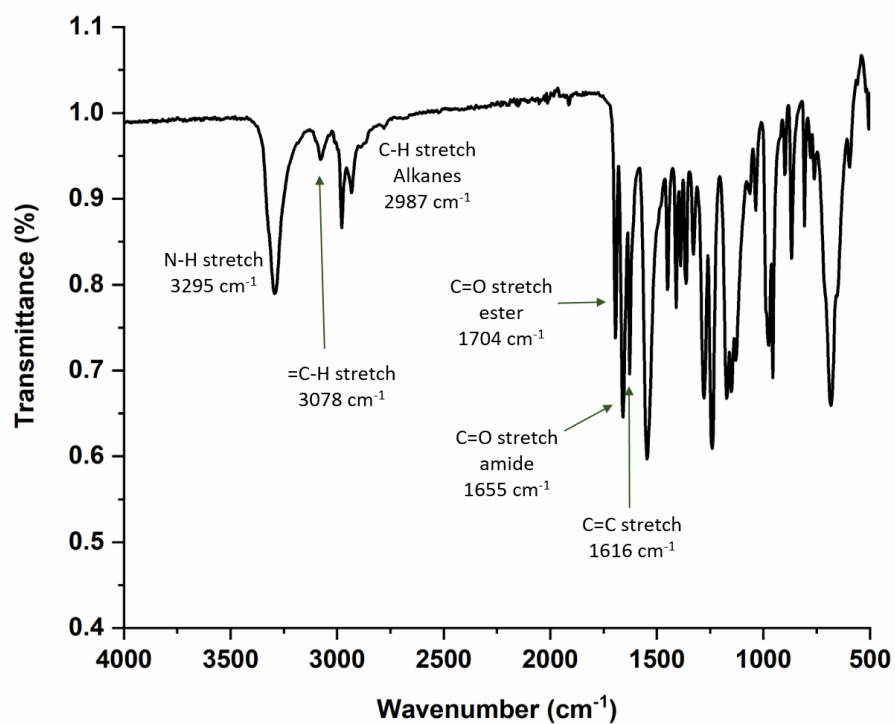
Figure 2.17 - IR spectrum of BocAEAM.
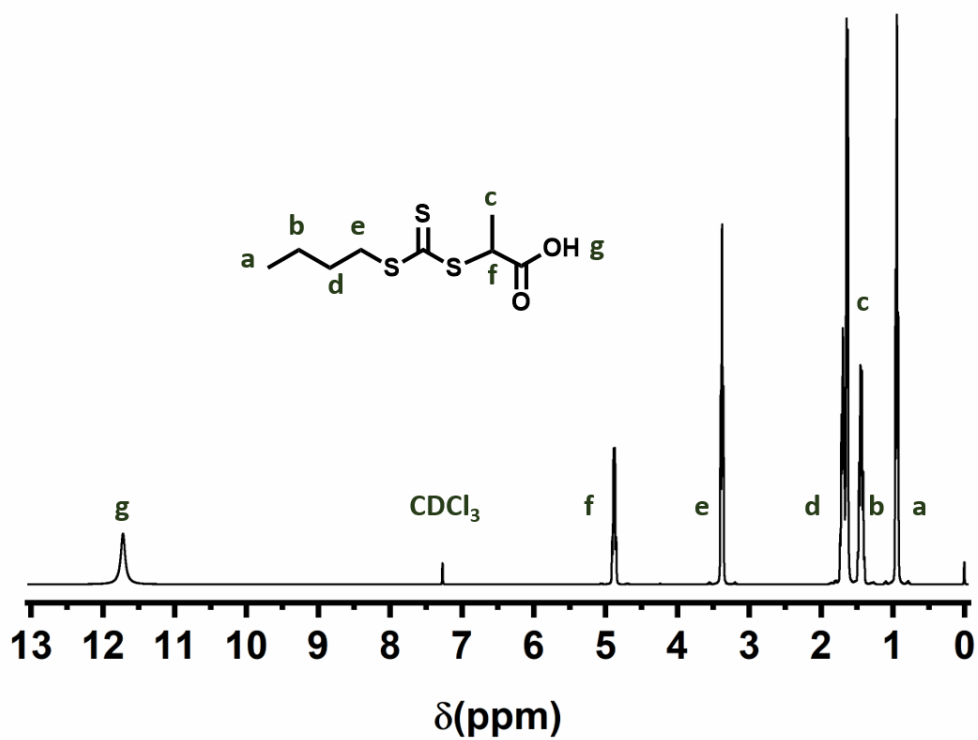
Figure 2.18 - ¹H NMR spectrum of PABTC in CDCl₃.
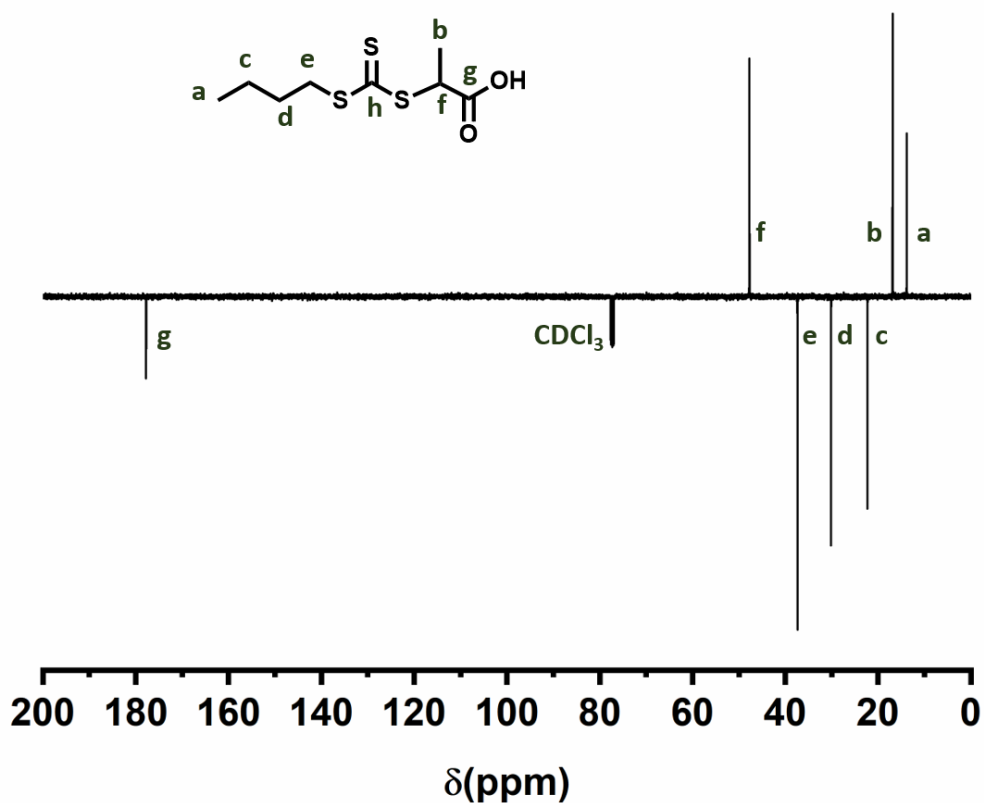
Figure 2.19 - ^{13}**C NMR spectrum of PABTC in CDCl₃.**
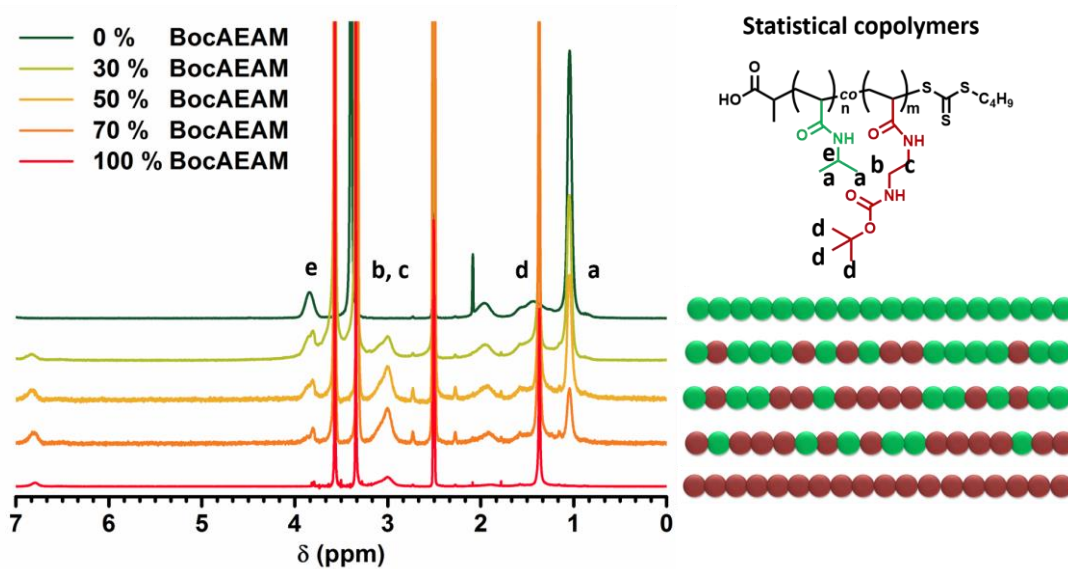
Figure 2.20 – ¹H NMR spectra in DMSO-d_6 of Boc-protected statistical copolymers for each composition.
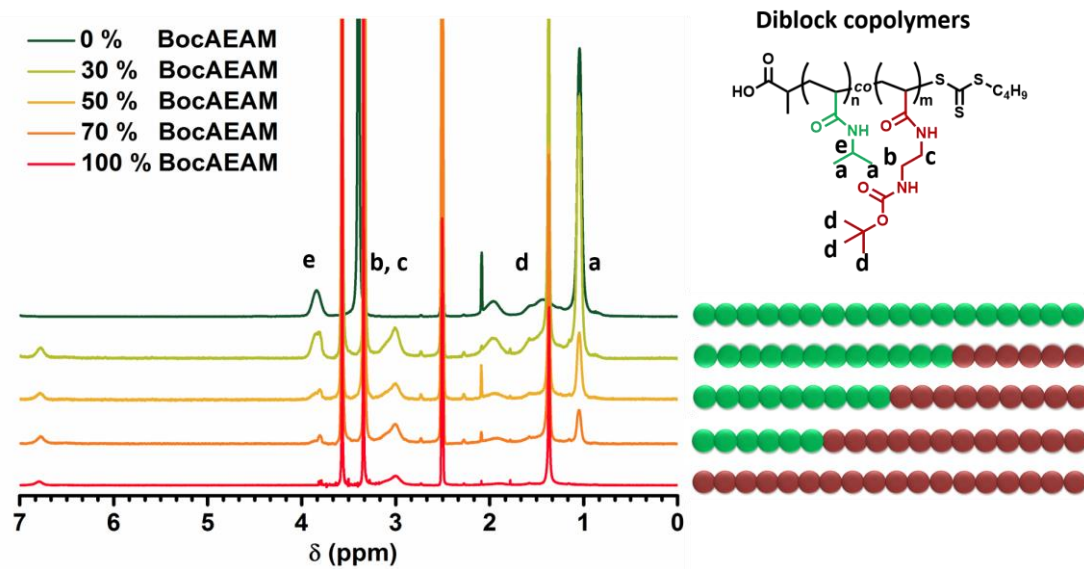
Figure 2.21 - ¹H NMR spectra in DMSO-d_6 of Boc-protected diblock copolymers for each composition.
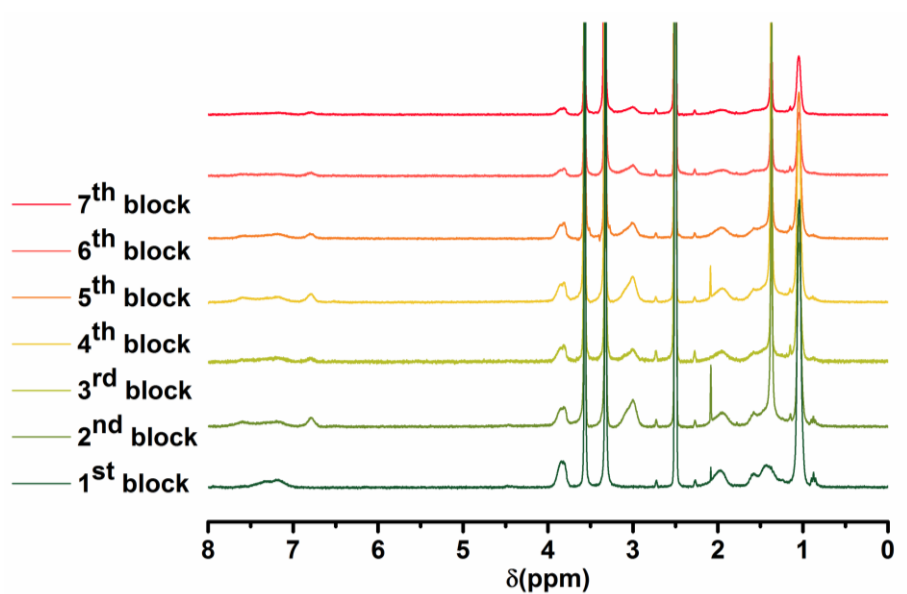
Figure 2.22 - ¹H NMR spectra in DMSO-d_6 of A-M30^{Boc} for each chain extension.
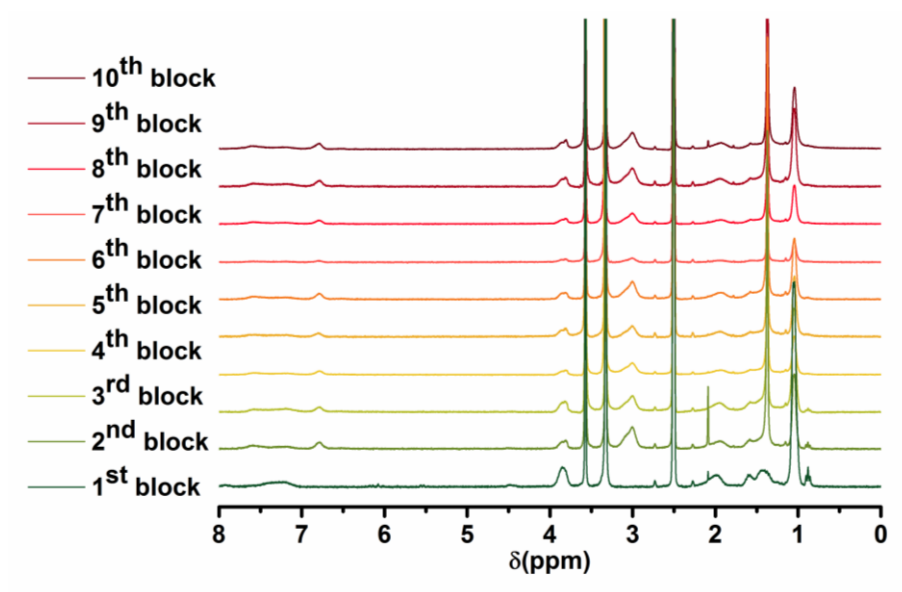
Figure 2.23 - ^{1}H NMR spectra in DMSO-d_6 of A-M50^{Boc} for each chain extension.
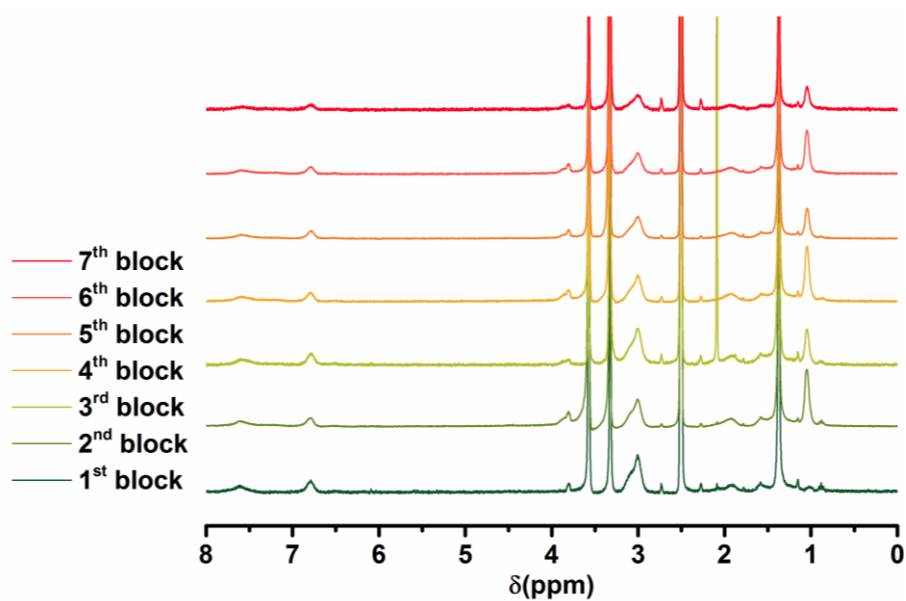
Figure 2.24 - ^{1}H NMR spectra in DMSO-d_6 of A-M70^{Boc} for each chain extension.
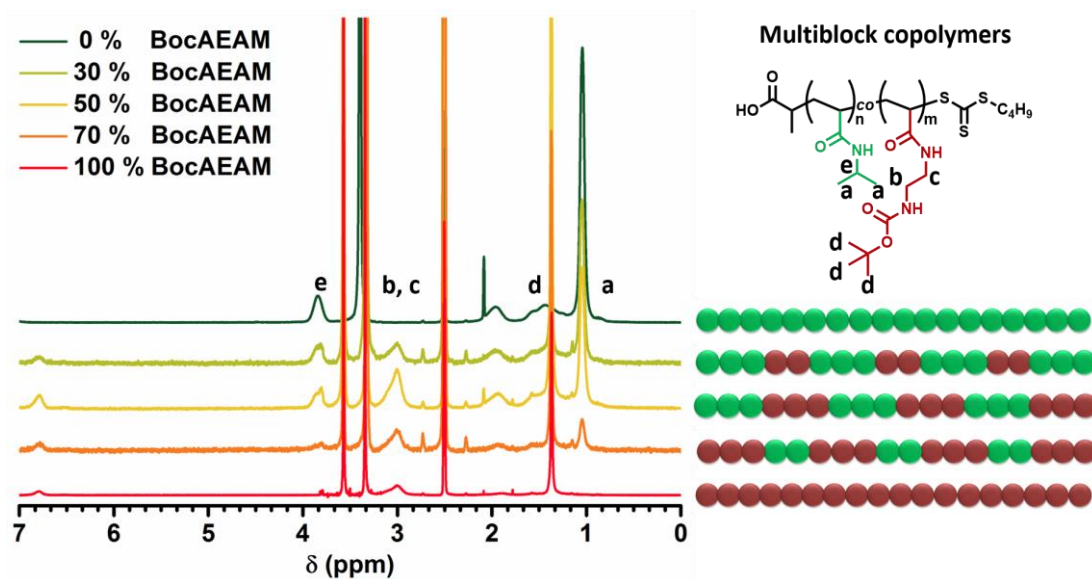
Figure 2.25 - ¹H NMR spectra in DMSO-d_6 of Boc-protected multiblock copolymers for each composition.
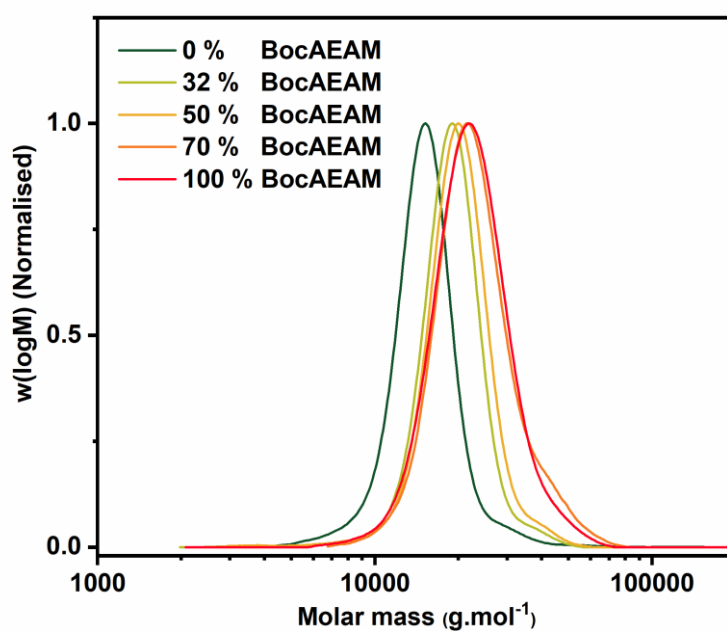
Figure 2.26 - DMF-SEC chromatograms for statistical copolymers of each composition.
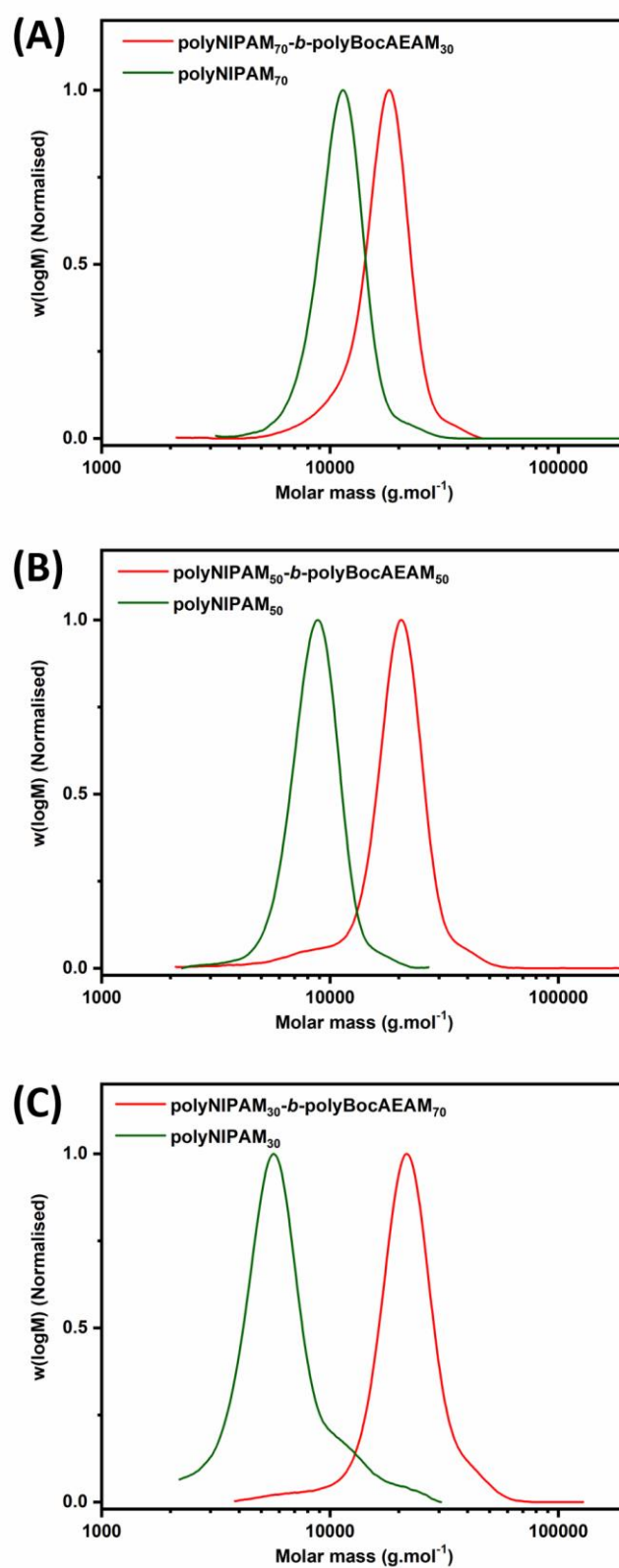
Figure 2.27 - DMF-SEC chromatograms for diblock copolymers with 30 % (A), 50 % (B) and 70 % (C) BocAEAM content.
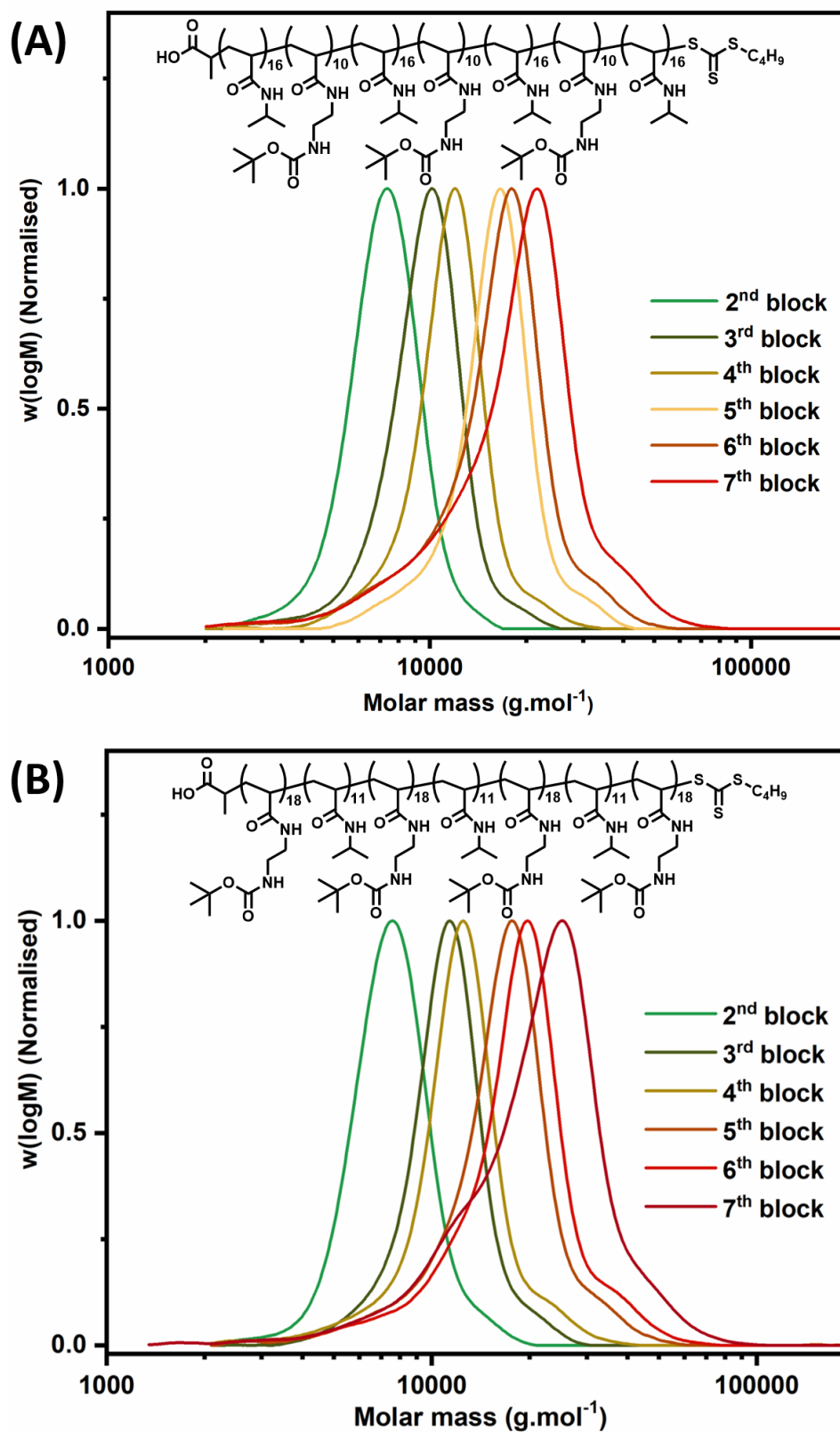
Figure 2.28 - DMF-SEC chromatograms for successive chain extensions of A-M30^{Boc} (A) and A-M70^{Boc} (B).
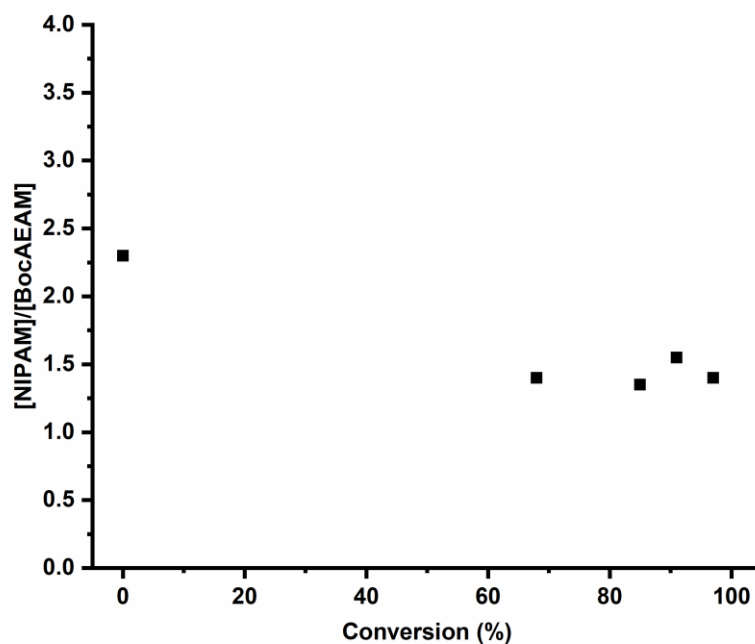
Figure 2.29 - Ratio of the concentration of remaining NIPAM and BocAEAM with overall conversion during the polymerisation of A-S30^Boc.
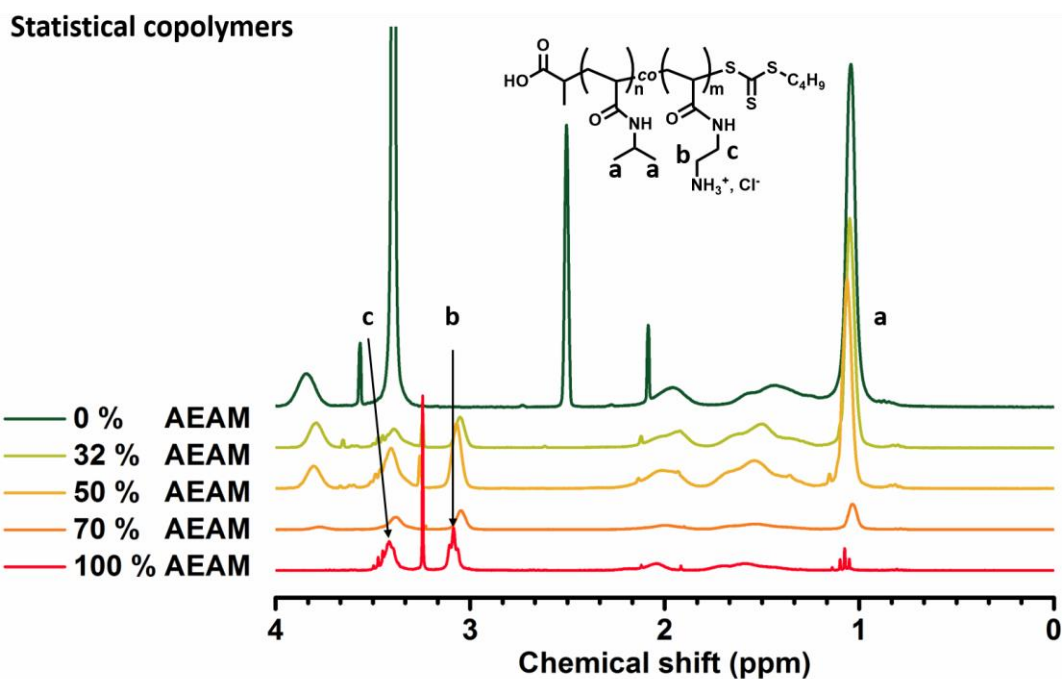
Figure 2.30 - ¹H NMR spectra in D₂O of the deprotected statistical copolymers of each composition and in DMSO-d_6 for H0.
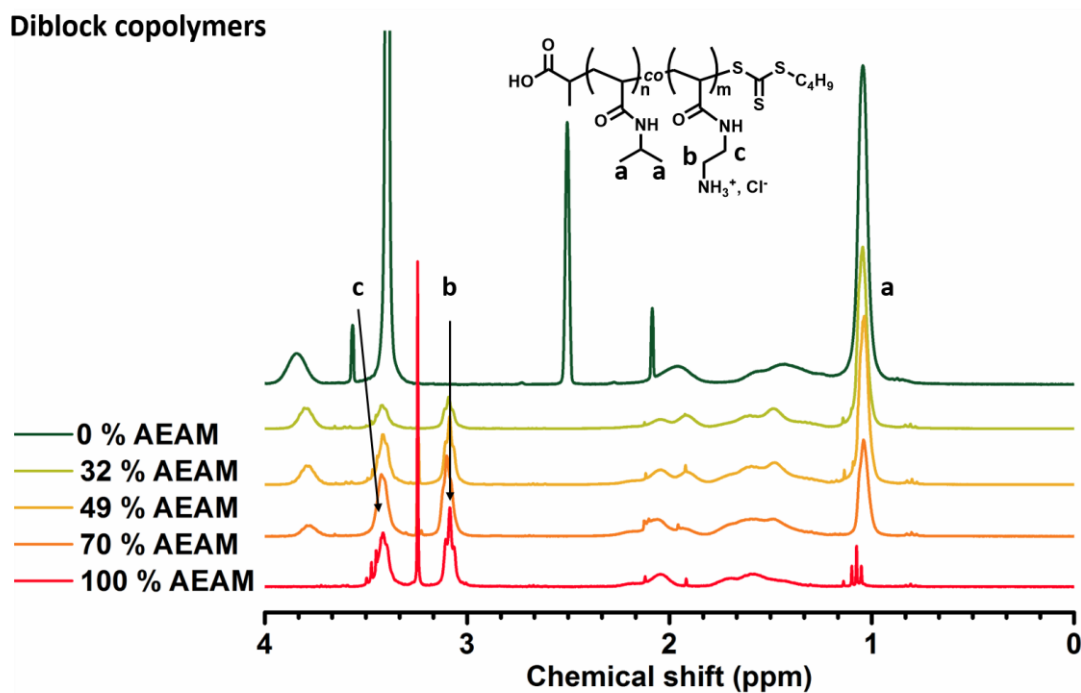
Figure 2.31 - ^{1}H NMR spectra in D$_2$O the deprotected diblock copolymers of each composition and in DMSO-d_6 for H0.
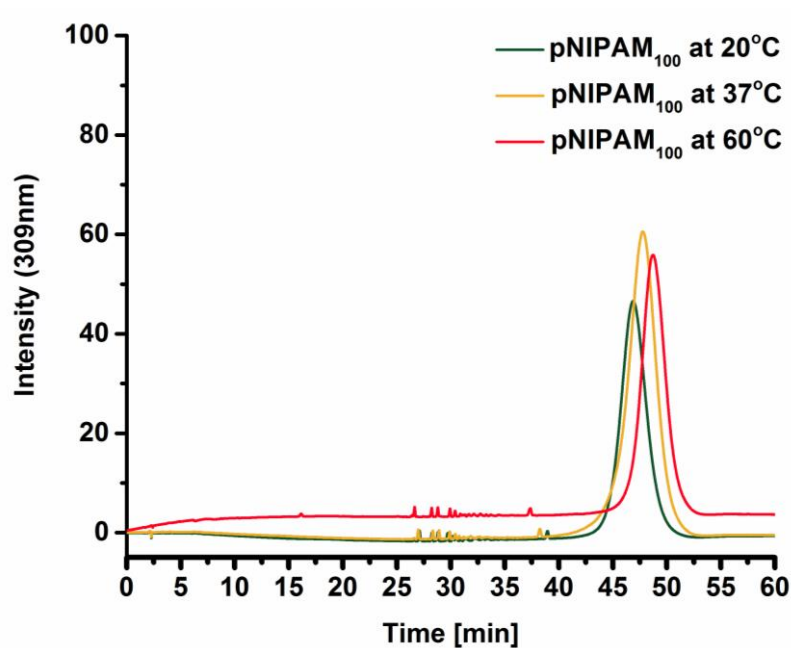
Figure 2.32 - HPLC chromatograms of H0 at 20, 37 and 60 °C with a gradient of 1 to 95 % ACN over 50 minutes.
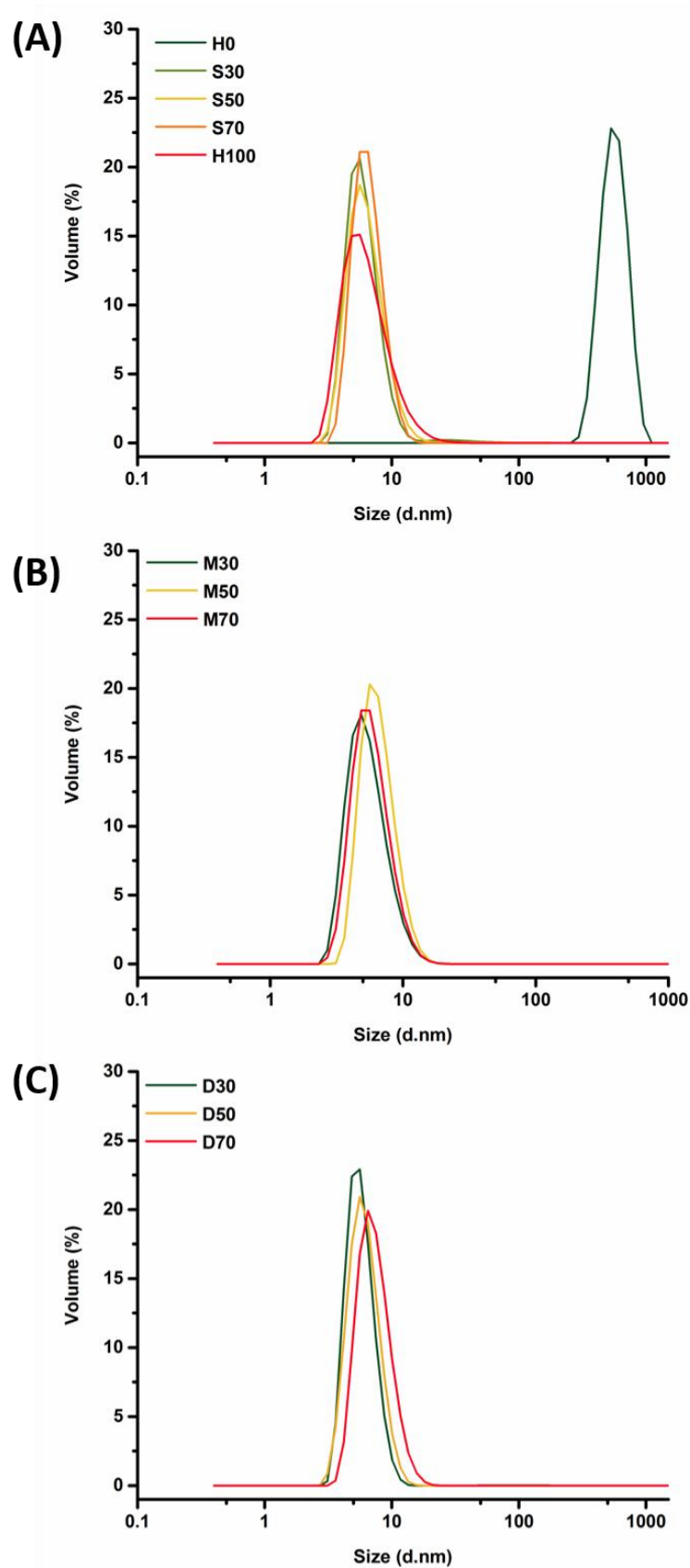
Figure 2.33 - Size distribution by volume by DLS of the homopolymers (A), statistical (A), diblock (B) and multiblock (C) copolymers at 1 mg mL^{-1} in PBS.
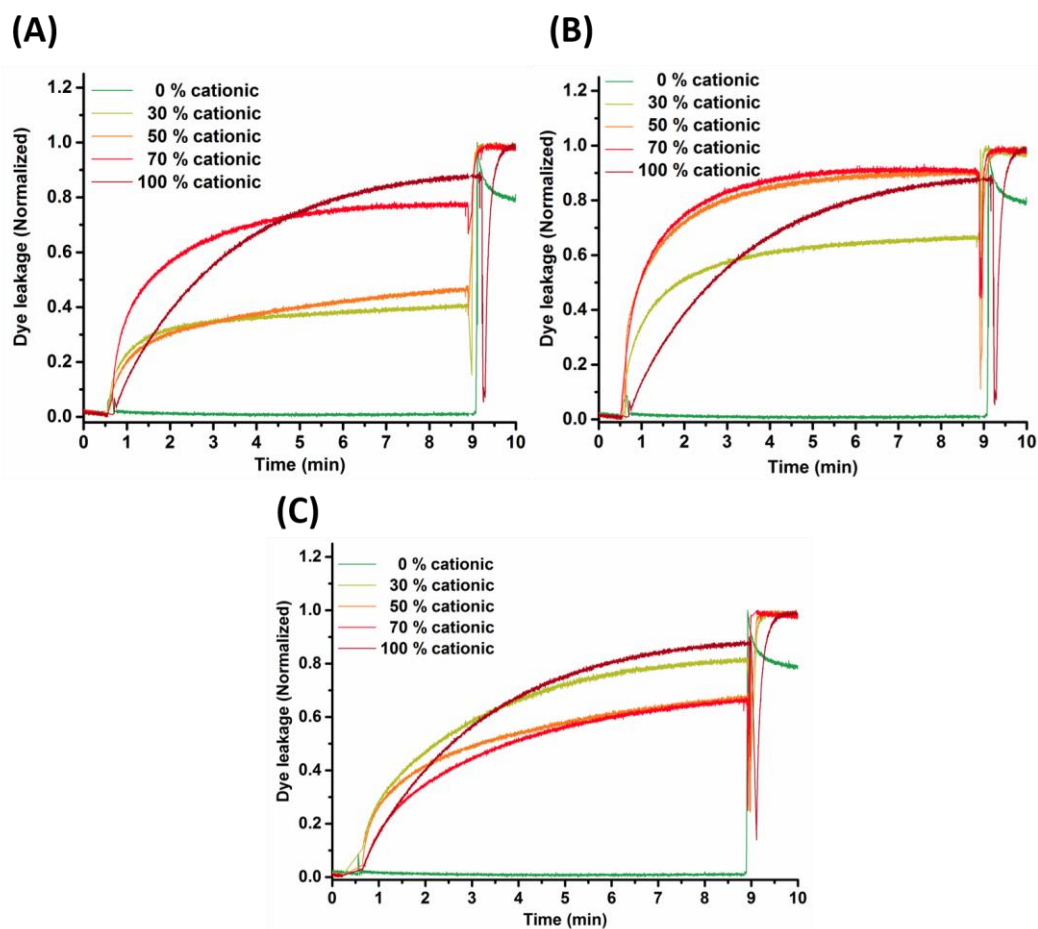
Figure 2.34 - Dye leakage study with (A) statistical (B) diblock and (C) multiblock copolymers on Gram-positive bacteria model. Fluorescence was read at 537 nm (emission) at an excitation wavelength of 492 nm. The sample was added at 30 s measurement time and vesicles were lysed by addition of Triton X at 9 min.
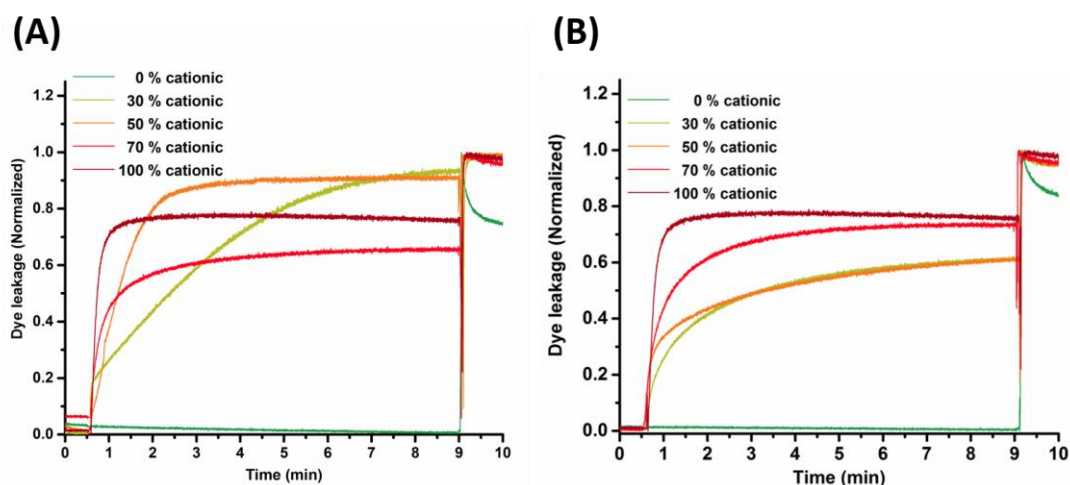
Figure 2.35 - Dye leakage study with statistical (A) and diblock (B) copolymers on Gram-negative bacteria model. Fluorescence was read at 537 nm (emission) at an excitation wavelength of 492 nm. The sample was added at 30 s measurement time and vesicles were lysed by addition of Triton X at 9 min.
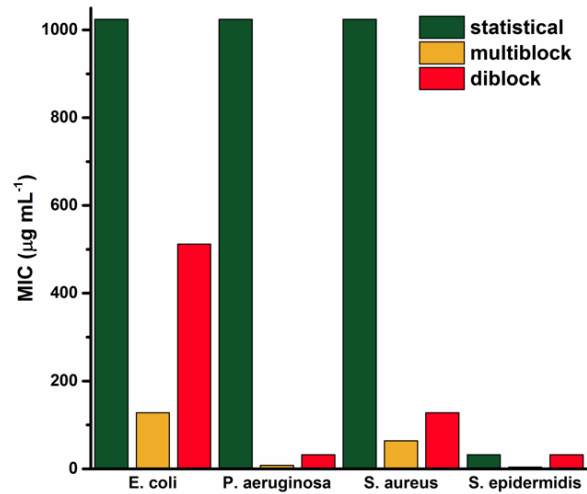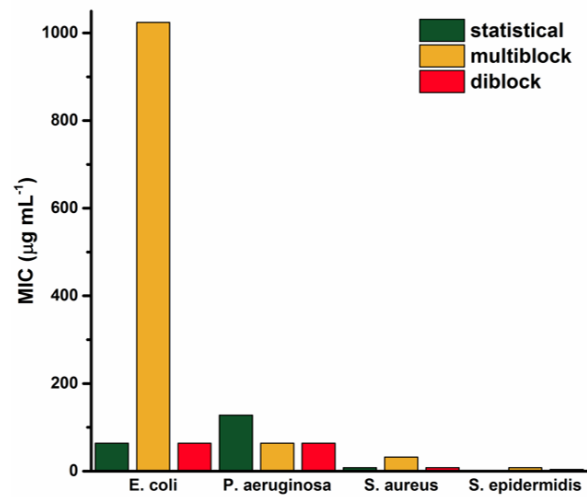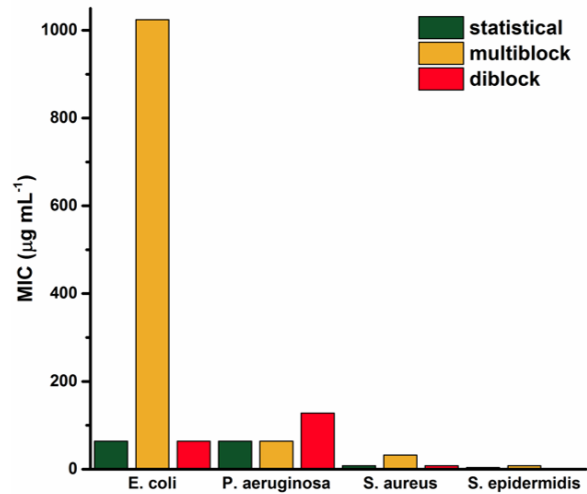
Figure 2.36 - MIC at 30 (A), 50 (B) and 70% (C) AEAM content of various segmentation for each bacteria species.
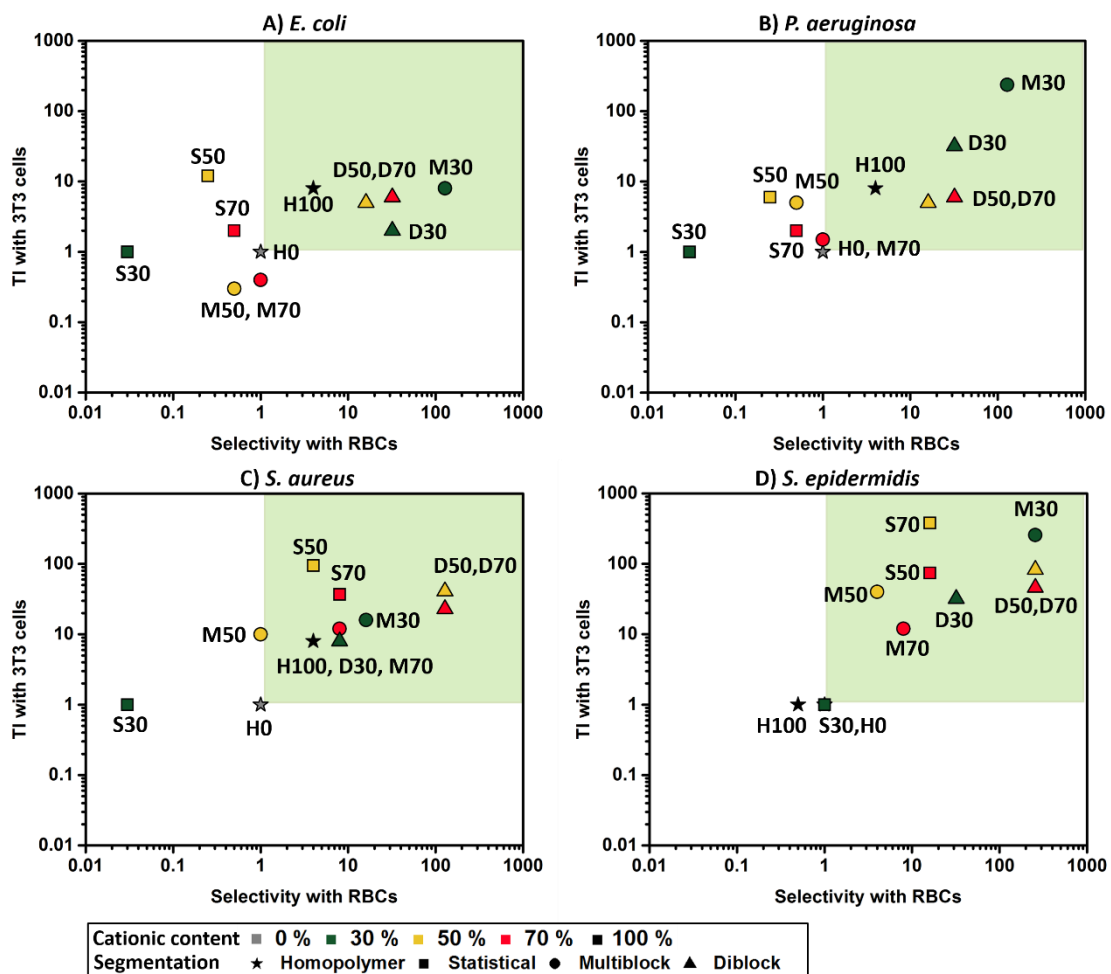
Figure 2.37 - TI of the SAMPs with NIH 3T3 cells against their selectivity with RBCs for *E. coli* **(A),** *P. aeruginosa* **(B),** *S. aureus* **(C) and** *S. epidermidis* **(D).**

2.6 Supporting Tables

Table 2.8 - Experimental conditions used for the synthesis of DP 100 homopolymer and statistical copolymers of NIPAM and BocAEAM.

Sample number		H0	A-S30[Boc]	A-S50[Boc]	A-S70[Boc]	A-H100[Boc]
BocAEAM content (%)		0	32	50	70	100
DP_{total}		104	105	105	105	98
NIPAM	$DP_{targeted}$	104	73	53	32	0
	$m_{monomer\ added}$ (mg)	226	317	226	136	0
BocAEAM	$DP_{targeted}$	0	32	52	73	98
	$m_{monomer\ added}$ (mg)	0	257	429	600	429
$m_{CTA\ added}$ (mg)		4.77	9.54	9.54	9.54	4.77
$V_{dioxane\ added}$ (mL)		0.533	0.980	0.980	0.980	0.533
$V_{water\ added}$ (mL)		0.132	0.266	0.266	0.266	0.132
V_{total} (mL)		1.834	1.246	1.246	1.246	0.665
$m_{VA\text{-}044\ total}$ (mg)		0.647	1.293	1.293	1.293	0.647
$[VA\text{-}044]_0$ (mol L^{-1})		$3.00\ 10^{-3}$	$3.00\ 10^{-3}$	$3.00\ 10^{-3}$	$3.00\ 10^{-3}$	$3.00\ 10^{-3}$
$[monomer]_0$ (mol L^{-1})		3.00	3	3	3	3
$[CTA]_0/[VA\text{-}044]_0$		10	10	10	10	10
L (%)[a]		92	92	92	92	92

[a] Livingness of the polymers, as defined in equation 2.6.

Table 2.9 - Experimental conditions used for the synthesis DP 100 diblock copolymers of NIPAM (NIP) and BocAEAM (BocA).

Sample number	A-D30^{Boc}		A-D50^{Boc}		A-D70^{Boc}	
BocA content (%)	30		49		70	
DP$_{total}$	103		90		99	
Cycles	1	2	1	2	1	2
Monomer	NIP	BocA	NIP	BocA	NIP	BocA
DP$_{targeted}$	72	31	46	44	29	70
m$_{monomer\ added}$ (mg)	339	275	226	429	226	1000
m$_{CTA\ added}$ (mg)	10.2	-	9.54	-	15.9	-
m$_{VA-044\ added}$ (mg)	0.970	0.595	0.862	0.718	1.04	1.84
V$_{dioxane\ added}$ (mL)	0.800	0.125	0.533	0.493	0.640	1.710
V$_{water\ added}$ (mL)	0.200	0.044	0.133	0.173	0.160	0.601
V$_{total}$ (mL)	1.000	1.169	0.666	1.332	0.800	3.111
m$_{VA-044\ total}$ (mg)	0.970	0.756	0.862	0.862	1.035	2.012
[VA-044]$_0$ (mol L^{-1})	3.00 10^{-3}	2.00 10^{-3}	4.00 10^{-3}	2.00 10^{-3}	4.00 10^{-3}	2.00 10^{-3}
[monomer]$_0$ (mol L^{-1})	3.00	1.10	3.00	1.50	2.50	1.50
[CTA]$_0$/[VA-044]$_0$	14	18	15	15	21	11
L (%)[a]	94	95	95	94	96	92
Cumulative L (%)	94	90	95	89	96	88

[a] Livingness of the polymers, as defined in equation 2.6.

Table 2.10 - Experimental conditions used for the synthesis of A-M30^{Boc}, the DP 100 heptablock copolymer of NIPAM (NIP) and BocAEAM (BocA) containing 30 % BocAEAM.

Cycles	1	2	3	4	5	6	7
Monomer	NIP	BocA	NIP	BocA	NIP	BocA	NIP
DP$_{targeted}$	18	10	18	10	18	10	18
m$_{monomer\ added}$ (mg)	226	238	226	238	226	238	226
m$_{CTA\ added}$ (mg)	26.5	-	-	-	-	-	-
m$_{VA-044\ added}$ (mg)	1.08	0.799	1.28	1.68	1.99	2.36	2.67
V$_{dioxane\ added}$ (mL)	0.533	0.261	0.460	0.405	0.351	0.350	0.281
V$_{water\ added}$ (mL)	0.132	0.082	0.129	0.173	0.136	0.157	0.180
V$_{total}$ (mL)	0.665	1.008	1.597	2.175	2.662	3.169	3.630
m$_{VA-044\ total}$ (mg)	1.078	0.98	1.552	2.113	2.587	3.079	3.527
[VA-044]$_0$ (mol L^{-1})	$5.00\ 10^{-3}$	$3.00\ 10^{-3}$	$3.00\ 10^{-3}$	$3.00\ 10^{-3}$	$3.00\ 10^{-3}$	$3.00\ 10^{-3}$	$3.00\ 10^{-3}$
[monomer]$_0$ (mol L^{-1})	3.00	1.10	1.25	0.51	0.75	0.35	0.55
[CTA]$_0$/[VA-044]$_0$	33	37	23	17	14	12	10
L (%)[a]	98	98	96	95	94	92	91
Cumulative L (%)	98	95	91	86	81	75	68

[a] Livingness of the polymers, as defined in equation 2.6.

Table 2.11 - Experimental conditions used for the synthesis of A-M50^{Boc}, the DP 100 decablock copolymer of NIPAM (NIP) and BocAEAM (BocA) containing 50 % BocAEAM.

Cycles	1	2	3	4	5	6	7	8	9	10
Monomer	NIP	BocA	NIP	BocA	NIP	BocA	NIP	BocA	NIP	BocA
$DP_{targeted}$	10	10	10	10	10	10	10	10	10	10
$m_{monomer\ added}$ (mg)	113	214	113	214	113	214	113	214	113	214
$m_{CTA\ added}$ (mg)	23.8	-	-	-	-	-	-	-	-	-
$m_{VA\text{-}044\ added}$ (mg)	0.862	0.601	0.747	0.815	1.00	1.15	1.23	1.39	1.59	2.07
$V_{dioxane\ added}$ (mL)	0.247	0.349	0.267	0.222	0.169	0.180	0.121	0.160	0.212	0.492
$V_{water\ added}$ (mL)	0.086	0.087	0.075	0.096	0.069	0.077	0.084	0.094	0.110	0.139
V_{total} (mL)	0.333	0.769	1.111	1.429	1.667	1.924	2.129	2.383	2.705	3.336
$m_{VA\text{-}044\ total}$ (mg)	0.862	0.746	1.078	1.293	1.617	1.865	2.064	2.31	2.622	3.233
$[VA\text{-}044]_0$ (mol L^{-1})	8.00 10^{-3}	3.00 10^{-3}	3.00 10^{-3}	3.00 10^{-3}	3.00 10^{-3}	3.00 10^{-3}	3.00 10^{-3}	3.00 10^{-3}	3.00 10^{-3}	3.00 10^{-3}
$[monomer]_0$ (mol L^{-1})	3.00	1.30	0.90	0.70	0.60	0.52	0.47	0.42	0.37	0.30
$[CTA]_0/[VA\text{-}044]_0$	38	43	30	23	20	17	16	14	12	10
L (%)[a]	98	98	97	96	95	95	94	94	93	91
Cumulative L (%)	98	96	93	89	85	81	76	71	66	60

[a] Livingness of the polymers, as defined in equation 2.6.

Table 2.12 - Experimental conditions used for the synthesis of A-M70^{Boc}, the DP 100 heptablock copolymer of NIPAM (NIP) and BocAEAM (BocA) containing 70 % BocAEAM.

Cycles	1	2	3	4	5	6	7
Monomer	BocA	NIP	BocA	NIP	BocA	NIP	BocA
$DP_{targeted}$	18	11	18	11	18	11	18
$m_{monomer\ added}$ (mg)	429	126	429	126	429	126	429
$m_{CTA\ added}$ (mg)	26.5	-	-	-	-	-	-
$m_{VA-044\ added}$ (mg)	1.07	1.13	1.55	1.80	2.16	2.49	2.82
$V_{dioxane\ added}$ (mL)	0.533	0.261	0.460	0.405	0.351	0.350	0.281
$V_{water\ added}$ (mL)	0.132	0.082	0.129	0.173	0.136	0.157	0.180
V_{total} (mL)	0.665	1.008	1.597	2.175	2.662	3.169	3.630
$m_{VA-044\ total}$ (mg)	1.078	1.4	1.94	2.343	2.812	3.266	3.731
$[VA-044]_0$ (mol L^{-1})	$5.00\ 10^{-3}$	$3.00\ 10^{-3}$	$3.00\ 10^{-3}$	$3.00\ 10^{-3}$	$3.00\ 10^{-3}$	$3.00\ 10^{-3}$	$3.00\ 10^{-3}$
$[monomer]_0$ (mol L^{-1})	2.00	0.77	1.00	0.46	0.69	0.33	0.52
$[CTA]_0/[VA-044]_0$	22	26	19	15	13	11	10
L (%)[a]	96	96	95	94	93	92	91
Cumulative L (%)	96	93	88	83	77	71	65

[a] Livingness of the polymers, as defined in equation 2.6.

Table 2.13. Experimental conditions and characterisation data for the synthesis of the diblock copolymers A-D30[Boc], A-D50[Boc], A-D70[Boc].

	Block n°	Monomer conversion[a] (%)	$M_{n,th}$[b] (g.mol^{-1})	$M_{n,SEC}$[c] (g.mol^{-1})	$Đ$[c]
A-D30[Boc]	1st	99	3400	10600	1.08
	2nd	>99	15000	16200	1.10
A-D50[Boc]	1st	>99	5400	8200	1.08
	2nd	>99	14900	17500	1.17
A-D70[Boc]	1st	>99	3500	5300	1.18
	2nd	>99	18500	19000	1.20

[a] Determined by ^{1}H NMR using equation 2.4.

[b] Theoretical molecular weight calculated from equation 2.5.

[c] Determined by SEC/RI in DMF using PMMA as molecular weight standards.

Table 2.14. Experimental conditions and characterisation data for the synthesis of the heptablock A-M30[Boc].

Block n°	Monomer conversion[a] (%)	$M_{n,th}$[b] (g.mol^{-1})	$M_{n,SEC}$[c] (g.mol^{-1})	$Đ$[c]
1st	99	2300	-	-
2nd	>99	4420	6800	1.08
3rd	>99	6500	9100	1.09
4th	>99	8600	10900	1.09
5th	>99	10630	14100	1.10
6th	>99	11800	14900	1.20
7th	>99	13800	15800	1.29

[a] Determined by ^{1}H NMR using equation 2.4.

 [b] Theoretical molecular weight calculated from equation 2.5.

[c] Determined by SEC/RI in DMF using PMMA as molecular weight standards.

Table 2.15. Experimental conditions and characterisation data for the synthesis of the decablock A-M50^{Boc}.

Block n°	Monomer conversion[a] (%)	$M_{n,th}$[b] (g.mol^{-1})	$M_{n,SEC}$[c] (g.mol^{-1})	$Đ$[c]
1st	99	1400	-	-
2nd	>99	3500	5300	1.07
3rd	>99	4600	6300	1.08
4th	>99	6800	9000	1.09
5th	>99	7900	11700	1.09
6th	>99	10100	12600	1.13
7th	>99	11200	13600	1.19
8th	>99	13300	14000	1.22
9th	>99	14500	14900	1.28
10th	>99	16600	17100	1.38

[a] Determined by ^{1}H NMR using equation 2.4.

[b] Theoretical molecular weight calculated from equation 2.5.

[c] Determined by SEC/RI in DMF using PMMA as molecular weight standards.

Table 2.16. Experimental conditions and characterisation data for the synthesis of the heptablock A-M70^{Boc}.

Block n°	Monomer conversion[a] (%)	$M_{n,th}$[b] (g.mol^{-1})	$M_{n,SEC}$[c] (g.mol^{-1})	Đ[c]
1st	99	4100	-	-
2nd	>99	5300	7100	1.08
3rd	>99	9200	10500	1.09
4th	>99	10400	11100	1.14
5th	>99	14300	14600	1.21
6th	>99	15500	15900	1.23
7th	>99	19400	17400	1.34

[a] Determined by ^{1}H NMR using equation 2.4

[b] Theoretical molecular weight calculated from equation 2.5.

[c] Determined by SEC/RI in DMF using PMMA as molecular weight standards.

Table 2.17 - Characterisation data of deprotected polymers.

	Sample	AEAM content (%)	$M_{n,th}$[a] (g mol^{-1})	Retention ratio[b] (%)	Z-average[c] (nm)	PDI[c]
Homopolymer	H0	0	12000	100	580	0.016
	A-H100	100	15000	0	7	0.223
Statistical	A-S30	32	13300	40	6	0.536
	A-S50	50	14070	20	7	0.695
	A-S70	70	14850	10	7	0.654
Multiblock	A-M30	30	12900	73	6	0.326
	A-M50	50	13400	37	7	0.615
	A-M70	70	14800	23	6	0.393
Diblock	A-D30	30	13000	87	6	0.808
	A-D50	49	12100	67	5	0.311
	A-D70	71	14000	50	8	0.313

[a] Theoretical molecular weight of the protected polymers calculated from equation 2.5.

[b] From HPLC data measured in water/ACN in a C18 column (gradient 1 to 95 % ACN in 50 minutes). Elution was calculated according to equation 2.3.

[c] Measured by DLS in Phosphate Buffer Saline (PBS) at 37°C and 1 mg mL^{-1}

Table 2.18 - Therapeutic index values of the SAMPs with Caco-2 cells.

Sample name	Therapeutic Index (TI) [b] Caco-2			
	E. coli	*P. aeruginosa*	*S. aureus*	*S. epidermidis*
H0	> 1	> 1	> 1	> 1
A-H100	< 8	< 8	< 8	< 1
A-S30	> 1	> 1	> 1	> 1
A-S50	1.4	0.7	11	45
A-S70	< 0.5	< 0.5	< 8	< 16
A-M30	2	38	5	77
A-M50	0.1	1	2	7.7
A-M70	< 0.3	< 1	< 8	< 8
A-D30	1.4	22	3	45
A-D50	1.2	1.2	10	19
A-D70	2	2	10	19

[a] IC$_{50}$ was determined as the concentration at which 50 % inhibition occurred.

[b] Therapeutic index (TI) was calculated as the ratio of the IC$_{50}$ towards Caco-2 with the MIC of the bacterial species.

2.7   References

1.   Antimicrobial resistance: Global report on surveillance; World Health Organization: 2014.

2.   Spellberg, B.; Guidos, R.; Gilbert, D.; Bradley, J.; Boucher, H. W.; Scheld, W. M.; Bartlett, J. G.; Edwards, J. J., The Epidemic of Antibiotic-Resistant Infections: A Call to Action for the Medical Community from the Infectious Diseases Society of America. *Clinical Infectious Diseases* **2008,** *46* (2), 155-164.

3.   Levy, S. B.; Marshall, B., Antibacterial resistance worldwide: causes, challenges and responses. *Nat Med* **2004,** *10*, S122-S129.

4.   Van Der Meer, J. W. M.; Fears, R.; Ter Meulen, V., Can we Tackle the Antibiotic Threat? *European Review* **2016,** *24* (1), 49-62.

5.   Bush, K.; Courvalin, P.; Dantas, G.; Davies, J.; Eisenstein, B.; Huovinen, P.; Jacoby, G. A.; Kishony, R.; Kreiswirth, B. N.; Kutter, E.; Lerner, S. A.; Levy, S.; Lewis, K.; Lomovskaya, O.; Miller, J. H.; Mobashery, S.; Piddock, L. J. V.; Projan, S.; Thomas, C. M.; Tomasz, A.; Tulkens, P. M.; Walsh, T. R.; Watson, J. D.; Witkowski, J.; Witte, W.; Wright, G.; Yeh, P.; Zgurskaya, H. I., Tackling antibiotic resistance. *Nat Rev Micro* **2011,** *9* (12), 894-896.

6.   Otto Cars; Högberg, L. D. M., Mary; Nordberg,Olle; Sivaraman,Satya; Lundborg,Cecilia S.; So,Anthony D.; Tomson,Gö, Meeting the challenge of antibiotic resistance. *British Medical Journal* **2008,** *337*.

7.   Brown, E. D.; Wright, G. D., Antibacterial drug discovery in the resistance era. *Nature* **2016,** *529* (7586), 336-343.

8.   Zasloff, M., Antimicrobial peptides of multicellular organisms. *Nature* **2002,** *415* (6870), 389-395.

9.   Hancock, R. E. W.; Sahl, H.-G., Antimicrobial and host-defense peptides as new anti-infective therapeutic strategies. *Nat Biotech* **2006,** *24* (12), 1551-1557.

10.   Izumiya, N., Kato, T., Aoyagi, H., Waki, M., Kondo, M., Synthetic Aspects of Biologically Active Cyclic Peptides-Gramicidin S and Tyrocidine. *Halsted Press* **1979**, 16-27.

11.   Ahmad, A.; Azmi, S.; Srivastava, R. M.; Srivastava, S.; Pandey, B. K.; Saxena, R.; Bajpai, V. K.; Ghosh, J. K., Design of Nontoxic Analogues of Cathelicidin-Derived Bovine Antimicrobial Peptide BMAP-27: The Role of Leucine as Well as Phenylalanine Zipper Sequences in Determining Its Toxicity. *Biochemistry* **2009,** *48* (46), 10905-10917.

12.   Seo, M.-D.; Won, H.-S.; Kim, J.-H.; Mishig-Ochir, T.; Lee, B.-J., Antimicrobial Peptides for Therapeutic Applications: A Review. *Molecules* **2012,** *17* (10), 12276.

13.   Ganewatta, M. S.; Tang, C., Controlling macromolecular structures towards effective antimicrobial polymers. *Polymer* **2015,** *63*, A1-A29.

14.   Hartlieb, M.; Williams, E. G. L.; Kuroki, A.; Perrier, S.; Locock, K., E. S. , Antimicrobial polymers: Mimicking amino acid functionality, sequence control and three-dimensional structure of host-defense peptides. *Curr. Med. Chem.* **2017,** *24*, 2115-2140.

15.   Kuroda, K.; Caputo, G. A., Antimicrobial polymers as synthetic mimics of host-defense peptides. *Wiley Interdisciplinary Reviews: Nanomedicine and Nanobiotechnology* **2013,** *5* (1), 49-66.

16. Engler, A. C.; Wiradharma, N.; Ong, Z. Y.; Coady, D. J.; Hedrick, J. L.; Yang, Y.-Y., Emerging trends in macromolecular antimicrobials to fight multi-drug-resistant infections. *Nano Today* **2012,** *7* (3), 201-222.

17. Locock, K. E. S.; Michl, T. D.; Valentin, J. D. P.; Vasilev, K.; Hayball, J. D.; Qu, Y.; Traven, A.; Griesser, H. J.; Meagher, L.; Haeussler, M., Guanylated Polymethacrylates: A Class of Potent Antimicrobial Polymers with Low Hemolytic Activity. *Biomacromolecules* **2013,** *14* (11), 4021-4031.

18. Gabriel, G. J.; Madkour, A. E.; Dabkowski, J. M.; Nelson, C. F.; Nüsslein, K.; Tew, G. N., Synthetic Mimic of Antimicrobial Peptide with Nonmembrane-Disrupting Antibacterial Properties. *Biomacromolecules* **2008,** *9* (11), 2980-2983.

19. Locock, K. E. S.; Michl, T. D.; Stevens, N.; Hayball, J. D.; Vasilev, K.; Postma, A.; Griesser, H. J.; Meagher, L.; Haeussler, M., Antimicrobial Polymethacrylates Synthesized as Mimics of Tryptophan-Rich Cationic Peptides. *ACS Macro Letters* **2014,** *3* (4), 319-323.

20. Ilker, M. F.; Nüsslein, K.; Tew, G. N.; Coughlin, E. B., Tuning the Hemolytic and Antibacterial Activities of Amphiphilic Polynorbornene Derivatives. *J. Am. Chem. Soc.* **2004,** *126* (48), 15870-15875.

21. Mowery, B. P.; Lee, S. E.; Kissounko, D. A.; Epand, R. F.; Epand, R. M.; Weisblum, B.; Stahl, S. S.; Gellman, S. H., Mimicry of Antimicrobial Host-Defense Peptides by Random Copolymers. *J. Am. Chem. Soc.* **2007,** *129* (50), 15474-15476.

22. Kuroda, K.; DeGrado, W. F., Amphiphilic Polymethacrylate Derivatives as Antimicrobial Agents. *J. Am. Chem. Soc.* **2005,** *127* (12), 4128-4129.

23. Kuroda, K.; Caputo, G. A.; DeGrado, W. F., The Role of Hydrophobicity in the Antimicrobial and Hemolytic Activities of Polymethacrylate Derivatives. *Chem. Eur. J.* **2009,** *15* (5), 1123-1133.

24. Muñoz-Bonilla, A.; Fernández-García, M., Polymeric materials with antimicrobial activity. *Progress in Polymer Science* **2012,** *37* (2), 281-339.

25. Timofeeva, L.; Kleshcheva, N., Antimicrobial polymers: mechanism of action, factors of activity, and applications. *Appl Microbiol Biotechnol* **2011,** *89* (3), 475-492.

26. Lam, S. J.; O'Brien-Simpson, N. M.; Pantarat, N.; Sulistio, A.; Wong, E. H. H.; Chen, Y.-Y.; Lenzo, J. C.; Holden, J. A.; Blencowe, A.; Reynolds, E. C.; Qiao, G. G., Combating multidrug-resistant Gram-negative bacteria with structurally nanoengineered antimicrobial peptide polymers. *Nature Microbiology* **2016,** *1*, 16162.

27. Phillips, D. J.; Harrison, J.; Richards, S.-J.; Mitchell, D. E.; Tichauer, E.; Hubbard, A. T. M.; Guy, C.; Hands-Portman, I.; Fullam, E.; Gibson, M. I., Evaluation of the Antimicrobial Activity of Cationic Polymers against Mycobacteria: Toward Antitubercular Macromolecules. *Biomacromolecules* **2017,** *18* (5), 1592-1599.

28. Muñoz-Bonilla, A.; Fernández-García, M., The roadmap of antimicrobial polymeric materials in macromolecular nanotechnology. *European Polymer Journal* **2015,** *65* (Supplement C), 46-62.

29. Saravanan, R.; Bhattacharjya, S., Oligomeric structure of a cathelicidin antimicrobial peptide in dodecylphosphocholine micelle determined by NMR spectroscopy. *Biochimica et Biophysica Acta (BBA) - Biomembranes* **2011,** *1808* (1), 369-381.

30. Oren, Z.; Lerman, J. C.; Gudmundsson, G. H.; Agerberth, B.; Shai, Y., Structure and organization of the human antimicrobial peptide LL-37 in phospholipid membranes: relevance to the molecular basis for its non-cell-selective activity. *The Biochemical journal* **1999,** *341 (Pt 3)* (Pt 3), 501-513.

31. Yao, D.; Guo, Y.; Chen, S.; Tang, J.; Chen, Y., Shaped core/shell polymer nanoobjects with high antibacterial activities via block copolymer microphase separation. *Polymer* **2013,** *54* (14), 3485-3491.

32. Costanza, F.; Padhee, S.; Wu, H.; Wang, Y.; Revenis, J.; Cao, C.; Li, Q.; Cai, J., Investigation of antimicrobial PEG-poly(amino acid)s. *RSC Advances* **2014,** *4* (4), 2089-2095.

33. Nguyen, T.-K.; Lam, S. J.; Ho, K. K. K.; Kumar, N.; Qiao, G. G.; Egan, S.; Boyer, C.; Wong, E. H. H., Rational Design of Single-Chain Polymeric Nanoparticles That Kill Planktonic and Biofilm Bacteria. *ACS Infectious Diseases* **2017,** *3* (3), 237-248.

34. Oda, Y.; Kanaoka, S.; Sato, T.; Aoshima, S.; Kuroda, K., Block versus Random Amphiphilic Copolymers as Antibacterial Agents. *Biomacromolecules* **2011,** *12* (10), 3581-3591.

35. Wang, Y.; Xu, J.; Zhang, Y.; Yan, H.; Liu, K., Antimicrobial and Hemolytic Activities of Copolymers with Cationic and Hydrophobic Groups: A Comparison of Block and Random Copolymers. *Macromolecular Bioscience* **2011,** *11* (11), 1499-1504.

36. Liu, R.; Chen, X.; Chakraborty, S.; Lemke, J. J.; Hayouka, Z.; Chow, C.; Welch, R. A.; Weisblum, B.; Masters, K. S.; Gellman, S. H., Tuning the Biological Activity Profile of Antibacterial Polymers via Subunit Substitution Pattern. *J. Am. Chem. Soc.* **2014,** *136* (11), 4410-4418.

37. Hadjichristidis, N.; Pispas, S.; Floudas, G., Dilute Solutions of Block Copolymers in Nonselective Solvents. In *Block Copolymers*, 2003; pp 195-202.

38. Hadjichristidis, N.; Pispas, S.; Floudas, G., Dilute Solutions of Block Copolymers in Selective Solvents. In *Block Copolymers*, 2003; pp 203-231.

39. Zamfir, M.; Lutz, J.-F., Ultra-precise insertion of functional monomers in chain-growth polymerizations. *Nature Communications* **2012,** *3*, 1138.

40. Moad, G.; Rizzardo, E.; Thang, S. H., Living Radical Polymerization by the RAFT Process – A Third Update. *Australian Journal of Chemistry* **2012,** *65* (8), 985-1076.

41. Perrier, S.; Takolpuckdee, P., Macromolecular design via reversible addition–fragmentation chain transfer (RAFT)/xanthates (MADIX) polymerization. *Journal of Polymer Science Part A: Polymer Chemistry* **2005,** *43* (22), 5347-5393.

42. Simula, A.; Nikolaou, V.; Anastasaki, A.; Alsubaie, F.; Nurumbetov, G.; Wilson, P.; Kempe, K.; Haddleton, D. M., Synthesis of well-defined α,ω-telechelic multiblock copolymers in aqueous medium: *in situ* generation of α,ω-diols. *Polym. Chem.* **2015,** *6* (12), 2226-2233.

43. Boyer, C.; Soeriyadi, A. H.; Zetterlund, P. B.; Whittaker, M. R., Synthesis of Complex Multiblock Copolymers via a Simple Iterative Cu(0)-Mediated Radical Polymerization Approach. *Macromolecules* **2011,** *44* (20), 8028-8033.

44. Martin, L.; Gody, G.; Perrier, S., Preparation of complex multiblock copolymers via aqueous RAFT polymerization at room temperature. *Polym. Chem.* **2015,** *6* (27), 4875-4886.

45. Gody, G.; Maschmeyer, T.; Zetterlund, P. B.; Perrier, S., Exploitation of the Degenerative Transfer Mechanism in RAFT Polymerization for Synthesis of Polymer of High Livingness at Full Monomer Conversion. *Macromolecules* **2014,** *47* (2), 639-649.

46. Gody, G.; Maschmeyer, T.; Zetterlund, P. B.; Perrier, S., Pushing the Limit of the RAFT Process: Multiblock Copolymers by One-Pot Rapid Multiple Chain Extensions at Full Monomer Conversion. *Macromolecules* **2014,** *47* (10), 3451-3460.

47. Hornung, C. H.; Nguyen, X.; Kyi, S.; Chiefari, J.; Saubern, S., Synthesis of RAFT Block Copolymers in a Multi-Stage Continuous Flow Process Inside a Tubular Reactor. *Australian Journal of Chemistry* **2013,** *66* (2), 192-198.

48.   Kuroki, A.; Martinez-Botella, I.; Hornung, C. H.; Martin, L.; Williams, E. G. L.; Locock, K. E. S.; Hartlieb, M.; Perrier, S., Looped flow RAFT polymerization for multiblock copolymer synthesis. *Polym. Chem.* **2017,** *8* (21), 3249-3254.

49.   Engelis, N. G.; Anastasaki, A.; Nurumbetov, G.; Truong, N. P.; Nikolaou, V.; Shegiwal, A.; Whittaker, M. R.; Davis, T. P.; Haddleton, D. M., Sequence-controlled methacrylic multiblock copolymers via sulfur-free RAFT emulsion polymerization. *Nat Chem* **2017,** *9* (2), 171-178.

50.   Barth, J.; Buback, M.; Hesse, P.; Sergeeva, T., Termination and Transfer Kinetics of Butyl Acrylate Radical Polymerization Studied via SP-PLP-EPR. *Macromolecules* **2010,** *43* (9), 4023-4031.

51.   Takahashi, H.; Palermo, E. F.; Yasuhara, K.; Caputo, G. A.; Kuroda, K., Molecular Design, Structures, and Activity of Antimicrobial Peptide-Mimetic Polymers. *Macromolecular Bioscience* **2013,** *13* (10), 1285-1299.

52.   Sambhy, V.; Peterson, B. R.; Sen, A., Antibacterial and Hemolytic Activities of Pyridinium Polymers as a Function of the Spatial Relationship between the Positive Charge and the Pendant Alkyl Tail. *Angew. Chem. Int. Ed.* **2008,** *47* (7), 1250-1254.

53.   Sovadinova, I.; Palermo, E. F.; Huang, R.; Thoma, L. M.; Kuroda, K., Mechanism of Polymer-Induced Hemolysis: Nanosized Pore Formation and Osmotic Lysis. *Biomacromolecules* **2011,** *12* (1), 260-268.

54.   Alidedeoglu, A. H.; York, A. W.; McCormick, C. L.; Morgan, S. E., Aqueous RAFT polymerization of 2-aminoethyl methacrylate to produce well-defined, primary amine functional homo- and copolymers. **2009,** *47* (20), 5405-5415.

55.   Figg, C. A.; Simula, A.; Gebre, K. A.; Tucker, B. S.; Haddleton, D. M.; Sumerlin, B. S., Polymerization-induced thermal self-assembly (PITSA). *Chemical Science* **2015,** *6* (2), 1230-1236.

56.   Lienkamp, K.; Kumar, K.-N.; Som, A.; Nüsslein, K.; Tew, G. N., "Doubly Selective" Antimicrobial Polymers: How Do They Differentiate between Bacteria? *Chem. Eur. J.* **2009,** *15* (43), 11710-11714.

57.   Gody, G.; Zetterlund, P. B.; Perrier, S.; Harrisson, S., The limits of precision monomer placement in chain growth polymerization. *Nature Communications* **2016,** *7*, 10514.

58.   Michl, T. D.; Locock, K. E. S.; Stevens, N. E.; Hayball, J. D.; Vasilev, K.; Postma, A.; Qu, Y.; Traven, A.; Haeussler, M.; Meagher, L.; Griesser, H. J., RAFT-derived antimicrobial polymethacrylates: elucidating the impact of end-groups on activity and cytotoxicity. *Polym. Chem.* **2014,** *5* (19), 5813-5822.

59.   Valdebenito, A.; Encinas, M. V., Effect of solvent on the free radical polymerization of N,N-dimethylacrylamide. *Polymer International* **2010,** *59* (9), 1246-1251.

60.   Hobson, L. J.; Feast, W. J., Poly(amidoamine) hyperbranched systems: synthesis, structure and characterization. *Polymer* **1999,** *40* (5), 1279-1297.

61.   Dewick, P. M., Essentials of Organic Chemistry: For Students of Pharmacy, Medicinal Chemistry and Biological Chemistry. Wiley: 2006; p 161.

62.   Suh, J.; Paik, H. J.; Hwang, B. K., Ionization of Poly(ethylenimine) and Poly(allylamine) at Various pH′s. *Bioorg. Chem.* **1994,** *22* (3), 318-327.

63.   Koper, G. J. M.; van Duijvenbode, R. C.; Stam, D. D. P. W.; Steuerle, U.; Borkovec, M., Synthesis and Protonation Behavior of Comblike Poly(ethyleneimine). *Macromolecules* **2003,** *36* (7), 2500-2507.

64.   Glöckner, G.; Müller, A. H. E., Gradient high-performance liquid chromatography of statistical and block copolymers of styrene and t-butyl methacrylate. *Journal of Applied Polymer Science* **1989,** *38* (9), 1761-1774.

65.   Ward, M. A. G., T.K., Thermoresponsive Polymers for Biomedical Applications. *Polymers* **2011,** *3*, 1215-1242.

66.   Nagarajan, R., Amphiphilic Surfactants and Amphiphilic Polymers: Principles of Molecular Assembly. In *Amphiphiles: Molecular Assembly and Applications*, American Chemical Society: 2011; Vol. 1070, pp 1-22.

67.   Epand, R. F.; Savage, P. B.; Epand, R. M., Bacterial lipid composition and the antimicrobial efficacy of cationic steroid compounds (Ceragenins). *Biochimica et Biophysica Acta (BBA) - Biomembranes* **2007,** *1768* (10), 2500-2509.

68.   Silhavy, T. J.; Kahne, D.; Walker, S., The Bacterial Cell Envelope. *Perspectives in Biology* **2010,** *2* (5), 1-16.

69.   Oddo, A.; Hansen, P. R., Hemolytic Activity of Antimicrobial Peptides. In *Antimicrobial Peptides: Methods and Protocols*, Hansen, P. R., Ed. Springer New York: New York, NY, 2017; pp 427-435.

70.   Angelis, I. D.; Turco, L., Caco-2 Cells as a Model for Intestinal Absorption. *Current Protocols in Toxicology* **2011,** *47* (1), 6-15.

71.   Caballero-Díaz, E.; Pfeiffer, C.; Kastl, L.; Rivera-Gil, P.; Simonet, B.; Valcárcel, M.; Jiménez-Lamana, J.; Laborda, F.; Parak, W. J., The Toxicity of Silver Nanoparticles Depends on Their Uptake by Cells and Thus on Their Surface Chemistry. **2013,** *30* (12), 1079-1085.

72.   Muller, P. Y.; Milton, M. N., The determination and interpretation of the therapeutic index in drug development. *Nat Rev Drug Discov* **2012,** *11* (10), 751-761.

73.   Gullberg, E.; Cao, S.; Berg, O. G.; Ilbäck, C.; Sandegren, L.; Hughes, D.; Andersson, D. I., Selection of Resistant Bacteria at Very Low Antibiotic Concentrations. *PLOS Pathogens* **2011,** *7* (7), 2158.

74.   Larnaudie, S. C.; Brendel, J. C.; Jolliffe, K. A.; Perrier, S., Cyclic peptide–polymer conjugates: Grafting-to vs grafting-from. *Journal of Polymer Science Part A: Polymer Chemistry* **2016,** *54* (7), 1003-1011.

Chapter 3 Effect of sequence on the selectivity of ammonium and guanidinium polymers towards MRSA
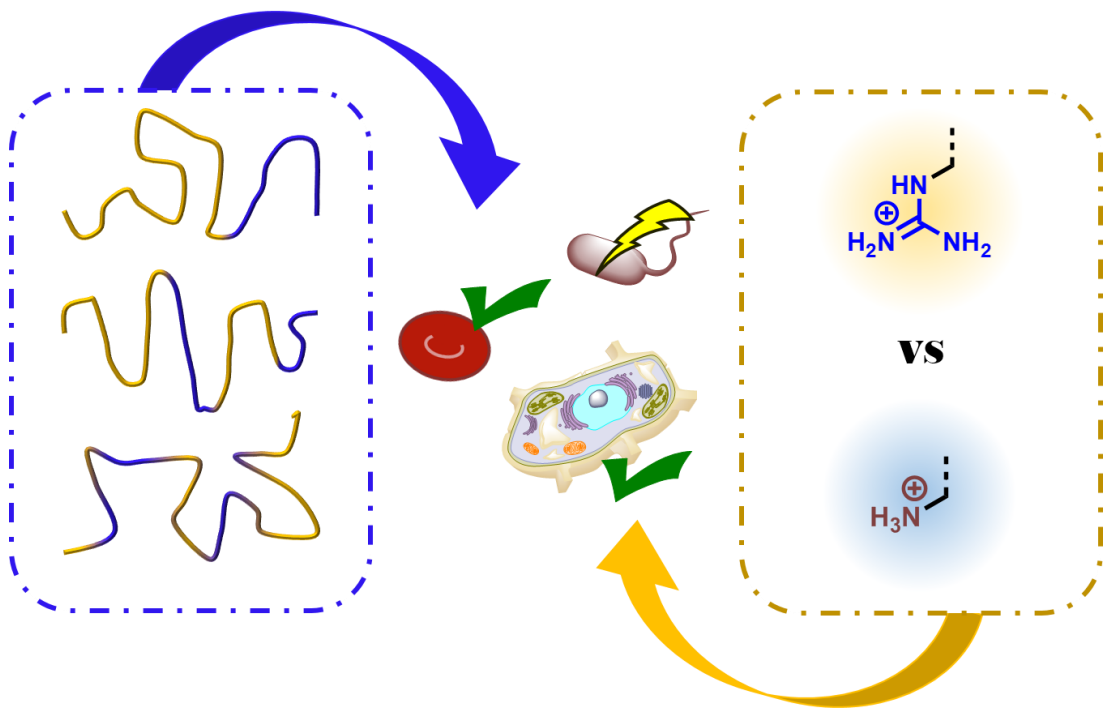
Abstract

As new treatments against MRSA are being investigated, cationic SMAMPs have been considered as potential long-term solutions to treating staphylococcal infections. The type of charge on SMAMPs has been reported to influence antimicrobial activity as well as haemocompatibility. In this chapter, the selectivity of guanidinium containing polymers towards RBCs and epithelial cells was compared to that of their ammonium counterparts for the treatment of MRSA. Firstly, a library of ammonium and guanidinium SMAMPs with varying monomer distribution was synthesised using RAFT polymerisation. Their compatibility with RBCs (both haemolysis and haemagglutination) and two human epithelial cell lines has been evaluated. The guanidinium polymers appeared to be slightly more toxic towards mammalian cells than their ammonium counterparts, but their haemocompatibility remained similar. Finally, the antimicrobial activity against both MSSA and MRSA was assessed. It was demonstrated that the guanidinium SMAMPs exhibited a higher potency towards MRSA than the ammonium copolymers. Furthermore, chapter 2 reported that monomer distribution can have a drastic effect on the biological properties of ammonium SMAMPs. Similar observations on selectivity were observed when investigating monomer distribution in guanidinium containing polymers. Although toxicity towards mammalian cells increased with increasing segregation of the cationic and hydrophobic functionalities, the antimicrobial activity of the diblock copolymers outperformed that of their tetrablock and statistical counterparts. Therefore, the guanidinium diblock appears to be the most potent candidate for applications against MRSA.

3.1 Introduction

Staphylococcus Aureus (*S. aureus*) is a common bacterial species in both community and hospital-acquired infections for which the methicillin-resistant strains (MRSA) are causing over 50 % of nosocomial infections in patients in intensive care units (ICUs) in the USA.[1] Vancomycin, a glycopeptide which inhibits cell wall synthesis, is currently the last-resort antibiotic being used to treat severe MRSA infections.[2] However, in the last 20 years, some *S. aureus* strains have developed reduced susceptibility or complete resistance towards vancomycin.[3] Moreover, the glycopeptide is associated with nephrotoxicity, particularly for invasive infections.[4] Therefore, an alternative to vancomycin which can circumvent the adaptability of *S. aureus* is urgently needed. One treatment strategy involves designing agents which target the bacterial membrane, as opposed to highly specific functions, to reduce the chance of bacteria developing resistance.[5] Antimicrobial peptides (AMPs) have been extensively investigated in this regard as their hydrophobic and cationic residues appear to efficiently disrupt bacterial membranes.[6-7] More importantly, the susceptibility of bacteria towards them seems to be maintained.[5]

Synthetic mimics of AMPs (SMAMPs) with various hydrophobic and cationic functionalities have been studied.[8] The type of charge can not only dictate the binding efficiency of a SAMP to bacterial membrane, but it is also interconnected to the overall amphiphilic balance of the material. Although the majority of naturally occurring AMPs consist largely of lysine or arginine residues, quaternary ammonium functionalities have been utilised in SMAMPs as their positive charge is independent to the pH of their environment.[9] However, polymers bearing quaternised amines were shown to be more hydrophilic than their primary amine equivalent at pH 6.[10] This observation can be attributed to the protonation of functionalities on a polymer chain being strongly influenced by neighbouring charges. Therefore, hydrophobic alkyl substituents (at least 4 carbons) had to be used on the quaternary amines of antimicrobial polypeptides in order to reach similar levels of antimicrobial activity as SMAMPs with primary amines.[11-12] Similarly, the effect of the type of charge was further investigated with methacrylamide-based copolymers bearing primary and tertiary amine pendant groups.[13] The SMAMPs with the highest content of primary amine were shown to be the most potent against bacteria. These results could be explained by a difference in binding affinity of the various cations to bacterial membranes. Despite increased levels of haemolysis induced by primary amine bearing polymers, these materials retained a higher selectivity compared to their quaternary counterparts.[10-11]

As arginine has as greater pK_a than lysine (12.5 and 8.9, respectively),[14-15] a considerable effect on the antimicrobial activity of the resulting polymers is expected when replacing one functionality by the other, although both functionalities would be protonated at physiological pH. Indeed, Tew and co-workers noted a superior antimicrobial potency for polyarginine mimics compared to polylysine mimics when using polyoxanorbornenes.[16] Similar results were obtained by Locock *et al.* with polymethacrylates: the antimicrobial activity of guanidinium polymers was higher than that of their ammonium counterparts whilst a low toxicity towards red blood cells was maintained.[17] However, the opposite trend was reported with the antimicrobial effect decreasing with increased guanidinium content, in a study using fully cationic polymethacrylamides with ammonium and guanidinium functionalities.[18] The discrepancy in the results could be due to the absence of hydrophobic character in the SMAMPs in the latter case. Additionally, the ammonium/guanidinium functional polymethacrylamide copolymers were shown to be more toxic towards mammalian cells with increasing guanidinium content.[18] Despite the promising results on the antimicrobial activity of guanidinium SMAMPs, beside haemocompatibility studies, the toxicity of the polymers towards mammalian cells has not been extensively investigated to the best of our knowledge.

Previous reports described the synthesis of guanidinium containing polymers by post-polymerisation functionalisation.[17, 19] Guanidinium monomers could also be directly polymerised with or without Boc protecting groups using ROMP or RAFT.[16, 20-22] In addition to being suitable for various types of monomers, the latter technique has been utilised to prepare polymers with precisely defined compositions and narrow molar mass distributions.[23-24]

In the previous chapter, the effect of monomer sequence on both the antimicrobial activity and the compatibility towards mammalian cells was highlighted using ammonium block copolymers synthesised by RAFT. However, such an effect has yet to be reported with other types of cationic groups. This chapter focuses on the synthesis of guanidinium copolymers with different monomer distributions (statistical, tetrablock and diblock copolymers) *via* RAFT polymerisation. In order to establish a comparison between ammonium and guanidinium SMAMPs, the compatibility with human epithelial cells in addition to their toxicity towards red blood cells was examined. Following this, their potency against MSSA and MRSA was investigated. Ultimately, this study establishes design parameters which may aid in the development of efficient treatment of MRSA.

3.2   Results and discussion

3.2.1   Synthesis and characterisation

In order to study the effect of the type of cationic group on the polymer activity against methicillin-susceptible *S. aureus* (MSSA) and MRSA, acrylamide monomers were used, guanidino-ethylacrylamide (GEAM) and amino-ethylacrylamide (AEAM), mimicking arginine and lysine respectively. The acrylamide monomer family is particularly suitable for the synthesis of multiblock copolymers *via* RAFT since acrylamides possess a high rate constant of propagation (k_p) and therefore, it is possible to polymerise them to high conversion with much lower initiator concentrations than other monomer families, such as methacrylates.[25] GEAM and AEAM monomers were synthesised with Boc protecting groups (diBocGEAM and BocAEAM, respectively) in order to avoid any aminolysis of the trithiocarbonate of the RAFT agent during the polymerisation process and to facilitate the characterisation of the materials (Figures 3.11-3.14). BocAEAM and diBocGEAM were both obtained with high yields after two-step syntheses as described in the literature.[20, 26] They were then separately copolymerised with *N*-isopropylacrylamide (NIPAM), which, in combination with AEAM at 70:30 molar ratio, has been shown to reduce the toxicity towards mammalian cells of cationic copolymers while maintaining antimicrobial properties.[26] Therefore, all polymers in this study were synthesised with 30 mol % of cationic monomer. The RAFT agent used for the synthesis was (propanoic acid)yl butyl trithiocarbonate (PABTC) as it is suitable for the polymerisation of acrylamides and its synthesis is facile and scalable.[26]

For each set of comonomers (BocAEAM and diBocGEAM, with NIPAM), a statistical, tetrablock and diblock copolymer (Figure 3.1) was synthesised to study the influence of monomer distribution on the antimicrobial activity. The final targeted degree of polymerisation (DP) was 100 for all the polymers, thus the shortest cationic blocks were of DP 15 (for the tetrablocks), which is expected to be high enough to ensure that the majority of polymer chains possess the correct monomer sequence.[27] All materials will be referred below according to the type of charge (G for guanidinium and A for ammonium), the amount of charge (here 30 molar % for all the polymers), their sequence (S for statistical, T for tetrablock and D for diblock) and labelled Boc when in their protected form (Table 3.1).
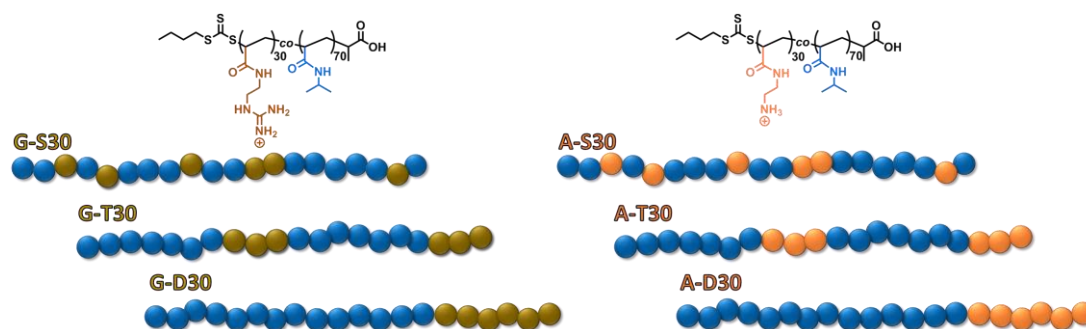
Figure 3.1 - Library of the synthesised guanidinium and ammonium polymers.

Table 3.1 - Synthesised Boc-protected polymers.

Co-monomer	Segmentation	Composition	Label
Amino-polymers	Statistical	$NIPAM_{70}$-*s*- $BocAEAM_{30}$	A-S30[Boc]
	Diblock	$NIPAM_{70}$-*b*- $BocAEAM_{30}$	A-D30[Boc]
	Tetrablock	$NIPAM_{35}$-*b*- $BocAEAM_{15}$-*b*-$NIPAM_{35}$-*b*- $BocAEAM_{15}$	A-T30[Boc]
Guanidino-polymers	Statistical	$NIPAM_{70}$-*s*- $BocGEAM_{30}$	G-S30[Boc]
	Diblock	$NIPAM_{70}$-*b*- $BocGEAM_{30}$	G-D30[Boc]
	Tetrablock	$NIPAM_{35}$-*b*- $BocGEAM_{15}$-*b*-$NIPAM_{35}$-*b*- $BocGEAM_{15}$	G-T30[Boc]

The polymerisation of BocAEAM and diBocGEAM required higher initiator concentrations than for the polymerisation of NIPAM. Furthermore, the first polymerisation cycle generally requires a higher initiator concentration than subsequent polymerisation cycles in order to fully consume the initial CTA.[28] Since the polymerisation of NIPAM required lower concentrations of initiator to achieve full monomer conversion, it was selected as the first block in each block copolymer synthesis in order to preserve a higher fraction of living chains going into subsequent block extensions. The polymerisation of diBocGEAM was undertaken at 46 °C since a loss of molar mass control was observed at higher temperatures (around 70 °C). The reaction conditions were optimised to maintain a high livingness of the polymer chains, which is necessary for the synthesis of multiblock copolymers (Tables 3.6-3.9).[28-29] Similarly to the polymerisation of poly(NIPAM-*co*-BocAEAM) described in chapter 2, the solvents used for the synthesis of poly(NIPAM-*co*-diBocGEAM) was a mixture of 1,4-dioxane/water (8:2, *v/v*). For the block copolymers G-T30[Boc] and G-D30[Boc], 7 % of EtOH was

added (which reduced the amount of dioxane), to help solubilise diBocGEAM further. Under these conditions, full monomer conversion was reached for each chain extension, allowing for the synthesis of the block copolymers in one pot (Figures 3.2A and 3.15). All polymers were obtained with the targeted molar mass and a low dispersity ($Đ \leq 1.24$) according to SEC analysis (Figures 3.2B, 3.16-3.18, Table 3.10). Similarly to chapter 2, low and high molar mass populations were observed on the SEC traces, which are probably due to initiator-derived chains and termination events, respectively. A shift to higher molar mass after each chain extension was confirmed with the SEC traces, but in most cases the experimental molar mass $M_{n,SEC}$ did not match the theoretical one $M_{n,th}$ (Table 3.10), which can be explained by the nature of the PMMA standards used for the calibration of the instrument.

A kinetic study of the statistical copolymer G-S30^{Boc} was undertaken using ^{1}H NMR and high performance liquid chromatography (HPLC) to determine the rate of incorporation for each monomer in the polymer. A similar study was undertaken for A-S30^{Boc} in chapter 2. No compositional drift was observed in both cases, meaning that the monomers are evenly distributed in both statistical copolymers (Figure 3.19).
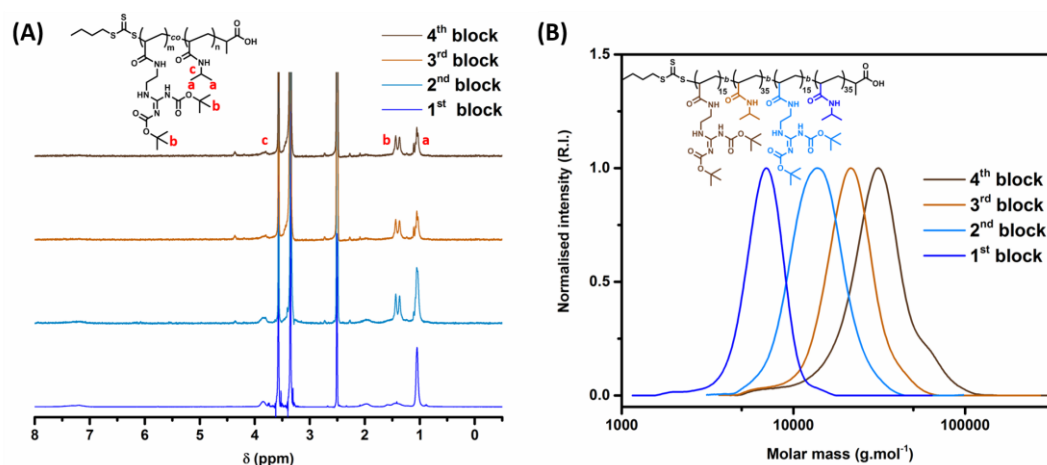
Figure 3.2 - ^{1}H NMR in DMS-d_6 (A) and DMF-SEC chromatograms (B) for successive chain extensions of G-T30^{Boc}.

Following the polymerisation process, the protected guanidinium copolymers were deprotected using TFA, with quantitative deprotection confirmed using ^{1}H NMR in D$_2$O (Figure 3.3).[20] D$_2$O was the only deuterated solvent which dissolved the final deprotected polymers, but was not suitable for the protected polymers, hence DMSO-d_6 had to be used prior to treatment with TFA. This deprotection method further justifies the choice of acrylamide monomers as they are more stable towards harsh acidic conditions than acrylates or methacrylates.[30] The cationic polymers were then dialysed against a solution containing

NaCl to replace the TFA counter-ions with Cl⁻ as shown by ¹⁹F NMR (Figure 3.20), and finally against distilled water to remove any traces of excess NaCl. The polymers were obtained as solids after freeze-drying. The counter-ion exchange was performed in order to directly compare the guanidinium copolymers to their ammonium analogues (which also possess a chloride counter-ion), as well as to enhance solubility and avoid any decrease in antimicrobial activity as reported by Tew and co-workers.[31]
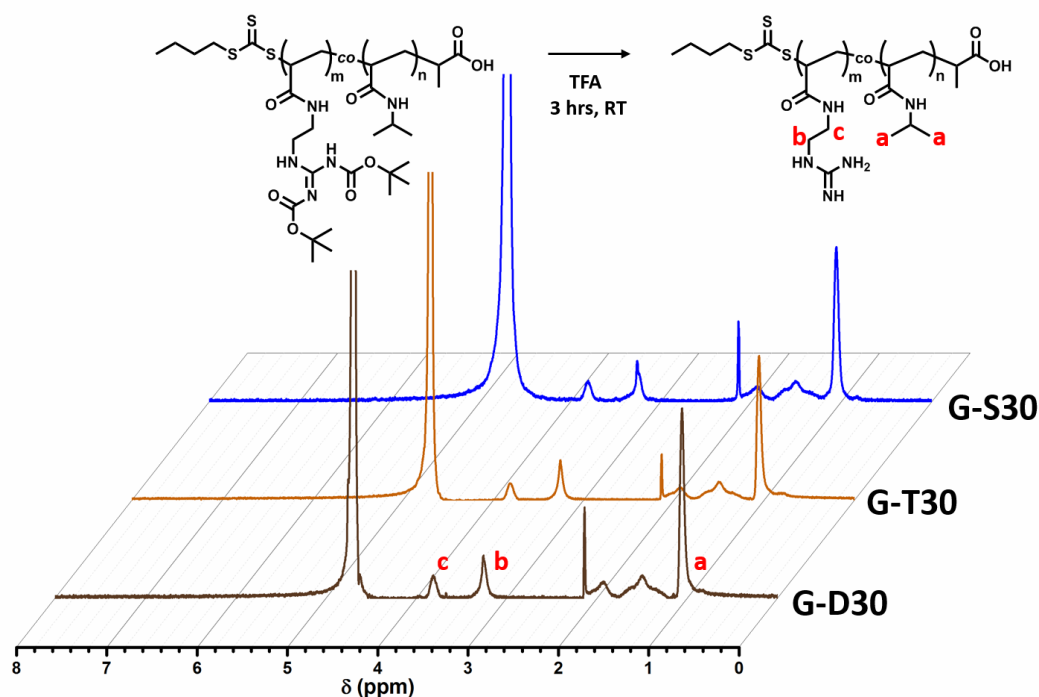
Figure 3.3 - ¹H NMR spectra in D₂O of G-S30, G-T30 and G-D30 after deprotection.

To identify the effect of monomer distribution on the physico-chemical properties of the polymer library, which could in turn alter their biological activity, characterisation of the polymers by reverse-phase HPLC was performed with H₂O/ACN as mobile phase (Figure 3.4, Table 3.11). The elution time of the polymers can be correlated to their hydrophobicity, where earlier elution times indicate less hydrophobicity. Preceding work examining the ammonium counterparts, but also other types of polyacrylamide-based multiblock copolymers, established a comparable trend between elution time of polymers with different compositions and hydrophobicity.[32] Reverse-phase HPLC of the guanidinium polymers indicated the following trend, with hydrophobicity of the polymers decreasing left to right; diblock (G-D30) > tetrablock (G-T30) > statistical (G-S30) according to Figure 3.4B. The cloud point temperature of statistical copolymers has been shown to be higher than that of their diblock counterparts.[33] This observation was attributed to the increase of the overall hydrophobicity

of the polymer chain with the segregation of the monomer types along the backbone. Similarly, in the case of G-D30, G-T30 and G-S30, the size of the discreet hydrophobic segments (here the polyNIPAM block) are likely affecting the overall hydrophobicity the polymer structures. The charge to hydrophobicity ratio strongly affects membrane interactions of SMAMPs and will not only alter their antimicrobial properties, but also their internalisation in mammalian cells.[20]

The determination of the pK_a of A-S50, A-M50 and A-D50 in chapter 2, demonstrated that some of the primary amines were not protonated at physiological pH. As mentioned previously, the pK_a of the guanidine moiety of arginine is around 12.5, hence even the incorporation into a polymer chain would not alter its acidity enough to have deprotonated guanidine groups at physiological pH.
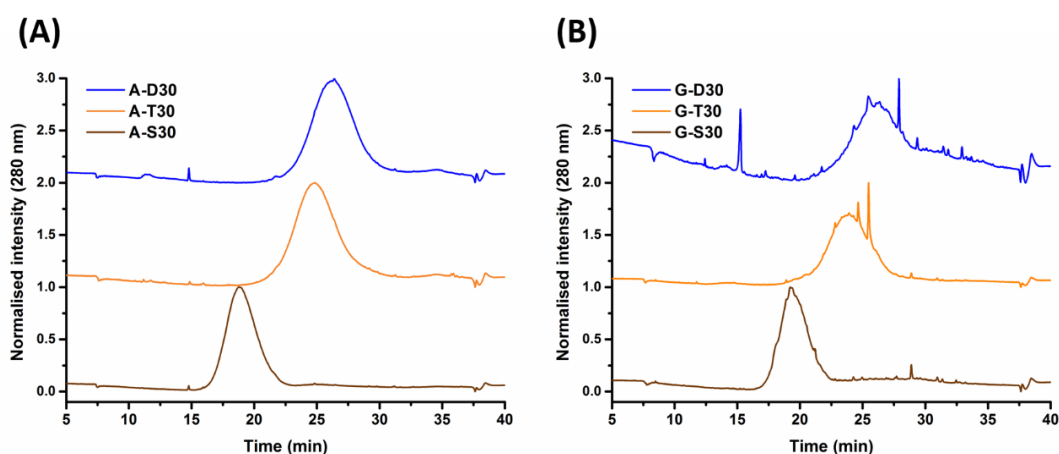
Figure 3.4 – RP-HPLC chromatograms of the ammonium (A) and the guanidinium polymers (B) with a gradient of 1 to 80 % ACN in 30 minutes with a 100 mm C18 column.

Next, the behaviour of the copolymers in solution was analysed by Dynamic Light Scattering (DLS) at 37 °C and pH 7.4 at the maximum concentration tested for the biological experiments (1024 μg.mL^{-1}). Since polyNIPAM is known to possess a lower critical solution temperature (LCST) in aqueous solution close to physiological temperatures, it was pertinent to demonstrate that the copolymers do not self-assemble under such conditions.[34] No self-assembly was observed for both the ammonium and guanidinium copolymers (Figure 3.21, Table 3.11). These results are in agreement with the general observation that the LCST of polymers increases when they are copolymerised with a non-temperature-responsive monomer.[35] Since no micellar formation was observed, any difference in the activity of the polymers can be directly correlated to the monomer sequence.

3.2.2 Toxicity of SMAMPs towards mammalian cells

3.2.2.1 Haemocompatibility of SMAMPs

As cationic polymers are known to be haemotoxic, defibrinated sheep blood was used to assess the haemocompatibility of the synthesised polymers up to 1024 μg.mL^{-1} over 2 hours at 37 °C, according to an adapted protocol from the literature.[36-37] Importantly, none of the ammonium polymers were haemolytic in contrast to Triton X, which was used as a positive control (Figure 3.5A). Amongst the guanidinium polymers, G-D30 induced 10% haemolysis at a concentration of 1000 μg.mL^{-1}, while the statistical and tetrablock counterparts (G-S30 and G-T30) were not haemolytic within the concentration range tested (Figure 3.5B).
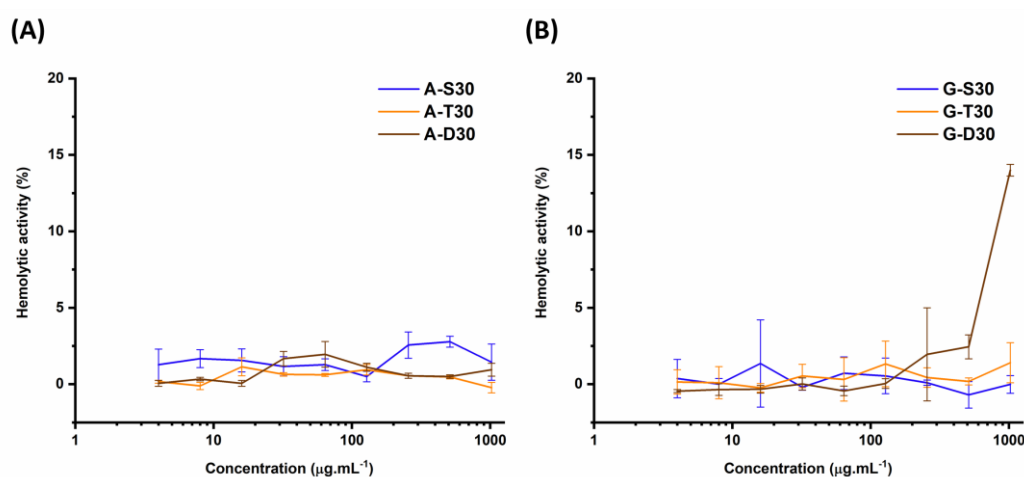
Figure 3.5 - Haemolytic activity of ammonium and guanidinium SMAMPs. Normalised haemolysis of sheep blood cells following incubation at 37 °C for 2 hours in PBS with ammonium (A) and guanidinium (B) SMAMPs.

Since the haemocompatibility of polymers encompasses both haemolytic and haemagglutination, the latter was studied with defibrinated sheep blood, using Concanavalin A as a positive control.[38] For guanidinium containing polymers, the aggregation of RBCs was observed with G-S30 and G-T30, from concentrations of 8 and 32 μg.mL^{-1}, respectively, while G-D30 did not induce haemagglutination (Table 3.2). Comparable results were obtained with the ammonium polymers as A-S30 and A-T30, which induced haemagglutination from concentrations of 64 and 128 μg.mL^{-1}, respectively, whereas A-D30 did not. These observations are in accordance with the study in chapter 2, in which the heptablock and statistical poly(NIPAM-co-AEAM) also induced the formation of RBC aggregates whilst the

diblock copolymer did not exhibit any toxicity.[26] This behaviour was explained by the distribution of cationic functionalities along the polymer backbone facilitating the cross-linking of RBCs.

The polymers which induced aggregation of red blood cells (statistical and tetrablock copolymers) were not haemolytic, suggesting that each aspect of haemotoxicity are relatively independent for the investigated materials. Combined, haemolysis and haemagglutination assays revealed that the diblocks A-D30 and G-D30 were the most haemocompatible systems, whereas the statistical and tetrablock SMAMPs induced haemotoxicity at low concentrations (Table 3.3).

Table 3.2 - SMAMP-induced erythrocytes aggregation. Observation of haemagglutination of sheep blood cells following incubation with ammonium and guanidinium SMAMPs in PBS for 2 hours at 37 °C.

sample /concentration (μg/mL)	1024	512	256	128	64	32	16	8	4	2
A-S30	++	++	+	+	+	-	-	-	-	-
A-T30	++	++	++	+	-	-	-	-	-	-
A-D30	-	-	-	-	-	-	-	-	-	-
G-S30	+++	+++	+++	++	++	+	+	+	-	-
G-T30	++	++	++	+	+	+	-	-	-	-
G-D30	-	-	-	-	-	-	-	-	-	-

Haemagglutination strength: +++ strong; ++ moderate; + weak; - none.

3.2.2.2 Compatibility towards human epithelial cells

As *S. aureus* was shown to persist within keratinocytes during skin infections,[39-40] SMAMPs need to exhibit a low toxicity towards these cells to warrant their clinical application. The toxicity of the two sets of polymers against human keratinocytes (HaCaT) was evaluated over a period of 24 hours using an XTT assay. The toxicity of the amine polymers towards HaCaT cells was surprisingly low, with an $IC_{50} > 1000$ μg.mL^{-1} for all three compositions (Figure 3.6 and Table 3.3), indicating that the monomer sequence did not influence the toxicity of these polymers at the tested concentrations. For each copolymer composition, the guanidinium polymers were shown to be more toxic than their corresponding

ammonium polymers. The difference between the two tetrablock copolymers (A-T30 and G-T30) and the two diblock copolymers (A-D30 and G-D30) was particularly significant (Figure 3.6B and 3.6C). This result is in agreement with a previously reported work studying methacrylamide-based statistical copolymers containing guanidinium and ammonium moeites.[18] By increasing the ratio of guanidinium to ammonium functionalities, the toxicity of the polymers were shown to increase towards MCF-7 epithelial cells. Indeed, due to their similarity to arginine-rich cell penetrating peptides, the guanidinium polymers could undergo enhanced interactions with mammalian cell membranes compared to their ammonium counterparts, which would affect their toxicity.[41]

Segregation of cationic and hydrophobic functionalities also significantly increased the toxicity of the ammonium and guanidinium SMAMPs towards epithelial cells. According to the IC_{50} values (Table 3.3), G-D30 appeared to be the most toxic, followed by G-T30 and G-S30. The toxicity observed with each polymer composition correlates to their overall hydrophobicity (determined *via* reverse-phase HPLC, Figure 3.4), indicating that an increase in hydrophobicity accounts for an increase in toxicity. Similarly, Neanmark and co-workers reported an increase in cytotoxicity with hydrophobicity by using poly(ethylenimine)s bearing aliphatic substituents of varying lengths.[42]

Table 3.3 - Comparison of the cytocompatibility of the ammonium and guanidinium SMAMPs. Haemocompatibility determined for sheep blood cells using haemolysis and haemagglutination assays and IC_{50} for HaCaT and A549 cells using XTT assays.

	Haemocompatibility		$IC_{50}^{[c]}$ ($\mu g.mL^{-1}$)	
	$HC_{10}^{[a]}$ ($\mu g.mL^{-1}$)	$c_H^{[b]}$ ($\mu g.mL^{-1}$)	HaCaT	A549
A-S30	> 1024	64	> 1024	> 1024
A-T30	> 1024	128	> 1024	700
A-D30	> 1024	> 1024	> 1024	400
G-S30	> 1024	8	> 1024	600
G-T30	> 1024	32	500	200
G-D30	1024	>1024	300	150

[a] HC_{10} is the minimum concentration at which at least 10 % of the maximum lysis was observed.

[b] c_H is the lowest concentration at which the polymers induce aggregation of RBCs.

[c] IC_{50} was determined as the concentration at which 50 % growth inhibition occurred.
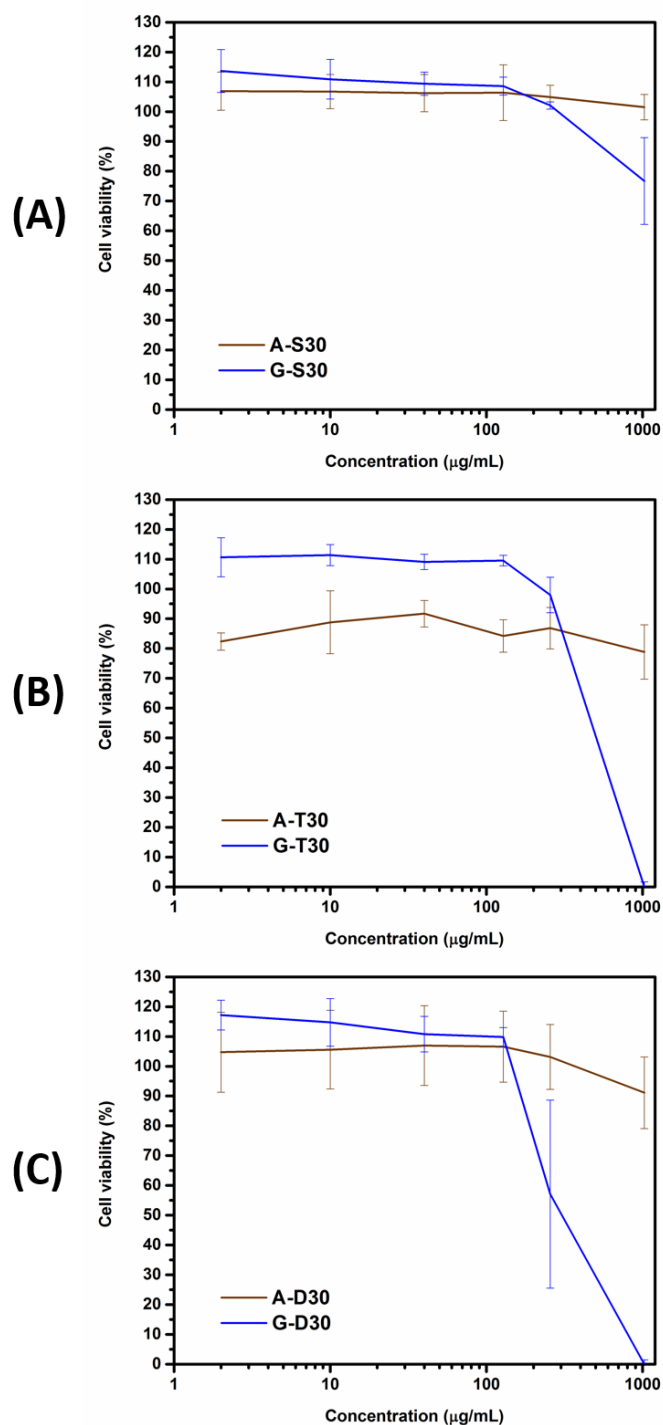
Figure 3.6 - Cytotoxicity of ammonium and guanidinium SMAMPs towards HaCaT. Viability of HaCaT cells incubated for 24 hours in presence of statistical (A), tetrablock (B) and diblock (C) ammonium and guanidinium SMAMPs using an XTT assay.

As pneumonia is another common ICU-acquired infection, the toxicity of the polymers towards lung epithelial cells (A549) was also evaluated over the course of 24 hours using an XTT assay (Figure 3.7).[43] With A549 cells, A-T30 and A-D30 were found to be toxic at relatively high concentrations (IC$_{50}$ of 700 and 400 µg.mL^{-1}), while the guanidinium counterparts were again more toxic (Figure 3.7 and Table 3.3). Similarly, the IC$_{50}$ decreased with increasing segregation of the co-monomers (G-S30 > G-T30 > G-D30). Taken together, the toxicity data revealed that toxicity increases with segregation, which was not shown before, to the best of our knowledge.
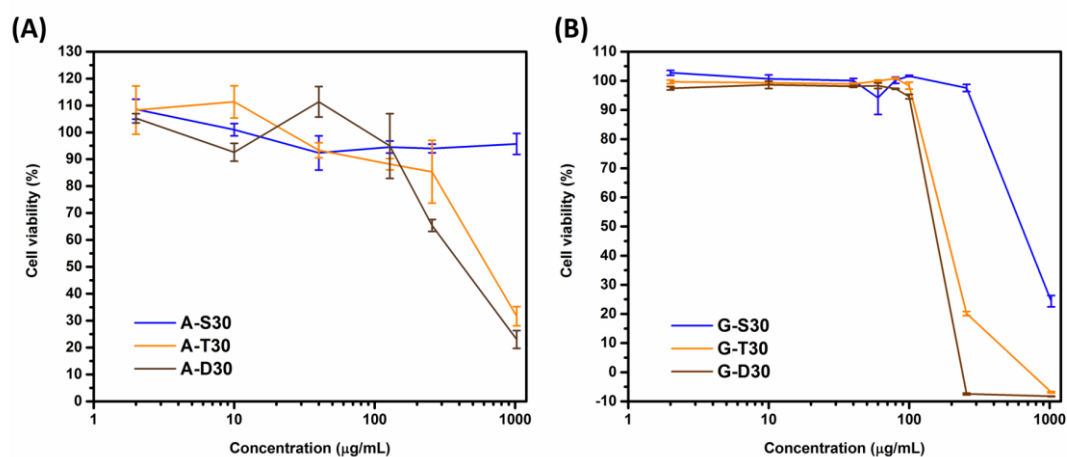
Figure 3.7 - Cytotoxicity of ammonium and guanidinium SMAMPs towards A549 cells. Viability of A549 cells incubated for 24 hours in presence of ammonium (A) and guanidinium (B) SMAMPs of various monomer sequence using an XTT assay.

3.2.3   Antimicrobial activity of SMAMPs

Two clinically relevant strains of *S. aureus* were used to evaluate their antimicrobial susceptibility towards the synthesised polymers: RN1 (NCTC 8325), a MSSA strain, which is widely used as a model strain, and USA300 JE2, a MRSA strain, which is more virulent than RN1.[44-45]

For both the ammonium and guanidinium polymers, the monomer distribution had a significant effect on their efficacy against *S. aureus* (Figure 3.8 and Table 3.4). The MIC value against the MSSA strain RN1 decreases with segmentation for the guanidinium polymers (Figure 3.8A). Indeed, for the polyarginine mimics, the statistical copolymer G-S30 appeared to be inactive against RN1 within the concentration range tested (MIC > 1000 µg.mL^{-1}), whereas the tetrablock G-T30 and diblock G-D30 copolymers exhibited relatively low MIC values (from 128 and 64 µg.mL^{-1}, respectively). The ammonium polymers followed the same

trend as the guanidinium SMAMPs, which was expected as it was found in chapter 2 that multiblock and diblock ammonium copolymers with 30 % charge content were more potent against bacteria than their statistical copolymer analogue. Additionally, it is worth noting that ammonium and guanidinium polymers of the same monomer sequence possessed similar MICs against the MSSA strain (Figure 3.8A). G-D30 an A-D30 were the most active against RN1 with a MIC of 64 μg.mL^{-1}. As indicated by DLS measurements, these copolymers were not expected to form any higher-order assemblies under the physiological conditions used (c ≤ 1024 μg.mL^{-1}). Therefore, the potency of the diblocks could be explained by the increase in hydrophobicity which accompanies the segregation of polyNIPAM into one discreet block: the more hydrophobic the polymer, the more toxic towards mammalian cells but also towards bacteria. Another hypothesis would be that the positive charges exert a synergistic effect when localised in a single segment of a macromolecule, enhancing bacterial attachment.

Similarly, the antimicrobial activity of the guanidinium SMAMPs against the MRSA strain JE2 increased with increasing segregation of cationic and hydrophobic functionality and their MIC values were similar to those observed against the MSSA strain (Figure 3.8B). Strikingly, the MIC values of G-T30 and G-D30 against JE2 (128 and 64 μg.mL^{-1}, respectively) were decreased two-fold compared to A-T30 and A-D30 (256 and 128 μg.mL^{-1}, respectively). Since the molar mass of the ammonium and guanidinium polymers are comparable (Table 3.11), the difference in the MIC values strongly suggests that the guanidinium copolymers were more potent than their ammonium counterparts, which is consistent with a previous study.[17] While the antimicrobial activity of polymers bearing primary amine moieties appear to derive from their attachment to bacterial membranes, followed by the formation of pores, polymers bearing guanidinium moieties could have a different antimicrobial mechanism. Indeed, the binding of guanidine units to phospholipids from bacterial membrane was shown to be more labile, hence allowing an efficient membrane crossing.[46] Recently, Good and co-workers reported that the antimicrobial activity of polyhexamethylene biguanidine is attributed to its differential access to, and subsequent condensation of, bacterial DNA over mammalian DNA, thereby inducing bacterial death.[47]
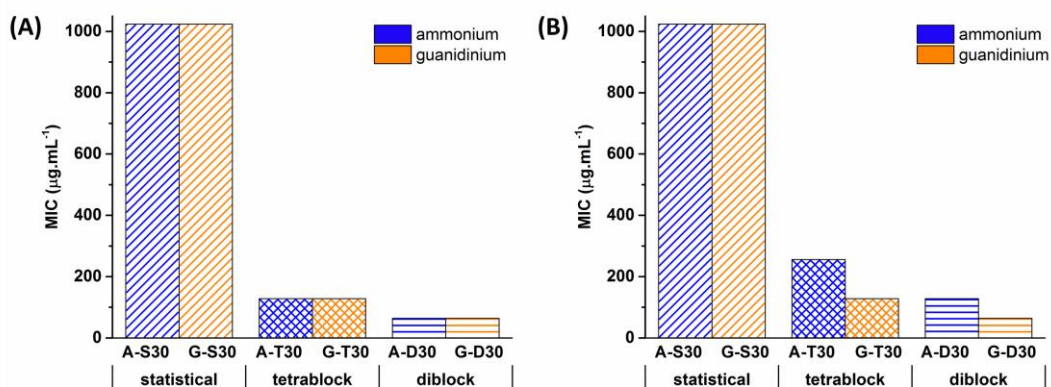
Figure 3.8 – Comparison of the MIC values of ammonium and guanidinium SMAMPs against MSSA RN1 (A) and MRSA JE2 (B).

The antimicrobial activity of the ammonium polymers against JE2 varied with monomer distribution in the same manner as with RN1. However, the MIC of A-T30 and A-D30 against JE2 (256 and 128 $\mu g.mL^{-1}$, respectively) was double that observed against RN1 (128 and 64 $\mu g.mL^{-1}$, respectively) as shown on Table 3.4. It is plausible that the reduced methicillin susceptibility of JE2 caused a change in its membrane composition and physical properties (thickness, surface charge) to that of RN1, which has been shown to influence the sensitivity of bacteria towards SMAMPs.[48-49]

Table 3.4 – Comparison of the antimicrobial activity of the SMAMPs. MIC values determined against MSSA RN1 and MRSA JE2.

	MIC[a] ($\mu g.mL^{-1}$)		MIC[a] ($nmol.mL^{-1}$)	
	RN1	JE2	RN1	JE2
A-S30	> 1024	> 1024	> 75	> 75
A-T30	128	256	10	20
A-D30	64	128	5	10
G-S30	> 1024	> 1024	> 75	> 75
G-T30	128	128	10	10
G-D30	64	64	5	5

[a] MIC is the minimum inhibitory concentration at which no visible bacterial growth can be observed.

3.2.4 Selectivity of SMAMPs for bacteria over mammalian cells

The selectivity of SMAMPs is defined as the ability to maximise their activity against bacteria whilst being non-toxic towards mammalian cells. Similarly to Chapter 2, this was evaluated by comparing the MIC of the polymer library towards a given bacterial strain against their compatibility with mammalian cells (Figures 3.9 and 3.10). The green region designates the area of the diagram in which the selectivity for bacteria over mammalian cells is superior to 1: the further from the diagonal line, the more selective the SMAMP. The ideal SMAMP would be located towards the top-left corner of the graph as it maximises antibacterial activity whilst being non-toxic to mammalian cells (Figure 3.9).

Remarkably, it is clear that segregation of the cationic and hydrophobic moieties in the copolymer compositions improves the selectivity. Indeed, the statistical copolymers A-S30 and G-S30 had the lowest selectivity for both RN1 and JE2. Despite an improved selectivity of tetrablock copolymers compared to their statistical equivalents, A-T30 and G-T30 do not favour interactions with bacteria over RBCs. The diblock copolymers (A-D30 and G-D30) exhibited a high selectivity towards RBCs, outperforming their statistical and tetrablock copolymer counterparts against RN1 and JE2. G-D30 seems to be the ideal candidate for the treatment of both MSSA and MRSA as it is the most potent but remains compatible with RBCs up to very high concentrations (Figure 3.9). These observations are confirmed by the selectivity values calculated in Table 3.5, according to Equation 2.1.
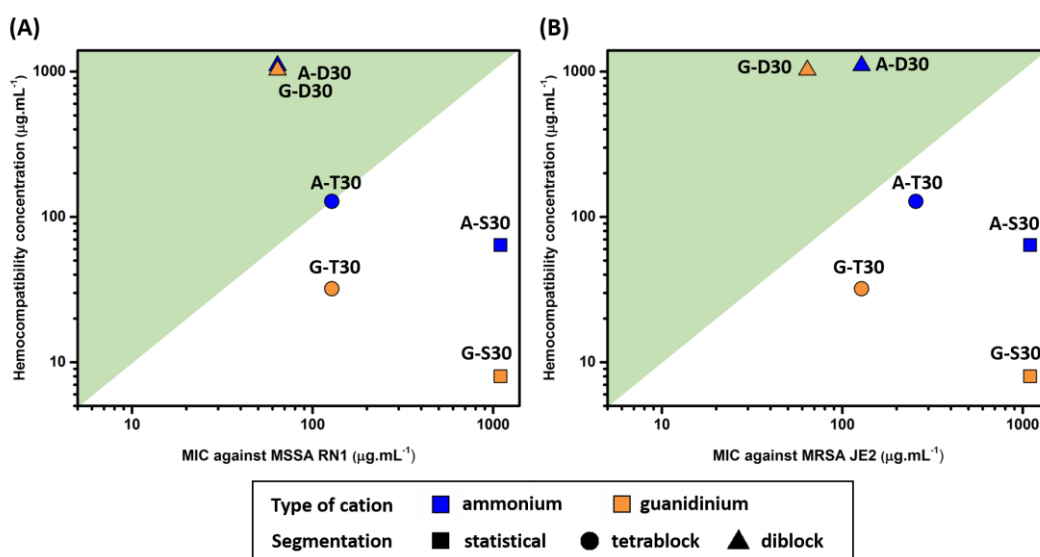
Figure 3.9 - Selectivity graphs of SMAMPs for MSSA RN1 (A) and MRSA JE2 (B) over RBCs. Haemocompatibility concentration (lowest value between HC_{10} and c_H, as shown in Table 3.3) against the MIC for MSSA RN1 (A) and MRSA JE2 (B), which values are reported in Table 3.4.

Table 3.5 - Selectivity of the SMAMPs for MSSA and MRSA over mammalian cells.
Selectivity values of the SMAMPs for MSSA RN1 and MRSA JE2 over RBCs (as calculated using equation 2.1) and TI values for RN1 and JE2 over HaCaT and A549 (as calculated using equation 2.2).

	Selectivity with RBCs[a]		Therapeutic Index (TI)[b] with HaCaT		Therapeutic Index (TI)[b] with A549	
	RN1	JE2	RN1	JE2	RN1	JE2
A-S30	< 0.1	< 0.1	< 1	< 1	< 1	< 1
A-T30	1	0.5	> 8	> 4	5	3
A-D30	> 16	> 8	> 16	> 8	6	3
G-S30	< 0.01	< 0.01	< 1	< 1	< 0.6	< 0.6
G-T30	0.3	0.3	4	4	2	2
G-D30	16	16	5	5	2	2

[a] Selectivity: lowest value between HC_{10} and c_H (haemocompatibility concentration) divided by the MIC of the bacterial strains concerned, as described in Equation 2.1.

[b] Therapeutic index (TI) was calculated as the IC_{50} of HaCaT or A549 for the SMAMP divided by the MIC of the bacterial species, as described in Equation 2.2.

Subsequently, the selectivity of SMAMPs for bacteria over HaCaT cells was established using Figure 3.10. It is noteworthy that except for the statistical copolymers A-S30 and G-S30, the synthesised SMAMPs were selective towards both MSSA and MRSA over HaCaT cells. In the case of the polylysine mimics, the diblock copolymer was the most selective for both RN1 and JE2 over keratinocytes. However, with the guanidinium polymers, the diblock and the tetrablock copolymer had similar levels of selectivity for both bacterial strains. Table 3.4 summarises the therapeutic indexes for all six compounds calculated using Equation 2.2. Comparable trends in selectivity towards MSSA and MRSA over A549 cells was observed according to Table 3.5: the diblock and tetrablock copolymers were the most selective with the lung epithelial cells out of both ammonium and guanidinium polymers. Although A-D30 has a similar level of selectivity to G-D30 and is slightly less toxic to HaCaT and A549 cells, the guanidinium diblock copolymer is a more promising alternative to vancomycin due to its higher potency against MRSA.
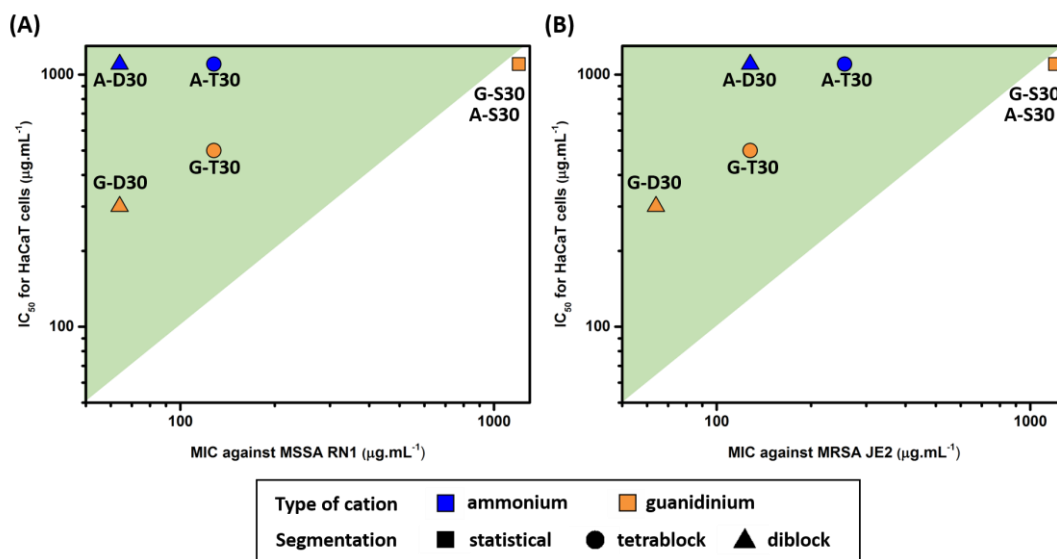
Figure 3.10 - Selectivity graphs of SMAMPs for MSSA RN1 (A) and MRSA JE2 (B) over HaCaT cells. IC_{50} towards HaCaT cells (values reported in Table 3.3) against the MIC for MSSA RN1 (A) and MRSA JE2 (B), which values are reported in Table 3.4.

3.3   Conclusion

Ammonium and guanidinium copolymers containing NIPAM as a co-monomer were successfully synthesised *via* RAFT polymerisation. By varying both the nature of the cationic functionality and the monomer distribution (statistical, tetrablock and diblock copolymers), the effect of charge and monomer distribution on the biological properties of SMAMPs was elucidated with both sets of polymers. Firstly, it was demonstrated that the type of charge affects the selectivity of SMAMPs. Indeed, the guanidinium containing polymers were more toxic towards epithelial cells than their ammonium counterparts, whilst a similar level of haemocompatibility was maintained. However, the guanidinium SMAMPs exhibited a stronger antimicrobial activity towards MRSA. This increased potency could be attributed to a different mechanism of action with bacteria, compared to the ammonium SMAMPs, with the polyarginine mimics acting intracellularly rather than disrupting bacterial membrane.

Finally, the influence of the monomer distribution on the characteristics of the SMAMPs was evaluated for both ammonium and guanidinium polymers. In both cases, the diblock copolymer exhibited a slightly higher toxicity towards epithelial cells than their statistical and tetrablock counterparts. However, the haemocompatibility was improved with a diblock structure, as no haemagglutination was observed for A-D30 and G-D30. More importantly, segregation of the cationic and hydrophobic functionalities drastically improved the potency against *S. aureus*. Despite bearing the same quantity of positive charges, the diblock copolymers were more active than the tetrablock copolymers, whilst the statistical copolymers did not exhibit any activity. Further investigations on the effect of segmentation in the interactions with bacterial membranes would help clarifying the advantage of a diblock copolymer structure over a statistical or tetrablock copolymer. After analysis of the selectivity of the library of polymers towards mammalian cell, G-D30 presented the best properties against MRSA.

3.4   Experimental

3.4.1   Materials

Acryloyl chloride (97 %), chloroform (CHCl$_3$, 99 %), dichloromethane (DCM, 99 %), 1,4-dioxane (99 %), ethylacetate (EtOAc, 99 %), ethylenediamine (≥99 %), triethylamine (NEt$_3$, ≥99 %) and trifluoroacetic acid (TFA, 99 %)) were purchased from Sigma-Aldrich and used without further purification. Sodium chloride (NaCl, Fischer-Scientific, ≥99 %), Boc-anhydride (Fluka, 98 %) and 2,2'-azobis[2-(2-imidazolin-2-yl)propane]dihydrochloride (VA-044, Wako) were also used without further purification. Mili-Q water was directly used as a solvent for polymerisations. N-isopropylacrylamide (NIPAM, Sigma-Aldrich, 97 %) was used after purification by recrystallization in n-hexane. Nutrient Agar, Dulbecco's Modified Eagle's Medium (DMEM), Müller-Hinton Broth (MHB), Trypsic Soy Broth (TSB), Roswell Park Memorial Institute medium (RPMI-1640) , Phosphate Buffered Saline (PBS) tablets, Concanavalin A (Con A) and Triton X were purchased from Sigma-Aldrich. 96-well plates were sourced from Thermo-Fischer. Milli-Q filtered water was used to prepare solutions, according to their recommended concentration and the solutions were autoclaved prior to their usage in order to ensure sterility. Defibrinated sheep blood was obtained from Fisher Scientific.

3.4.2   Methods

3.4.2.1   Nuclear Magnetic Resonance (NMR) Spectroscopy

^{1}H NMR spectra were recorded on a Bruker Advance 300 spectrometer (300 MHz) at 27 °C in DMSO, CDCl$_3$ or D$_2$O. For ^{1}H NMR, the delay time (dl) was 2 s. Chemical shift values (δ) are reported in ppm. The residual proton signal of the solvent was used as internal standard.

3.4.2.2   Size exclusion chromatography (SEC)

Molar mass distributions were measured using an Agilent 390-LC MDS instrument equipped with differential refractive index (DRI), viscometry (VS), dual angle light scatter (LS) and dual wavelength UV detectors. The system was equipped with 2 x PLgel Mixed D columns (300 x 7.5 mm) and a PLgel 5 μm guard column. The eluent was DMF with 5 mmol NH$_4$BF$_4$ additive. Samples were run at 1 mL min^{-1} at 50°C. Poly(methyl methacrylate) standards (Agilent EasyVials) were used for calibration between 955,000 - 550 gmol^{-1}. Analyte samples were filtered through a nylon membrane with 0.22 μm pore size before injection. Respectively, experimental molar mass (M$_{n,SEC}$) and dispersity ($Đ$) values of synthesized polymers were determined by conventional calibration using Agilent GPC/SEC software.

3.4.2.3 Mass spectrometry (MS)

MS analysis was carried out with Agilent1100 HPLC coupled with Agilent 6130B single quadruple mass spectrometer equipped with electrospray ionisation source. Mobile phase was 80 % methanol with 20 % water at flow rate at 0.2ml.min^{-1}. Mass spectrometer was operated in electrospray positive ion mode with a scan range 50-500 m/z. Source conditions are: capillary at 4000V; nebuliser gas (N$_2$) at 15 psi; dry gas (N$_2$) at 7 L.min^{-1}; Temperature at 300 °C. Calibration was done with ESI tuning mix from Agilent.

3.4.2.4 High performance liquid chromatography (HPLC)

HPLC was performed using an Agilent 1260 infinity series stack equipped with an Agilent 1260 binary pump and degasser. The flow rate was set to 1.0 mL min^{-1} and samples were injected using Agilent 1260 autosampler with a 100 µL injection volume. The temperature of the column was set at 37 °C. The HPLC was fitted with an Agilent C18 column (100 x 4.6 mm) with 5 micron packing (100Å). Detection was achieved using an Agilent 1260 variable wavelength detector. UV detection was monitored at λ = 309 nm. Methods were edited and run using Agilent OpenLAB online software and data was analysed using Agilent OpenLAB offline software. Mobile phase solvents used were HPLC grade (ACN was 'far UV') and consisted of mobile phase A: 100 % ACN, 0.04 % TFA; mobile phase B: 100 % water, 0.04 % TFA with a gradient of 1 to 80 % ACN over 30 minutes.

3.4.2.5 Dynamic Light Scattering measurements.

DLS measurements were taken using a Malvern instruments Zetasizer Nano at 37 °C with a 4 mW He-Ne 633 nm laser at a scattering angle of 173° (back scattering). For DLS aggregation studies, 1.024 mg of polymer sample was dissolved in 1 mL of PBS buffer at pH 7.4 and a total of 0.5 mL of the solution was introduced in a 1.5 mL polystyrene cuvette after filtering with a 0.2 µm filter.

3.4.2.6 Haemolysis and haemagglutination assays

Sheep red blood cells (RBCs) were prepared by washing defibrinated sheep blood with PBS *via* centrifugation. Polymers were dissolved in PBS. Polymers were dissolved in PBS. The normalisation was done using positive controls (50 µg mL^{-1} Concanavalin A for haemagglutination and 2 % Triton X-100 in PBS for haemolysis) and negative control (PBS) which were included on each plate. A suspension of 3 % in volume of RBCs was added to each well and the contents were mixed before being incubated at 37°C for 2 hours. The 96-well plates were centrifuged at 600 x g for 10 minutes then 100 µL of the supernatant was

transferred into a new plate. The absorbance at 540 nm was measured and normalised using the positive and negative control.

3.4.2.7   Eukaryotic Cell Lines and Growth Conditions

HaCaT human keratinocytes were grown in a 50:50 mixture of Ham's F12 and Dulbecco's Modified Eagle's Medium (DMEM) supplemented with 10% of foetal calf serum, 1% of 2 mM glutamine and 1%. Both cell lines were grown as adherent monolayers at 37 °C in a 5% CO_2 humidified atmosphere and passaged at approximately 70-80% confluence.

3.4.2.8   *In vitro* growth inhibition assays

The anti-proliferative activity of the polymers was determined in HaCaT human keratinocytes. 96-well plates were used to seed 5000 cells per well which were left to pre-incubate with drug-free medium at 37 °C for 24 hours before adding different concentrations of the compounds to be tested (1024 µg mL^{-1} – 32 µg mL^{-1}). A drug exposure period of 24 hours was allowed. The XTT assay was used to determine cell viability. The IC_{50} values (concentrations which caused 50% of cell death), were determined as duplicates of triplicates in two independent sets of experiments and their standard deviations were calculated.

3.4.2.9   Bacterial Strains and Growth Conditions

The utilised bacterial strains were *S. aureus* USA 300 LAC JE2 and NCTC 8325 RN1. Bacteria were grown in TSB at 37°C at 250 rpm for 18 hours.

3.4.2.10 Antibacterial susceptibility tests

Antibacterial susceptibility was studied using two strains of *Staphylococcus aureus* (*S. aureus*): RN1 and JE2. Minimum inhibitory concentrations (MICs) were determined according to the standard Clinical Laboratory Standards Institute (CLSI) broth microdilution method (M07-A9-2012). A single colony of bacteria was picked up from a fresh (24 hour) culture plate and inoculated in 5 mL of Mueller-Hinton (MH) broth, then incubated at 37 °C overnight. On the next day, the concentration of cells was assessed by measuring the optical density at 600 nm (OD_{600}). Culture suspension was then diluted to an $OD_{600} = 0.1$ with RPMI with 0.165 mol L^{-1} of MOPS in order to reach a bacterial concentration of ~ 10^8 colony forming unit per mL (CFU mL^{-1}). The solution was diluted further by 100-fold to obtain a concentration of 10^6 CFU mL^{-1}. Polymers were dissolved in distilled water and 100 µL of each test polymer was added to micro-wells followed by the addition of the same volume of bacterial suspension (10^6 CFU mL^{-1}). The micro-well plates were incubated at 37 °C for 24 hours, and growth was evaluated by measuring the OD_{600} using a plate reader. Triplicates were performed for each

concentration and readings were taken twice. The growth in the well was normalised using negative controls, wells without any bacteria introduced, and positive controls, wells only containing bacterial solution.

3.4.3 Synthesis

3.4.3.1 Synthesis of 1,3-Di-Boc-guanidinoethyl acrylamide diBocGEAM
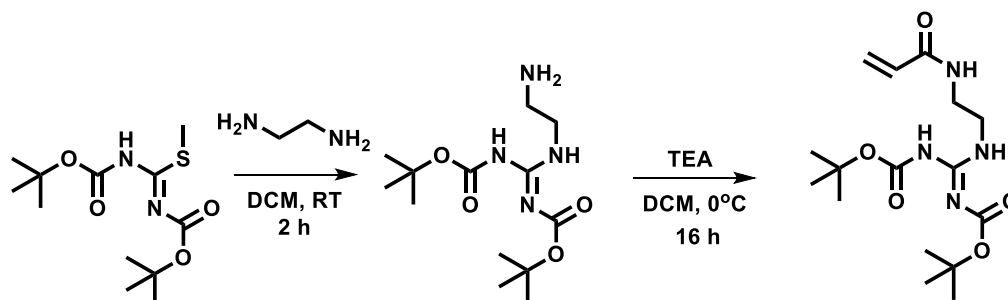
The monomer was synthesised according to the literature.[20]

Synthesis of 2-[1,3-Bis(tert-butoxycarbonyl)guanidine]ethylamine. A solution of 1,3-Bis(*tert*-butoxycarbonyl)-2-methyl-2-thiopseudourea (6.50 g, 27.6 mmol) in DCM (50 mL) was added dropwise to a solution of ethylenediamine (3.77 g, 4.20 mL, 77.3 mmol) in DCM (60 mL), and the reaction was stirred at RT for 2 hours. Following washes with 3 x 50 mL of water and 2 x 50 mL of brine, the product was dried over $MgSO_4$ and the solvent was removed by rotary evaporation to obtain a white solid (6.76 g, 22.3 mmol, 80%). ^{1}H NMR (300 MHz, 298 K, CDCl$_3$, δ): 11.51 (s, 1H, NH), 8.64 (s, 1 H, NH), 4.51 (s, 1H, NH), 3.46 (t, 2H, CH$_2$), 2.88 (t, 2H, CH$_2$), 1.49 (s, 9H, CH$_3$), 1.44 (s, 9H, CH$_3$) as shown on Figure 3.11.

Synthesis of 2-[1,3-Bis(tert-butoxycarbonyl)guanidine]ethyl acrylamide. 2-[1,3-Bis(tert-butoxycarbonyl)guanidine]ethylamine (6.56 g, 21.6 mmol) was dissolved in 150 mL of DCM with TEA (2.63 g, 3.62 mL, 26.0 mmol) and cooled in an ice-bath. A solution of acryolyl chloride (1.96 g, 1.7 mL, 21.6 mmol) in 50 mL of DCM was added dropwise. After leaving the reaction to stir overnight at RT, 300 mL of saturated NaHCO$_3$ was added to the reaction mixture and extracted with 3 x 300 mL of DCM. The organic fractions were collected and dried over $MgSO_4$. The product was isolated by removing the solvent and purified by chromatography column (hexane/EtOAc) to yield a white solid (6.4 g, 18.0 mmol, 83 %); mp=142 °C. ^{1}H NMR (300 MHz, 298 K, CDCl$_3$, δ): 11.40 (s, 1H, NH), 8.69 (t, 5.1 Hz, 1H, NH), 8.12 (t, 1H, amide proton), 6.21 – 6.25 (dd, *J*=18 Hz, *J*=1 Hz, 1H, vinyl proton), 6.11 – 6.16 (dd, *J*=15 Hz, *J*=12 Hz, 1H, vinyl proton), 5.55 – 5.57 (dd, *J*=9 Hz, *J*=3 Hz, 1H, vinyl proton), 3.60 (m, 2H, CH$_2$), 3.50 (m, 2H, CH$_2$), 1.59 (s, 9H, CH$_3$), 1.51 (s, 9H, CH$_3$) as shown

on Figure 3.12. ^{13}C NMR (300 MHz, 298 K, CDCl$_3$, δ): 166.1 (CH$_2$=CH−(C=O)−NH−), 163.1 (−NH−(C=N−)−NH−), 158.0 (=N−(C=O)−O−), 153.3 (=N−(C=O)−O−), 131.8 (CH$_2$=C−(C=O)−), 125.7 (CH$_2$=C−), 84.0 (−O−C((CH$_3$)$_3$), 79.9 (−O−C((CH$_3$)$_3$), 42.2 (−NH−CH$_2$−CH$_2$−NH−) 40.6 (−NH−CH$_2$−CH$_2$−NH−), 28.3 (−O−C((CH$_3$)$_3$) as shown on Figure 3.13. MS: [M+Na]$^+$ 379.41 (calculated), 379.3 (found). The IR spectrum of diBocGEAM can be found on Figure 3.14.

3.4.3.2 Synthesis of G-S30^{Boc}

DiBocGEAM (320 mg, 0.900 mmol), NIPAM (238 mg, 2.10 mmol) and PABTC (7.15 mg, 0.0300 mmol) were dissolved in 1200 µL of 1,4-dioxane and 100 µL of water. 194 µL of a 5 mg.mL^{-1} stock solution of VA-044 in water was added to the mixture which was introduced in a test tube equipped with a mechanical stirrer and a rubber septum. The solution was degassed with nitrogen for *ca.* 15 min and the polymerisation was then performed in a thermostated oil bath. After the desired polymerisation time, the test tube was withdrawn from the oil bath.

3.4.3.3 Multiblock copolymer synthesis by iterative RAFT polymerisation
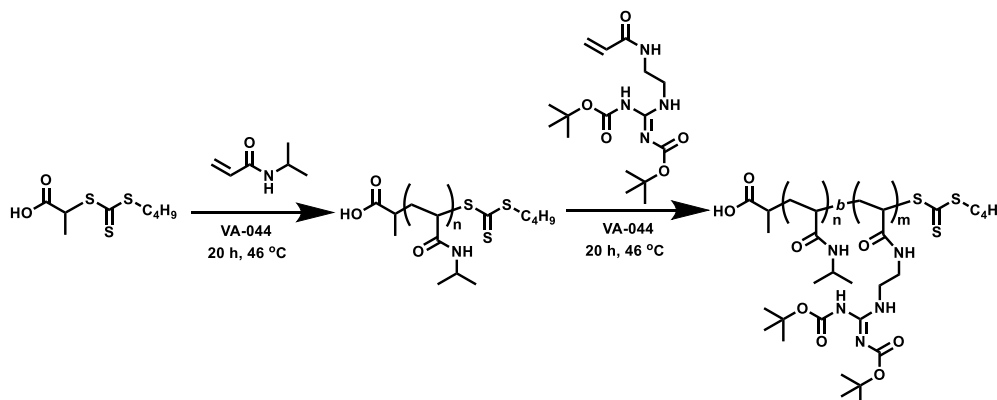
Typical synthesis of the initial block. For the synthesis of the first block of G-D30^{Boc}, NIPAM (249 mg, 2.20 mmol) and PABTC (7.49 mg, 0.0300 mmol) were dissolved in 700 µL of 1,4-dioxane and 33 µL of water. 142 µL of a 5 mg.mL^{-1} stock solution of VA-044 was added to the mixture which was introduced in a test tube equipped with a mechanical stirrer and a rubber septum. The solution was degassed with nitrogen for *ca.* 20 min and the polymerisation was then performed in a thermostated oil bath at 46 °C. After 6 hours, the test tube was withdrawn from the oil bath and a sample was taken for ^{1}H NMR and SEC analysis.

Typical synthesis of subsequent blocks. The test tube with the reaction mixture was opened and diBocGEAM (336 mg, 0.900 mmol) was added with 240 µL of 1,4-dioxane and 60 µL of a 10 mg.mL^{-1} stock solution of VA-044 in water. After the mixture was sealed with a septum,

the solution was degassed for *ca*. 20 min, then placed in an oil bath set at 46 °C for the polymerisation to occur. The tube was withdrawn from the oil bath after 6 hours and a sample was taken for ^{1}H NMR and SEC analysis. The quantity of reagents needed for the tetrablock copolymers can be found in Tables 3.7-3.10.

Monomer conversion, theoretical molecular weight $M_{n,th}$ and livingness were determined as detailed in chapter 2.

3.4.3.4   RAFT Polymerisation Kinetics for G-S30^{Boc}

The polymerisation kinetics and resulting composition of G-S30^{Boc} were investigated using ^{1}H NMR spectroscopy in DMSO-d_6. As the vinyl protons of NIPAM and diBocGEAM cannot be readily distinguished, the overall monomer conversion (diBocGEAM and HEA combined) was followed by ^{1}H NMR spectroscopy using an external standard (1,3,5-trioxane). Additionally, RP-HPLC was used to determine the relative concentration of each monomer in the reaction mixture over time (Eclipse Plus C18, 3.5 µm, 4.6 x 100 mm, H_2O/ACN). Calibration curves were established with NIPAM and diBocGEAM in order to determine the concentration of each monomer in the kinetic samples. The ratio of NIPAM to diBocGEAM was calculated and used in conjunction with the overall monomer conversion in order to determine the relative conversion of each monomer over time and deduce the compositional drift (Figure 3.18). The conversion of diBocGEAM and NIPAM over time are comparable to one another, indicating the absence of profound compositional drift.

3.4.3.5   Deprotection of the polymers

The polymers were dissolved in TFA and stirred for 3 hours at 40°C. The TFA was then removed and the polymers were precipitated in diethyl ether. In order to replace the TFA counter-ion, the polymers were dialysed against a NaCl solution, followed by dialysis against distilled water.

3.5   Supporting Figures
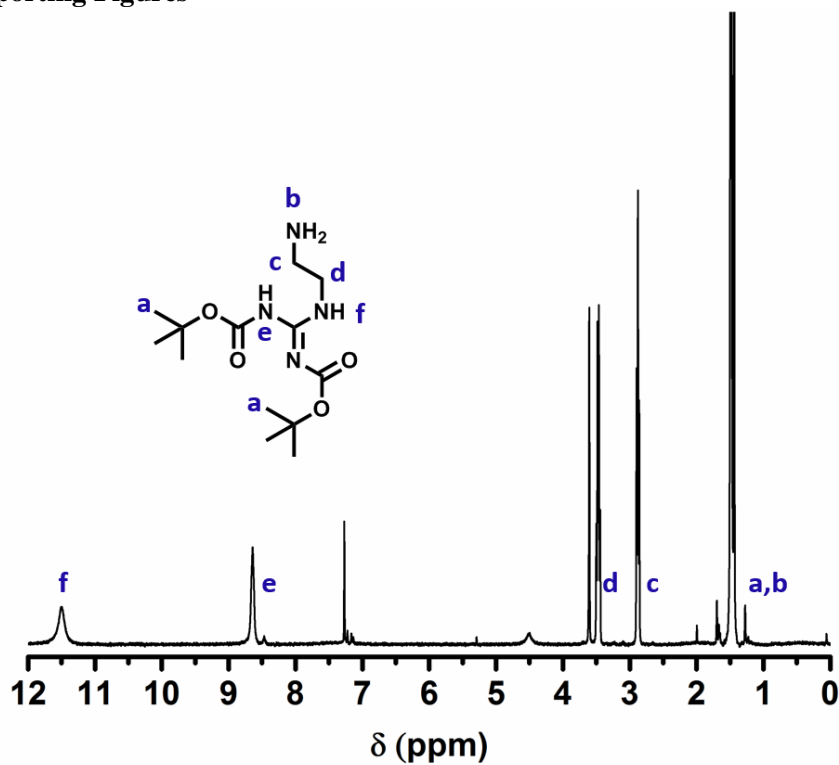
Figure 3.11 - ^{1}**H NMR spectrum of the intermediate product 2-[1,3-Bis(tert-butoxycarbonyl)guanidine]ethylamine in CDCl$_3$.**
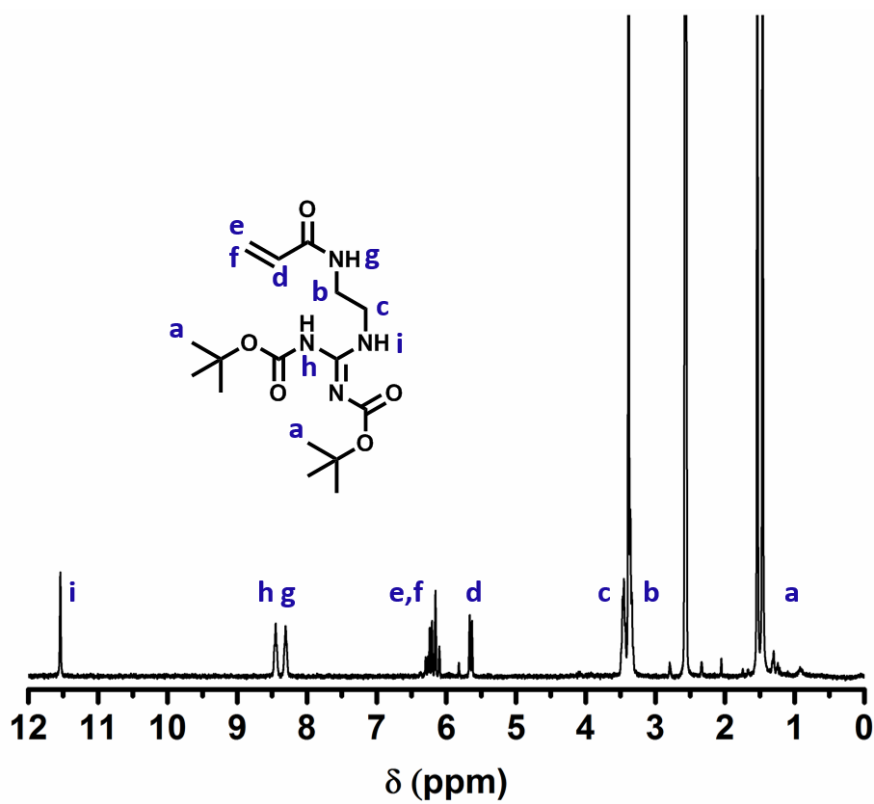
Figure 3.12 - ^{1}**H NMR spectrum of diBoc-GEAM in CDCl$_3$.**
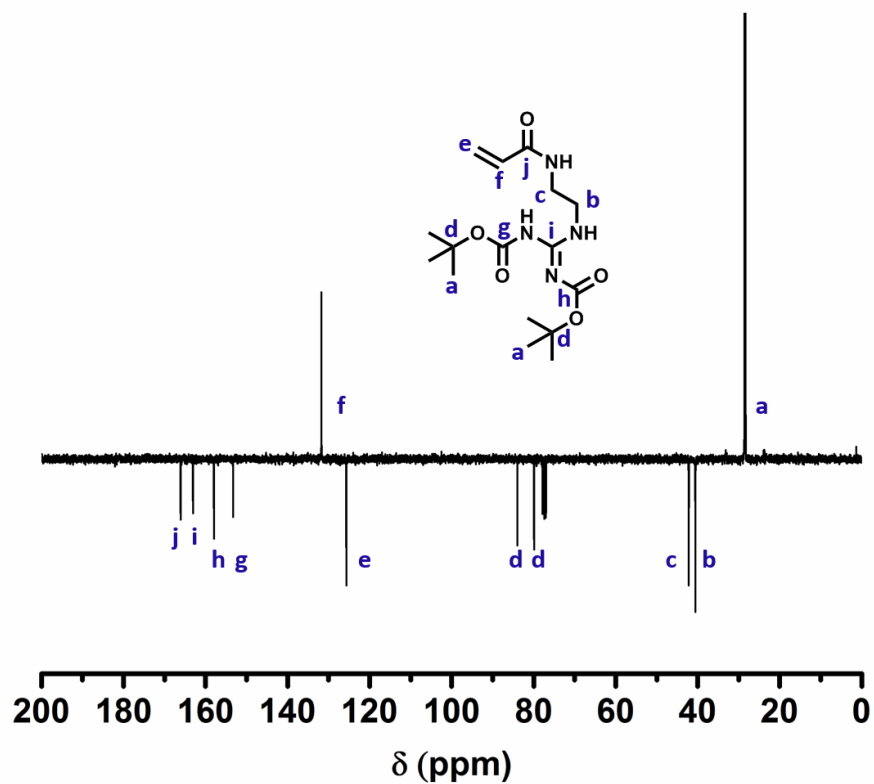
Figure 3.13 - ^{13}C NMR spectrum of diBoc-GEAM in CDCl$_3$.
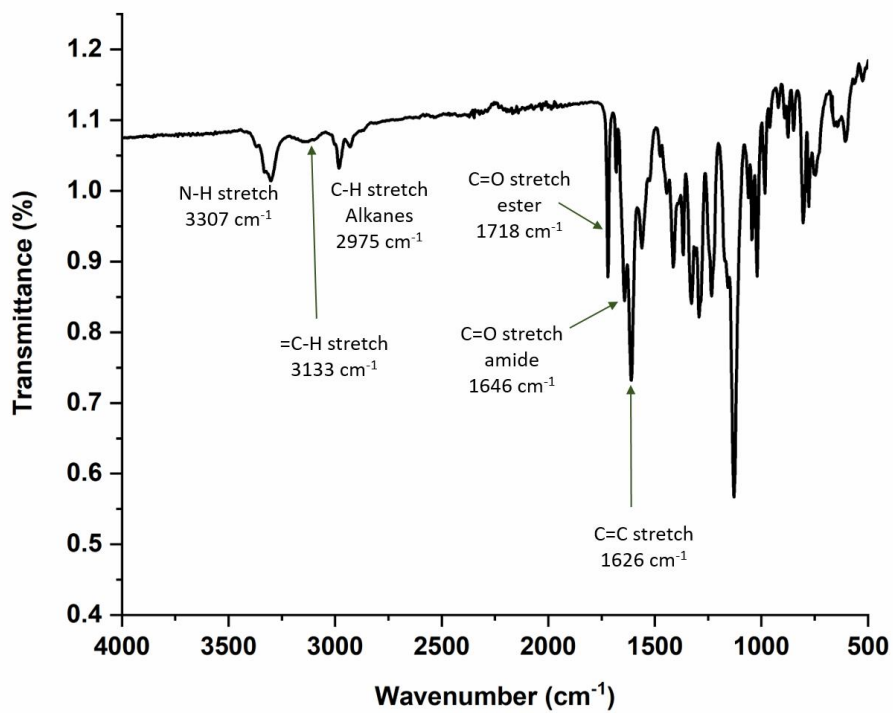
Figure 3.14 - IR spectrum of diBocGEAM.
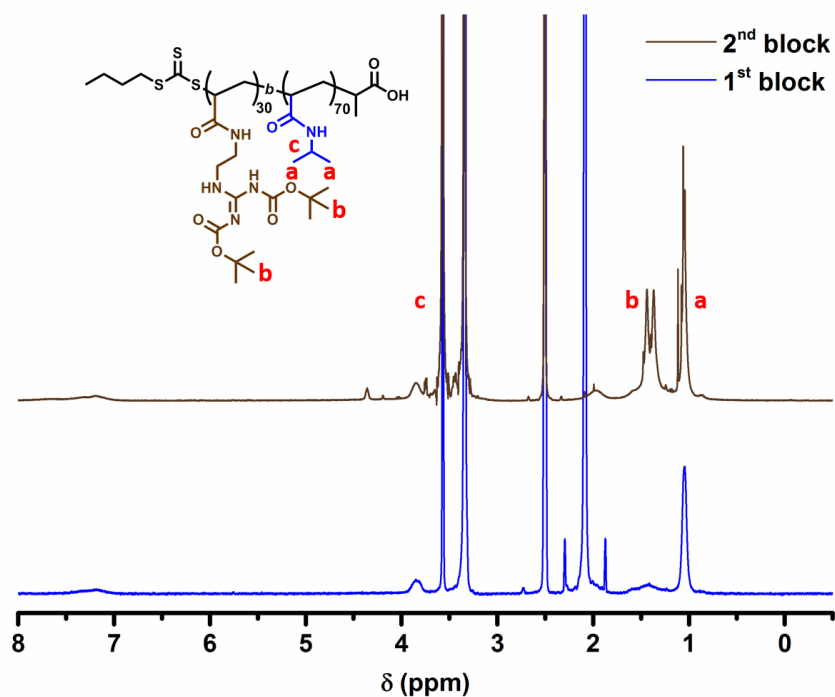
Figure 3.15 - ^{1}H NMR spectra in DMSO-d_6 of **G-D30^{Boc}** for each chain extension.
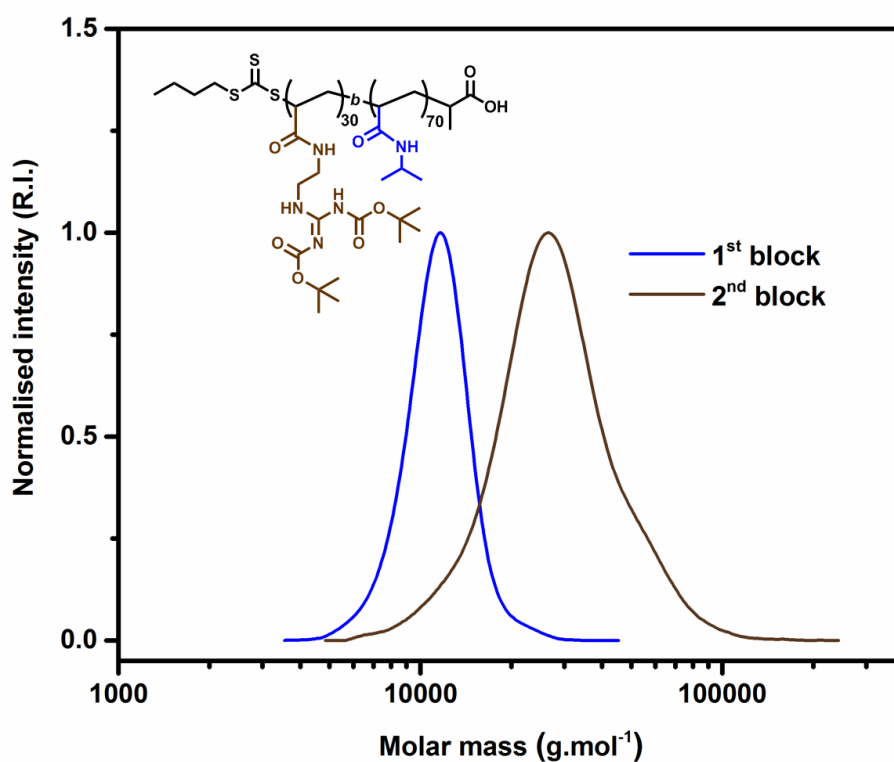
Figure 3.16 - DMF-SEC chromatograms for successive chain extensions of G-D30^{Boc}.
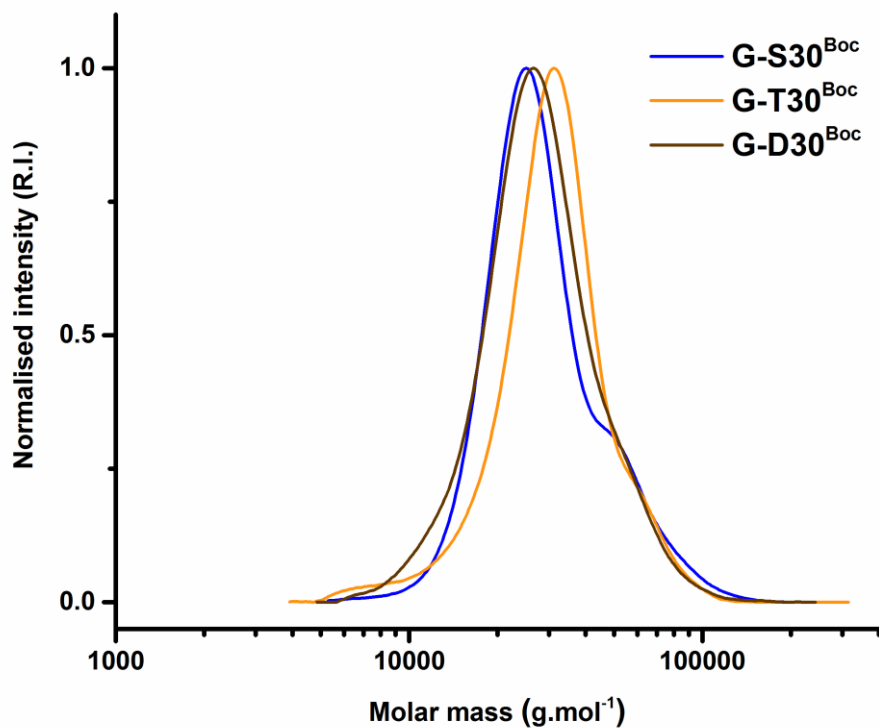
Figure 3.17 - DMF-SEC chromatograms for G-S30^{Boc}, G-T30^{Boc} and G-D30^{Boc}.
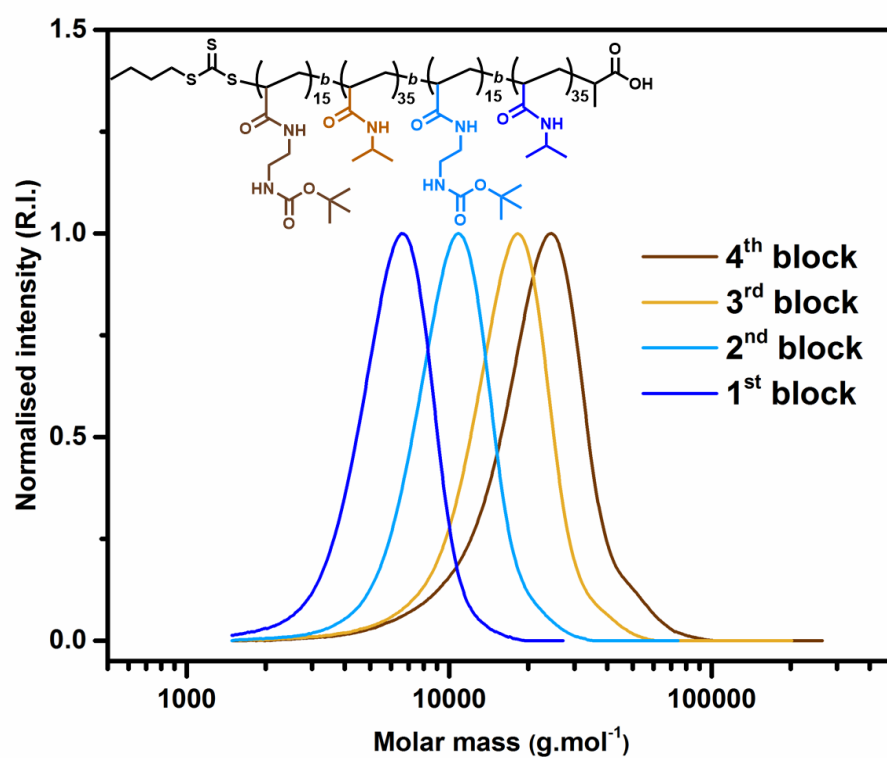
Figure 3.18 - DMF-SEC chromatograms for successive chain extensions of A-T30^{Boc}.
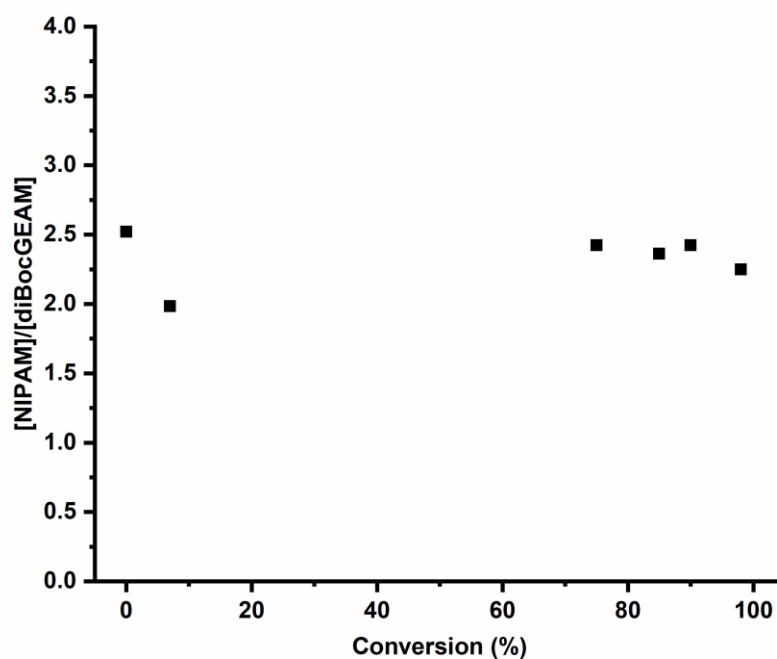
Figure 3.19 - Ratio of the concentration of remaining NIPAM and BocAEAM with overall conversion during the polymerisation of G-S30^{Boc}.
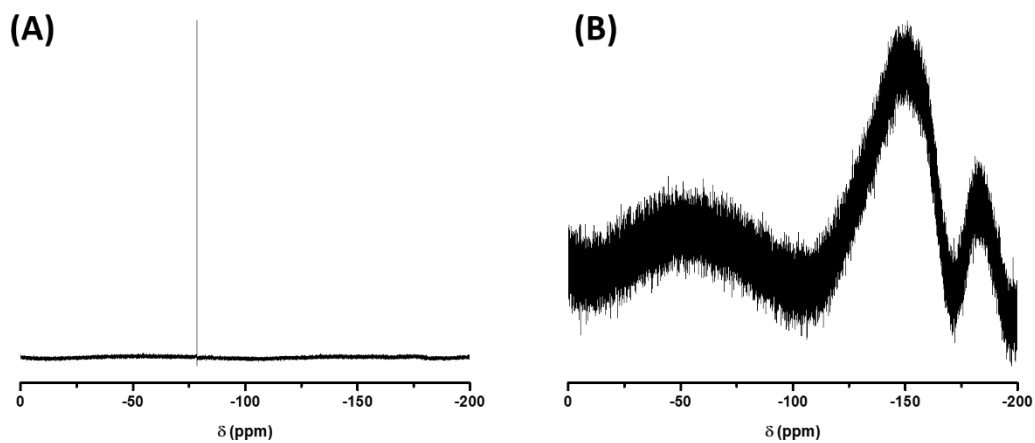
Figure 3.20 - ^{19}F NMR spectra in D$_2$O of G-S30 before (A) and after (B) dialysis against NaCl.
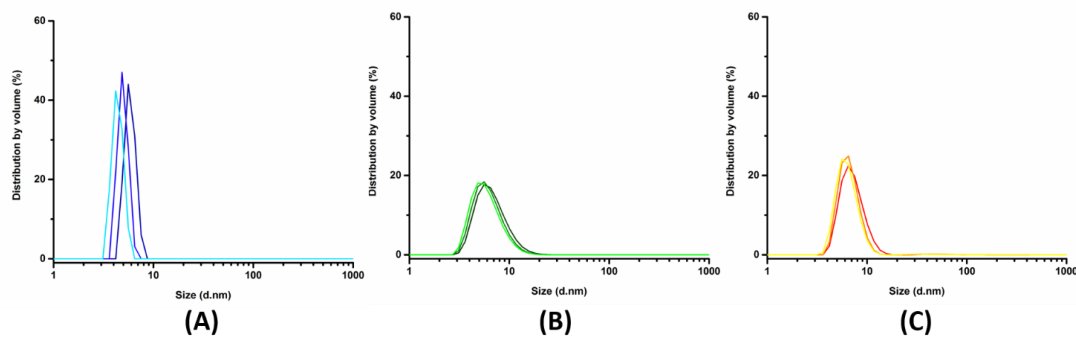
Figure 3.21 - Volume distribution of G-S30 (A), G-T30 (B), G-D30 (C) by DLS in PBS at 37 °C at 1.024 mg.mL^{-1} Size and PDI are shown in Table 3.11.

3.6 Supporting Tables

Table 3.6 - Experimental conditions used for the synthesis of S30^{Boc}.

Sample number		S30^{Boc}
BocGEAM content (%)		32
DP$_{total}$		105
NIPAM	DP$_{targeted}$	73
	m$_{monomer\ added}$ (mg)	238
BocGEAM	DP$_{targeted}$	32
	m$_{monomer\ added}$ (mg)	321
m$_{CTA\ added}$ (mg)		7.15
V$_{dioxane\ added}$ (mL)		1.200
V$_{water\ added}$ (mL)		0.300
V$_{total}$ (mL)		1.500
[VA-044]$_0$ (mol L^{-1})		2.00 10^{-3}
[monomer]$_0$ (mol L^{-1})		2
[CTA]$_0$/[VA-044]$_0$		10
L (%)[a]		92

[a] Livingness of the polymers, as defined in equation 2.6.

Table 3.7 - Experimental conditions used for the synthesis DP 100 diblock copolymers of NIPAM and diBocGEAM.

Sample number	D30[Boc]	
BocGEAM content (%)	30	
DP_{total}	103	
Block n°	1	2
Monomer	NIPAM	BocGEAM
$DP_{targeted}$	63	31
$m_{monomer\ added}$ (mg)	249	336
$m_{CTA\ added}$ (mg)	7.49	-
$m_{VA\text{-}044\ added}$ (mg)	1.14	0.724
$V_{dioxane\ added}$ (mL)	0.704	0.240
$V_{water\ added}$ (mL)	0.176	0.060
V_{total} (mL)	0.880	1.180
$[VA\text{-}044]_0$ (mol L^{-1})	$2.50\ 10^{-3}$	$1.90\ 10^{-3}$
$[monomer]_0$ (mol L^{-1})	2.50	0.80
$[CTA]_0/[VA\text{-}044]_0$	14	18
L (%)[a]	94	95
Cumulative L (%)	94	90

[a] Livingness of the polymers, as defined in equation 2.6.

Table 3.8 - Experimental conditions used for the synthesis of G-T30^{Boc}.

Block n°	1	2	3	4
Monomer	NIPAM	BocGEAM	NIPAM	BocGEAM
$DP_{targeted}$	33	15	33	15
$m_{monomer\ added}$ (mg)	147	199	147	199
$m_{CTA\ added}$ (mg)	8.85	-	-	-
$m_{VA-044\ added}$ (mg)	0.420	0.437	0.525	0.703
$V_{dioxane\ added}$ (mL)	0.420	0.165	0.230	0.176
$V_{EtOH\ added}$ (mL)	-	0.055	-	0.044
$V_{water\ added}$ (mL)	0.100	0.060	0.060	0.056
V_{total} (mL)	0.520	0.800	1.090	1.366
$[VA-044]_0$ (mol L^{-1})	2.50 10^{-3}	1.70 10^{-3}	1.50 10^{-3}	1.60 10^{-3}
$[monomer]_0$ (mol L^{-1})	2.50	0.70	1.20	0.41
$[CTA]_0/[VA-044]_0$	29	27	23	17
L (%)[a]	97	99	96	95
Cumulative L (%)	97	97	94	89

[a] Livingness of the polymers, as defined in equation 2.6.

Table 3.9 - Experimental conditions used for the synthesis of A-T30^{Boc}.

Block n°	1	2	3	4
Monomer	NIPAM	BocAEAM	NIPAM	BocAEAM
$DP_{targeted}$	37	15	33	15
$m_{monomer\ added}$ (mg)	79.0	64.0	79.0	64.0
$m_{CTA\ added}$ (mg)	4.77	-	-	-
$m_{VA-044\ added}$ (mg)	0.226	0.144	0.138	0.285
$V_{dioxane\ added}$ (mL)	0.224	0.066	0.167	0.116
$V_{water\ added}$ (mL)	0.056	0.030	0.042	0.057
V_{total} (mL)	0.280	0.375	0.583	0.732
$[VA\text{-}044]_0$ (mol L^{-1})	$2.50\ 10^{-3}$	$1.50\ 10^{-3}$	$1.00\ 10^{-3}$	$1.50\ 10^{-3}$
$[monomer]_0$ (mol L^{-1})	2.50	0.80	1.20	0.40
$[CTA]_0/[VA\text{-}044]_0$	29	36	34	18
L (%)[a]	97	98	97	95
Cumulative L (%)	97	95	93	88

[a] Livingness of the polymers, as defined in equation 2.6.

Table 3.10 - Characterisation data of the final Boc-protected polymers.

	Block n°	Polymer composition	$M_{n,th}$[a] (g mol^{-1})	$M_{n,SEC}$[b] (g mol^{-1})	$Đ$[b]
G-S30^{Boc}	*N.A.*	pdiBocGEAM$_{30}$-*s*-pNIPAM$_{70}$	18900	25900	1.24
G-D30^{Boc}	1st	pNIPAM$_{70}$	10900	11000	1.07
	2nd	pNIPAM$_{70}$-*b*-pdiBocGEAM$_{30}$	17900	24900	1.24
G-T30^{Boc}	1st	pNIPAM$_{35}$	3970	6300	1.09
	2nd	pNIPAM$_{35}$-*b*-pdiBocGEAM$_{15}$	9320	12800	1.14
	3rd	pNIPAM$_{35}$-*b*-pdiBocGEAM$_{15}$-*b*-pNIPAM$_{35}$	13000	19400	1.15
	4th	pNIPAM$_{35}$-*b*-pdiBocGEAM$_{15}$-*b*-pNIPAM$_{35}$-*b*-pdiBocGEAM$_{15}$	18400	27200	1.23
A-S30^{Boc}	*N.A.*	pBocAEAM$_{30}$-*s*-pNIPAM$_{70}$	15400	17900	1.09
A-D30^{Boc}	1st	pNIPAM$_{70}$	8390	10600	1.08
	2nd	pNIPAM$_{70}$-*b*-pBocAEAM$_{30}$	15000	16000	1.10
A-T30^{Boc}	1st	pNIPAM$_{35}$	3860	5560	1.15
	2nd	pNIPAM$_{35}$-*b*-pBocAEAM$_{15}$	6650	9310	1.16
	3rd	pNIPAM$_{35}$-*b*-pBocAEAM$_{15}$-*b*-pNIPAM$_{35}$	10300	14770	1.20
	4th	pNIPAM$_{35}$-*b*-pBocAEAM$_{15}$-*b*-pNIPAM$_{35}$-*b*-pBocAEAM$_{15}$	13050	18800	1.27

[a] Theoretical molecular weight of the protected polymers calculated from equation 2.5.

[b] Determined for the protected polymers by SEC/RI in DMF using PMMA as molecular weight standards.

Table 3.11 - Characterisation data of deprotected polymers.

Sample	Cationic content (%)	$M_{n,th}$[a] (g mol^{-1})	Elution ratio[b] (%)	Size[c] (nm)	PDI[c]
A-S30	32	13300	54	6	0.6
A-T30	29	13100	69	10	0.4
A-D30	30	13000	77	6	0.9
G-S30	32	13900	53	4	1.0
G-T30	31	13200	72	6	0.4
G-D30	30	13100	78	7	0.6

[a] Theoretical molecular weight of the protected polymers calculated from equation 2.5.

[b] From HPLC data measured in water/ACN in a C18 column (gradient 1 to 80 % ACN in 45 minutes). The elution ratio was calculated according to equation 2.3 using the elution time.

[c] Measured by DLS in Phosphate Buffer Saline (PBS) at 37˚C and 1 mg mL^{-1} using the volume distribution.

3.7   References

1.   Cosgrove, S. E.; Sakoulas, G.; Perencevich, E. N.; Schwaber, M. J.; Karchmer, A. W.; Carmeli, Y., Comparison of Mortality Associated with Methicillin-Resistant and Methicillin-Susceptible Staphylococcus aureus Bacteremia: A Meta-analysis. *Clinical Infectious Diseases* **2003,** *36* (1), 53-59.

2.   Liu, C.; Chambers, H. F.; Kaplan, S. L.; Karchmer, A. W.; Levine, D. P.; Rybak, M. J.; Murray, B. E.; Bayer, A.; Talan, D. A.; Cosgrove, S. E.; Daum, R. S.; Fridkin, S. K.; Gorwitz, R. J., Clinical Practice Guidelines by the Infectious Diseases Society of America for the Treatment of Methicillin-Resistant Staphylococcus aureus Infections in Adults and Children. *Clinical Infectious Diseases* **2011,** *52* (3), e18-e55.

3.   McGuinness, W. A.; Malachowa, N.; DeLeo, F. R., Vancomycin Resistance in Staphylococcus aureus. *The Yale journal of biology and medicine* **2017,** *90* (2), 269-281.

4.   Hidayat, L. K.; Hsu, D. I.; Quist, R.; Shriner, K. A.; Wong-Beringer, A., High-dose vancomycin therapy for methicillin-resistant staphylococcus aureus infections: Efficacy and toxicity. *Archives of Internal Medicine* **2006,** *166* (19), 2138-2144.

5.   Van Bambeke, F.; Mingeot-Leclercq, M.-P.; Struelens, M. J.; Tulkens, P. M., The bacterial envelope as a target for novel anti-MRSA antibiotics. *Trends in Pharmacological Sciences* **2008,** *29* (3), 124-134.

6.   Zasloff, M., Antimicrobial peptides of multicellular organisms. *Nature* **2002,** *415* (6870), 389-395.

7.   Hartlieb, M.; Williams, E. G. L.; Kuroki, A.; Perrier, S.; Locock, K., E. S. , Antimicrobial polymers: Mimicking amino acid functionality, sequence control and three-dimensional structure of host-defense peptides. *Curr. Med. Chem.* **2017,** *24*, 2115-2140.

8.   Ganewatta, M. S.; Tang, C., Controlling macromolecular structures towards effective antimicrobial polymers. *Polymer* **2015,** *63*, A1-A29.

9.   Findlay, B.; Zhanel, G. G.; Schweizer, F., Cationic Amphiphiles, a New Generation of Antimicrobials Inspired by the Natural Antimicrobial Peptide Scaffold. **2010,** *54* (10), 4049-4058.

10.   Palermo, E. F.; Lee, D.-K.; Ramamoorthy, A.; Kuroda, K., Role of Cationic Group Structure in Membrane Binding and Disruption by Amphiphilic Copolymers. *The Journal of Physical Chemistry B* **2011,** *115* (2), 366-375.

11.   Palermo, E. F.; Sovadinova, I.; Kuroda, K., Structural Determinants of Antimicrobial Activity and Biocompatibility in Membrane-Disrupting Methacrylamide Random Copolymers. *Biomacromolecules* **2009,** *10* (11), 3098-3107.

12.   Engler, A. C.; Shukla, A.; Puranam, S.; Buss, H. G.; Jreige, N.; Hammond, P. T., Effects of Side Group Functionality and Molecular Weight on the Activity of Synthetic Antimicrobial Polypeptides. *Biomacromolecules* **2011,** *12* (5), 1666-1674.

13.   Paslay, L. C.; Abel, B. A.; Brown, T. D.; Koul, V.; Choudhary, V.; McCormick, C. L.; Morgan, S. E., Antimicrobial Poly(methacrylamide) Derivatives Prepared via Aqueous RAFT Polymerization Exhibit Biocidal Efficiency Dependent upon Cation Structure. *Biomacromolecules* **2012,** *13* (8), 2472-2482.

14.   Griffiths, M. Z.; Alkorta, I.; Popelier, P. L. A., Predicting pKa Values in Aqueous Solution for the Guanidine Functional Group from Gas Phase Ab Initio Bond Lengths. **2013,** *32* (4), 363-376.

15.   Dewick, P. M., Essentials of Organic Chemistry: For Students of Pharmacy, Medicinal Chemistry and Biological Chemistry. Wiley: 2006; p 161.

16.   Gabriel, G. J.; Madkour, A. E.; Dabkowski, J. M.; Nelson, C. F.; Nüsslein, K.; Tew, G. N., Synthetic Mimic of Antimicrobial Peptide with Nonmembrane-Disrupting Antibacterial Properties. *Biomacromolecules* **2008,** *9* (11), 2980-2983.

17.   Locock, K. E. S.; Michl, T. D.; Valentin, J. D. P.; Vasilev, K.; Hayball, J. D.; Qu, Y.; Traven, A.; Griesser, H. J.; Meagher, L.; Haeussler, M., Guanylated Polymethacrylates: A Class of Potent Antimicrobial Polymers with Low Hemolytic Activity. *Biomacromolecules* **2013,** *14* (11), 4021-4031.

18.   Exley, S. E.; Paslay, L. C.; Sahukhal, G. S.; Abel, B. A.; Brown, T. D.; McCormick, C. L.; Heinhorst, S.; Koul, V.; Choudhary, V.; Elasri, M. O.; Morgan, S. E., Antimicrobial Peptide Mimicking Primary Amine and Guanidine Containing Methacrylamide Copolymers Prepared by Raft Polymerization. *Biomacromolecules* **2015,** *16* (12), 3845-3852.

19.   Budhathoki-Uprety, J.; Peng, L.; Melander, C.; Novak, B. M., Synthesis of Guanidinium Functionalized Polycarbodiimides and Their Antibacterial Activities. *ACS Macro Letters* **2012,** *1* (3), 370-374.

20.   Martin, L.; Peltier, R.; Kuroki, A.; Town, J. S.; Perrier, S., Investigating Cell Uptake of Guanidinium-Rich RAFT Polymers: Impact of Comonomer and Monomer Distribution. *Biomacromolecules* **2018,** *19* (8), 3190-3200.

21.   Treat, N. J.; Smith, D.; Teng, C.; Flores, J. D.; Abel, B. A.; York, A. W.; Huang, F.; McCormick, C. L., Guanidine-Containing Methacrylamide (Co)polymers via aRAFT: Toward a Cell Penetrating Peptide Mimic. *ACS macro letters* **2012,** *1* (1), 100-104.

22.   Sarapas, J. M.; Backlund, C. M.; deRonde, B. M.; Minter, L. M.; Tew, G. N., ROMP- and RAFT-Based Guanidinium-Containing Polymers as Scaffolds for Protein Mimic Synthesis. *Chemistry (Weinheim an der Bergstrasse, Germany)* **2017,** *23* (28), 6858-6863.

23.   Perrier, S., 50th Anniversary Perspective: RAFT Polymerization—A User Guide. *Macromolecules* **2017,** *50* (19), 7433-7447.

24.   Moad, G.; Rizzardo, E.; Thang, S. H., Living Radical Polymerization by the RAFT Process – A Third Update. *Australian Journal of Chemistry* **2012,** *65* (8), 985-1076.

25.   Gody, G.; Maschmeyer, T.; Zetterlund, P. B.; Perrier, S., Exploitation of the Degenerative Transfer Mechanism in RAFT Polymerization for Synthesis of Polymer of High Livingness at Full Monomer Conversion. *Macromolecules* **2014,** *47* (2), 639-649.

26.   Kuroki, A.; Sangwan, P.; Qu, Y.; Peltier, R.; Sanchez-Cano, C.; Moat, J.; Dowson, C. G.; Williams, E. G. L.; Locock, K. E. S.; Hartlieb, M.; Perrier, S., Sequence Control as a Powerful Tool for Improving the Selectivity of Antimicrobial Polymers. *ACS Appl. Mater. Interfaces* **2017,** *9* (46), 40117-40126.

27.   Gody, G.; Zetterlund, P. B.; Perrier, S.; Harrisson, S., The limits of precision monomer placement in chain growth polymerization. *Nature Communications* **2016,** *7*, 10514.

28.   Gody, G.; Maschmeyer, T.; Zetterlund, P. B.; Perrier, S., Pushing the Limit of the RAFT Process: Multiblock Copolymers by One-Pot Rapid Multiple Chain Extensions at Full Monomer Conversion. *Macromolecules* **2014,** *47* (10), 3451-3460.

29.   Martin, L.; Gody, G.; Perrier, S., Preparation of complex multiblock copolymers via aqueous RAFT polymerization at room temperature. *Polym. Chem.* **2015,** *6* (27), 4875-4886.

30.   Smets, G.; Hesbain, A. M., Hydrolysis of polyacrylamide and acrylic acid–acrylamide copolymers. *Journal of Polymer Science* **1959,** *40* (136), 217-226.

31.   Lienkamp, K.; Madkour, A. E.; Kumar, K.-N.; Nüsslein, K.; Tew, G. N., Antimicrobial Polymers Prepared by Ring-Opening Metathesis Polymerization: Manipulating

Antimicrobial Properties by Organic Counterion and Charge Density Variation. *Chem. Eur. J.* **2009,** *15* (43), 11715-11722.

32. Peltier, R.; Bialek, A.; Kuroki, A.; Bray, C.; Martin, L.; Perrier, S., Reverse-phase high performance liquid chromatography (RP-HPLC) as a powerful tool to characterise complex water-soluble copolymer architectures. *Polym. Chem.* **2018,** *9* (46), 5511-5520.

33. Hou, L.; Wu, P., Comparison of LCST-transitions of homopolymer mixture, diblock and statistical copolymers of NIPAM and VCL in water. *Soft Matter* **2015,** *11* (14), 2771-2781.

34. Wei, H.; Cheng, S.-X.; Zhang, X.-Z.; Zhuo, R.-X., Thermo-sensitive polymeric micelles based on poly(N-isopropylacrylamide) as drug carriers. *Progress in Polymer Science* **2009,** *34* (9), 893-910.

35. Feil, H.; Bae, Y. H.; Feijen, J.; Kim, S. W., Effect of comonomer hydrophilicity and ionization on the lower critical solution temperature of N-isopropylacrylamide copolymers. *Macromolecules* **1993,** *26* (10), 2496-2500.

36. Oddo, A.; Hansen, P. R., Hemolytic Activity of Antimicrobial Peptides. In *Antimicrobial Peptides: Methods and Protocols*, Hansen, P. R., Ed. Springer New York: New York, NY, 2017; pp 427-435.

37. Sovadinova, I.; Palermo, E. F.; Huang, R.; Thoma, L. M.; Kuroda, K., Mechanism of Polymer-Induced Hemolysis: Nanosized Pore Formation and Osmotic Lysis. *Biomacromolecules* **2011,** *12* (1), 260-268.

38. Locock, K. E. S.; Michl, T. D.; Stevens, N.; Hayball, J. D.; Vasilev, K.; Postma, A.; Griesser, H. J.; Meagher, L.; Haeussler, M., Antimicrobial Polymethacrylates Synthesized as Mimics of Tryptophan-Rich Cationic Peptides. *ACS Macro Letters* **2014,** *3* (4), 319-323.

39. Annual epidemiological report : Antimicrobial resistance and health care-associated infections In *European Centre For Disease Prevention And Control*, 2014.

40. von Eiff, C.; Becker, K.; Metze, D.; Lubritz, G.; Hockmann, J.; Schwarz, T.; Peters, G., Intracellular Persistence of Staphylococcus aureus Small-Colony Variants within Keratinocytes: A Cause for Antibiotic Treatment Failure in a Patient with Darier's Disease. *Clinical Infectious Diseases* **2001,** *32* (11), 1643-1647.

41. Bechara, C.; Sagan, S., Cell-penetrating peptides: 20 years later, where do we stand? *FEBS Lett.* **2013,** *587* (12), 1693-1702.

42. Neamnark, A.; Suwantong, O.; K. C, R. B.; Hsu, C. Y. M.; Supaphol, P.; Uludağ, H., Aliphatic Lipid Substitution on 2 kDa Polyethylenimine Improves Plasmid Delivery and Transgene Expression. *Molecular Pharmaceutics* **2009,** *6* (6), 1798-1815.

43. Rubinstein, E.; Kollef, M. H.; Nathwani, D., Pneumonia Caused by Methicillin-Resistant Staphylococcus aureus. *Clinical Infectious Diseases* **2008,** *46* (Supplement_5), S378-S385.

44. Herbert, S.; Ziebandt, A.-K.; Ohlsen, K.; Schäfer, T.; Hecker, M.; Albrecht, D.; Novick, R.; Götz, F., Repair of global regulators in Staphylococcus aureus 8325 and comparative analysis with other clinical isolates. *Infection and immunity* **2010,** *78* (6), 2877-2889.

45. Bæk, K. T.; Gründling, A.; Mogensen, R. G.; Thøgersen, L.; Petersen, A.; Paulander, W.; Frees, D., β-Lactam resistance in methicillin-resistant Staphylococcus aureus USA300 is increased by inactivation of the ClpXP protease. *Antimicrobial agents and chemotherapy* **2014,** *58* (8), 4593-4603.

46. Sakai, N.; Matile, S., Anion-Mediated Transfer of Polyarginine across Liquid and Bilayer Membranes. *J. Am. Chem. Soc.* **2003,** *125* (47), 14348-14356.

47.   Chindera, K.; Mahato, M.; Kumar Sharma, A.; Horsley, H.; Kloc-Muniak, K.; Kamaruzzaman, N. F.; Kumar, S.; McFarlane, A.; Stach, J.; Bentin, T.; Good, L., The antimicrobial polymer PHMB enters cells and selectively condenses bacterial chromosomes. *Scientific Reports* **2016,** *6*, 23121.

48.   García, A. B.; Viñuela-Prieto, J. M.; López-González, L.; Candel, F. J., Correlation between resistance mechanisms in Staphylococcus aureus and cell wall and septum thickening. *Infection and drug resistance* **2017,** *10*, 353-356.

49.   Kawada-Matsuo, M.; Komatsuzawa, H., Factors affecting susceptibility of Staphylococcus aureus to antibacterial agents. *Journal of Oral Biosciences* **2012,** *54* (2), 86-91.

Chapter 4   Targeting intracellular MRSA with guanidinium polymers and elucidating the structure-activity relationship
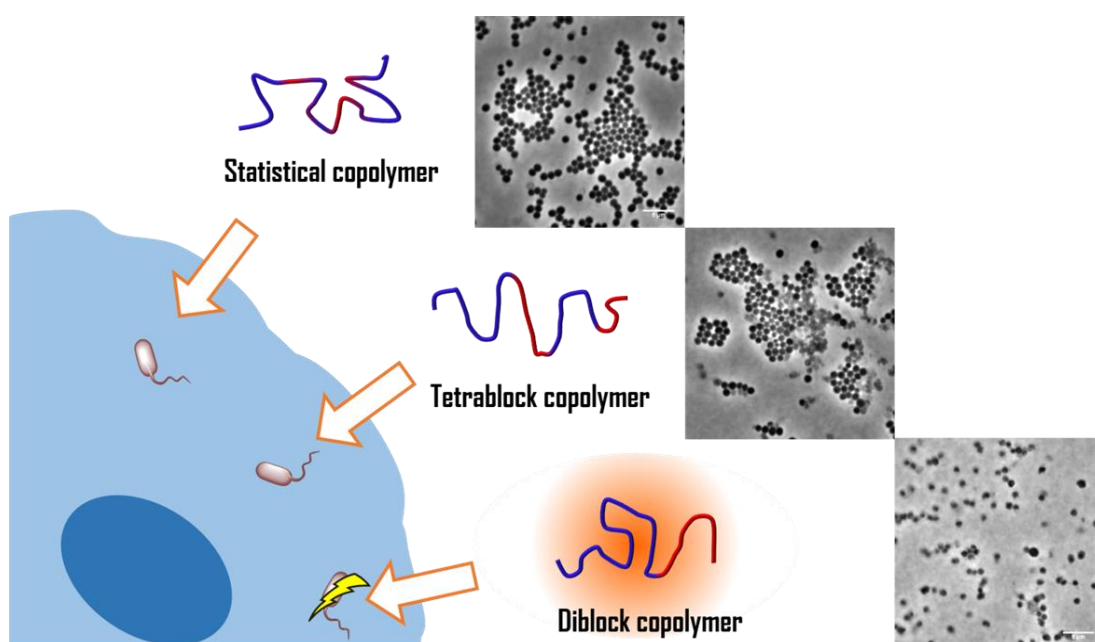
Abstract

Intracellular persistence of bacteria represents a clinical challenge as bacteria can thrive in an environment harboured from high concentrations of antibiotics and phagocytes. This persistence, combined with decreasing bacterial susceptibility to antibiotics make the need for an alternative to current infection treatments urgent. To tackle infections whilst overcoming antibiotic resistance, SMAMPs are interesting candidates as they exhibit a very high antimicrobial activity. In addition to bearing structural similarities to CPPs, the guanidinium containing SMAMPs were shown to be very potent against MRSA in chapter 3. Therefore, they were further investigated in the treatment of intracellular *S. aureus* in keratinocytes. Varying the distribution of functional monomers was shown to have a substantial influence on the interactions of the polymers with bacterial membranes: the diblock copolymer bound the fastest, followed by the tetrablock, whereas no binding was observed with the statistical copolymer. This trend was consistent with that of the antimicrobial activity of the guanidinium polymers. The reduction in activity of the tetrablock compared to the diblock was attributed to the isopropyl functionalities of the polyNIPAM block hindering the cationic functionalities when in the middle of the polymer chain. However, these alkyl chains seemed to promote the antimicrobial activity of guanidinium containing SMAMPs. In parallel, it was observed that all three polymers had comparable levels of internalisation into keratinocytes, *via* both energy-dependent and independent pathways. These results led to the investigation of the efficiency of the SMAMPs against intracellular bacteria in keratinocytes. The diblock structure was the most active, reducing the amount of intracellular MSSA and MRSA by two-fold compared to the statistical and tetrablock copolymers. Here, a potential treatment for intracellular, multi-drug resistant bacteria is presented, using a simple and scalable strategy.

4.1   Introduction

Staphylococcus aureus (*S. aureus*) is one of the major causes of both community and hospital-acquired infections, methicillin-resistant *S. aureus* (MRSA) being associated with a mortality rate fivefold higher than that of methicillin-sensitive strains (MSSA) amongst patients in Europe.[1-2] This issue is exacerbated with the ability of *S. aureus* to persist intracellularly.[3-4] The presence of *S. aureus* inside epithelial and phagocytic cells has been associated with skin infections, tonsillitis and rhinosinusitis.[5-8] Unfortunately, the most commonly employed antibiotics (such as vancomycin, oxacillin, and gentamycin) are not effective against intracellular bacteria since they are not efficiently internalised by the host cells, which enables *S. aureus* to survive.[9-10] In order to address this issue, antibiotic loaded liposomes and nanoparticles have been explored.[11] Although these systems were internalised by infected mammalian cells and efficiently killed intracellular bacteria, the stability and the drug loading efficiency of nanoparticles and liposomes were shown to be limited.[12-13] To circumvent these challenges, recent work has focused on the use of low molecular weight vectors capable of promoting intracellular delivery of antibiotics.[14] Amongst those systems, cell penetrating peptides (CPPs) conjugated to antibiotics significantly reduced bacterial growth in intracellular environments.[15-16] However, the rapid development of resistance against antibiotics calls for more sustainable treatment.[12, 17-19]

In this context, various studies have looked into antimicrobial peptides (AMPs), as they appeared to have a broad activity range. More recently, synthetic polymers, designed to be analogous to AMPs (SMAMPs), have been developed since they possess greater versatility and potential for scale-up compared to AMPs.[20-21] Interestingly, SMAMPs do not evoke bacterial resistance as their mechanism of action is based on interactions with the negatively charged surface of bacterial membrane.[22-23] Previous reports demonstrated that ammonium- and guanidinium-rich SMAMPs were potent towards a broad spectrum of bacteria.[24] Among those, guanidinium-rich materials, mimicking arginine-rich peptide sequences, seemed particularly active against MRSA, as highlighted in chapter 3.

In parallel, a wide range of guanidinium-rich polymers were also designed, to mimic the proficiency CPPs possess for cellular uptake.[25-27] Although the mechanism of cell uptake has not been entirely elucidated, the guanidinium moieties are thought to interact with membrane phospholipids *via* electrostatic interactions and H-bonding, followed by both endocytosis and direct translocation through the membrane.[28] The stereochemistry of the polymeric backbone was demonstrated not to impair the internalisation of the guanidinium-rich polymers, but other parameters such as the number of guanidinium units or the overall

hydrophobicity of the polymer were reported to alter cellular uptake.[26, 29] By exploiting their antimicrobial activity in combination with their ability to enter eukaryotic cells, guanidinium rich polymers could be a promising alternative to antibiotics currently used against intracellular bacteria.[30-31] In this case, the usual drawbacks associated with the use of a cargo such as drug attachment/ encapsulation or release would be bypassed, since the polymer is simultaneously performing the role of vector and therapeutic agent.

A guanidinium-containing SMAMP, polyhexamethylene biguanidine (PHMB), which is utilised as a disinfectant, has been reported to be efficient against intracellular *S. aureus* in keratinocytes.[32-33] However, reports of potential carcinogenic effects on humans, and increasing regulation over its use highlight the need for an alternative to PHMB.[34] In light of recent studies, the biological properties of SMAMPs can be improved upon by modifying the distribution of cationic and hydrophobic functionalities along the polymeric backbone.[35-36] Indeed, the segregation of cationic and hydrophobic moieties appears to enhance the bactericidal effect whilst promoting haemocompatibility, yet PHMB has an alternating sequence inherent to the nature of its synthesis. Varying the monomer distribution in guanidinium containing copolymers could potentially improve their intracellular activity and reduce their haemotoxicity.

Well-defined guanidinium-rich block copolymers with controlled monomer distributions have been successfully prepared using RAFT polymerisation, and materials made using this approach represent an attractive alternative to PHMB due to the synthetic versatility which RAFT polymerisation offers.[29, 37]

In chapter 3, the synthesis of statistical, tetrablock and diblock guanidinium-rich copolymers, using the acrylamide monomer guanidinoethyl acrylamide (GEAM), was described in detail. In the present chapter, fluorescently-labelled derivatives of these guanidinium-rich copolymers were prepared in order to study the interactions of SMAMPs with bacterial membranes. The influence of the length of the polyGEAM domains as a result of varying monomer distribution was also investigated, using polyGEAM homopolymers of similar molar mass to the cationic block(s) of the tetrablock and diblock copolymer SMAMPs. The final focus of this study was to investigate the intracellular activity of the guanidinium containing polymers within keratinocytes as a potential staphylococcal skin infection therapy.

4.2 Results and discussion

4.2.1 Synthesis of Bodipy acrylamide (BodipyAM)

The comparison of the antimicrobial activity between ammonium and guanidinium containing copolymers in chapter 3 demonstrated that the guanidinium copolymers were more active against MRSA than their ammonium copolymer counterparts. In order to carry out bacterial binding and mammalian cell uptake assays, the guanidinium polymers were functionalised using a Bodipy dye. Bodipy-derived dyes are known to have a high quantum yield and have been extensively used to label polymers.[38] An additional advantage of Bodipy derivatives is their non pH-dependent fluorescence, within the limits of their stability, which is necessary for accurate intracellular tracking of materials. Here, an acrylamide derivative of the Bodipy dye was synthesised to allow its incorporation in the guanidinium copolymers in a RAFT polymerisation chain-extension step (Scheme 4.1). Firstly, Bodipy acid (**1**) was synthesised in 2 steps according to the literature.[39] ^{1}H NMR spectra of all intermediates can be found in section 4.5, Figures 4.10-4.12. **1** was then modified to obtain a *N*-hydroxysuccinimide (NHS) functionalised Bodipy (NHS-Bodipy, **2**). **2** was then coupled with amino-ethylacrylamide (AEAM, **3**), obtained by deprotection of BocAEAM. Since AEAM was not soluble in organic solvents, most probably due to its positive charge, **1** was functionalised with NHS in DMF prior to reaction with AEAM in water, to limit hydrolysis. The obtained Bodipy acrylamide (BodipyAM, **4**) was fluorescent with λ_{ex}=525 nm and λ_{em}=537 nm (Figure 4.1).
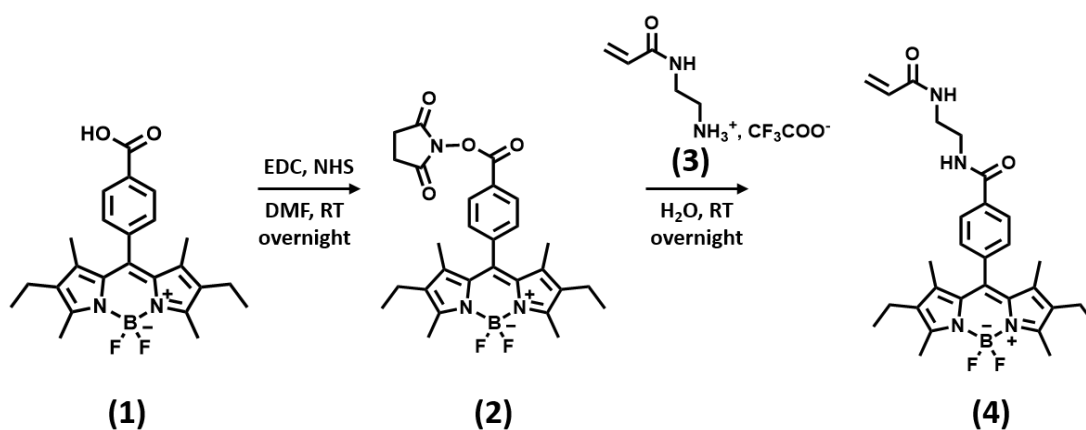
Scheme 4.1 - Synthesis of BodipyAM from Bodipy acid.
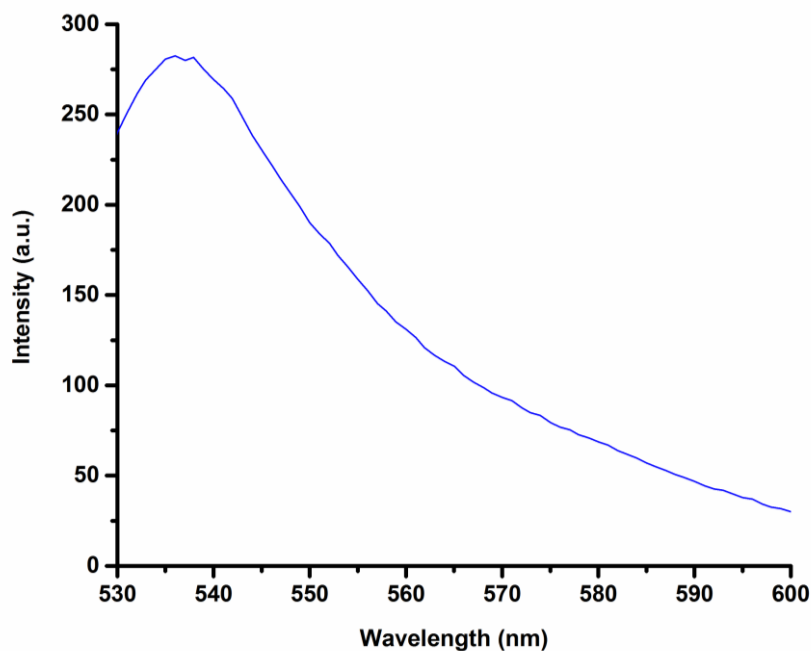
Figure 4.1- Emission spectrum of BodipyAM (λ_{ex}=525 nm).

4.2.2 Labelling of polymers

The guanidinium-rich copolymers from chapter 3 contained NIPAM as co-monomer, and were synthesised by RAFT polymerisation with different monomer distributions: statistical, tetrablock and diblock copolymers (G-S30, G-T30 and G-D30, respectively) (Table 4.2). The incorporation of (on average) one unit of BodipyAM per polymer chain was first attempted *via* the chain extension of the Boc-protected polymers using RAFT. Following the chain extension with BodipyAM, the Boc protecting group of the polymer was hydrolysed using TFA. Once the deprotection was complete, the polymer did not exhibit any fluorescence (Figures 4.2 and 4.13). A possible explanation would be that the Bodipy moiety might degrade under the harsh acidic conditions used in the deprotection step.
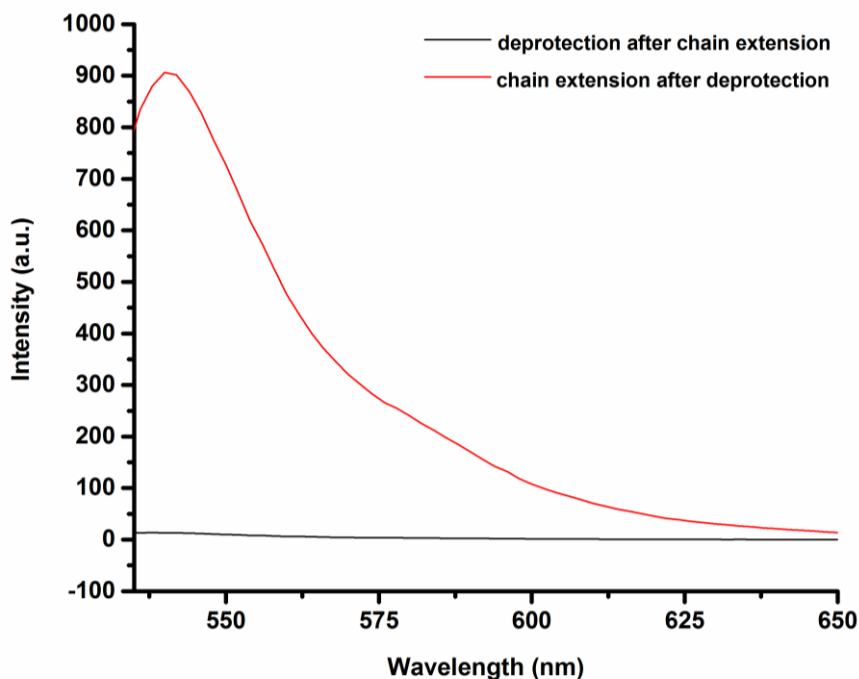
Figure 4.2 – Emission spectra of Bodipy functionalised polymers (λ_{ex}=525 nm).

To circumvent this issue, the guanidinium copolymers were chain-extended with BodipyAM in their deprotected forms. The polymerisations were performed in a mixture of an acetate buffer (pH 5) and acetone (8/2) to limit aminolysis and solubilise BodipyAM, respectively. The excess dye was removed by precipitation in diethyl ether after further diluting the mixture with acetone. The Bodipy labelled statistical, tetrablock and diblock copolymers (G-S30[Bodipy], G-T30[Bodipy] and G-D30[Bodipy], respectively), which contained less than 5 % of free dye, were characterised using high performance liquid chromatography (HPLC) and fluorescence spectroscopy (Scheme 4.2, Figures 4.2, 4.3 and 4.13). The intrinsic fluorescence was determined for each polymer in order to obtain a correction factor used to account for a difference in the incorporation of BodipyAM between the three copolymers (Table 4.7). The fluorescence HPLC spectrum overlapped with that at 280 nm for each copolymer, indicating their fluorescence.
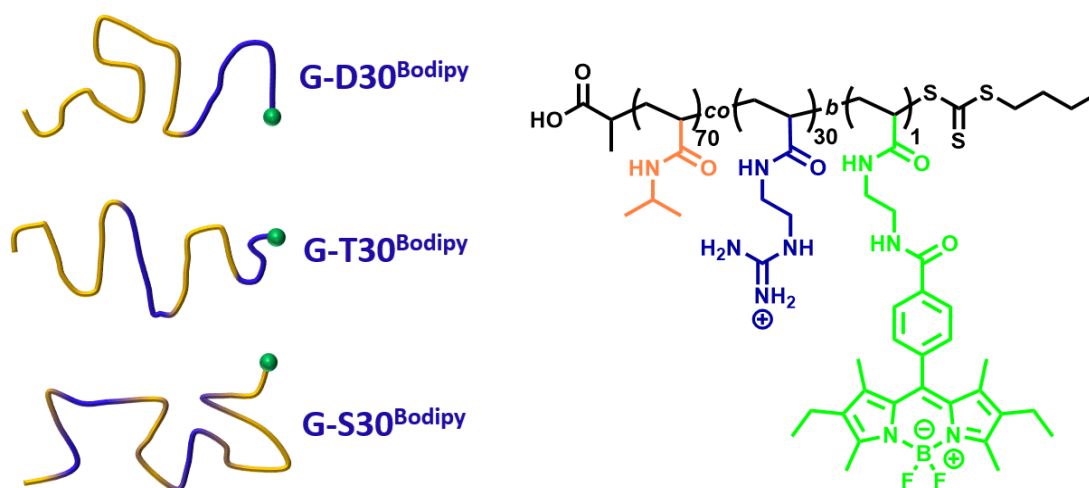
Scheme 4.2 – Library of Bodipy functionalised guanidinium polymers.
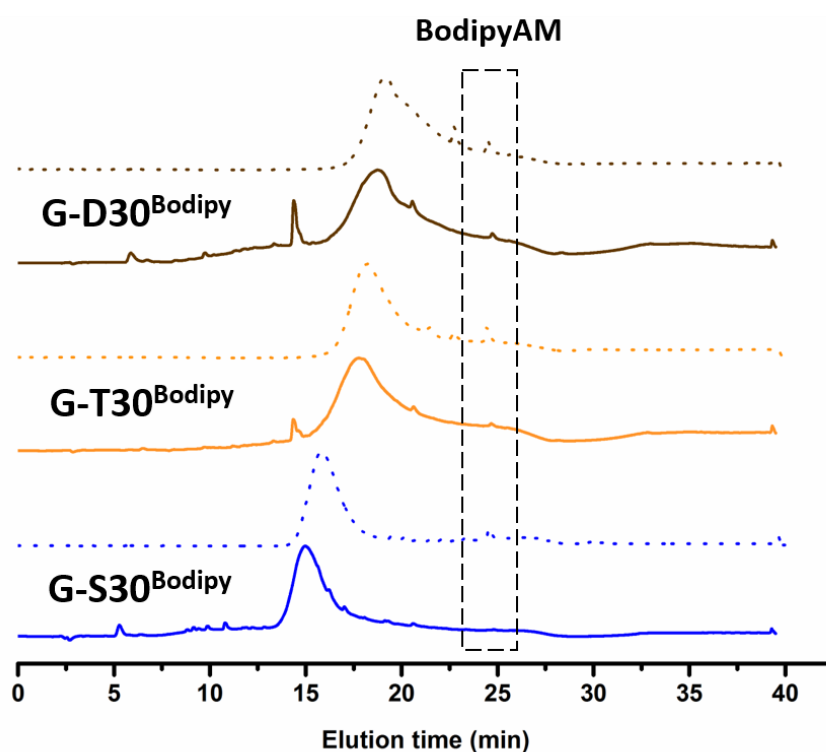
Figure 4.3 - HPLC chromatograms of the fluorescent polymers (solid line – λ=280nm; dashed line - λ$_{ex}$=525 nm and λ$_{em}$=537 nm) with a gradient of 1 to 95 % ACN in 35 minutes with a 100 mm C18 column.

4.2.3   Interactions with bacterial membrane

The antimicrobial activity of the guanidinium SMAMPs towards JE2, a MRSA strain, was assessed in chapter 3. Interestingly, their potency increased with segregation of functional

regions: G-S30 did not exhibit any activity within the concentration tested (MIC > 1000 μg.mL^{-1}), whereas G-T30 and G-D30 were both active with MIC values of 128 and 64 μg.mL^{-1}, respectively. The variation in the minimum inhibitory concentration (MIC) values could either be explained by a difference in bacterial binding or ability to efficiently kill bacteria.

In order to determine if the binding efficiency between bacteria and guanidinium copolymers was influenced by monomer distribution, the Bodipy-functionalised guanidinium polymers were utilised. In mass concentration, the MIC of the fluorescent polymers were double that of their unlabelled counterparts (256 and 128 μg.mL^{-1} for G-T30^{Bodipy} and G-D30^{Bodipy}, respectively), as shown in Table 4.3. Although the MIC values of the fluorescent polymers (in molar concentration) against both RN1 and JE2 were slightly higher to that of the unlabelled polymers, a significant antimicrobial activity was maintained after incorporation of BodipyAM, in turn validating the experiment (Table 4.3). The MRSA strain JE2 was incubated at 37 °C with each polymer at a concentration of 128 μg.mL^{-1} for 15, 30 and 120 minutes (Figure 4.4). For the 30 and 120 minute time points, propidium iodide (PI), which stains bacteria possessing a compromised membrane, was added 15 minutes prior to the end of the experiments. The bacterial suspensions were then washed and fixed on a glass slide to be viewed using an optical microscope. Three different filters were utilised to assess the interactions between the polymers and bacterial membranes: the brighfield (BF) channel, the green channel (Bodipy functionalised polymers) and the red channel (PI stained bacteria).

As there was no staining with PI for the 15 minute time point, in order to demonstrate that the bacterial binding of guanidinium polymers is independent of the presence of PI, Figure 4.4A displays only the BF and green channel (including a merge of the two). The images indicate that G-D30^{Bodipy} was bound to bacteria within 15 minutes of incubation. According to the BF image, the bacteria appeared to be compromised in the presence of G-D30^{Bodipy}, as the shape of the majority of the bacterial population is poorly defined. In contrast, G-S30^{Bodipy} and G-T30^{Bodipy} did not appear to bind bacteria as effectively within this timeframe, evidenced by the absence of noticeable fluorescence in the green channel. Additionally, the shape of the bacteria remained intact, indicating that the polymers did not compromise bacterial membrane.
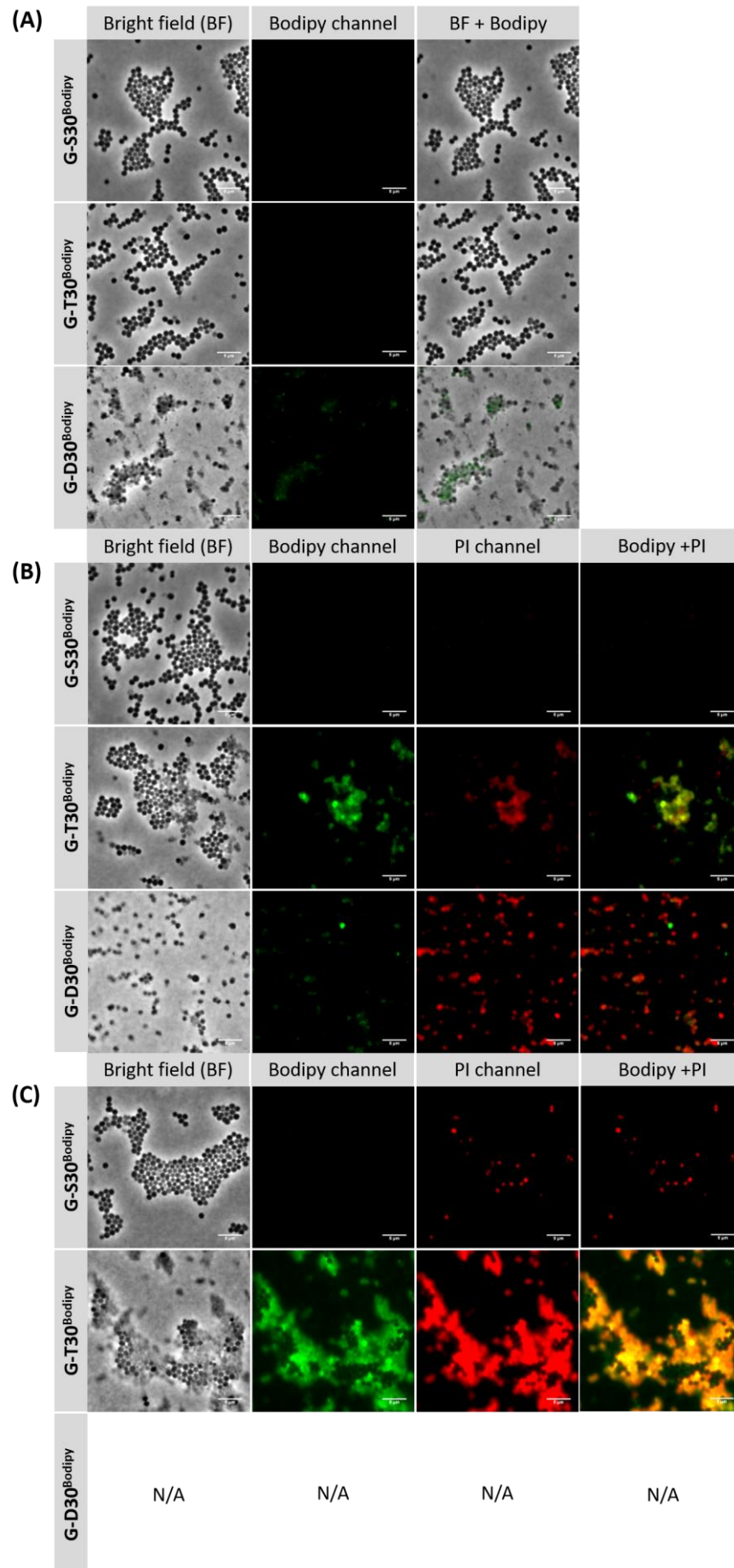
Figure 4.4 – Bacterial membrane interactions of SMAMPs. Binding assay with JE2 of the guanidinium SMAMPs after 15 minutes without PI (A) Binding assay with JE2 after 30 minutes in presence of PI (B) Binding assay with JE2 after 2 hours in presence of PI, no image was presented for G-D30 after 2 hours no bacteria were left under these conditions (C). The scale bar represents 5 µm.

For the 30 minute time-point, Figure 4.4B displays images from the BF, Bodipy, PI channels and a merge of the Bodipy and PI channels. Following 30 minutes of incubation, both G-T30^{Bodipy} and G-D30^{Bodipy} bound to bacteria. Although the fluorescence intensity appeared to be greater following incubation with G-T30^{Bodipy} than G-D30^{Bodipy} for this time point, the BF images reveal that the number of bacteria was significantly lower following treatment with G-D30^{Bodipy}. Furthermore, after 30 minutes in presence of G-D30^{Bodipy}, most of the visible bacteria possess polymer bound to their surface and a compromised membrane, as can be seen with the overlay image of the Bodipy and PI channels, and are unhealthy, as indicated by their shape (BF). These pores would allow the polymers to diffuse out of the cell, which could explain a reduction in fluorescence intensity. Interestingly, bacteria interacting with G-T30^{Bodipy} were also exclusively the ones stained by PI. These results demonstrate that membrane attachment and disruption occur jointly and in a short time span: within 15 minutes, the polymer binds and disrupts the membrane. This observation would question the hypothesis that guanidinium-rich polymers induce cell death *via* a different mechanism to pore formation.[40] These results are in contradiction to a study from Tew *et al.*, which investigated the effect of guanidinium-functional polyoxanorbornene on the membrane integrity of *S. aureus* using PI.[40] Although the polymer showed a bactericidal effect against *S. aureus*, none of the bacteria were stained with PI after 30 minutes, indicating that bacterial membrane was not compromised. Comparable observations were reported by Good and co-workers after treatment of *E.coli* with PHMB. No permeability of bacterial membrane was observed in presence of PHMB after 60 minutes at 37 °C, when using SYTOX$^®$ Green as a membrane integrity probe, despite the potency of the polymer against *E. coli*. Following this experiment, it was suggested that complexation of PHMB with bacterial DNA was responsible for the antimicrobial character of the polymer, which could also be the mechanism of action of guanidinium-functional polyoxanorbornene.[41] The disruption of membrane integrity associated with G-T30 and G-D30 could be due to the action of the isopropyl groups of the NIPAM units - the polyoxanorbornene and PHMB did not bear any pendant alkyl chains, hence could likely cross bacterial membrane without compromising it (Scheme 4.3).[40] In the present case, both pore formation and bacterial DNA binding could be occurring and collectively contributing towards bacterial death.
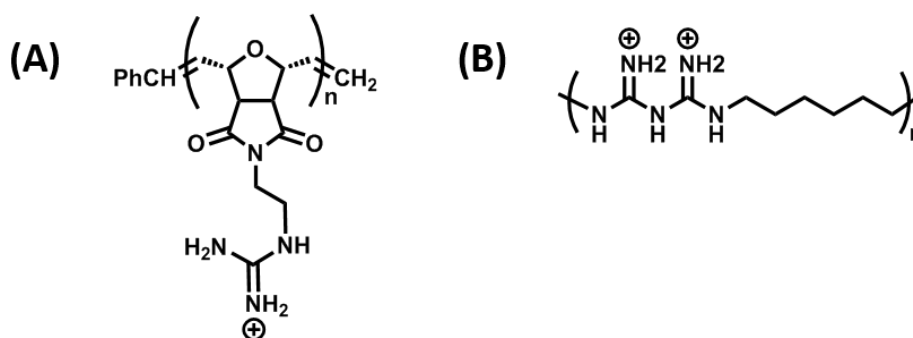
Scheme 4.3 – Chemical structure of (A) polyguanidinium oxanorbornene[40] and (B) PHMB[41].

Following incubation with G-D30^{Bodipy} for 2 hours, no bacteria were observed, most probably because they were killed and subsequently removed during the washing step (Figure 4.3C). In the presence of G-T30^{Bodipy} more bacteria were stained after 2 hours of incubation, compared to 30 minutes. Again, co-localisation between G-T30^{Bodipy} and PI reinforces the previous observation that membrane disruption is a consequence of polymer binding. The BF image confirms the loss in membrane integrity for the majority of bacteria following 2 hours of incubation with G-T30^{Bodipy}. Although no bacteria were stained by G-S30^{Bodipy}, even after 2 hours, a few of them were stained with PI. A negative control experiment with PBS and PI was performed and no membrane disruption was found (Figure 4.14). Therefore, in the case of G-S30^{Bodipy}, the statistical copolymer would have interacted with JE2 over the course of 2 hours, hence inducing membrane disruption, but to a limited extent.

In summary, G-D30^{Bodipy} underwent stronger interactions with the bacteria compared to G-T30^{Bodipy} (within 15 to 30 minutes, respectively), whilst G-S30^{Bodipy} only had limited interactions with JE2 even after 2 hours (Figure 4.3C). This trend correlates with the MIC values, as the tested concentration (128 µg.mL^{-1}) corresponds to the MIC of G-D30^{Bodipy} and half that of G-T30^{Bodipy} (G-S30^{Bodipy} was not active up to 1000 µg.mL^{-1}), as shown in Table 4.3.

4.2.4   Synthesis and properties of guanidinium homopolymers

The difference in the MIC values of the guanidinium polymers raises the question whether there is a minimum length requirement of the cationic block for the polymer to interact with bacterial membrane. To investigate this, guanidinium homopolymers of DP 15

and 30, which corresponds to the DP of the cationic block(s) in G-T30 and G-D30, respectively, were synthesised. As with the copolymers, polyGEAM$_{15}$ and polyGEAM$_{30}$ were synthesised by RAFT polymerisation of diBocGEAM followed by hydrolysis to remove the Boc protecting groups (Tables 4.4 and 4.5, Figures 4.5 and 4.15). Additionally, the role of the isopropyl (NIPAM) functionalities in the antimicrobial activity of G-S30, G-T30 and G-D30 can be elucidated in the following study.

The antimicrobial activity of the homopolymers was tested against two clinically relevant strains: a MSSA and MRSA strain, RN1 (NCTC 8325) and JE2 (USA 300), respectively (Figure 4.6A, Table 4.6). The MIC of the homopolymers polyGEAM$_{15}$ and polyGEAM$_{30}$ were similar (7 nmol.mL^{-1} for both), meaning that the molar mass of the homopolymers did not appear to affect the antimicrobial activity in this particular case. These results would assert that a cationic block of DP 15 was sufficient to promote effective interaction with bacterial membrane. However, as G-T30 did not bind as efficiently to bacteria as G-D30 (Figure 4.4), it is plausible that the polyNIPAM block sterically hinders the interaction of the polyGEAM block with bacterial membrane in the tetrablock copolymer structure.
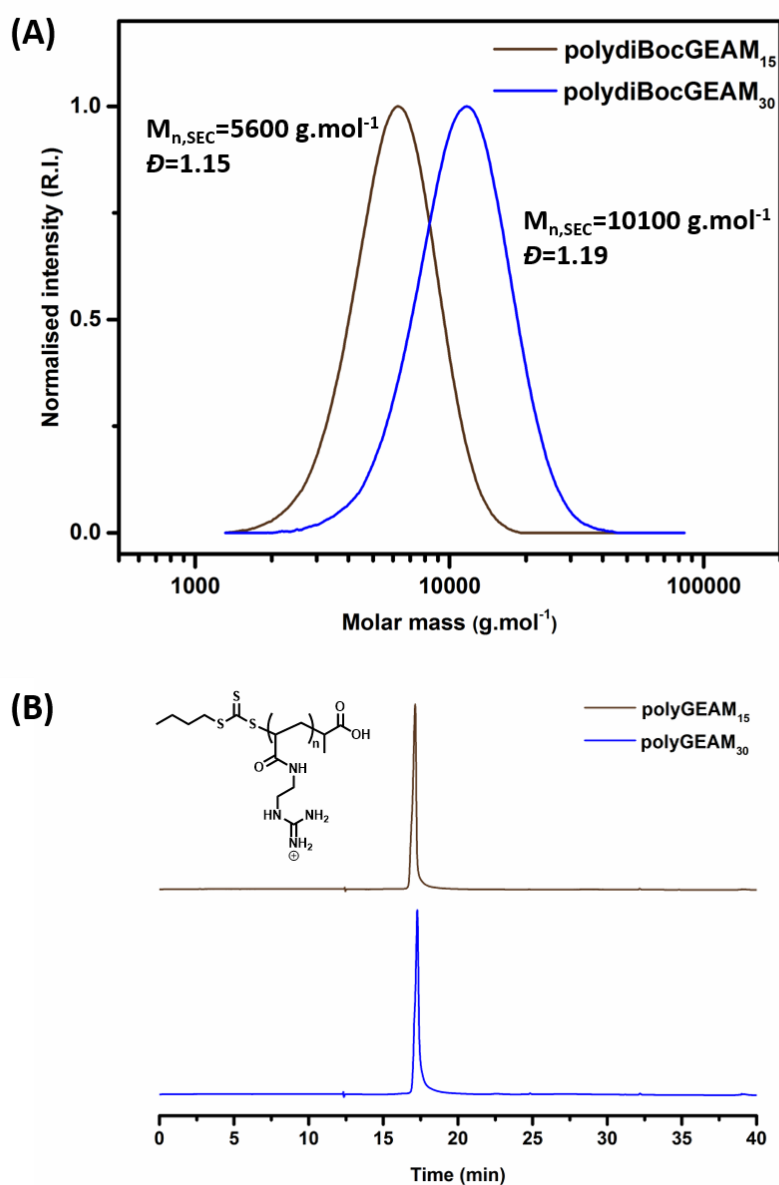
Figure 4.5 - Characterisation of the guanidinium homopolymers. (A) DMF-SEC chromatograms of polydiBocGEAM$_{15}$ and polydiBocGEAM$_{30}$. (B) RP-HPLC chromatograms of the guanidinium homopolymers with a gradient of 1 to 80 % ACN in 30 minutes with a 100 mm C18 column (λ=280 nm).

The effect of the isopropyl moieties on the antimicrobial activity of the copolymers was evaluated by comparing the potency of the copolymers with the cationic homopolymers of similar polyGEAM length. If the hydrophobic moieties are considered as "non-active" towards bacteria, the standard MIC values should be corrected to account for the content of "active" moieties in the respective polymers by multiplying the MIC expressed in molar concentration with the molar percentage of guanidinium functionalities in each polymer.

According to Figure 4.6 A, the re-evaluated MIC of G-T30 and G-D30 was less than half that of polyGEAM$_{15}$ and polyGEAM$_{30}$, respectively. This suggests that the polyNIPAM blocks participate in the antimicrobial activity of the polymers.
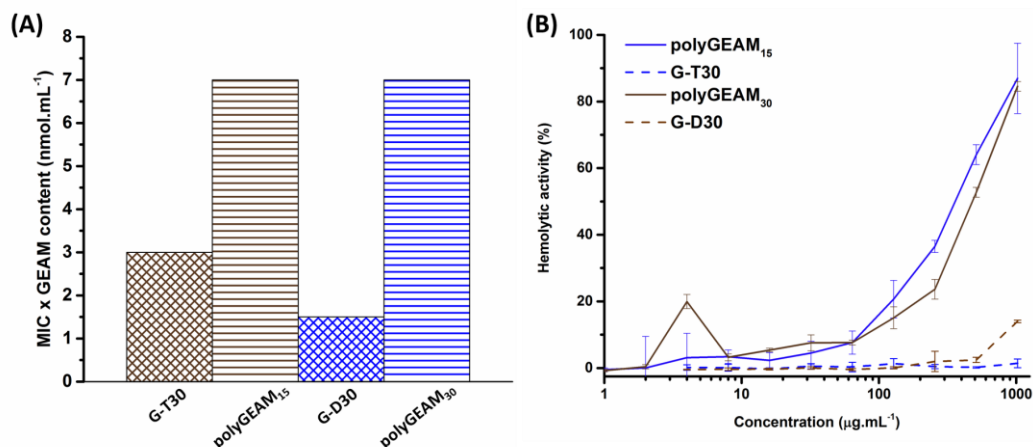
Figure 4.6 – Antimicrobial and haemolytic activities of the guanidinium homopolymers. (A) Corrected MIC of polyGEAM and the guanidinium block copolymers against MRSA strain JE2 obtained by multiplying the MIC expressed in molar concentration with the molar percentage of guanidinium functionalities in each polymer. (B) Haemolytic activity of the guanidinium homopolymers and their associated copolymers. Normalised haemolysis of sheep blood cells following incubation at 37 °C for 2 hours in PBS with guanidinium SMAMPs.

In order to estimate the influence of the co-monomer on the biocompatibility of the guanidinium polymers, the toxicity of the cationic homopolymers towards mammalian cells was evaluated. The haemocompatibility was first studied by incubating the polymers with defibrinated sheep blood over 2 hours at 37 °C. Not only did polyGEAM$_{15}$ and polyGEAM$_{30}$ induce haemagglutination at concentrations as low as 2 µg.mL^{-1}, but they also caused over 10 % of haemolysis from 128 µg.mL^{-1} (Table 4.1 and Figure 4.6B).

Table 4.1 – Guanidinium homopolymers induced erythrocytes aggregation. Observation of haemagglutination of sheep blood cells following incubation with guanidinium SMAMPs in PBS for 2 hours at 37 °C.

sample /concentration (μg/mL)	1024	512	256	128	64	32	16	8	4	2	1	0.5
G-S30	+++	+++	+++	++	++	+	+	+	-	-	-	-
G-T30	++	++	++	+	+	+	-	-	-	-	-	-
G-D30	-	-	-	-	-	-	-	-	-	-	-	-
polyGEAM$_{15}$	+++	+++	+++	+++	+++	++	+	+	+	+	-	-
polyGEAM$_{30}$	+++	+++	+++	+++	+++	+++	++	++	++	++	+	-

Haemagglutination strength: +++ strong; ++ moderate; + weak; - none.

To further investigate the toxicity of the polymers against mammalian cells, an XTT assay was performed on HaCaT (human keratinocytes) and A549 (lung epithelial) cells. The toxicity profile was very acute for both cationic homopolymers towards HaCaT cells (Figure 4.7) following 20 hours incubation. The IC$_{50}$ values, which is the minimum concentration required for a 50 % cell growth inhibition, were as low as 40 and 60 μg.mL^{-1} for polyGEAM$_{30}$ and polyGEAM$_{15}$, respectively. Similar results were obtained with A549 cells (Figure 4.16).
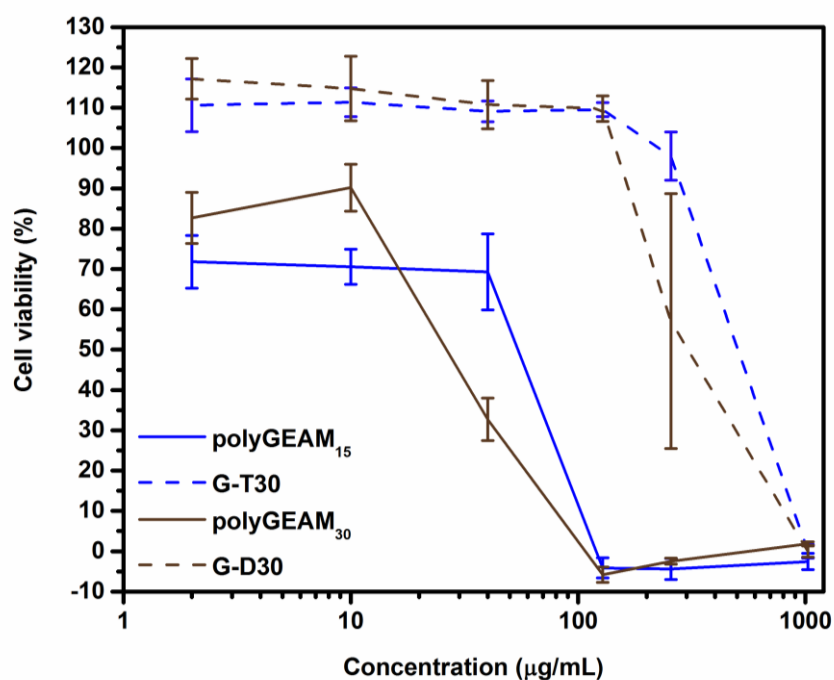
Figure 4.7 – Cytotoxicity of guanidinium SMAMPs towards HaCaT cells. Viability of HaCaT cells incubated for 24 hours in presence of guanidinium homopolymers and their associated copolymers using an XTT assay.

This set of experiments confirms that the cationic homopolymers were toxic towards RBCs and epithelial cells from a low concentration and that the incorporation of NIPAM in the guanidinium-rich copolymers reduce their toxicity *in vitro*. Most importantly, the isopropyl functionalities seem to enhance the potency of the guanidinium polymers towards bacteria, which is consistent with previous work investigating the role of hydrophobic domains in SMAMPs.[42] Due to the dual action of the guanidinium-rich materials against bacteria, the isopropyl functionalities could promote pore formation within bacterial membrane, but also improve membrane crossing followed by possible condensation of bacterial DNA, in the hypothesis of a dual action of the guanidinium materials against bacteria.

4.2.5   Effect of segmentation on cell uptake of guanidinium copolymers

As mentioned previously, in addition to mimicking the action of AMPs, guanidinium containing polymers resemble CPPs. The potency of SMAMPs on intracellular bacteria strongly depends on their ability to enter mammalian cells. Therefore, the uptake of the guanidinium-rich polymers by keratinocytes was studied to elucidate the effect of monomer

distribution on their internalisation. For this assay, HaCaT cells were incubated at 37 °C for 2 and 16 hours with the Bodipy-labelled polymers at a concentration of 128 µg.mL^{-1}. The extent of uptake was quantified by measuring cellular fluorescence using a plate-reader, followed by correction with the intrinsic fluorescence of each copolymer (Figure 4.8 and Table 4.7). Following 2 hours incubation with G-S30, G-T30 and G-D30, similar levels of cellular fluorescence were observed in each case. Comparable levels of were also observed for all three SMAMPs fluorescence following 16 hours of incubation (Figure 4.8), with only a slight increase in uptake observed despite the substantially longer incubation time (from 2 to 16 hours), indicating that the internalisation of the guanidinium containing polymers occured mostly during the first 2 hours of incubation. With this copolymer system, monomer distribution does not seem to have a significant impact on the internalisation of the SMAMPs by HaCaT cells. On the contrary, Martin *et al.* reported a decrease in the cellular uptake of guanidinium-rich copolymers with increasing segregation of functionalities (from statistical to tetrablock to diblock copolymer).[29] This discrepancy could be explained by the hydrophobicity of the overall materials as the polymers in the mentioned study used more hydrophilic co-monomers than NIPAM. Indeed, there is strong evidence that the hydrophobicity of cationic polymers largely influences the extent of cell uptake.[43]

The uptake mechanism of the guanidinium polymers was further investigated by incubating the cells at 4 °C for 2 hours. At this temperature, not only energy-dependent uptake pathways are inhibited, but the overall hydrophobicity of the SMAMPs might be decreased due to the thermo-responsiveness of polyNIPAM.[44] The internalisation of all three polymers was drastically reduced at 4 °C by over 70 % compared to that at 37 °C (Figure 4.8), which was also observed in the work by Martin *et al.*, indicating that the guanidinium polymers are taken up *via* both membrane permeation and endocytosis.[29] However, the difference in internalisation was not as substantial with the DMA and HEA copolymers, which could possibly be explained by a decrease in hydrophobicity of poly(GEAM-*co*-NIPAM) further reducing the cellular uptake of the copolymers at 4 °C. Moreover, the levels of uptake at 4 °C were comparable for G-S30, G-T30 and G-D30. As a result, the ratio of polymer present in endosomes and in the cytosol should be similar for all three SMAMPs. Nonetheless, the guanidinium containing polymers are likely to escape from endosomes due to their highly charged nature, as demonstrated with arginine-rich peptides, hence interact with bacteria present in the cytosol.[45-46]
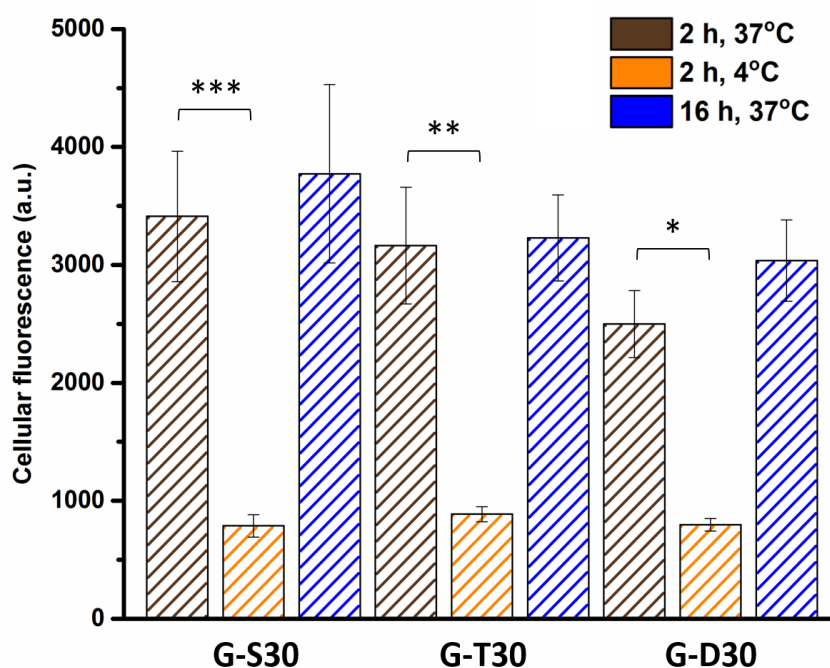
Figure 4.8 – Comparison of cell uptake of guanidinium polymers with architecture. Cellular fluorescence measured for HaCaT cells in presence of 128 µg.mL^{-1} of guanidinium polymers for the indicated time and temperature. *: p ≤ 0.05; **: p ≤ 0.01; ***: p ≤ 0.001.

4.2.6 Effect of segmentation on potency against intracellular bacteria

Since the guanidinium polymers exhibited both antimicrobial activity and ability to be taken up efficiently by mammalian cells, their activity against intracellular bacteria was finally explored. To investigate this, HaCaT cells were infected either with the MSSA strain RN1, or with the MRSA strain JE2, by incubating them for 2 hours. The infected cells were then treated with a mixture of gentamicin and lysostaphin for 30 minutes to kill extracellular bacteria as described in the literature.[47] Finally, the infected cells were incubated with the guanidinium compounds at a non-cytotoxic concentration of 128 μg.mL^{-1} at 37 °C for 2 hours. Lysostaphin was used as a negative control (at a concentration of 5 μg.mL^{-1}) as this enzyme is known to be ineffective against intracellular bacteria, whilst killing extracellular bacteria, which can be released by infected cells.[3] Following incubation with the guanidinium-rich copolymers, the cells were lysed using a saponin solution. The lysate was diluted and plated to obtain a bacterial count for each sample (Figure 4.9). The experiment was repeated 3 times in triplicates.

Similar levels of intracellular MSSA RN1 were recovered following treatment with G-S30 or G-T30 compared to the lysostaphin control (Figure 4.9A). This result indicates that the polymers inhibited the proliferation of extracellular bacteria released during the treatment to a comparable extent to lysostaphin, but did not inhibit the growth of intracellular *S. aureus*. This would help containing the infection to an extent but would not be sufficient to treat infections. Interestingly, G-D30 was the most active against intracellular RN1, reducing the number of bacteria by two-fold compared to lysostaphin (Figure 4.9A).

Furthermore, treatment with G-S30 and G-T30 revealed survival levels of intracellular MRSA JE2 bacteria comparable to the lysostaphin treated control (Figure 4.9B). In contrast, G-D30 was active against intracellular JE2 with a 50 % growth inhibition of intracellular MRSA following 2 hours of treatment. Interestingly, the cell uptake assay demonstrated that all three compounds were internalised in keratinocytes to a similar extent and a similar fashion (ratio of endocytosis to energy-independent pathways). These results narrow down the possible explanations for a difference in activity against intracellular bacteria, which is most likely due to the divergence in antimicrobial activity between the three polymers (MIC>1024 μg.mL^{-1} for G-S30, and MIC=128 and 64 μg.mL^{-1} for G-T30 and G-D30, respectively, against both RN1 and JE2). Indeed, G-D30 exhibited the highest antimicrobial activity towards planktonic RN1 and JE2. The improved potency of G-D30 against both MSSA and MRSA is responsible for the superior activity against intracellular bacteria compared to its statistical and tetrablock copolymer counterparts (Figure 4.9).
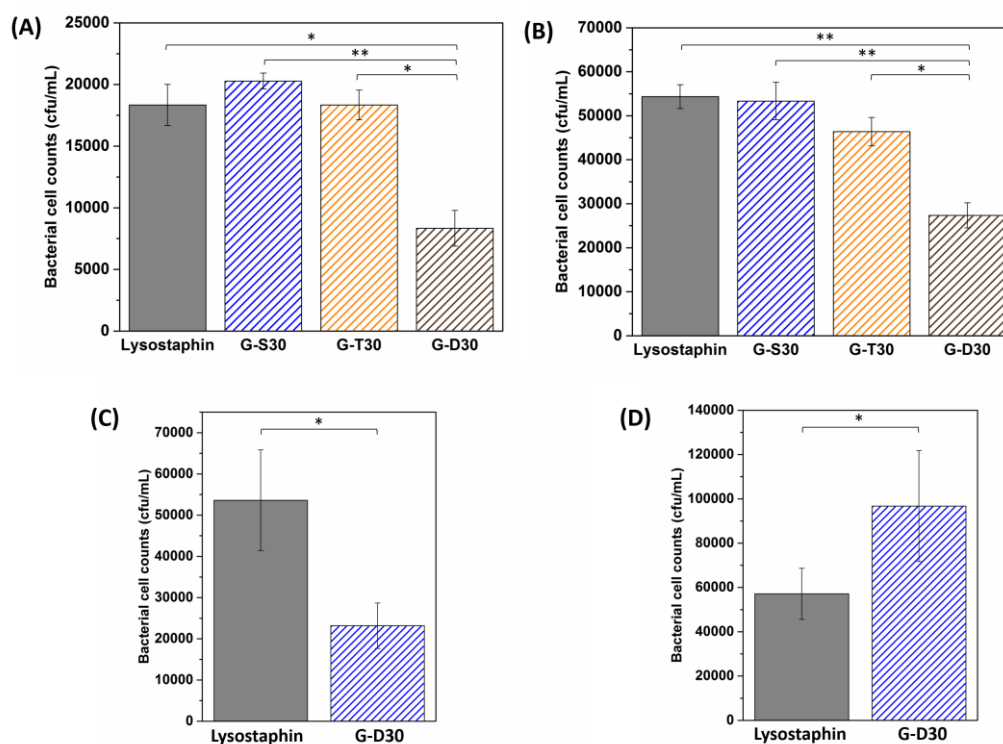
Figure 4.9 –Intracellular activity of guanidinium polymers in HaCaT cells. Counts of intracellular bacteria after a polymer treatment at 128 µg.mL^{-1} at 37 °C for 2 hours against RN1 (A) JE2 (B). Treatment with G-D30 at 40 µg.mL^{-1} for 2 hours against RN1 (C) JE2 (D). *: p ≤ 0.05; **: p ≤ 0.01; ***: p ≤ 0.001.

Following the experiments performed at 128 µg.mL^{-1}, treatment of intracellular bacteria with G-D30 was undertaken at a lower polymer concentration (40 µg.mL^{-1}) for 2 hours, in order to assess variation in activity against intracellular bacteria with concentration. A similar level of inhibition (40 % of bacteria recovered compared to the lysostaphin control) against RN1 at this concentration as at 128 µg.mL^{-1} (Figure 4.9C). Although the concentration of polymer treatment is of 40 µg.mL^{-1}, the intracellular concentration of G-D30 might reach a similar level to the MIC value of G-D30 against planktonic RN1 (64 µg.mL^{-1}). However, G-D30 was not effective against intracellular JE2 at 40 µg.mL^{-1} (Figure 4.9D). A possible explanation could be that, as previously discussed, JE2 is less susceptible to SMAMPs compared to RN1 due to its resistance to methicillin. As G-D30 did not exhibit any toxicity at 128 µg.mL^{-1} against the various types of mammalian cells tested, the guanidinium diblock copolymer represents a promising candidate for the use in intracellular killing of MRSA and MSSA.

Although inhibition of half of intracellular MRSA was achieved by treating infected keratinocytes with G-D30, scope for improvement was identified for a complete eradication of intracellular bacteria. *S. aureus* was shown to be internalised by mammalian cells *via* phagocytosis, following which various factors such as the type of host cell or the bacterial growth phase come into play.[48] In the majority of cases, *S. aureus* seems to be present in defined locations within the host cell: inside endosomes where they can replicate, in the cytosol if they escape from endosomes, or in phagolysosomes (result of the fusion of a lysosome with a phagosome).[48] Although the bacteria should be eradicated by the innate immune system, *S. aureus* has been reported to persist within phagosomes for prolonged periods.[49] Having the bacteria compartmentalised either in endosomes or in phagolysosomes renders them difficult to access. This could explain why the action of the SMAMPs on intracellular *S. aureus* was not optimal. Despite phagosomes fusing with late endosomes, the likelihood of a phagosome containing bacteria merging with an endosome comprising a SMAMP is small.[50] However, Good *et al.* reported eradication of 90 % of intracellular *S. aureus* in keratinocytes after treatment with PHMB at 4 μg.mL^{-1}, during which co-localisation of the SMAMP with bacteria was observed.[32] The greater intracellular efficiency of PHMB could also be explained by a more efficient internalisation into keratinocytes compared to that of G-D30. However, as previously mentioned, the fate of intracellular *S. aureus* strongly depends on experimental conditions.[48] In the study with PHMB, the protocol and the bacterial strain employed to obtain intracellular bacteria differ from that used for the present work, which could have resulted in a different ratio of bacteria in the cytosol compared to that in endosomes and makes a direct comparison between the two studies difficult.

4.3   Conclusion

The previous chapter in this thesis demonstrated that varying monomer distribution in guanidinium-rich copolymers influences their antimicrobial activity. Elsewhere, it has been shown that varying the monomer distribution in a similar copolymer system influences their cellular uptake.[29] Combining these two themes, this chapter aimed to utilise the guanidinium-rich polymers introduced in chapter 3 to determine the influence of monomer distribution on activity against intracellular bacteria, which has been an ongoing clinical challenge.

G-D30 was demonstrated to be the most efficient at attaching to bacterial membrane, followed by G-T30, whilst no binding was observed with G-S30. This reduced binding affinity is probably not due to the reduction in the size of the cationic block as polyGEAM$_{15}$ and polyGEAM$_{30}$ exhibited similar antimicrobial activity. The difference between G-D30 and G-T30 could instead be attributed to the isopropyl functionalities hindering the guanidinium moieties from interacting with the negatively charged phospholipids present on bacterial membranes. Nonetheless, there is strong evidence that these hydrophobic functionalities are necessary for both antimicrobial activity and their internalisation into mammalian cells. Indeed, the isopropyl functionalities from the polyNIPAM block of G-D30 and G-T30 were likely responsible for permeabilising bacterial membranes as it was demonstrated elsewhere that guanidinium homopolymers did not compromise bacterial membrane. This hypothesis was confirmed with the decrease in antimicrobial activity of polyGEAM homopolymers which contained no polyNIPAM.

Interestingly, all three SMAMPs were shown to be internalised in keratinocytes to comparable levels *via* both active and passive mechanisms. This result was expected due to their resemblance to the structure of CPPs. Despite their cellular uptake, the statistical and tetrablock copolymers did not appear to be active towards intracellular *S. aureus.* The diblock guanidinium copolymer G-D30 particularly attracted attention as it inhibited the growth of both intracellular MSSA and MRSA by 50 % over 2 hours. Therefore, the optimised copolymer microstructure for the reduction of intracellular and extracellular MRSA appears to be the diblock copolymer G-D30, which could find applications in the treatment of infections, whilst limiting antibiotic induced-bacterial resistance.[2] In order to further reduce the amount of intracellular bacteria, variation in the hydrophobic functionality, overall charge content or other bacteria-targeting moiety could be investigated.

4.4   Experimental

4.4.1   Materials.

Boron trifluoride diethyl etherate (BF$_3$.OEt$_2$), chloroform (CHCl$_3$), 2,3-dichloro-5,6-, dichloromethane (DCM), dicyano-1,4-benzoquinone (DDQ), 1,4-dioxane, 1-Ethyl-3-(3-dimethylaminopropyl)carbodiimide (EDC), ethylacetate (EtOAc), hexane, methanol (MeOH), *N*-hydroxysuccinimide (NHS), triethylamine (TEA) and trifluoroacetic acid (TFA) were purchased from Sigma-Aldrich and used without further purification. 2,2'-azobis[2-(2-imidazolin-2-yl)propane]dihydrochloride (VA-044, Wako), 4-carboxybenzaldehyde (Alfa-Aesar), 2,4-dimethylethylpyrrole (Acros Organic) and propidium iodide (PI, Thermo-Fisher) were also used without further purification. Nutrient Agar, Dulbecco's Modified Eagle's Medium (DMEM), Müller-Hinton Broth (MHB), Roswell Park Memorial Institute medium (RPMI-1640) , Phosphate Buffered Saline (PBS) tablets, Concanavalin A (Con A) and Triton X were purchased from Sigma-Aldrich. 96-well plates were sourced from Thermo-Fischer. Milli-Q filtered water was used to prepare solutions, according to their recommended concentration and the solutions were autoclaved prior to their usage in order to ensure sterility. Defibrinated sheep blood was obtained from Fisher Scientific.

4.4.2   Methods.

4.4.2.1   Nuclear Magnetic Resonance (NMR) Spectroscopy.

^{1}H NMR spectra were recorded on a Bruker Advance 300 spectrometer (300 MHz) at 27 °C in DMSO, CDCl$_3$ or D$_2$O. For ^{1}H NMR, the delay time (dl) was 2 s. Chemical shift values (δ) are reported in ppm. The residual proton signal of the solvent was used as internal standard.

4.4.2.2   Size exclusion chromatography (SEC).

Molar mass distributions were measured using an Agilent 390-LC MDS instrument equipped with differential refractive index (DRI), viscometry (VS), dual angle light scatter (LS) and dual wavelength UV detectors. The system was equipped with 2 x PLgel Mixed D columns (300 x 7.5 mm) and a PLgel 5 µm guard column. The eluent was DMF with 5 mmol NH$_4$BF$_4$ additive. Samples were run at 1 mL min^{-1} at 50°C. Poly(methyl methacrylate) standards (Agilent EasyVials) were used for calibration between 955,000 - 550 gmol^{-1}. Analyte samples were filtered through a nylon membrane with 0.22 µm pore size before injection. Respectively, experimental molar mass (M$_{n,SEC}$) and dispersity (*Đ*) values of synthesized polymers were determined by conventional calibration using Agilent GPC/SEC software.

4.4.2.3 Fluorescence spectrometer

The fluorescent intensity was monitored using Agilent Technologies Cary Eclipse Fluorescence Spectrophotometer. The solutions of vesicles were introduced in a polystyrene cuvette for the measurements.

4.4.2.4 High performance liquid chromatography (HPLC)

HPLC was performed using an Agilent 1260 infinity series stack equipped with an Agilent 1260 binary pump and degasser. The flow rate was set to 1.0 mL min^{-1} and samples were injected using Agilent 1260 autosampler with a 100 μL injection volume. The temperature of the column was set at 37 °C. The HPLC was fitted with a phenomenex Lunar C18 column (150 x 4.6 mm) with 5 micron packing (100Å). Detection was achieved using an Agilent 1260 variable wavelength detector. UV detection was monitored at λ = 309 nm. Methods were edited and run using Agilent OpenLAB online software and data was analysed using Agilent OpenLAB offline software. Mobile phase solvents used were HPLC grade (ACN was 'far UV') and consisted of mobile phase A: 100 % ACN, 0.04 % TFA; mobile phase B: 100 % water, 0.04 % TFA with a gradient of 1 to 95 % ACN over 35 minutes.

4.4.2.5 Bacterial Strains and Growth Conditions

The utilised bacterial strains were *S. aureus* USA 300 LAC JE2 and NCTC 8325 RN1. Bacteria were grown in TSB at 37 °C at 250 rpm for 18 hours.

4.4.2.6 Antibacterial susceptibility tests

Antibacterial susceptibility was studied using two strains of *Staphylococcus aureus* (*S. aureus*): RN1 and JE2. Minimum inhibitory concentrations (MICs) were determined according to the standard Clinical Laboratory Standards Institute (CLSI) broth microdilution method (M07-A9-2012). A single colony of bacteria was picked up from a fresh (24 hour) culture plate and inoculated in 5 mL of Mueller-Hinton (MH) broth, then incubated at 37 °C overnight. On the next day, the concentration of cells was assessed by measuring the optical density at 600 nm (OD$_{600}$). Culture suspension was then diluted to an OD$_{600}$ = 0.1 with MHB in order to reach a bacterial concentration of $\sim 10^8$ colony forming unit per mL (CFU mL^{-1}). The solution was diluted further by 100 fold to obtain a concentration of 10^6 CFU mL^{-1}. Polymers were dissolved in distilled water and 100 μL of each test polymer was added to micro-wells followed by the addition of the same volume of bacterial suspension (10^6 CFU mL^{-1}). The micro-wellplates were incubated at 37 °C for 24 hours, and growth was evaluated by measuring the OD$_{600}$ using a plate reader. Triplicates were performed for each concentration and readings were taken twice. The growth in the well was normalised using negative controls, wells without any bacteria introduced, and positive controls, wells only containing bacterial solution.

4.4.2.7   Bacterial membrane interactions

Antibacterial susceptibility was studied using two strains of *Staphylococcus aureus* (*S. aureus*): RN1 and JE2. Bacteria were picked up from a frozen aliquot inoculated in 5 mL of Trypsic Soy Broth (TSB), then incubated at 37 °C overnight. On the next day, the concentration of bacteria was assessed by measuring the optical density at 600 nm (OD_{600}). Culture suspension was then diluted to an $OD_{600} = 1$ with TSB and 1 mL of the diluted suspension was centrifuged at 5000 rpm for 5 minutes. Solutions of the labelled polymers were prepared with a final concentration of 128 $\mu g.mL^{-1}$ in PBS. The bacteria were resuspended in the polymer solution and incubated at 37 °C for 15 minutes and 2 hours whilst shaking. The solutions were then centrifuged, the supernatant removed and 110 μL of a 300 μM solution of propidium iodide (PI) was added. After incubating at 37 °C for another 15 minutes, the bacteria were washed with PBS and finally the pellet was resuspended in 100 μL of PBS of which 5 μL was placed on a glass slide covered with an agarose gel. Upon drying, 20 μL of DAPI was added and the cover slip was placed upon the sample. The samples were using a Leica DMi8 fluorescence microscope equipped with a FITC filter (480nm/40) used to view BodipyAM and a TXR filter (560nm/40) to image PI.

4.4.2.8   Eukaryotic Cell Lines and Growth Conditions

HaCaT human keratinocytes were grown in a 50:50 mixture of Ham's F12 and Dulbecco's Modified Eagle's Medium (DMEM) supplemented with 10 % of foetal calf serum, 1 % of 2 mM glutamine and 1 %. Both cell lines were grown as adherent monolayers at 37 °C in a 5 % CO_2 humidified atmosphere and passaged at approximately 70-80 % confluence.

4.4.2.9   Cell uptake assay

HaCaT cells were seeded (2×10^4 cells/well) in a black 96-well plate with clear bottom. After 24 hours, the cells were incubated with fluorescent polymers (128 and 40 $\mu g.mL^{-1}$) for 2 or 16 hours depending on the specified conditions. In order to stain the nucleus of the cells, Hoescht 33342 was added to each well 15 minutes prior to the end of the incubation time. For the experiment performed at 4 °C, the plate was placed in the fridge 30 min prior to the polymer treatment. The wells were viewed after washing and replacing with fresh media using a Cytation3 Cell Imaging Multi-Mode Reader™ from Biotek®. Gen5™ was used to isolate individual cells with the blue channel. The background was removed with a rolling ball model (20 μm) and intracellular fluorescence was determined using the RFP filter (λ_{ex}=531 nm, λ_{em}=593 nm) to view the Bodipy-functionalised polymers. Two separate experiments were conducted with triplicates.

4.4.2.10 Invasion assay

The intracellular infection was performed on HaCaT cells using RN1 and JE2. 24-well plates were used to seed 2×10^5 cells per well which were left to pre-incubate with antibiotic-free medium at 37 °C for 10 hours. A single colony of bacteria was inoculated in LSB overnight. The inoculum was diluted to reach an OD=0.15 and were incubated for 2 hours to reach OD=1. After a 1:200 dilution, 1 mL of the bacterial solution was added in each well and the cells were incubated for another 2 hours at 37 °C. The medium was then removed and the wells were washed with 1 mL of PBS. 500 µL of a solution of 50 µg.mL^{-1} of gentamicin and 20 µg.mL^{-1} of lysostaphin in DMEM was added and the plate was left at 37 °C for 30 min to kill the extracellular bacteria. The solution was removed and the wells were washed with PBS. 500 µL of polymer solution was added and the plate was incubated at 37 °C for 2 hours, using a solution of 5 µg.mL^{-1} of lysostaphin as a negative control. 1 mL of a solution of 0.5 % of saponin was added to disrupt the membrane of mammalian cells. After 10 minutes at 37 °C, serial dilution of each well in PBS was undertaken following a thorough detachment of the cells. Each serial dilution was then plated on an Agar plate and left in the incubator overnight. The number of bacteria was counted on the next day.

4.4.2.11 Statistical analysis of data

The statistical significance of the differences between cfu/mL recovered from various groups was analysed using the One-way ANOVA test. Differences were considered significant if $P \leq 0.05$.

4.4.3   Synthesis

4.4.3.1   Synthesis of BodipyAM
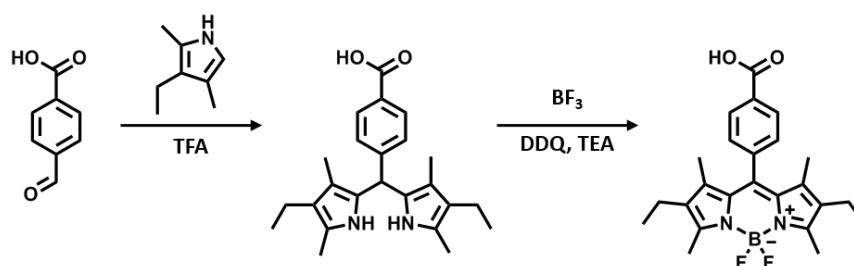
Synthesis of Bodipy acid. Bodipy acid was synthesised according to the literature.[51] 4-carboxybenzaldehyde (0.61g, 4.06 mmol) and 2,4-dimethylethylpyrrole (1.00 g, 1.10 mL, 8.12 mmol) were dissolved in 150 mL of DCM. After addition of a few drops of TFA, the pale yellow mixture turned red. The solution was left to stir at RT overnight. A solution of DDQ

(0.92 g, 4.06 mmol) dissolved in 100 mL of DCM was added to the reaction mixture. After stirring at RT for 4 hours, TEA (6.16 g, 8.5 mL, 60.9 mmol) was introduced, followed by a dropwise addition of $BF_3.OEt_2$ (9.22 g, 9 mL, 65.0 mmol). The reaction was left to stir for 2 hours at RT. The reaction mixture was washed with 3 x 250 mL of water, then dried over $MgSO_4$. The solvent was removed and the product was purified by silica gel chromatography column (EtOAc/hexane, 90:10) to yield a purple solid (110 mg, 259 µmol, 6 %). ^{1}H NMR (300 MHz, 298 K, $CDCl_3$, δ): 8.23 (d, *J*=6 Hz, 2H, **H**Ar proton), 7.47 (d, *J*=6 Hz, 2H, **H**Ar proton), 2.55 (s, 6H, CH_3), 2.30 (q, 4H, H**CH**2CH_3), 1.28 (s, 6H, **H**Ar), 0.99 (t, 6H, HCH_2**CH**3) as shown on Figure 4.10.
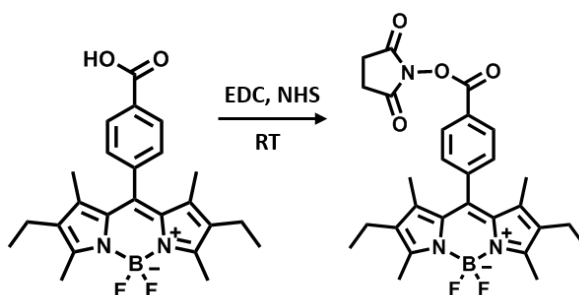
Synthesis of NHS-Bodipy. Bodipy acid (20 mg, 47 µmol) was dissolved in 2 mL of DMF with EDC (13.6 mg, 71 µmol) and NHS (10.8 mg, 94 µmol). The reaction mixture was left to stir overnight. Upon addition of 2 mL of $CHCl_3$, the solution was washed with 3 x 2 mL of water and dried over $MgSO_4$. The solvent was removed to yield a purple powder (24 mg, 46 µmol, 98 %). ^{1}H NMR (300 MHz, 298 K, $CDCl_3$, δ): 8.23 (d, *J*=6 Hz, 2H, **H**Ar proton), 7.47 (d, *J*=6 Hz, 2H, **H**Ar proton), 2.89 (s, 2H, CO-**CH**2-**CH**2-CO), 2.55 (s, 6H, CH_3), 2.30 (q, 4H, H**CH**2CH_3), 1.28 (s, 6H, **H**Ar), 1.00 (t, 6H, HCH_2**CH**3) as shown on Figure 4.11.
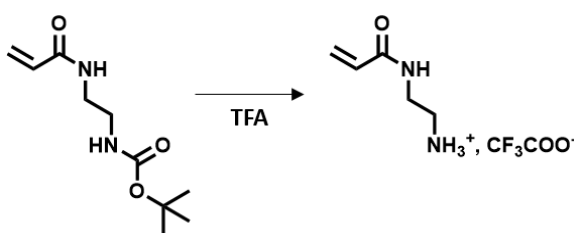
Synthesis of *N*-(2-aminoethyl)acrylamide. *Tert*-butyl (2-acrylamidoethyl)carbamate (BocAEAM) was synthesised according to the literature.[36] The Boc protecting group was removed by adding TFA (500 µL) in 500 µL of EtOH with BocAEAM (100 mg, 0.47 mmol). The product was isolated by rotary evaporation. ^{1}H NMR (300 MHz, 298 K, D_2O, δ): 6.24-6.20 (dd, *J*=12 Hz, *J*=6 Hz, 1H, vinyl proton), 6.16-6.12 (dd, *J*=16 Hz, *J*=2 Hz, 1H, vinyl

proton), 5.74-5.71 (dd, J=9 Hz, J=2 Hz, 1H, vinyl proton), 3.56 (t, 2H, CO-NH-C**H**$_2$), 3.16 (t, 2H, C**H**$_2$-NH$_2$).
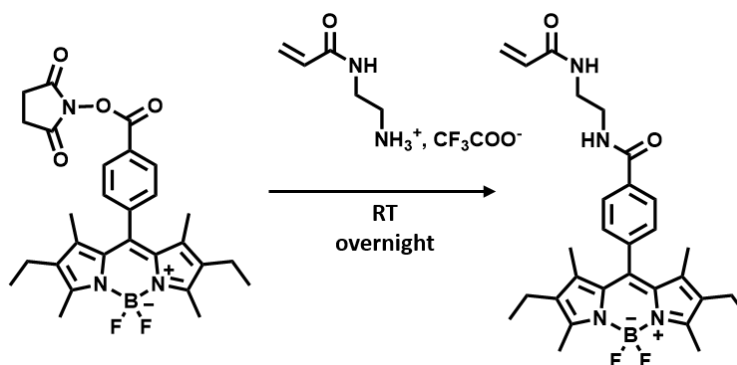
Synthesis of Bodipy acrylamide. NHS-Bodipy (24 mg, 46 μmol) was dissolved in a 2 mL water/THF mixture (40:60) with N-(2-aminoethyl)acrylamide (6.9 mg, 46 μmol) and NaHCO$_3$ (5.8 mg, 69 μmol). The reaction mixture was left to stir at RT overnight. The solvent was removed and the product was dissolved in 7 mL of CHCl$_3$. After washing with 3 x 2 mL of water, the organic layer was dried over MgSO$_4$. The solvent was removed to yield a purple powder (15 mg, 29 μmol, 64 %). ^{1}H NMR (300 MHz, 298 K, CDCl$_3$, δ): 7.95 (d, J=6Hz, 2H, **H**Ar proton), 7.39 (d, J=6Hz, 2H, **H**Ar proton), 6.36-6.31 (dd, J=15 Hz, J=1 Hz, 2H, vinyl proton), 6.20-6.11 (dd, J=18 Hz, J=9 Hz, 2H, vinyl proton), 5.72-5.69 (dd, J=9 Hz, J=1 Hz, 1H, vinyl proton), 3.69 (d, 4H, NH-C**H**$_2$-C**H**$_2$-NH$_2$), 2.54 (s, 6H, CH$_3$), 2.29 (q, 4H, HC**H**$_2$CH$_3$), 1.26 (s, 6H, **H**Ar), 0.99 (t, 6H, HCH$_2$C**H**$_3$) as shown on Figure 4.12. MS: [M+Na]$^+$=543.42 (calculated), 543.4 (found).

4.4.3.2   Synthesis of Bodipy functionalised polymers
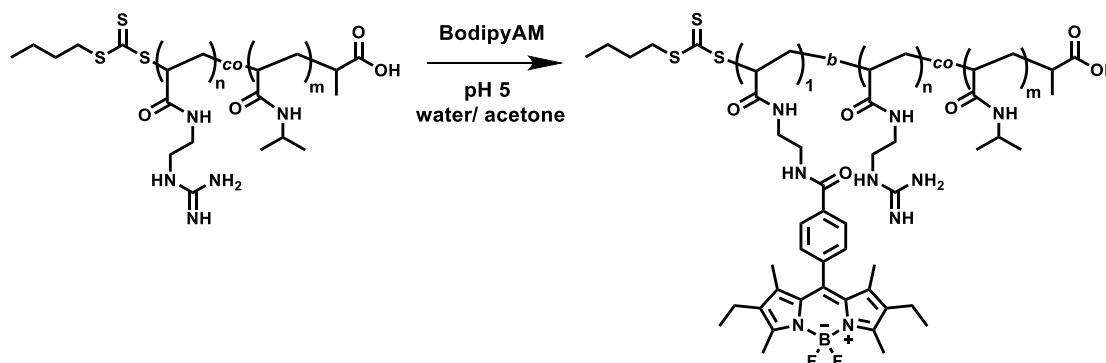
G-D30 (13.9 mg, 1 μmol) was dissolved in an acetate buffer (pH 5). A solution of Bodipy acrylamide (0.5 mg, 1 μmol) in acetone was added, as well as a stock solution of VA-044 in H_2O. The reaction mixture was degassed for 15 min, then placed in an oil bath at 46 °C for 5 hours. Similar reactions were performed on G-S30 and G-T30.

	Concentration (mol.L^{-1})	Mass (mg)
Initiator VA-044	1.0 10^{-3}	0.162
polyGEAm-*co*-NIPAm	2.0 10^{-3}	13.9
Bodipy acrylamide	2.0 10^{-3}	0.520

4.5   Supporting Figures
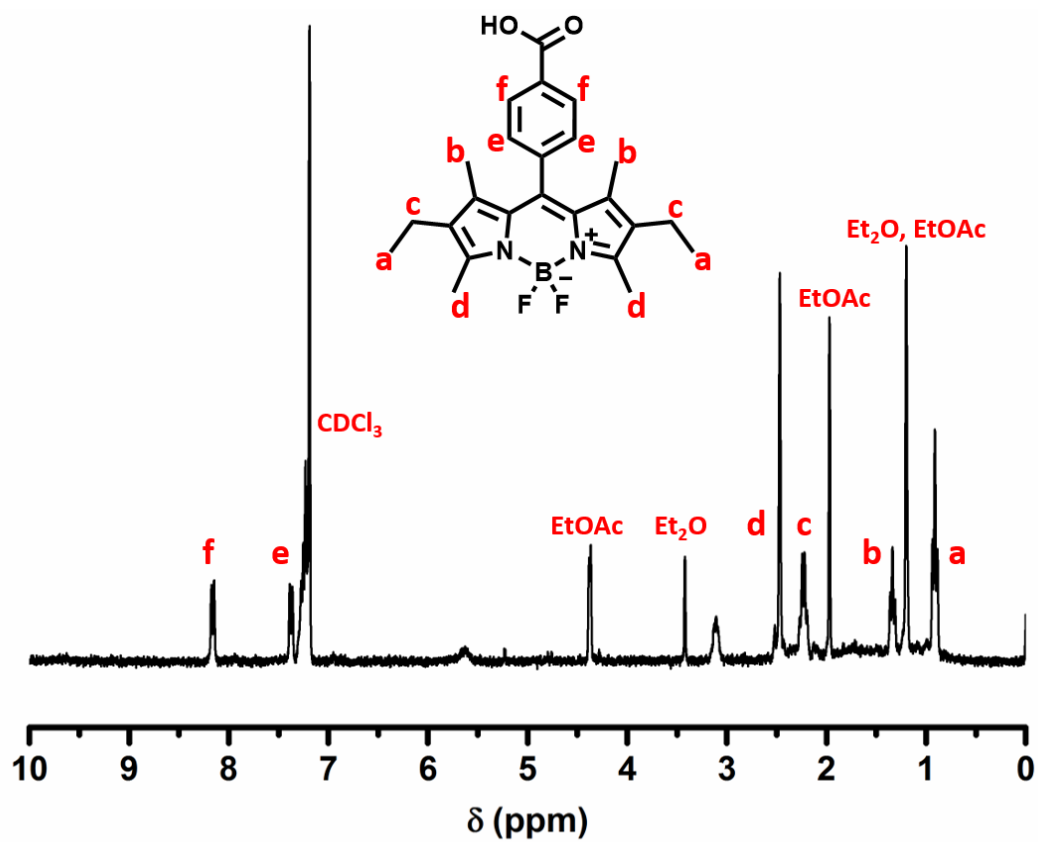
Figure 4.10 - ^{1}H NMR spectrum of Bodipy acid in CDCl$_3$.
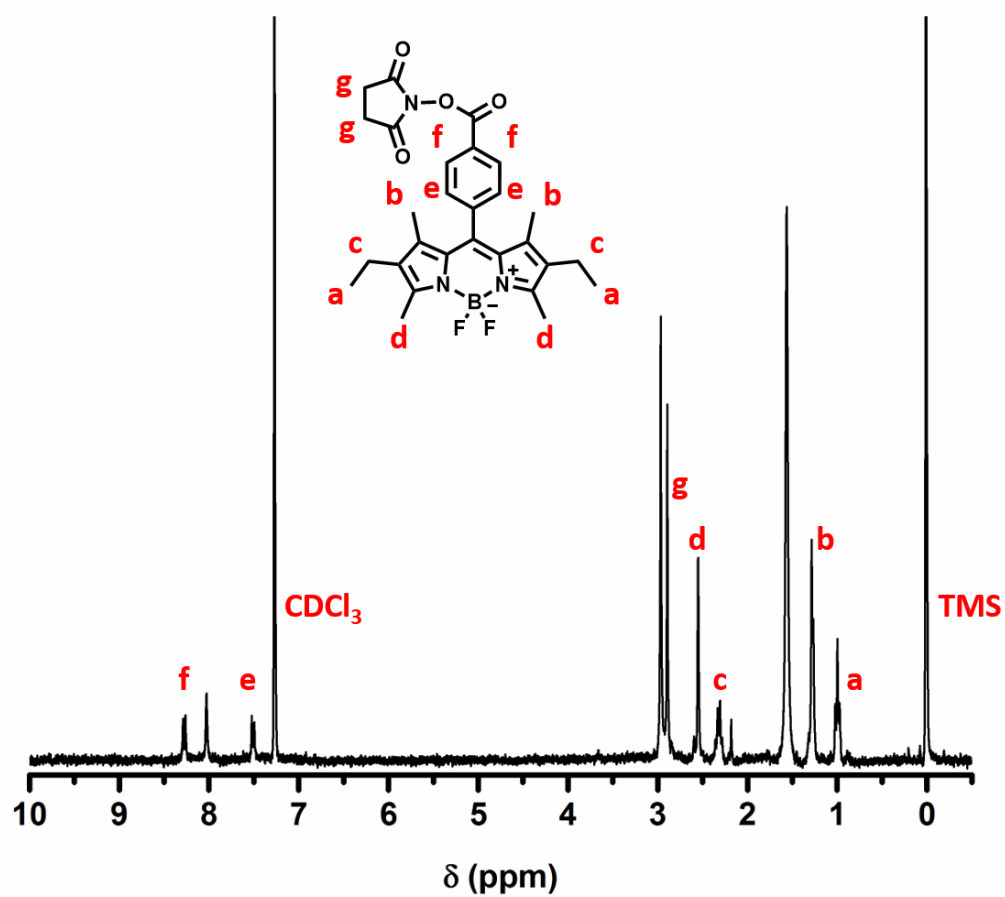
Figure 4.11 - ^{1}H NMR spectrum of NHS-Bodipy in CDCl$_3$.
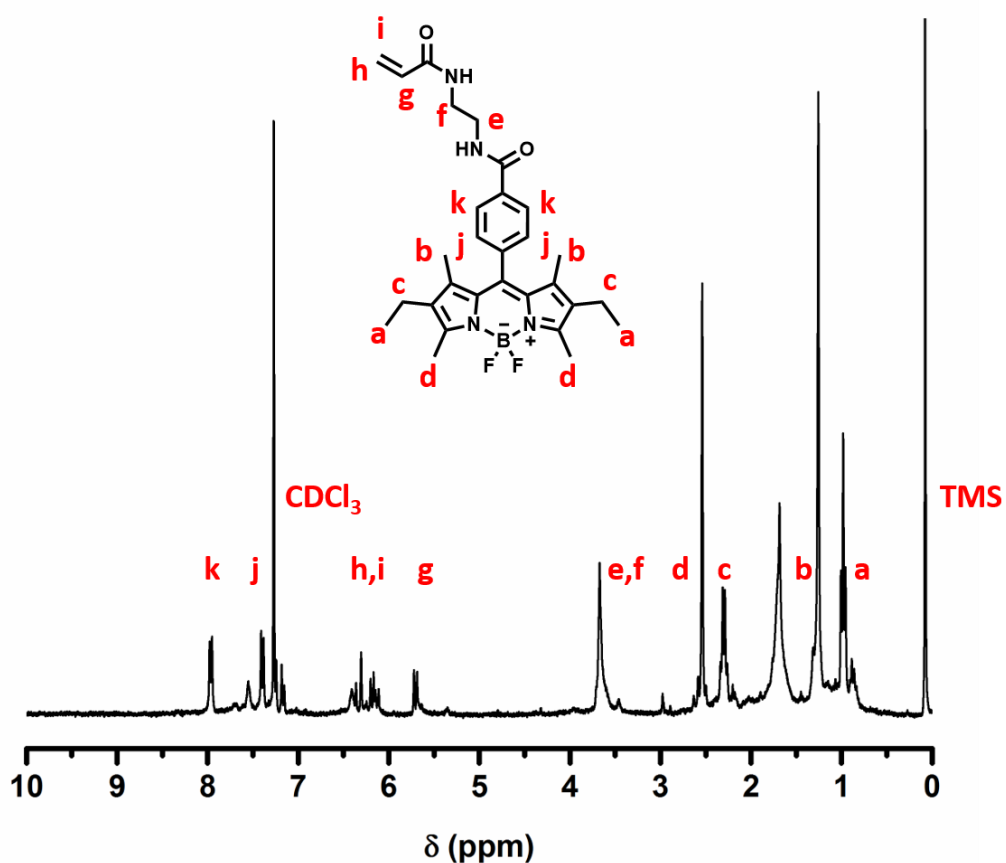
Figure 4.12 - ^{1}**H NMR spectrum of Bodipy acrylamide in CDCl$_3$.**
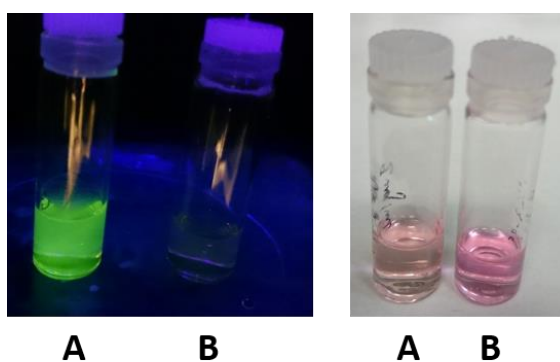
Figure 4.13 - Photos of 1 mg.mL^{-1} solution of the Bodipy functionalised polymers with (A) chain extension after deprotection and (B) deprotection after chain extension.
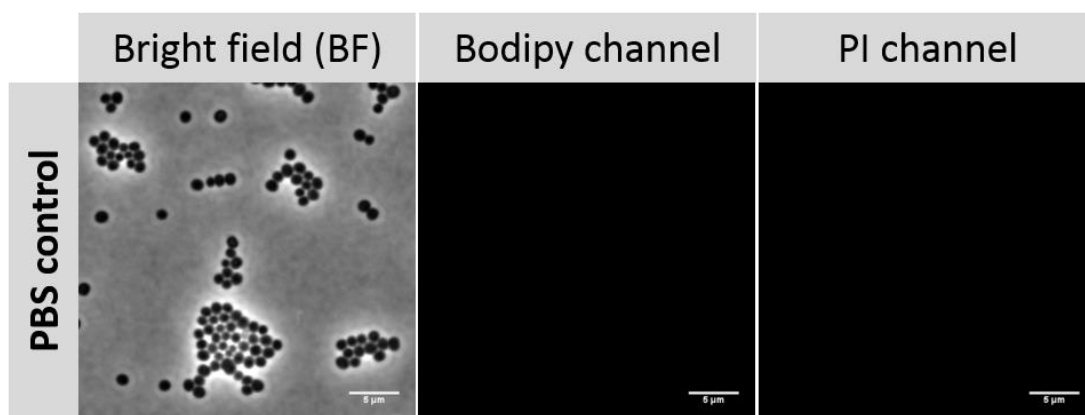
Figure 4.14 - Negative control for the binding assay with MRSA strain JE2 after 2 hours in presence of PI. Microscopy images with the BF, green and red channels. The scale bar represents 5 μm.
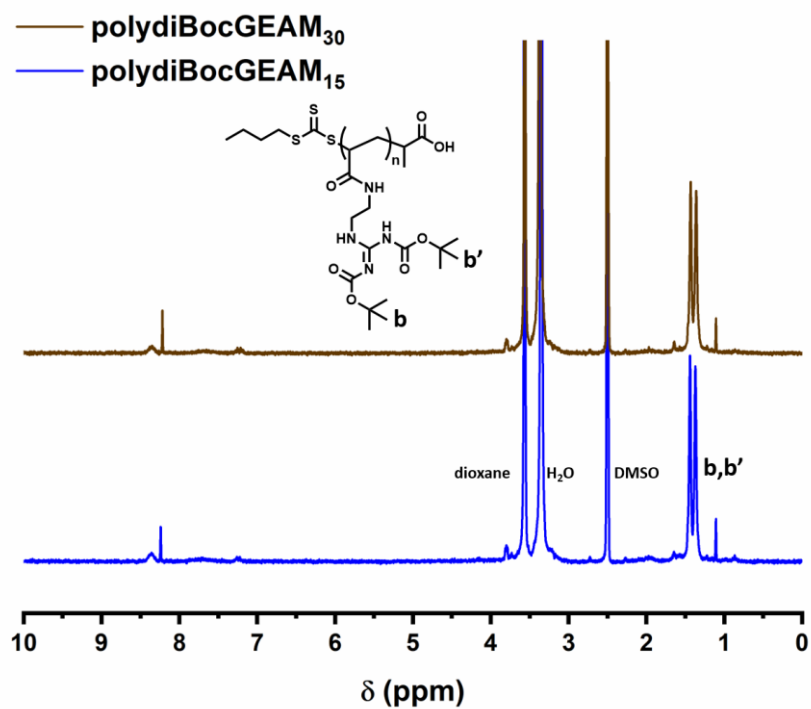
Figure 4.15 - ^{1}H NMR spectra of polydiBocGEAM$_{15}$ and polydiBocGEAM$_{30}$ in DMSO-d_6.
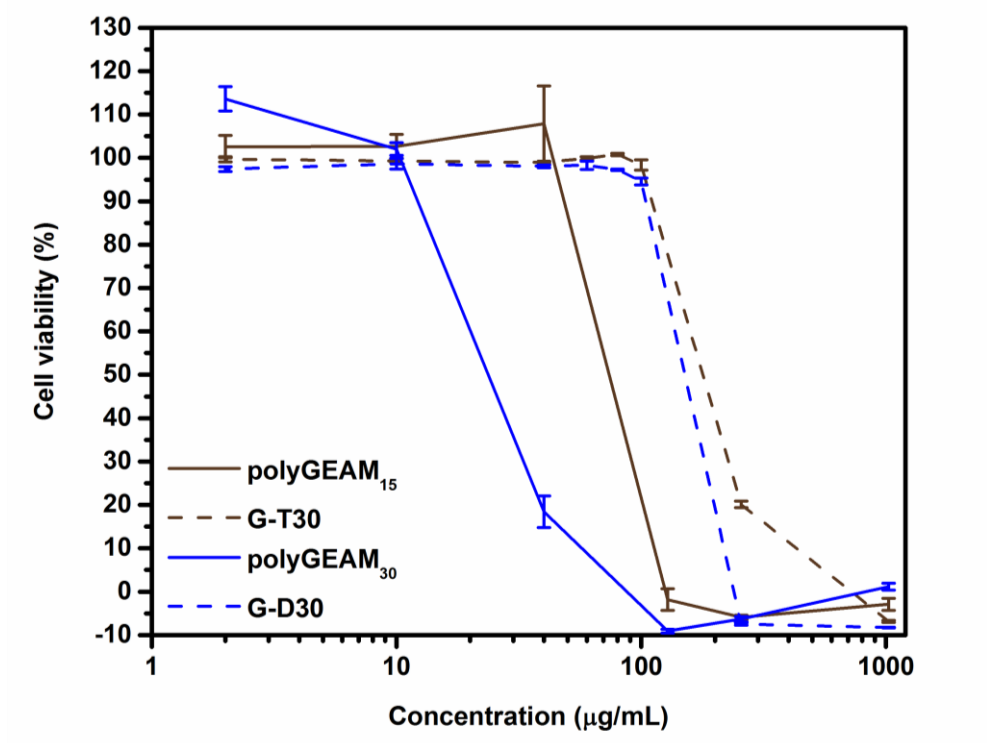
Figure 4.16 – Cytotoxicity of guanidinium SAMPs towards A549 cells. Viability of HaCaT cells incubated for 24 hours in presence of guanidinium homopolymers and their associated copolymers using an XTT assay.

4.6 Supporting Tables

Table 4.2 - Synthesised Boc-protected polymers.

Statistical copolymer	$NIPAM_{70}$-*s*- $BocGEAM_{30}$	G-S30
Tetrablock copolymer	$NIPAM_{35}$-*b*- $BocGEAM_{15}$-*b*- $NIPAM_{35}$-*b*- $BocGEAM_{15}$	G-T30
Diblock copolymer	$NIPAM_{70}$-*b*- $BocGEAM_{30}$	G-D30

Table 4.3 - Antimicrobial activity of the Bodipy functionalised compounds

		$MIC^{[a]}$ ($\mu g.mL^{-1}$)		$MIC^{[a]}$ ($nmol.mL^{-1}$)	
		RN1	JE2	RN1	JE2
Arginine mimics	G-S30	> 1024	> 1024	> 75	> 75
	G-T30	128	128	10	10
	G-D30	64	64	5	5
Bodipy functionalised	Bodipy G-S30	> 1024	> 1024	> 70	> 70
	Bodipy G-T30	256	256	16	16
	Bodipy G-D30	128	128	8	8

[a] MIC is the minimum inhibitory concentration at which no visible bacterial growth can be observed.

Table 4.4 - Experimental conditions used for the synthesis of polydiBocGEAM$_{15}$ and polydiBocGEAM$_{30}$.

	polydiBocGEAM$_{15}$	polydiBocGEAM$_{30}$
DP$_{targeted}$	14	26
m$_{monomer\ added}$ (mg)	71	107
m$_{CTA\ added}$ (mg)	3.18	2.38
m$_{VA-044\ added}$ (mg)	0.324	0.404
V$_{dioxane\ added}$ (mL)	0.268	0.400
V$_{water\ added}$ (mL)	0.065	0.100
V$_{total}$ (mL)	0.333	0.500
[VA-044]$_0$ (mol L^{-1})	3.00 10^{-3}	2.50 10^{-3}
[monomer]$_0$ (mol L^{-1})	0.60	0.60
[CTA]$_0$/[VA-044]$_0$	13	8
L (%)[a]	94	91

[a] Livingness of the polymers, as defined in equation 2.6.

Table 4.5 – DMF-SEC data of the Boc-protected guanidinium homopolymers.

	$M_{n,th}$[a] (g.mol^{-1})	$M_{n,SEC}$[b] (g.mol^{-1})	Đ
polydiBocGEAM$_{15}$	5200	5600	1.15
polydiBocGEAM$_{30}$	9500	10100	1.19

[a] Theoretical molecular weight of the protected polymers calculated from equation 2.5.

[b] Determined for the protected polymers by SEC/RI in DMF using PMMA as molecular weight standards.

Table 4.6 – MIC values for the guanidinium homopolymers.

Compounds		MIC[a] ($\mu g.mL^{-1}$)		MIC[a] ($nmol.mL^{-1}$)		MIC x % GEAM[b] ($nmol.mL^{-1}$)	
		RN1	JE2	RN1	JE2	RN1	JE2
Poly(NIPAM-*co*-GEAM)	G-S30	> 1024	> 1024	> 75	> 75	> 25	> 25
	G-T30	128	128	10	10	3	3
	G-D30	64	64	5	5	1.5	1.5
polyGEAM	polyGEAM$_{15}$	16	16	7	7	7	7
	polyGEAM$_{30}$	32	32	7	7	7	7

[a] MIC is the minimum inhibitory concentration at which no visible bacterial growth can be observed.

[b] Corrected MIC with the molar % of GEAM content.

Table 4.7 - Fluorescence intensity and correction factor due to the discrepancies in the intrinsic fluorescence of the polymers (calculated using a calibration curve).

	Slope α[a]	Correction factor β[b]	Original value[c]	Corrected value
G-S30	9.57	1.00	3412	3412
G-T30	5.21	1.84	1723	3164
G-D30	4.99	1.92	1303	2499

[a] Fluorescence intensity=α.[concentration]

[b] $\beta_i = \alpha(G\text{-}S30)/ \alpha_i$

[c] Cellular fluorescence values obtained for intracellular fluorescence of HaCaT after 2 hours at 37 °C

4.7   References

1.   Köck, R.; Becker, K.; Cookson, B.; van Gemert-Pijnen, J. E.; Harbarth, S.; Kluytmans, J.; Mielke, M.; Peters, G.; Skov, R. L.; Struelens, M. J.; Tacconelli, E.; Witte, W.; Friedrich, A. W., Systematic literature analysis and review of targeted preventive measures to limit healthcare-associated infections by meticillin-resistant Staphylococcus aureus. *Euro Surveillance* **2014,** *19* (29), 20860.

2.   Annual epidemiological report : Antimicrobial resistance and health care-associated infections In *European Centre For Disease Prevention And Control*, 2014.

3.   Garzoni, C.; Kelley, W. L., *Staphylococcus aureus*: new evidence for intracellular persistence. *Trends in Microbiology* **2009,** *17* (2), 59-65.

4.   Singer, A. J.; Talan, D. A., Management of Skin Abscesses in the Era of Methicillin-Resistant Staphylococcus aureus. **2014,** *370* (11), 1039-1047.

5.   Lubritz, G.; Peters, G.; Becker, K.; von Eiff, C.; Metze, D.; Hockmann, J.; Schwarz, T., Intracellular Persistence of Staphylococcus aureus Small-Colony Variants within Keratinocytes: A Cause for Antibiotic Treatment Failure in a Patient with Darier's Disease. *Clinical Infectious Diseases* **2001,** *32* (11), 1643-1647.

6.   Soong, G.; Paulino, F.; Wachtel, S.; Parker, D.; Wickersham, M.; Zhang, D.; Brown, A.; Lauren, C.; Dowd, M.; West, E.; Horst, B.; Planet, P.; Prince, A., Methicillin-resistant Staphylococcus aureus adaptation to human keratinocytes. *mBio* **2015,** *6* (2), e00289-15.

7.   Zautner, A. E.; Krause, M.; Stropahl, G.; Holtfreter, S.; Frickmann, H.; Maletzki, C.; Kreikemeyer, B.; Pau, H. W.; Podbielski, A., Intracellular Persisting Staphylococcus aureus Is the Major Pathogen in Recurrent Tonsillitis. *PLOS ONE* **2010,** *5* (3), e9452.

8.   Chaponnier, C.; Kampf, S.; Clement, S.; Lew, D.; Huggler, E.; Schrenzel, J.; Francois, P.; Vaudaux, P.; Lacroix, J.-S., Evidence of an Intracellular Reservoir in the Nasal Mucosa of Patients with Recurrent Staphylococcus aureus Rhinosinusitis. *The Journal of Infectious Diseases* **2005,** *192* (6), 1023-1028.

9.   Krut, O.; Sommer, H.; Krönke, M., Antibiotic-induced persistence of cytotoxic Staphylococcus aureus in non-phagocytic cells. *Journal of Antimicrobial Chemotherapy* **2004,** *53* (2), 167-173.

10.   Bastos, M. d. C. d. F.; Coutinho, B. G.; Coelho, M. L. V., Lysostaphin: A Staphylococcal Bacteriolysin with Potential Clinical Applications. *Pharmaceuticals* **2010,** *3* (4), 1139.

11.   Pinto-Alphandary, H.; Andremont, A.; Couvreur, P., Targeted delivery of antibiotics using liposomes and nanoparticles: research and applications. *International Journal of Antimicrobial Agents* **2000,** *13* (3), 155-168.

12.   Sémiramoth, N.; Meo, C. D.; Zouhiri, F.; Saïd-Hassane, F.; Valetti, S.; Gorges, R.; Nicolas, V.; Poupaert, J. H.; Chollet-Martin, S.; Desmaële, D.; Gref, R.; Couvreur, P., Self-Assembled Squalenoylated Penicillin Bioconjugates: An Original Approach for the Treatment of Intracellular Infections. *ACS Nano* **2012,** *6* (5), 3820-3831.

13.   Lutwyche, P.; Cordeiro, C.; Wiseman, D. J.; St-Louis, M.; Uh, M.; Hope, M. J.; Webb, M. S.; Finlay, B. B., Intracellular delivery and antibacterial activity of gentamicin encapsulated in pH-sensitive liposomes. *Antimicrobial agents and chemotherapy* **1998,** *42* (10), 2511-2520.

14.   Boonyarattanakalin, S.; Hu, J.; Dykstra-Rummel, S. A.; August, A.; Peterson, B. R., Endocytic Delivery of Vancomycin Mediated by a Synthetic Cell Surface Receptor: Rescue

of Bacterially Infected Mammalian Cells and Tissue Targeting In Vivo. *J. Am. Chem. Soc.* **2007,** *129* (2), 268-269.

15.   Nepal, M.; Mohamed, M. F.; Blade, R.; Eldesouky, H. E.; N. Anderson, T.; Seleem, M. N.; Chmielewski, J., A Library Approach to Cationic Amphiphilic Polyproline Helices that Target Intracellular Pathogenic Bacteria. *ACS Infectious Diseases* **2018,** *4* (9), 1300-1305.

16.   Lei, E. K.; Pereira, M. P.; Kelley, S. O., Tuning the Intracellular Bacterial Targeting of Peptidic Vectors. *Angew. Chem. Int. Ed.* **2013,** *52* (37), 9660-9663.

17.   Yang, S.; Han, X.; Yang, Y.; Qiao, H.; Yu, Z.; Liu, Y.; Wang, J.; Tang, T., Bacteria-Targeting Nanoparticles with Microenvironment-Responsive Antibiotic Release To Eliminate Intracellular Staphylococcus aureus and Associated Infection. *ACS Appl. Mater. Interfaces* **2018,** *10* (17), 14299-14311.

18.   Laxminarayan, R.; Duse, A.; Wattal, C.; Zaidi, A. K. M.; Wertheim, H. F. L.; Sumpradit, N.; Vlieghe, E.; Hara, G. L.; Gould, I. M.; Goossens, H.; Greko, C.; So, A. D.; Bigdeli, M.; Tomson, G.; Woodhouse, W.; Ombaka, E.; Peralta, A. Q.; Qamar, F. N.; Mir, F.; Kariuki, S.; Bhutta, Z. A.; Coates, A.; Bergstrom, R.; Wright, G. D.; Brown, E. D.; Cars, O., Antibiotic resistance—the need for global solutions. *The Lancet Infectious Diseases* **2013,** *13* (12), 1057-1098.

19.   Ellington, J. K.; Harris, M.; Hudson, M. C.; Vishin, S.; Webb, L. X.; Sherertz, R., Intracellular Staphylococcus aureus and antibiotic resistance: Implications for treatment of staphylococcal osteomyelitis. *Journal of Orthopaedic Research* **2006,** *24* (1), 87-93.

20.   Zasloff, M., Antimicrobial peptides of multicellular organisms. *Nature* **2002,** *415* (6870), 389-395.

21.   Ganewatta, M. S.; Tang, C., Controlling macromolecular structures towards effective antimicrobial polymers. *Polymer* **2015,** *63*, A1-A29.

22.   Huang, K.-S.; Yang, C.-H.; Huang, S.-L.; Chen, C.-Y.; Lu, Y.-Y.; Lin, Y.-S., Recent Advances in Antimicrobial Polymers: A Mini-Review. *International journal of molecular sciences* **2016,** *17* (9), 1578.

23.   Van Bambeke, F.; Mingeot-Leclercq, M.-P.; Struelens, M. J.; Tulkens, P. M., The bacterial envelope as a target for novel anti-MRSA antibiotics. *Trends in Pharmacological Sciences* **2008,** *29* (3), 124-134.

24.   Hartlieb, M.; Williams, E. G. L.; Kuroki, A.; Perrier, S.; Locock, K. E. S., Antimicrobial Polymers: Mimicking Amino Acid Functionali ty, Sequence Control and Three-dimensional Structure of Host-defen se Peptides. *Current Medicinal Chemistry* **2017,** *24* (19), 2115-2140.

25.   Treat, N. J.; Smith, D.; Teng, C.; Flores, J. D.; Abel, B. A.; York, A. W.; Huang, F.; McCormick, C. L., Guanidine-Containing Methacrylamide (Co)polymers via aRAFT: Toward a Cell Penetrating Peptide Mimic. *ACS macro letters* **2012,** *1* (1), 100-104.

26.   Wender, P. A.; Mitchell, D. J.; Pattabiraman, K.; Pelkey, E. T.; Steinman, L.; Rothbard, J. B., The design, synthesis, and evaluation of molecules that enable or enhance cellular uptake: peptoid molecular transporters. *Proceedings of the National Academy of Sciences of the United States of America* **2000,** *97* (24), 13003-13008.

27.   Cooley, C. B.; Trantow, B. M.; Nederberg, F.; Kiesewetter, M. K.; Hedrick, J. L.; Waymouth, R. M.; Wender, P. A., Oligocarbonate Molecular Transporters: Oligomerization-Based Syntheses and Cell-Penetrating Studies. *J. Am. Chem. Soc.* **2009,** *131* (45), 16401-16403.

28.   Wender, P. A.; Galliher, W. C.; Goun, E. A.; Jones, L. R.; Pillow, T. H., The design of guanidinium-rich transporters and their internalization mechanisms. *Advanced Drug Delivery Reviews* **2008,** *60* (4), 452-472.

29.   Martin, L.; Peltier, R.; Kuroki, A.; Town, J. S.; Perrier, S., Investigating Cell Uptake of Guanidinium-Rich RAFT Polymers: Impact of Comonomer and Monomer Distribution. *Biomacromolecules* **2018,** *19* (8), 3190-3200.

30.   Herce, H. D.; Garcia, A. E.; Cardoso, M. C., Fundamental Molecular Mechanism for the Cellular Uptake of Guanidinium-Rich Molecules. *J. Am. Chem. Soc.* **2014,** *136* (50), 17459-17467.

31.   Locock, K. E. S.; Michl, T. D.; Valentin, J. D. P.; Vasilev, K.; Hayball, J. D.; Qu, Y.; Traven, A.; Griesser, H. J.; Meagher, L.; Haeussler, M., Guanylated Polymethacrylates: A Class of Potent Antimicrobial Polymers with Low Hemolytic Activity. *Biomacromolecules* **2013,** *14* (11), 4021-4031.

32.   Kamaruzzaman, N. F.; Firdessa, R.; Good, L., Bactericidal effects of polyhexamethylene biguanide against intracellular Staphylococcus aureus EMRSA-15 and USA 300. *Journal of Antimicrobial Chemotherapy* **2016,** *71* (5), 1252-1259.

33.   Ansorg, R.; Rath, P.-M.; Fabry, W., Inhibition of the Anti-staphylococcal Activity of the Antiseptic Polihexanide by Mucin. *Arzneimittelforschung* **2003,** *53* (05), 368-371.

34.   Opinion on Polyaminopropyl Biguanide (PHMB). Submission III ed.; European Commission, 2017.

35.   Judzewitsch, P. R.; Nguyen, T.-K.; Shanmugam, S.; Wong, E. H. H.; Boyer, C., Towards Sequence-Controlled Antimicrobial Polymers: Effect of Polymer Block Order on Antimicrobial Activity. *Angew. Chem. Int. Ed.* **2018,** *57* (17), 4559-4564.

36.   Kuroki, A.; Sangwan, P.; Qu, Y.; Peltier, R.; Sanchez-Cano, C.; Moat, J.; Dowson, C. G.; Williams, E. G. L.; Locock, K. E. S.; Hartlieb, M.; Perrier, S., Sequence Control as a Powerful Tool for Improving the Selectivity of Antimicrobial Polymers. *ACS Appl. Mater. Interfaces* **2017,** *9* (46), 40117-40126.

37.   Gody, G.; Maschmeyer, T.; Zetterlund, P. B.; Perrier, S., Pushing the Limit of the RAFT Process: Multiblock Copolymers by One-Pot Rapid Multiple Chain Extensions at Full Monomer Conversion. *Macromolecules* **2014,** *47* (10), 3451-3460.

38.   Squeo, B. M.; Gregoriou, V. G.; Avgeropoulos, A.; Baysec, S.; Allard, S.; Scherf, U.; Chochos, C. L., BODIPY-based polymeric dyes as emerging horizon materials for biological sensing and organic electronic applications. *Progress in Polymer Science* **2017,** *71*, 26-52.

39.   Summers, G. H.; Lefebvre, J.-F.; Black, F. A.; Stephen Davies, E.; Gibson, E. A.; Pullerits, T.; Wood, C. J.; Zidek, K., Design and characterisation of bodipy sensitizers for dye-sensitized NiO solar cells. *Physical Chemistry Chemical Physics* **2016,** *18* (2), 1059-1070.

40.   Gabriel, G. J.; Madkour, A. E.; Dabkowski, J. M.; Nelson, C. F.; Nüsslein, K.; Tew, G. N., Synthetic Mimic of Antimicrobial Peptide with Nonmembrane-Disrupting Antibacterial Properties. *Biomacromolecules* **2008,** *9* (11), 2980-2983.

41.   Chindera, K.; Mahato, M.; Kumar Sharma, A.; Horsley, H.; Kloc-Muniak, K.; Kamaruzzaman, N. F.; Kumar, S.; McFarlane, A.; Stach, J.; Bentin, T.; Good, L., The antimicrobial polymer PHMB enters cells and selectively condenses bacterial chromosomes. *Scientific Reports* **2016,** *6*, 23121.

42.   Kuroda, K.; Caputo, G. A.; DeGrado, W. F., The Role of Hydrophobicity in the Antimicrobial and Hemolytic Activities of Polymethacrylate Derivatives. *Chem. Eur. J.* **2009,** *15* (5), 1123-1133.

43.   Liu, Z.; Zhang, Z.; Zhou, C.; Jiao, Y., Hydrophobic modifications of cationic polymers for gene delivery. *Progress in Polymer Science* **2010,** *35* (9), 1144-1162.

44.   Wei, H.; Cheng, S.-X.; Zhang, X.-Z.; Zhuo, R.-X., Thermo-sensitive polymeric micelles based on poly(N-isopropylacrylamide) as drug carriers. *Progress in Polymer Science* **2009,** *34* (9), 893-910.

45.   Varkouhi, A. K.; Scholte, M.; Storm, G.; Haisma, H. J., Endosomal escape pathways for delivery of biologicals. *J. Control. Release* **2011,** *151* (3), 220-228.

46.   Kamaruzzaman, N. F.; Chong, S. Q. Y.; Edmondson-Brown, K. M.; Ntow-Boahene, W.; Bardiau, M.; Good, L., Bactericidal and Anti-biofilm Effects of Polyhexamethylene Biguanide in Models of Intracellular and Biofilm of Staphylococcus aureus Isolated from Bovine Mastitis. *Frontiers in microbiology* **2017,** *8*, 1518-1518.

47.   Korea, C. G.; Balsamo, G.; Pezzicoli, A.; Merakou, C.; Tavarini, S.; Bagnoli, F.; Serruto, D.; Unnikrishnan, M., Staphylococcal Esx proteins modulate apoptosis and release of intracellular Staphylococcus aureus during infection in epithelial cells. *Infection and immunity* **2014,** *82* (10), 4144-4153.

48.   Fraunholz, M.; Sinha, B., Intracellular Staphylococcus aureus: live-in and let die. *Frontiers in cellular and infection microbiology* **2012,** *2*, 43-43.

49.   Sendi, P.; Proctor, R. A., *Staphylococcus aureus* as an intracellular pathogen: the role of small colony variants. *Trends in Microbiology* **2009,** *17* (2), 54-58.

50.   Harrison, R. E.; Bucci, C.; Vieira, O. V.; Schroer, T. A.; Grinstein, S., Phagosomes fuse with late endosomes and/or lysosomes by extension of membrane protrusions along microtubules: role of Rab7 and RILP. *Molecular and cellular biology* **2003,** *23* (18), 6494-6506.

51.   Brizet, B.; Goncalves, V.; Bernhard, C.; Harvey, P. D.; Denat, F.; Goze, C., DMAP-BODIPY Alkynes: A Convenient Tool for Labeling Biomolecules for Bimodal PET–Optical Imaging. *Chem. Eur. J.* **2014,** *20* (40), 12933-12944.

Chapter 5   Conclusion and outlook

Since the effectiveness of antibiotics against bacteria is progressively diminishing, the need for alternative treatments of bacterial infections is becoming a pressing clinical issue. In an attempt to aid the development of such alternatives, SMAMPs have been extensively studied in order to determine the important features which confer effective antimicrobial activity. The scope of this thesis was to establish the relationship between the primary microstructure of cationic SMAMPs and their antimicrobial activity, thereby outlining synthetic approaches for optimising the selectivity of such materials.

Chapter 2 focused on the synthesis of a library of SMAMPs containing a primary amine functional acrylamide monomer (AEAM), designed to mimic lysine, and a hydrophobic co-monomer (NIPAM). The library contained several general compositions with a range of AEAM content (0, 30, 50, 70 and 100 molar %), while for each general composition the monomer distribution was also varied (statistical, multiblock and diblock copolymer microstructures). Statistical and block copolymers with controlled molar mass and molar mass distribution were readily obtained *via* RAFT polymerisation. The potency of the SMAMP library against four different strains of bacteria (two Gram-negative and two Gram-positive) was evaluated, in addition to their compatibility towards mammalian cells. In addition to the AEAM content, the monomer distribution of the copolymer systems was found to affect the physico-chemical and biological properties of the SMAMPs.

As monomer distribution had a significant impact on the selectivity of the ammonium polymers, another series of cationic polymer was studied to demonstrate that these observations may be true for other copolymer compositions containing different cationic moieties. In chapter 3, copolymers incorporating 30 % of a guanidinium functional acrylamide (GEAM) monomer, designed to mimic arginine, and NIPAM were synthesised with variation in their monomer distribution (statistical, tetrablock and diblock copolymers). Again, well-defined polymers were prepared using RAFT polymerisation, and analogous ammonium (AEAM-based) counterparts were prepared following protocols established in chapter 2. The main aim of this chapter was to establish the influence of the nature of positive moieties, and their distribution along polymer backbone, on their selectivity towards MSSA and MRSA. These bacterial strains were of particular interest since reduced susceptibility have emerged against vancomycin, which is the last resort antibiotic currently used against MRSA. The type of positive charge and segregation of cationic and hydrophobic functionalities affected the

antimicrobial activity as well as the toxicity of the polymers towards mammalian cells, and can hence be used to tune the properties of SMAMPs.

In addition to an increasing resistance, another challenge antibiotics currently need to tackle during infections is the intracellular persistence of bacteria. In parallel to being explored as SMAMPs, guanidinium containing polymers have successfully been utilised to mimic CPPs in previous studies, and are therefore interesting candidates for the treatment of intracellular bacteria. In this context, chapter 4 concerns the use of the guanidinium-rich polymers introduced in chapter 3 towards the reduction of intracellular MSSA and MRSA within keratinocytes. To investigate this, the polymers were fluorescently-labelled with a Bodipy-functional acrylamide monomer. The influence of monomer distribution on the cellular uptake of the SMAMPs as well as the effect on their interactions with bacterial membrane were determined. Following these experiments, the treatment of intracellular bacteria with guanidinium containing polymers was explored.

The synthesis of statistical and (multi)block copolymers *via* RAFT polymerisation was a simple and versatile method which enabled the preparation of ammonium- and guanidinium-containing polymers. As quantitative monomer conversion was obtained for each block extension, all copolymers syntheses could be performed in a one-pot fashion. By optimising the reaction conditions, polymers with a targeted molar mass and narrow molar mass distributions were obtained ($Đ \leq 1.38$).

From these studies, some key parameters were found to significantly influence the biological properties of the polymers.

Effect of charge to hydrophobicity ratio

Firstly, the charge to hydrophobicity ratio played an important role, as previously reported in the literature. By characterising the cationic polymers by reverse-phase HPLC, the charge to hydrophobicity ratio was demonstrated to increase with increasing AEAM content. Not only did haemolytic activity increase with increasing AEAM content, but haemagglutination was also shown to be favoured, with polymers with an AEAM content of 50 % or above possessing very poor haemocompatibility. Additionally, the toxicity of the cationic polymers to other mammalian cells was enhanced with increasing charge to hydrophobicity ratio. Indeed, the incorporation of NIPAM into the SMAMPs was shown to drastically improve the compatibility of the materials towards mammalian cells. Therefore, it is necessary to establish an optimal AEAM content for any new system based on these copolymer compositions. Additionally, it is worth noting that the selectivity of SMAMPs

towards RBCs decreased when the AEAM content was increased. However, no clear trend was observed with varying charge to hydrophobicity ratio for the selectivity of the SMAMPs towards fibroblasts. For clarity purposes, the following points will be discussing the cationic polymers with 30 % of charge content.

Effect of the type of charge

Despite possessing a comparable content of cationic monomer, the ammonium and guanidinium SMAMPs had different biological properties. Indeed, a slight increase in toxicity towards epithelial cells was observed with guanidinium containing polymers, whereas similar levels of haemocompatibility (both haemolytic activity and haemagglutination) was observed for each type of cationic copolymer. Interestingly, the guanidinium moiety seemed to promote the potency of SMAMPs against MRSA compared to ammonium functionality. This increase could be attributed to a difference in the mechanism of antimicrobial action of the cationic polymers. The ammonium polymers were demonstrated to be membrane active: a fluorescent dye was encapsulated in lipid vesicles, mimicking bacterial membranes, and by monitoring fluorescence levels dye leakage was observed in the presence of the ammonium SMAMPs. Although membrane disruption was also observed with the guanidinium tetrablock and diblock copolymers using PI staining on an MRSA strain, previous work with guanidinium polymers bearing no pendant alkyl groups reported a mechanism of action based on DNA complexation rather than pore formation. When in combination with cationic functionalities, the presence of hydrophobic isopropyl groups from NIPAM could induce bacterial death by disrupting membrane integrity. Therefore, both mechanisms - bacterial DNA binding and membrane disruption - could be taking place simultaneously in presence of the guanidinium copolymers, hence enhancing their antimicrobial activity compared to ammonium analogues. However, the mechanism of action of guanidinium SMAMPs towards bacteria should be further investigated to confirm their complexation to bacterial DNA. Furthermore, the selectivity towards RBCs were similar for both types of cationic polymers, but the guanidinium containing SMAMPs exhibited lower selectivity towards epithelial cells than the ammonium copolymer counterparts.

Effect of segregation of the cationic and hydrophobic functionalities

In addition to the aforementioned features, the distribution of monomers along the backbone played an important role in adjusting the properties of SMAMPs. The first effect which was observed, as characterised by HPLC, with both ammonium and guanidinium

polymers was the change in the overall hydrophobicity of the chain with monomer sequence: the more segregated the cationic and hydrophobic functionalities (diblock > multiblock > statistical copolymer), the more hydrophobic the polymer. Importantly, for the cationic copolymers (ammonium and guanidinium functional) with 30 % charge content, monomer distribution had an impact on antimicrobial activity. Indeed, A-M30 and A-D30 had a significantly greater activity than A-S30 towards both Gram-negative and Gram-positive bacteria. However, there was no distinct trend observed between A-M30 and A-D30 regarding the MIC against all bacterial strain. For the guanidinium containing polymers, G-S30 was non active, whereas G-T30 and G-D30 were both active against MSSA and MRSA, with the diblock copolymer being the most potent. From these results, the antimicrobial activity of SMAMPs seems to increase when the cationic and hydrophobic functionalities are segregated. This trend was not only independent of the type of cationic moiety, but also of the formation of any self-assembly, since no aggregates were observed within the range of concentrations tested. By studying the membrane interactions of guanidinium polymers with a MRSA strain, the reduction of the MIC values with segregation of functionality was correlated to the degree of efficiency with which they interact with bacterial membranes. Indeed, the diblock copolymer interacted with bacteria faster than the tetrablock copolymer, whereas the statistical counterpart did not exhibit any attachment. The lower rate of membrane interaction of G-T30 compared to G-D30 was not due to the length of the cationic block of G-T30 being inadequate to interact with bacterial membrane, shown by comparing polyGEAM of DP 15 and 30, which both interacted in similar ways with membranes. This reduced efficiency could instead be explained by the isopropyl functionalities of the polyNIPAM block which, when present in the middle of the polymer chain, hinder the positive charges from the phospholipids of bacterial membrane. Therefore, the polyNIPAM block should be segregated from the cationic domain for an optimised bacterial binding.

Surprisingly, monomer distribution did not have a significant effect on the haemolytic activity of SMAMPs, whereas haemagglutination was shown to be affected. For both ammonium and guanidinium containing polymers, although the diblock copolymers did not induce aggregation of red blood cells, their statistical and tetrablock counterparts did. Indeed, the distribution of cationic monomers along the polymer backbone (for the tetrablock and statistical copolymers) could be promoting the cross-linking of red blood cells.

On the contrary, toxicity towards mammalian cells from tissues was shown to increase with segregation of functionalities for both types of cationic copolymers, using two epithelial cell lines and fibroblasts. This trend was similar to that of the potency of SMAMPs against bacteria. Indeed, the increase in toxicity of the cationic polymers could also be explained by

enhancement of membrane interactions with mammalian cells when the isopropyl functionalities are segregated from the cationic groups.

Subsequently, the effect of monomer distribution on the selectivity of SMAMPs was evaluated. The diblock copolymers A-D30 and G-D30 displayed the highest selectivity towards RBCs due to their great haemocompatibility combined with high antimicrobial activity against most bacterial strains tested. Although the toxicity towards epithelial cells and fibroblasts increased with segregation of functionality, the effect was not as significant as that on antimicrobial activity. Therefore, the diblock copolymers possessed the highest therapeutic index compared to the multiblock and statistical counterparts.

In addition to mimicking AMPs, guanidinium containing copolymers display structural similarities with cell-penetrating peptides (CPPs), a pertinent design feature for treatment against intracellular bacteria. Although, as mentioned earlier, monomer distribution altered the interactions of the polymers with mammalian cells, it did not affect the internalisation of guanidinium SMAMPs in keratinocytes, as all three polymer compositions (statistical, tetrablock and diblock copolymers) resulted in comparable levels of uptake. The cell uptake by keratinocytes was dictated by both endocytosis and energy-independent pathways. Additionally, the isopropyl functionalities from polyNIPAM were likely to promote the internalisation of the guanidinium-rich SMAMPs into mammalian cells, since they increased the overall hydrophobicity of the polymers.

Finally, segregation of the cationic and hydrophobic functionalities was shown to be necessary for activity against intracellular MSSA and MRSA. Indeed, the statistical and tetrablock guanidinium copolymers did not inhibit the growth of intracellular bacteria, as similar amounts of bacteria were recovered with a lysostaphin treatment, a control antibiotic which can only treat extracellular bacteria. However, G-D30 halved the quantity of intracellular MSSA and MRSA compared to the lysostaphin treatment, within 2 hours. The increased activity of G-D30 towards intracellular bacteria was attributed to a greater antimicrobial activity, as all three polymers had similar internalisation levels into keratinocytes.

One of the major challenges with the use of SMAMPs to eradicate intracellular bacteria is the colocalisation of the cationic polymers with bacteria within the cell. Due to the guanidinium polymers being internalised by keratinocytes *via* both energy-dependent and independent pathways, the polymers would be located in endosomes as well as in the cytosol. Nonetheless, the cationic character of the polymers should allow them to escape from endosomes, hence most of the internalised SMAMPs would eventually be present in the

cytosol of the keratinocytes. However, the guanidinium polymers utilised only possess 30 % molar content of GEAM, which might not be sufficient to efficiently induce endosomal escape. It would be of great interest to vary the size of the polymers or increase the charge content of these guanidinium copolymers to enhance their colocalisation with bacteria, though this would most probably significantly enhance the toxicity of the SMAMPs and reduce their uptake, as seen previously.

In addition to these findings, the cationic polymers did not seem to elicit any bacterial resistance. Indeed, the MIC of the ammonium polymers against an MRSA strain remained constant over the course of 4 weeks. This experiment demonstrated that the cationic SMAMPs could be promising alternatives to currently used antibiotics such as vancomycin.

To conclude, RAFT polymerisation has been demonstrated to be a powerful technique for screening libraries of functional SMAMPs, importantly providing access to subtle levels of microstructural control (i.e. multiblock copolymers), which allowed for the investigation of structure-activity relationships. The effect of charge to hydrophobicity ratio as well as type of charge were shown to impact the selectivity of the polymers. However, monomer distribution had a more significant effect on the interactions of the polymers with bacterial and mammalian cells, as it can render a non-antimicrobial active and non-haemocompatible polymer, G-S30, into a SMAMP inhibiting the growth of intracellular MRSA, G-D30, by sole segregation of cationic and hydrophobic functionalities. Taken together, the observations made in the various studies which comprise this thesis will hopefully be useful for the design and development of future SMAMPs in clinical treatment.

List of publications

1. Antimicrobial polymers: Mimicking amino acid functionality, sequence control and three-dimensional structure of host-defense peptides. M. Hartlieb; E. G. L. Williams; **A. Kuroki**; S. Perrier; K. Locock, E. S., *Current Medicinal Chemistry* **2017**, 24, 1-1.

2. Sequence control as a powerful tool for improving the selectivity of antimicrobial polymers, **A. Kuroki**; P. Sangwan; Y. Qu; R. Peltier; C. Sanchez-Cano; J. Moat; C. G. Dowson; E. G. L. Williams; K. E. S. Locock; M. Hartlieb; S. Perrier, *ACS Applied Materials & Interfaces* **2017**, 9, 40117-40126.

3. Looped flow raft polymerization for multiblock copolymer synthesis, **A. Kuroki**; I. Martinez-Botella; C. H. Hornung; L. Martin; E. G. L. Williams; K. E. S. Locock; M. Hartlieb; S. Perrier, *Polymer Chemistry* 2017, 8, 3249-3254.

4. Investigating cell uptake of guanidinium-rich raft polymers: Impact of comonomer and monomer distribution, L. Martin; R. Peltier; **A. Kuroki**; J. S. Town; S. Perrier, *Biomacromolecules* **2018**, 19, 3190-3200.

5. Reverse-phase high performance liquid chromatography (rp-hplc) as a powerful tool to characterise complex water-soluble copolymer architectures, R. Peltier; A. Bialek; **A. Kuroki**; C. Bray; L. Martin; S. Perrier, *Polymer Chemistry* **2018**, 9, 5511-5520.

6. Stimuli-Responsive Membrane Activity of Cyclic-Peptide-Polymer Conjugates, M. Hartlieb; S. Catrouillet; **A. Kuroki**; C. Sanchez-Cano; R. Peltier; S. Perrier, *Chemical Science* **2019**, Accepted Manuscript.

7. Targeting intracellular, multi-drug resistant *Staphylococcus aureus* with guanidinium polymers by elucidating the structure-activity relationship, **A. Kuroki**; A. Kengmo-Tchoupa; M. Hartlieb; R. Peltier; K. E. S. Locock; M. Unnikrishnan; S. Perrier, **2019**, Submitted for publication.

8. The type VII secretion system protects Staphylococcus aureus against antimicrobial host fatty acids, A. Kengmo Tchoupa; R. Jones; **A. Kuroki**; M. Alam; S. Perrier; Y. Chen; M. Unnikrishnan, **2019**, Submitted for publication.